Rapid detection of Avian Influenza Virus - Towards point of care diagnosis

Dhumpa, Raghuram

Publication date:
2011

Document Version
Publisher's PDF, also known as Version of record

Raghuram Dhumpa

Rapid detection of Avian Influenza Virus - Towards point of care diagnosis

2011

DTU Vet
National Veterinary Institute
Technical University of Denmark

Hangoevej 2
DK-8200 Aarhus N
Denmark
Phone +45 35 88 60 00
Fax +45 35 88 60 01

www.vet.dtu.dk

Rapid detection of Avian Influenza Virus
- Towards point of care diagnosis

PhD Thesis

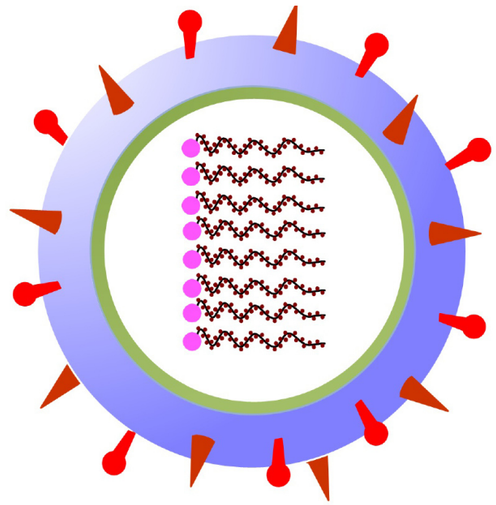

Raghuram Dhumpa
March 2011

DTU Vet
National Veterinary Institute

Rapid detection of Avian Influenza Virus - Towards point of care diagnosis

Ph.D Thesis

Raghuram Dhumpa

National veterinary Institute
Technical University of Denmark

March 2011

DTU Vet
National Veterinary Institute

Dedicated to my dear friends & family

கற்றது கைமண் அளவு, கல்லாதது
உலகளவு -- ஔவையார்

What is learnt is a handful of sand, while what is unknown is the size of the world -- Avvaiyar

ABSTRACT

Bird flu or Avian flu is an infectious disease caused by an influenza A virus of the *Orthomyxoviridae* family. Avian influenza virus (AIV) causes significant economic losses to the poultry industry worldwide and threatens human life with a pandemic. Pandemic of AIV is the human infection caused by the appearance of a “new” influenza virus as a result of antigenic shift or antigenic drift. Several outbreaks of AIV caused by the rapid spread of infection have been identified. Therefore, there is an urgent need for rapid diagnostic methods that would enable early detection and improved measurements to control the AIV outbreak. Classical method for detection and identification of AIV is time consuming (3-10 days), laborious, requires high amount of virus for detection and also special laboratory facilities and trained staff. Molecular diagnostic systems using RT-PCR amplification have significantly improved the speed, sensitivity and specificity of detecting AIV but are still cumbersome, expensive and time-consuming (1-2 days). In both classical and molecular diagnosis, the transportation of sample to the near-by reference or diagnostic laboratory is needed, and this will increases the time for diagnostic result. A simple approach would be to have a point-of-care (POC) diagnostic test at or near the site of sample collection to provide results in very short time and that can improve medical decision-making. The available commercial POC tests that are used for screening of influenza A virus are rapid (5-30 minutes), but have low sensitivity and false negative results are of major concern. Ultimately, the miniaturization of molecular diagnostics using Lab-on-a-chip (LOC) systems could provide the next-generation rapid POC diagnostics.

This study has been focused on developing rapid diagnostic methods for the identification and subtyping of the AIV towards POC diagnosis. The first step in molecular diagnostic is sample preparation which is the key to the success of diagnosis. To address this, a novel method was developed for selective separation and purification of AIV from chicken faecal sample using monoclonal antibody (mAb) conjugated magnetic beads where RNA extraction step is not required. The developed bead-based system was able to capture, concentrate and purify all of the 16 H subtypes of AIV from the AIV spiked faecal samples, demonstrating the efficiency of the mAb conjugated beads and the developed method. Subsequently, the newly developed bead-

based method was used in a microfluidic magnetic microsystem for the automation of sample preparation. Using LOC system with a Cyclic-Olefin-Copolymer (COC) polymer chip, the RT-PCR was miniaturized and the entire process was detected in less than 2 h. This integrated LOC system has a great potential for POC clinical diagnostics.

Subtyping of AIV is important in the diagnosis to identify the pathogenic virus. A DNA microarray-based solid-phase PCR approach has been developed for rapid detection of influenza virus types A and simultaneous identification of pathogenic virus subtypes of H5 and H7. This solid-phase RT-PCR method combines a reverse-transcription amplification of RNA extract in the liquid-phase with sequence-specific nested PCR on the solid phase. The examination of 33 avian faecal and tracheal swab specimens was completed in less than 2 h with 94% accuracy. Subsequently, the approach of solid-phase-PCR was extended to a microfluidic chip to reduce sample and reagent consumption. The whole processing time for identifying and simultaneously subtyping AIV was further reduced to 1h.

Apart from the RT-PCR method, two immunological methods based on; fluorescent DNA barcode and fluorescent beads were also developed for rapid detection and identification of the AIV. In both methods, the detection involved sandwiching of the target AIV between monoclonal antibodies for nucleoproteins and for matrix proteins. In the fluorescent DNA barcode-based immunoassay, fluorophore-tagged oligonucleotides were used as surrogates for signal detection with sensitivity comparable to conventional RT-PCR for allantoic fluid containing H16N3 AIV. While in the fluorescent bead-based immunoassay, the fluorescent beads were used as the direct detection signal from AIV. In both methods the entire detection time was less than 2 h.

Keywords: Avian Influenza Virus - Diagnostics – Faecal sample - Sample Preparation - Magnetic Beads – RT-PCR – Microfluidics – Magnetic microsystem – Lab-on-a-chip – Solidphase PCR – Microarray – Biobarcode immunoassay – Fluorescent beads.

SAMMENDRAG (Danish)

Fugle influenza eller Aviær influenza er en infektiøs lidelse, der skyldes smitte med et influenza A virus af *Orthomyxoviridae* familien. Verden over har sygdoms udbrud i fjerkræ forsaget af Aviær influenza virus (AIV) givet store tab fjerkræindustrien, og der hersker stor frygt for at smitten kan overføres til mennesker og udvikle sig til en verdensomspændende pandemi. En pandemi kan opstå når mennesker bliver følsomme for AIV virus, som følge af ændringer i det oprindelige virus. Dette kan ske ved mutation eller små ændringer i virus genomet, hvorved der opstår nye ukendte typer. Som følge af en meget hurtig spredning af virus er der indtil nu påvist en del mindre udbrud med AIV. For at kunne kontrollere disse udbrud er det meget nødvendigt at have hurtige og sikre metoder til at påvise infektionen så tidligt i forløbet så muligt. Påvisning af AIV med de klassiske metoder med dyrkning af virus er meget langsommelig og arbejdskrævende og langsommelig (3-10 dage); ydermere er metoderne ikke særlig følsomme og kræver sikrede laboratorie faciliteter samt trænet personale. Indførelsen af molekylære påvisningsmetoder som reverse transcription polymerase chain reaction (RT-PCR), har øget følsomhed og specificiteten i analysen væsentligt, og man kan nu få svar indenfor 1-2 dage, men metoden er stadigvæk arbejdskrævende og bekostelig.

Uafhængigt af påvisningsmetoden, tager det tid at transportere prøver til det nærmeste kvalificerede laboratorium, hvilket det øger tiden inden en diagnose kan stilles. En simpel måde at løse dette problem på er at anvende point-of-care (POC) diagnostiske tests, hvor påvisningen foretage ude ved den smittede patient. Der findes allerede i dag kommercielle hurtigtest kits som kan give svar indenfor 5-30 minutter, men de har oftest for lav følsomhed til at kunne stille en sikker diagnose. Til næste generations POC diagnostiske test vil det derfor være interessant at nedskalere de hidtidige molekylære påvisnings metoder, således at de kan anvendes i et mikro laboratorium som feks i ”Lab-on-a-chip” (LOC) systemer.

Dette studie har fokuseret på at udvikle hurtig-diagnostiske metoder til at identificere og typebestemme AIV. Det første vigtige trin i diagnosticering med molekylære metoder er en god prøveforberedelse. For at optimere denne, er der blevet udviklet en ny metode baseret på

monoklonale antistoffer (mAb) bundet til magnetiske kugler, til selektivt at binde og oprense viruspartikler fra kyllingegødning, hvilket overflødiggør oprensning af RNA.

Med det udviklede kuglebaserede oprensningssystem var det muligt at binde og oprense alle 16 H AIV subtyper fra gødningsprøver tilsat virus eksperimentelt. Efterfølgende blev dette system overført til et mikrofluidisk magnetisk mikrosystem, hvori prøveforberedelsen kunne automatiseres. RT-PCR blev nedskaleret således at det kunne foregå i et LOC system baseret på en Cyclic-Olefin-Copolymer (COC) polymer chip. Hele forløbet fra oprensning til påvisning kunne ske på mindre end to timer, så dette integrerede LOC system har derfor et stort potientale som fremtidigt POC testkit.

Typning af AIV er vigtig for at kunne adskille de sygdomsfremkaldende virus fra de ufarlige. Et DNA microarray-baseret solid-phase PCR, er blevet udviklet til både at kunne påvise Influenza A samt vise de H5 og H7 undertyper som er sygdomsfremkaldende. Denne solid-phase RT-PCR metode kombinerer RT amplifikationen af oprenset RNA i væskefasen, med en sekvensspecifik nested PCR i Solid phasen. Undersøgelsen af 33 svabere fra kloak eller svælg fra fugle kunne foretages på mindre end 2 timer og med en nøjagtighed på 94 %. Dette system blev også overført til et microfluidic chip system for at reducere prøve og reagens mængden. Proces tiden for denne detektions og typnings metode kunne herefter nedsættes med 1 time.

Udover RT-PCR detektions metoden blev der også udviklet en immunologisk metode baseret dels på fluorescerende DNA stregkoder samt på fluorescerende kugler. Med begge metoder påvistes AIV som en sandwich med monoklonale antistoffer rettet imod nucleoproteiner og matrix proteiner. I det fluorescerende DNA stregkode baserede immunoassay brugtes korte fluorescensmærkede nukleotider som erstatning for traditionel signal forstærkning, og metoden kunne påvise virus med en følsomhed tilsvarende konventionel RT-PCR i allantois væske indeholdende AIV H16N3. Med det immunoassay baseret på fluorescerende kugler foretages direkte detektion af signal fra AIV. Med begge metoder var detektionstiden mindre end 2 timer.

PREFACE AND ACKNOWLEDGEMENT

This thesis is submitted in partial fulfilment of the requirements for the Ph.D degree at Technical University of Denmark (DTU). This work was carried out at the Laboratory of Applied Micro-Nanotechnology (LAMINATE), National Veterinary Institute, Technical University of Denmark. The project was funded by DTU Globalization-food pathogen project no. 8 and grant no. 150627.

First, I would like to express my thanks and sincere gratitude to my advisor, senior scientist Dr. Dang Doung Bang for giving me an opportunity to pursue my doctoral studies. Also for his extended support during the entire tenure of my Ph.D was memorable. I express my deep sense of gratitude to my co-supervisor, Associate Prof. Dr. Anders Wolff for his fruitful discussions. Likewise, I would like to thank my head of the department Dr. Flemming Bager for his support.

My thesis would not have been complete without collaboration with the Avian virology group. I was very fortunate to associate with Dr. Kurt Handberg and Dr. Poul Henrik Jørgensen for their helps and thoughtful advices. I enjoyed the most working with Hanne, Lisbeth, Tanja, Susanne Jespersen, Susanne Stubbe, Søs and also Anne (especially for her home baked cakes☺).

I would also like to thank my external project collaborators Sun Yi, Minqiang Bu and Ivan from BioLabchip group at DTU- Nanotech and many thanks to Dr. Jesus Ruano-López and his colleagues at Ikerlan, Spain.

My special thanks go to Jonas and Steen for being helpful from the day one of my Ph.D. I would like to express my sincere thanks to Cuong for his comments and proofreading the thesis. Also I thank my group members Xuan, Tram, Zoreah, Søren Peter, Morten, Joana, Huong, Yiping Li and Yuliang Liu for being cheerful colleagues. Thanks to colleagues from other groups and staff members in the department for their kindness and help.

I would also like to express my thanks to all my friends and well-wishers in Aarhus and Copenhagen who offered help and support during several occasions. We had wonderful time together.

I would like to express my loving thanks to my family, my sister, and friends for their constant moral support and encouragement in spite of being far away, without which I would not have made it this far. Finally, I would like to thank my wife Dhivyaa for her unwavering support and care, especially during the final months of my thesis.

Raghuram Dhumpa
January 2011 Aarhus, Denmark

I. Table of content

II. List of publications

Peer-review Journals

i. Dhumpa, R., Handberg, K.J., Jørgensen, P.H., Yi, Sun., Wolff,A., Bang, D.D., (**2011**). Rapid detection of avian influenza virus in chicken faecal samples by immunomagnetic capture RT-PCR assay. Diagnostic Microbiology and Infectious Diseases, 69,258-265.

ii. Dhumpa, R., Bu,M., Handberg, K.J., Wolff,A., Bang, D.D (**2010**). Rapid sample preparation for detection and identification of avian influenza virus from chicken faecal samples using magnetic bead microsystem. Journal of Virological Methods, 169, 228–231

iii. Yi, S., Dhumpa, R., Bang, D.D., Handberg, K.J., Wolff, A (**2011**). DNA Microarray Based Solid Phase RT-PCR for Rapid Detection and Identification of Avian Influenza Virus. Diagnostic Microbiology and Infectious Diseases, 69, 432–439.

iv. Yi, S., Dhumpa, R., Bang, D.D., Handberg, K.J., Wolff, A. (**2011**). A lab-on-a-chip device for rapid identification of avian influenza viral RNA by solid-phase PCR. Lab chip, 11, 1457-1463.

v. Cao, C., Dhumpa, R., Bang, D.D., Ghavifekr, Z., Høgberg, J., and Wolff, A. (**2010**). Detection of avian influenza virus by fluorescent DNA barcode-based immunoassay with sensitivity comparable to PCR. Analyst, 135, 337-342.

International conference presentation and proceedings (*presenter)

- Dhumpa, R.*, Handberg, K.J., Wolff, A., Bang, D.D., (2008). "Monoclonal antibody coated magnetic beads for rapid identification of Avian Influenza Virus (AIV) in Danish broiler". Poster presentation at poster at Lab-On-a-Chip World Congress, Barcelona, Spain, May 2008.
- Dhumpa, R.*, Handberg, K.J., Wolff, A., Bang, D.D., (2008). "Monoclonal antibody coated magnetic bead microsystem for rapid identification of avian influenza virus (AIV)". Oral presentation at MED-VET-NET 4th Annual scientific meeting, St. Malo, France, June 2008
- Dhumpa, R.*, Bu, M., Handberg, K.J., Wolff, A., Bang, D.D., (2009). "Rapid sample preparation using magnetic bead microsystem for detection and identification of avian influenza virus from chicken faecal samples". Oral presentation at NanoBioTech-conference-2009, Montreux, Switzerland, November 2009.
- Dhumpa, R.*, Berganzo, J., Ruano-López, J.M., Wolff, A., Bang, D.D., (2010). "Microfluidic System for on Chip Sample Preparation and Immunodetection of Avian Influenza Virus". Poster presentation at Lab-on-a-Chip European Congress, Dublin, Ireland, May 2010.
- Bang, D.D.*, Dhumpa, R., Cao, C., Florian, L., Berganzo, J., Walczak, R., Liu, Y., Bu, M., Yi, S., Dzuiban, J., Ruano, J.M. and Wolff, A. (2010). "A trip from a tube to a chip applied micro and nanotechnology in biotechnology", veterinary and life sciences. Proceeding Series of the International Federation of Medical and Biological Engineering (ISSN 1680-0737), p: 290-294.
- Yi, S., Bang, D.D., Dhumpa, R., Handberg, K.J., Wolff,A.*(2009). A Lab on a chip device for rapid identification of Avian Influenza virus μTAS 2009 Vol. 1, p: 697-698.
- Cao, C.*, Dhumpa, R., Bang, D.D., Ghavifekr, Z., Høgberg, J., and Wolff, A., (2009). "Detection of Avian Influenza virus with PCR like sensitivity by fluorescent DNA bare code based immunoassay" μTAS 2009 Vol.2. p:1614-1616.
- Bang, D. D.*, Dhumpa. R., Cuong, C., Florian,L., Berganzo, J., Walczak, R., Liu, Y., Bu, M., Yi, S., Dzuiban, J., Ruano, J. M., and Wolff, A. (2010). "A trip from a tube to a chip applied micro and nanotechnology in biotechnology, veterinary and life sciences", 3rd Electronic System Integration Technology Conference, Brussels, Belgium.

III. List of abbreviations

AGID	Agar gel immunodiffusion
AIV	Avian influenza virus
BSA	Bovine Serum Albumin
BSL-3	Bio safety level-3
COC	Cyclic-Olefin-Copolymer
CP	Capture probe
CY5	Cyanine-5
dNTP	deoxynucleotide triphosphate
EDC	1-ethyl-3-(3-dimethylaminopropyl) carbodiimide
EID50	50% Egg infectious dosage
ELISA	Enzyme linked immunosorbent assay
FIA	Fluorescent immunoassay
FITC	Fluorescein isothiocyanate
HA	Haemagglutination
HA0	Haemagglutinin precursor
HAU	Haemagglutination Unit
HPAI	Highly pathogenic avian influenza
IVPI	Intravenous pathogenicity index
IVRD	Influenza virus resource database
LOC	Lab-on-a-chip
LPAI	Low pathogenic avian influenza
MDCK	Madin-Darby canine kidney
MMP	Magnetic microparticle
mRNA	Messenger RNA
NA	Neuraminidase
OIE	Office International Des Epizooties
PBS	Phosphate buffered saline
PCR	polymerase chain reaction

PD	Primer dimmer
PDMS	polydimethyl siloxane
PFU	Plaque forming unit
PMK	Primary monkey kidney
PMP	Polystyrene microparticle
POC	Point of care
RBC	Red blood cell
RNA	Ribonucleic acid
RNP	Ribonucleoprotein
RT-PCR	Reverse transcription polymerase chain reaction
SA	Sialic acid
SDS	sodium dodecyl sulphate
SNP	Single-nucleotide polymorphisms
SPF	Specific pathogen free
SSC	standard saline citrate
SVR	Surface to volume ratio
TAQ	Thermus aquaticus
TCID50	50% Tissue culture infectious dosage
WHO	World health organization

Chapter 1

Introduction and thesis outline

Avian Influenza infection is caused by Influenza A virus belonging to the *Orthomyxoviridae* family. Avian influenza virus (AIV) have been affecting all types of wild birds and occasionally aquatic bird species [1]. The wild life species serve as a reservoir of all Influenza A viruses over a long period and have been the source of infection in domestic poultry and mammals. Transmission of AIV to domestic poultry is introduced primarily through direct or indirect contact with infected birds.

Based on the ability of AIV to cause disease and mortality in experimental infection of four to eight weeks-old chickens, the AIV is classified as either highly pathogenic avian influenza (HPAI) or low pathogenic avian influenza (LPAI)[2;3]. The HPAI virus H5N1 which affected birds in Eurasia and Africa continues to spread and to pose a challenge to animal and human health. The first known instance of human infection with AIV H5N1 was reported in Hong Kong in 1997. Since then the pandemic started spreading around the world. So far a total number of 507 cases of human Avian Influenza A/(H5N1) infection with 59.56% death ratio (302/507) was reported by Wold Health Organisation (WHO) on 18th October 2010 [4]. The pandemic could have resulted from either antigenic drift or avian viral strain re-assortment with a human strain (antigenic shift). Cross species infection between humans and other mammals continues to threat the world of a pandemic influenza. In poultry, several outbreaks of AIV caused culling of several millions birds and created a huge economic loss in poultry industry worldwide [5]. The outbreaks of AIV have been characterized by the rapid spread of infection emphasizing the need for rapid diagnostic methods that would enable early detection and improve measures to control the AIV. This thesis aimed to development rapid diagnosis methods for the detection of avian influenza virus.

The classical method for detection and identification of AIV is time consuming (3-10 days), laborious, requires high amount of virus for detection and also special laboratory facilities and trained staffs (Chapter 3). On the other hand, molecular diagnostic systems using reverse

transcriptase polymerase chain reaction (RT-PCR) amplification have significantly improved the speed, sensitivity and specificity for the detection of AIV but are still cumbersome, expensive and time-consuming (1-2 days) (Chapter 4). In both classical and molecular diagnostics, the transportation of sample to the near-by reference or diagnostic laboratory is needed, which further increases the time for diagnostic result. A simple approach would be to have a point-of-care (POC) diagnostic test at or near the site of sample collection which could provide result instantly or in a very short time and can improve medical decision-making. The available commercial POC tests are mainly based on immunoassays which detect influenza viral antigen and are used for screening of influenza A within 5-30minutes. However these POC poses low sensitivity and false negative results are a major concern. Ultimately, the miniaturization of the molecular diagnostics using Lab-on-a-chip (LOC) systems could provide the next-generation rapid POC diagnostics (Chapter 5).

In order to develop such rapid diagnostic system, a simple and robust sample preparation for RT-PCR is required (Chapter 6). In this study, a magnetic bead based system has been developed to separate, concentrate and purify AIV from faecal sample. The beads were conjugated with monoclonal antibodies against the AIV nucleoprotein, which is conserved in all the AIV. The bead captured virus was detected by RT-PCR without RNA extraction, due to effective removal of RT-PCR inhibitors. The developed bead-based assay showed a detection limit comparable to the RNA extraction and the classical virus isolation method. The advantage of using magnetic beads in sample preparation is that it can be automated using magnetic microfluidic system. The miniaturization of RT-PCR for AIV has been performed on a lab-on-a-chip system with a Cyclic-Olefin-Copolymer (COC) microfluidic chip. Using this system the entire process was detected in less than 2 h.

Along with the detection and identification of AIV, it is important to be able to subtype AIV and understand the pathogenicity (Chapter 7). To address this, a DNA microarray based solid-phase PCR has been developed for rapid detection of influenza virus types A and simultaneous identification of pathogenic virus subtypes H5 and H7. This solid-phase RT-PCR method combines reverse-transcription amplification of extracted RNA in the liquid-phase with sequence specific nested PCR on the solid phase. A simple UV cross-linking method was used to

immobilize the DNA probes over an unmodified glass surface, which makes solid-phase PCR a convenient possibility for AIV screening. The testing of 33 avian faecal and tracheal swab specimens was completed in less than 2 hours with 94% accuracy. This work was extended to a LOC device for fast AIV screening by integrating DNA microarray-based solid-phase PCR on a microfluidic chip. Furthermore, by incorporating the microarray into a microchamber-based PCR chip, sample and reagent consumption was greatly reduced. The whole process for identifying and simultaneously subtyping AIV was reduced to 1h and the sample volume used in the microfluidic chip was at least 10 times less than specified in the literature. Subtyping of all the 16 HA types is essential for the identification of circulating strains that could emerge as a pandemic influenza virus. This is addressed in the last part of the thesis where preliminary results on the development of primers and probes for detecting of AIV and simultaneous HA subtyping (H1-H16) are discussed.

Apart from the PCR based detection, two immunological based methods; fluorescent DNA barcode based and fluorescent bead based methods for detection of AIV were presented (Chapter 8). In both cases, the detection involves sandwiching of the target AIV between the monoclonal antibodies of nucleoproteins and matrix proteins. In the fluorescent DNA barcode-based immunoassay, fluorophore-tagged oligonucleotides are used as a detection signal whereas in the fluorescent bead-based immunoassay fluorescent beads were used as detection signals. The advantages of each method for rapid detection of are discussed.

Chapter 2

Avian Influenza

Influenza A viruses causes annual epidemics and occasional pandemics that have claimed the lives of millions. The three genera of Influenza viruses are classified by their antigenic differences as A, B and C. Among the three, Influenza A virus is known to be an infectious agent in birds (Avian) and some mammals.

AIV is a spherically shaped virus with an average diameter of 100nm (Figure 2.1). The surface of AIV comprises distinctive peaks with two major glycoprotein's: haemagglutinin (HA) and neuraminidase (NA) with a ratio of 4-5 to 1. Due to the antigenic drift of these two proteins, AIV is classified into 16 haemagglutinin subtypes (H1-H16) and 9 neuraminidase subtypes (N1-N9). The possible combinations of influenza A virus with both HA and NA form 144 sub-types and so far 103 have been found in wild birds [6;7]. The complete AIV genome is 13,588 nucleotides long and consists of 8 segments of single stranded, negative sense ribonucleic acid (RNA): haemagglutinin (HA) gene; neuraminidase (NA) gene; matrix (M) gene; nonstructural gene; nucleoprotein (NP) gene; and three polymerases: PA, PB1 and PB2 genes[6].

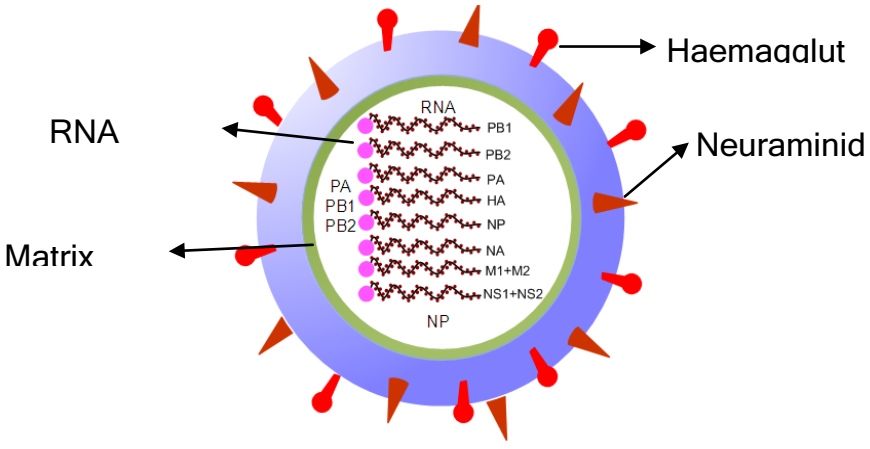

Figure 2.1 Structure of Avian Influenza Virus (reproduced from ref [8])

The 11-13 nucleotides at the 3' end and 5' end of genome are conserved and are complementary to each other [9]. Each segment is encapsulated in a separate nucleocapsid and is surrounded by an envelope. The AIV genome encodes 11 proteins which include the structural and non-structural proteins [9]. Virions (complete virus particle) are composed of 18-37% lipids by weight[10].

2.1 Terminology

Isolates of AIV are termed by their source of isolation, location, year, etc. For example, the strain H16N3 – A/Gull/Denmark/68110/02 is identified as:

A: stands for the species of influenza (A, B or C).

Gull: the species in which the virus was found

Denmark: the place where this specific virus was isolated

68110: an identification number to differentiate the isolation from other AIV isolated at the same place

02: represents the year 2002

H16: stands for the sixteenth of sixteen known types of haemagglutinin.

N3: stands for the third of nine known types of neuraminidase.

Other examples include: H7N7-2 A/Chicken/Netherland/2993/03 and H5N1 A/Chicken/Scotland/ 59 06.04/67.

2.2 Influenza virus replication

Replication of Influenza virus is divided into four phases: (1) virus attachment and penetration into the host cell; (2) transcription of the viral genome and translation of viral proteins; (3) replication of the viral RNA; and (4) assembly of the virions and subsequent release from the host cell [11](Figure 2.2).

(1) V*irus attachment and penetration*: The Influenza virus is attaching to the host cell by HA glycoprotein, which is considered as a primary protein responsible for binding to receptor sites and activating virus infectivity[12]. HA is synthesized as a precursor (HA0) and is subsequently cleaved by a host cell trypsin-like protease to HA1 and HA2 subunits[13]. The infection process is initiated by HA1 binding to receptor sites i.e. sialic acid (N-acetylneuraminic acid) and

penetration of the virus particle into the cell by HA2 membrane fusion [14]. Due to the acidic environment of the host cell the adsorbed virus is internalized as an endosome and the viral capsid is degraded.

(2)*Transcription and translation*: The eight segments of ribonucleoprotein (RNP) are transported into the host cell nucleus where messengerRNA (mRNA) synthesis and replication take place. As the segments enter the nucleus, the viral endonuclease cleaves the 5' end of the host capped, methylated mRNA about 13-15 bases from the 5' end. The cleaved part of the host mRNA is used as a primer by the virus to synthesize and to elongate leading to the formation of a complimentary plus strand of mRNA. These mRNA's undergo a translation process in the cytoplasm resulting in the formation of polypeptides which are subsequently cleaved to form viral proteins[9].

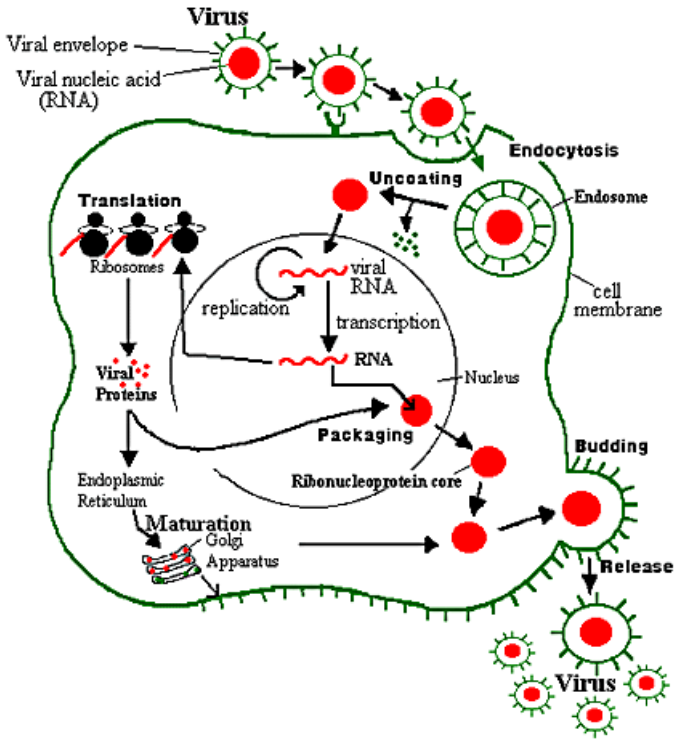

Figure 2.2 Replication of influenza A virus (from ref [15])

3) *Genome Replication*: During the replication of viral RNA genome, a different type of complementary RNA (cRNA) is produced which is a positive strand of anti-genome. This cRNA strand serves as a template for the production of negative strand viral genomic segments with the

help of polymerase protein (PA). The newly synthesized negative stranded RNA's are associated with NP and form ribonucleoprotein (RNP)[9].

(4) *Assembly and release*: The RNP's are transported into the host cell cytoplasm where other proteins are then assembled to form virons. On maturity the virus buds through the outer cell membrane and the NA protein cleaves terminal sialic acid from glycoproteins and the virus thus become free from the host cell[9].

2.3 Avian influenza pathogenicity

Based on the ability to cause disease and mortality by the influenza A virus in poultry, the AIV is classified into two pathotypes: highly pathogenic avian influenza (HPAI) and low pathogenic avian influenza (LPAI)[2;6]. The laboratory criteria to evaluate the pathogenicity consist of an intravenous pathogenicity index (IVPI) test where the AIV strain is inoculated intravenously into 6-week-old chicken. The IVPI is calculated based on the mortality of the birds, by following the protocols from the World Organization for Animal Health (Office International des Epizooties, OIE)[2]. The HPAI have an IVPI greater than 1.2 or alternatively cause at least 75% mortality within 10 days. The other criterion is the presence of multiple basic amino acids with minimum sequence motif R-X-R/K-R (R-Argenine, K-Lysine, X-variable amino acid) at the HA0 cleavage site found to be associated with HPAI viruses[16;17].

During the viral infection the precursor HA0 is cleaved post-translationally at a conserved Arginine residue by host-produced proteases into two subunits HA1 and HA2 before the protein is functional and virus particles are infectious. The cleavage occurs by trypsin-like proteases which are present in tissue of respiratory and gastrointestinal tract of the host. However, with multiple basic amino acids (R or K) present at the HA cleavage site, the HA0 precursor becomes cleavable by a wide range of proteases. This allows the virus to replicate also in other organs than respiratory and gastrointestinal tract resulting in high mortality and leading to HPAI virus [1;13]. So far, the HPAI viruses have been restricted to two subtypes; H5 and H7, although not all viruses of these subtypes are HPAI. Table 2.1 shows the list of H5 and H7 subtype AIV viruses which are identified as both HPAI and LPAI viruses based on the presence of multiple

amino acids[18]. The viruses of subtype H1 to H4, H6, and H8 to H16 are all LPAI. Some H5 and H7 subtypes which do not have IVPI greater than 1.2 and the absence of multiple R or K amino acids are considered as LPAI viruses (Table 2.1).

Table 2.1: Few examples of H5 & H7 AI amino acid sequences across the cleavage site (HA1/HA2)[18]. The multiple basic amino acids for HPAI are shown in red.

Virus	**Subtype**	**Motif (HA1/HA2)**	**Pathogenicity**
A/laughing gull/AK/296/75	H5N3	PSIGE----R/GLF	LPAI
A/chicken/Italy/RA9097/98	H5N9	PQKET----R/GLF	LPAI
A/duck/Ireland/113/83	H5N8	PQ**RKRKK**--R/GLF	HPAI
A/chicken/Scotland/59	H5N1	PQ**RKK**----R/GLF	HPAI
A/chicken/Italy/1487/97	H5N2	PQ**RRKKR**-R/GLF	HPAI
A/chicken/Thailand/04 (1, 2, 3)	H5N1	PQ**RERRRKK**R/GLF	HPAI
A/avian/Texas/04	H5N2	PQ**RKK**R/GLF	HPAI
A/ruddy turnstone/NJ/65/85	H7N3	PEKPK---TR/GLF	LPAI
A/duck/OH/10/88	H7N8	PESPK----TR/GLF	LPAI
A/duck/Victoria/76	H7N7	PEIPK----KRGLF	LPAI
A/finch/CA/28710-8/93	H7N8	PEIPK----ER/GLF	LPAI
A/poultry/Chile/2002	H7N3	PEKPKTR/GLF	LPAI
A/FPV/Brescia/02	H7N1	PS**KKR**---**KK**R/GLF	HPAI
A/turkey/England/63	H7N3	PETP**K**---**RRR**R/GLF	HPAI
A/chicken/Leipzig/79	H7N7	PEIP**K**---**KK**GR/GLF	HPAI
A/chicken/NL/2003	H7N7	PEIP**KRRR**R/GLF	HPAI

2.4 Influenza virus variation

During the viral replication cycle a high mutation rate of $\geq 7.3 \times 10^{-5}$ per nucleotide base per cycle of replication occurs, which corresponds to one nucleotide exchange per genome[19]. This error rate is due to the lack of proofreading by viral RNA polymerase in contrast to the DNA polymerase. The frequent mutations (substitutions, deletions, insertions) in the viral genes cause

changes to viral proteins resulting in antigenic drift. Some of these mutations occurring at the antigenic sites of the virus can reduce or inhibit the binding of neutralising antibodies. This either increases the virulence of the strain or generate of a new strain that rapidly spread within a non-specific immune population[20]. In poultry, it was shown that the LPAI virus which was circulating in the natural wild birds for several months underwent antigenic drift and became a HPAI virus[21].

Another major variation in viral proteins is called antigenic shift and is responsible for pandemics occurring at irregular intervals[22]. Antigenic shift occurs if the host cell is simultaneously infected by two or more strains of influenza A virus. A genetic exchange or re-assortment takes place among the viruses and forms a progeny virus with a new HA (with or without a new NA)[23]. It has been shown that pigs are susceptible to both human and avian type influenza virus, and they are therefore considered to be the viral mixing vessel for genetic re-assortment[24;25]. Another possibility of antigenic shift is the direct introduction of strain without re-assortment from animal reservoir to humans[22].

2.5 AIV transmission

The wild life species serve as a reservoir of all Influenza A viruses over a long period and have been the source of infection in domestic poultry and mammals (Figure 2.3)[3;26-28]. Most of the influenza viruses, except the HPAI, cause mild primary respiratory infection in birds[3]. The introduction of H5 or H7 subtypes of LPAI viruses may adapt in poultry and cause a mutation at the HA cleavage site leading to the formation of a HPAI type. Transmission of AIV to domestic poultry is introduced primarily through direct or indirect contact with infected birds, movement of infected poultry, contaminated equipments, vehicles, etc. Other sources of infection transmission can be infected bird droppings, saliva, nasal secretions, faeces, or blood [26;29].

It has been reported that AIV infective faeces may contain virus up to concentrations of 8.8 log10 EID_{50} (50% Egg infectious dose) per gram and the virus can remain active over 30 days at 0 °C with a five fold decrease in mean EID value [30]. The stability of the virus has also been

found to increase over the years. Transmission of AIV from wild birds to poultry depends upon the exposure interface where an adequate infectious dose for a given strain may be achieved[27].

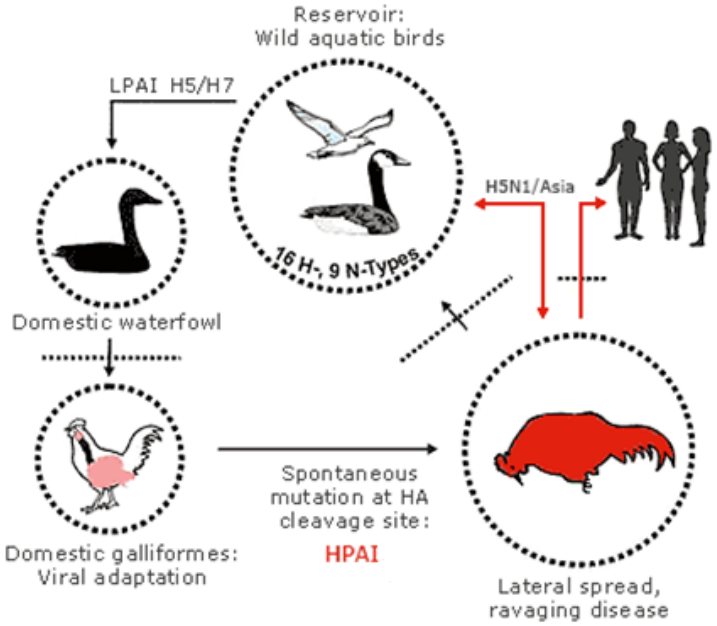

Figure 2.3 Scheme of avian influenza pathogenesis and epidemiology (dotted lines with arrows represent species barriers) (from ref[31]).

In general the transmission of avian influenza to humans is limited and its replication is not efficient[32]. This species barrier is due to the variation of receptors for influenza viruses in birds and other species. The HA protein of AIV binds to host (e.g. chicken) cell sialic acid (SA) linked to galactose by α-2,3 linkage (SA α-2,3) while in humans the binding site is α-2,6 linkage (SA α-2,6)[33]. Subtypes of the AIV such as H5 and H7 have acquired mutations in HA that can have affinity for both avian and human receptors and cause disease [1;34;35]. Human cases of AIV infection were acquired by close contact with infected birds, consumption of undercooked or raw poultry products and handling of sick or dead birds without proper protection[35;36]. In a few cases, there had been human to human transmission among family members[37] or health care workers[38].

2.6 Pandemic

Pandemic of AIV is the human infection caused by the appearance of a “new” influenza virus as a result of antigenic shift or antigenic drift[39]. The first known outbreak of HPAI occurred in

northern Italy in 1878 which caused extremely high mortality in chickens. The first confirmed outbreak of HPAI was reported in Scotland in 1959. Since then, more than 28 outbreaks have been recorded worldwide, of which half of them have occurred in the past 10 years[40]. The first known case of AIV H5N1 human infection was reported in Hong Kong in 1997. Since then the pandemic started to spread and affected birds in Eurasia and Africa and continued to pose a challenge to animal and human health[35]. So far a total number of 507 cases of human Avian Influenza A/(H5N1) infection with 59.56% death ratio (302/507) was reported by World Health Organisation (WHO) on 18th October 2010 [41]. Several outbreaks of AIV caused culling of tens of millions of birds and created a major economic loss in poultry industry around the world [3;40;42;43].

2.7 Surveillance and control of AI

The AIV has crossed the species barrier and become more virulent over time. To inspect these changes in the behaviour of the virus, an efficient surveillance is necessary. The current surveillance studies are addressed in 4 major lines of investigation: 1) early detection of HPAI viruses; 2) ecology and epidemiology of LPAI virus in host populations; 3) diversity and evolution of viral strains within wild birds; and 4) identification of the pathogens that infect individual birds or population, often as part of multipathogen surveillance[44]. Improving pandemic surveillance additionally requires more research in secure laboratory settings to investigate the viral reassortment, biological behaviour, and transmissibility[39].

The active surveillance for AIV in wild birds could act as an early warning system to identify areas of higher risk that can be controlled through vaccination. Surveillance can also provide the latest possible strains to determine the closest possible vaccine match. Although vaccines and antiviral drugs are key strategies to prevent severe illness and death from pandemic influenza, development of such vaccines and drugs have scientific barriers[45]: The diversities present in the HA and NA surface glycoproteins and its antigenic drift and antigenic shift pose a challenge in the development of such vaccine in advance of an outbreak[46]. At the same time, the strong host immunity created by the vaccine could be a driving force to antigenic drift in the AI [47].

Chapter 3

Diagnosis of AIV

Correct diagnosis of AIV provides information about the viral isolate and can reduce the spread of infection.

3.1 Specimens collection

The starting point of every diagnosis is collection of specimens and the successful detection depends on the sample type, the method to collect the sample, the quality of sample, and the handling conditions and time. Safety precautions must also be taken while collecting and handling the sample to avoid exposure to infectious agents. Therefore, care is taken from the time of specimen collection to the time of sample processing in the laboratory to provide valid results.

The AIV infects both respiratory and intestinal tract of poultry and waterfowl. Birds infected with AI shed viruses in their faeces and these can be a source of transmission to other birds. Due to high replication of virus; swab of oropharyngeal, cloacal and faecal droping are the choice of specimens for AI culture isolation, nucleic acid based assays, and antigen immunoassays respectively. Other specimens such as blood, biopsies of lung, spleen, intestinal tract are also included. The collected specimens are placed in 1-3 ml plastic tubes with sterile isotonic transport medium containing antibiotics such as penicillin (2,000 units/ ml), streptomycin (2 mg/ ml), gentamicin (50 mcg/ ml) and mycostatin (1,000 units/ ml) and protein (Bovine Serum Albumin (BSA). During transportation, the antibiotics in the medium eliminate the growth of microflora and the protein prevents the degradation of live virus. The specimens are cooled to 4^{o}C and immediately transported to the laboratory for diagnosis. The specimens are not allowed to be freezed in order to avoid freezing and thawing of the virus which has been shown to reduce the viral titre value [48]. In case of long transportation, the specimens are frozen and transported on dry ice. The transportation of specimens has to follow the OIE guidance[2].

3.2 Isolation of influenza virus

Virus isolation (VI) represents the gold standard and the official method for detection of AI viruses[2]. The method can be applied for all types of samples including clinical, laboratory, swabs, organs, faeces, and other organic and inorganic materials. The AIV are recovered from the specimens by one of the following methods a) classical culture of the AIV virus using specific pathogen free (SPF) egg; b) tissue culture based isolation. The classical culture method of AIV is viral propagation in embryonating SPF chicken eggs. The specimen with appropriate antibiotic medium is inoculated in the chorioallantoic sac (CAS) (Figure 3.1a) of 9-11 day-old fertilized egg and the infected eggs are incubated at 37°C for 4-7 days. After the incubation, the eggs are candled to test the survival of the embryos (Figure 3.1b). The allantoic fluid from the dead or dying embryos is harvested (about 10 ml) and used for further characterization of virus.

a) b)

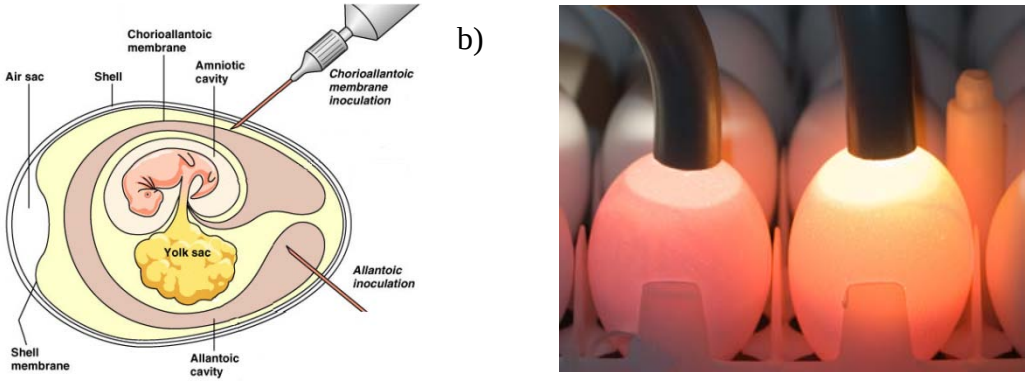

Figure 3.1 a) Scheme of virus inoculation in to chorioallantoic sac of a embryonated chicken egg[49] b) Light shown over eggs to test their survival[50].

For the tissue culture method, primary monkey kidney (PMK) or Madin-Darby canine kidney (MDCK) cells are widely used in the diagnostic laboratories for viral isolation. The cell lines support the growth of AIV (Figure 3.2). This method is simple and the cell lines are easy to maintain. In case of vaccine production for humans, the propagation of the virus on MDCK cells is preferred since these cells resemble the original human isolate more closely than virus propagation in eggs[51]. Although the cell culture method can be performed in 24 hours, a superior growth of the AIV is achieved in embryonated eggs and therefore the method has been the choice for veterinary diagnostic[52].

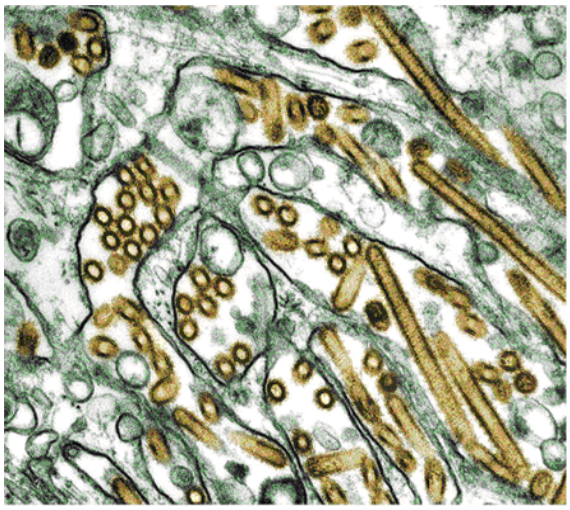

Figure 3.2 A colorized transmission electron micrograph of Avian influenza A H5N1 viruses (seen in gold) grown in MDCK cells (seen in green)[53].

Virus isolation method is labour intensive and time consuming due to the handling of individual sample. Moreover, the method requires viable virus to be present in the sample. In some cases, the viral viability may be adversely affected by the sample collection, storage and transportation conditions which may lead to false-negative results[54]. Finally, virus isolation needs a higher level of biosafety level (BSL-3) laboratory facilities and special equipments.

3.3 Haemagglutination assay

Haemagglutination assay is commonly used to detect the propagation or presence of influenza virus in cell culture or SPF eggs by haemagglutinating activity. Haemagglutinin (HA) is one of the surface glycoprotein present on the envelope of Influenza virus particles. The HA binds to the erythrocytes through sialic acid receptors present on the cells surface forming a lattice. As the virus and erythrocytes contain multiple binding sites for each other, agglutination can be visualised and distinguished from other non agglutinated erythrocytes. The HA test is performed according to OIE standard method [55]. Initially, 25µl of PBS buffer is filled in every well of a microtitre 96-well V-bottomed plate. Then, 25µl of a virus sample is added in each well in the first row of the plate and a two fold dilution is made across each row for the entire plate. Finally,

25µl of 0.5% chicken red blood cells (RBC) is added to all the wells and the plate is incubated at room temperature for 30min. Results are read by tilting the plate 45 degrees and HA activity is determined by the formation of tear shaped streaming of RBC(Figure 3.3). The HA titre value is calculated as the highest dilution in which complete agglutination (no streaming) is observed and is represented as a HA units (HAU)[2]. The HA titre value can be used to describe the virus concentration[56;57]. The HA assay is relatively insensitive and requires a higher amount of virus (approx 10^7 particles) for one HAU[58].

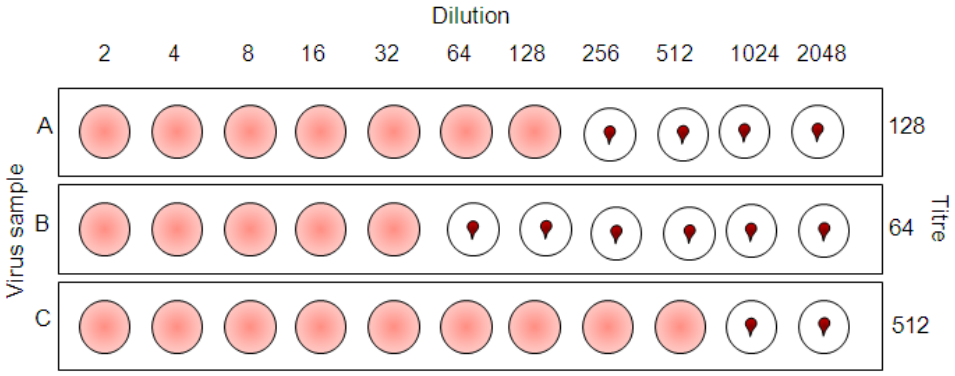

Figure 3.3 Haemagglutination assay(reproduced from ref[59])

3.4 Haemagglutination inhibition

The HA subtype of the virus isolate is characterized by Haemagglutination inhibition (HI) assay. The HI test is also used to detect the specificity of antibodies of the HA subtypes which are produced in response to AIV infection. In the HI test, the antibodies bind to the virus/antigen and inhibit the formation of the agglutination with RBC's (Figure 3.4)[60]. The HI titre is the reciprocal of the highest dilution of serum that inhibits the Haemagglutination completely. The HI assay is relatively easy and inexpensive to perform but the assay has low sensitivity. Since the HI titre depends on the virus antigen that can be highly variable within a subtype, the interpretation of the results is a challenge [61].

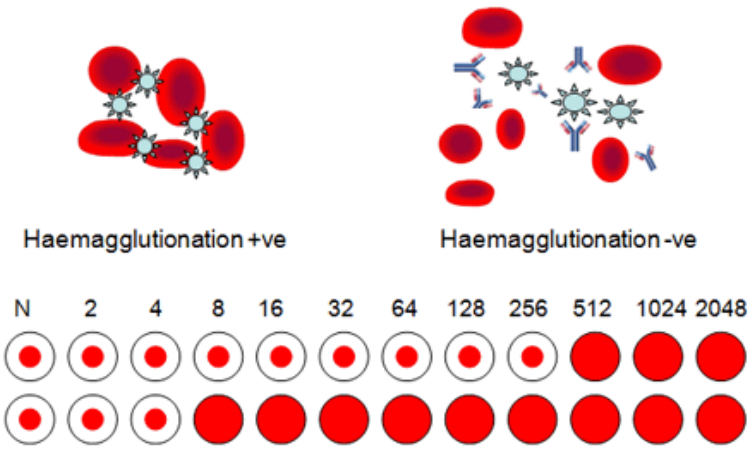

Figure 3.4 Haemagglutination inhibition assay[62]. A haemagglutination +ve reaction is formed when the blood cells and AIV bind to each forming a lattice. In the presence of antibodies specific to AIV subtype, the agglutination effect is inhibition (-ve reaction).

3.5 Neuraminidase inhibition assay

Like the HI assay, neuraminidase inhibition (NI) assay is performed to characterize the neuraminidase subtype of virus. Neuraminidase (NA) is a glycoprotein present on the surface of AIV that cleaves terminal sialic acid and releases AIV from the host cells. The viral neuraminidase activity is inhibited by antisera that are prepared against a NA antigen from reference strains [63]. In this method a fetuin substrate is added to the virus-antisera mixture and the released N-acetyl neuraminic acid (NANA) is determined by colorimetric assay of thiobarbituric acid (Figure 3.5). NI assay is cumbersome and requires large volume of multiple hazardous chemicals. The method is not suitable for large numbers of samples.

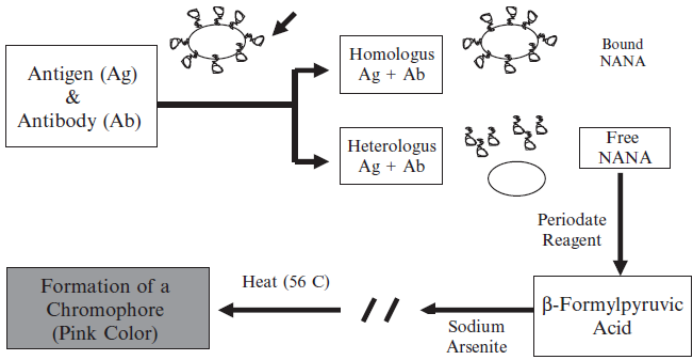

Figure 3.5 Neuraminidase inhibition [64]. The inhibition of viral enzymatic acitivity by specific antibodies forms the basis of the neuraminidase inhibition assay. Interaction of free N-acetyl

neuraminic acid (NANA) with formylpyruvic acid and sodium arsenite for the formation of a pink chromophore.

3.6 Agar gel immunodiffusion

Agar gel immunodiffusion (AGID) is a serology test. The test is used to detect antibodies that are produced in response to an AIV infection. Unlike the HI assay, the AGID detects the antibodies against the AIV internal proteins; the NP and the matrix 1 (M1) protein. These proteins are antigenically similar in all AIV. The antigens (Virus) may be prepared by concentrating the virus from an AIV infective allantoic fluid or extracting the infected chorioallantoic membranes. These antigens are tested against known positive antisera [2].

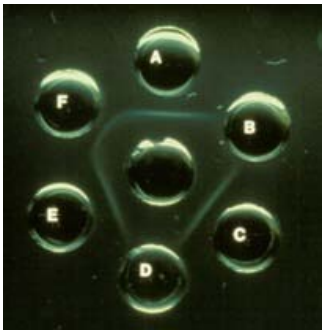

Figure 3.6 Agar gel immunodiffusion. Wells B and D are AGID negative reactions and all other wells are AGID positive reactions[65].

AGID is based on the formation of Immuno-precipitation. When an antibody and an antigen are placed proximity in agar wells; they diffuse and react with each other to form a visible white aggregate (Figure 3.6). A 1% agarose in 0.1M PBS buffer slide or plate is prepared and cylindrical wells with approximately 5mm in diameter and 2-5 mm apart are made in the agar. Fifty µl of sample, control and reference antibody are added to the cylindrical wells and the plate is incubated for 12 to 48h. After incubation, the formation of precipitin lines confirms the presence of the antibodies. AGID is a simple and inexpensive assay to perform but it is time consuming to detect some weak positive reactions. In addition, the amount of antibodies produced in immune response to AIV varies between species and this limits the sensitivity of the assay. Furthermore, the result of the assay only confirms the presence or absence of AIV rather than the subtype of the infected virus. The assay is therefore of less importance as a tool for AIV screening since several wild birds are known to be the natural reservoir of AIV[66].

3.7 Enzyme-Linked Immunosorbent Assay

Enzyme-linked Immunosorbent Assay or ELISA is another serology test to detect antibodies, against AIV using colorimetric detection. In an antigen-capture ELISA, purified matrix or nucleoprotein antigens are attached to a 96-well microtitre flat-bottomed plate and the sample containing the antibody is applied over the surface so that it can bind to the antigen. A second enzyme linked antibody (the “detection” antibody) is added to the well to form a sandwich structure. Unbound products in each addition step are removed with a washing step. The assay is then quantified by measuring the amount of labelled antibody bound to the matrix, through the use of a colorimetric substrate (Figure 3.7).

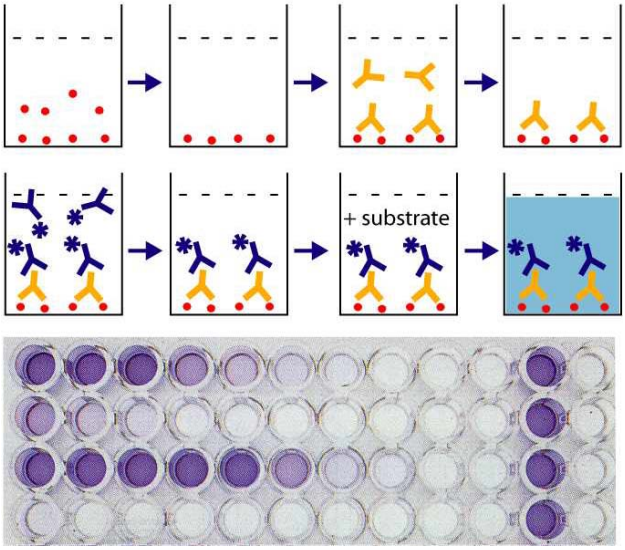

Figure 3.7 Enzyme-linked Immunosorbent Assay[67]

Antigen-capture ELISA is a fast, specific and inexpensive method that can be applied for large number of samples in routine diagnosis. Commercial ELISA kits are also available for the detection of influenza virus. The test of these kits are quick (within 15 minutes) but are usually less sensitive and are often for specific species [68;69]. An alternative to specific species antigen-capture ELISA is the competitive ELISA which can be applied in case to detect diverse species such as chicken, ducks, swan, etc. [70;71].

3.8 AIV Inactivation

Inactivation of AIV, especially HPAI viruses, is required to avoid the potential health hazard. The inactivated viruses are often used as materials in a development of methods for diagnosing AIV. As the AIV is a low thermal stable virus [72], the inactivation can be performed at temperatures above 50 °C [73]. Chemicals such as beta propiolactone or formaldehyde are commonly used for inactivation of the AIV. A combined effect of heat and high hydrostatic pressure have also been reported to inactivate the AIV[74]. After the inactivation, the sample is often tested for infectious activity by inoculating in to SPF egg. The allantoic fluid from infected egg is harvested and tested for any AIV growth using HA assay and the AIV virus is considered inactive by a negative HA assay. Inactivation of virus is a critical requirement in the production of vaccine.

3.9 Virus Quantification

Quantification of viral particles in a sample is critical for investigations of their ecological role and the viral infection. The ability of virus to spread must, to some extent relate to the amount of virus released by the respiratory or intestinal route. The viral quantification can be classified in to two types: physical and biological assays[75]. The physical assays can only quantify the presence or absence of virus but not the nature of infection; such methods are Haemagglutination tests, electron microscopic particle counts, optical density measurements or immunological methods[75]. The biological assays can quantify the viral infectious particles such methods are plaque assay, cell culture or in vivo (SPF eggs) virus cultivation.

3.9.1 Plaque Assay

The plaque assay is a standard method for determining and representing the quantification of the AIV in terms of infectious dose. The assay is based on the ability of a single infectious virus particle to produce a macroscopic area of cytopathology on a cultured cell monolayer called a *plaque*. Figure 3.8 shows the plaque assay used to quantify the virus from a sample. The sample

with unknown viral concentration is serially diluted in an appropriate medium and a known dilution volume is seeded onto confluent monolayer cell culture.

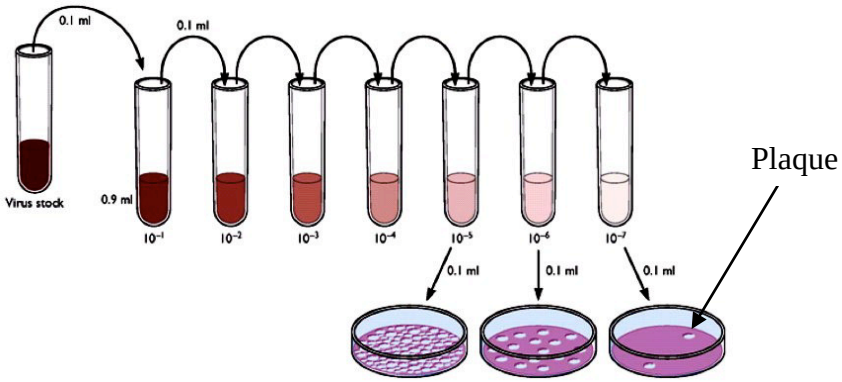

Figure 3.8 Plaque assay method (reproduced from [76])

The infected cells are covered with a mixture of semisolid nutrient of the growth medium and agar and the plate is incubated at 37^{o}C for several h. The semisolid medium prevents the secondary plaque formation through indiscriminated spreading of infection. In order to visualize the plaques formed, the monolayer cell culture is stained with dyes such as neutral red and subsequently enumerated (Figure 3.8). The concentration of virus is calculated from the dilution factor using the formula:

$$\frac{\text{No. of plaques}}{d \times V} = \text{pfu/ ml}$$

d= dilution factor

V = volume of diluted virus added to the well

The resulting plaque forming unit (pfu) per milliliter is the number of the infectious particles present in the sample. The plaque assay measures only the infectious particles and this can be a fraction of particles such as 1 in 10 to 1 in 10,000 from a given sample. This difference of infectious particle in sample could be due to a) damage of the virus particles while purification, b) presence of empty or defective particles or c) the virus requires a specific metabolic state of cell for infection. Errors are also inherent while performing a serial dilution of the sample[77].

3.9.2 Infectious dosage determination

This method can be performed using a cell culture (50% tissue culture infective dosage, $TCID_{50}$) or an embryonated chicken egg (50% egg infective dosage, EID_{50}). In both cases the sample

containing virus is serially diluted. Each dilution with multiple replicates is inoculated in to the cell culture or the egg at 37^{o}C and incubated for 3 or 4 days. The results of the tests are calculated based on the observation of the cytopathic effect in the cultured cells or the death of the embryonic in the viral inoculated eggs. An index is calculated from the observation of percentage for positive and negative infection above 50% of dead embryo's using Reed-Muench formula[78]:

$$\text{Index} = \frac{(\%\text{ of positive infection above 50\%}) - 50\%}{(\%\text{ of positive infection above 50\%}) - (\%\text{ of positive infection below 50\%})}$$

This index number is applied to the dilution of virus that produced positive infection immediately above 50 percent. For e.g., if the 10^{-6} dilution cause positive infection immediately above 50 percent, the index number say 0.7 is applied to this dilution and expressed as $10^{6.7}$EID50/ ml or TCID/ ml.

Several research groups working with virus use different quantification method to express the amount of viruses used in their studies. Although a one-to-one correlation between the various quantitative assays is not possible, the difference in magnitude of detection between the assays is as below[77].

Method	**Amount (per milliliter)**
Egg infectious dosage method	10^{9} EID_{50}
Plaque formation method	10^{8} PFU
Haemagglutination assay	10^{3} HA units

Chapter 4

Molecular Diagnostics

Classical methods for detection and identification of AIV samples are time consuming (4-10 days), laborious, expensive, and require special laboratory facilities and trained staff. Over the last decade, the use of molecular methods based on nucleic acid amplification for genetic identification have improved the sensitivity and speed for diagnosis of AIV [79].

4.1 RT-PCR

Polymerase chain reaction (PCR) is a powerful molecular technique, which is widely used to amplify a single or few copies of DNA to several-million-fold or more copies (Figure 4.1). To utilize the technique for AIV detection, a copy of DNA, complimentary (cDNA) to viral RNA is synthesised using a reverse transcriptase (RT) enzyme and random hexanucleotides or a sequence specific primer. The sequence of interest located within the cDNA is amplified using a heat stable polymerase enzyme from the bacterium Thermus aquaticus (TAQ) and primers. The sequence is selected by these primers which binds to the target region and serves as a starting point (3'-end of the primer) for DNA synthesis.

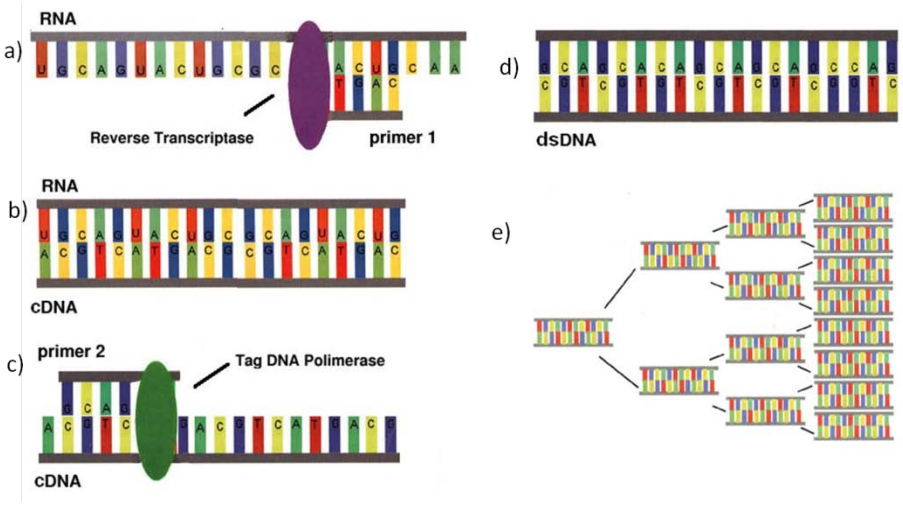

Figure 4.1. Reverse transcriptase polymerase chain reaction (from ref [80]). a)The first strand of cDNA is synthesized using RT enzyme, which adds complementary nucleotide bases to the RNA strand at the primer annealing site creating a strand of cDNA (b). In the PCR reaction (c), Taq polymerase adds complementary nucleotides beginning at the primer annealing site and a double stranded cDNA is produced (d). The three step process of denaturation, primer annealing and extension are repeated for 30-40 cycles (e) to yield over billion copies of double stranded DNA molecules identical to the initial template RNA fragment.

The RT step can be performed either as a separate reaction (two-step PCR) [81] or along with PCR reaction in one tube (one-step PCR) using a temperature between 45 °C and 60 °C depending on the properties of the reverse transcriptase. The amplification of a DNA sequence typically involves 30-40 PCR cycles and each cycle requires three steps: denaturing, annealing and extension. In the first denaturing step, the double stranded DNA (dsDNA) is melted at approximately 94ºC to form single strands DNA (ssDNA). In the annealing step the specific primers binds (anneal) to the single strands of the target DNA. The annealing temperature is normally between 50 ºC to 65 ºC depending on the length and on the guanine/cytosine (GC) content of the selected primers. Finally, the extension step where the TAQ polymerase adds deoxynucleotide triphosphate bases (dNTP's) to the primer on the 3' side takes place. The extension occur around 72ºC at 50-100 nucleotides per sec.

Depending on the aim of the study to detect, different genes of AIV are selected as the target for RT-PCR to detect AIV. The presence of AIV can be confirmed by targeting highly conversed genes in all influenza A viruses such as matrix (M) [82] or nucleoprotein (NP) [83;84]. Fouchier et al., [82] first designed a set of primers, M52C and M253R, of matrix gene and used for diagnosis purpose. The PCR end point analysis was performed by gel electrophoresis. The method was used for clinical diagnostic and was found to be about 100-folds more sensitive than the classical virus isolation method. This increased sensitivity of 100-fold is likely due to the detection of RNA from incompletely packaged virus particles or viral RNA from infected cells[85].

4.2 Real time RT-PCR

Conventional end-point RT-PCR has several disadvantages such as time consuming, non-automated method with risk of cross-contamination. In order to overcome these disadvantages, a real-time RT-PCR (rRT-PCR) approach was introduced to detect AIV. The rRT-PCR eliminates the post-amplification steps increasing the reliability and reproducibility of the assay. In rRT-PCR the amplified DNA is detected by monitoring the fluorescence emitted as the reaction progresses in real time. The two common methods used for detecting PCR product are a) non-specific intercalating dye (e.g. SYBR green) which becomes fluorescent when binding to double stranded DNA and b) sequence specific approach using TaqMan probes. The TaqMan probes are oligonucleotides longer than the primers and are designed to anneal to an internal region of a PCR product to increase the specificity of real-time PCR assays. TaqMan probes contain a report dye on the 5' base and a quenching dye on the 3' base.

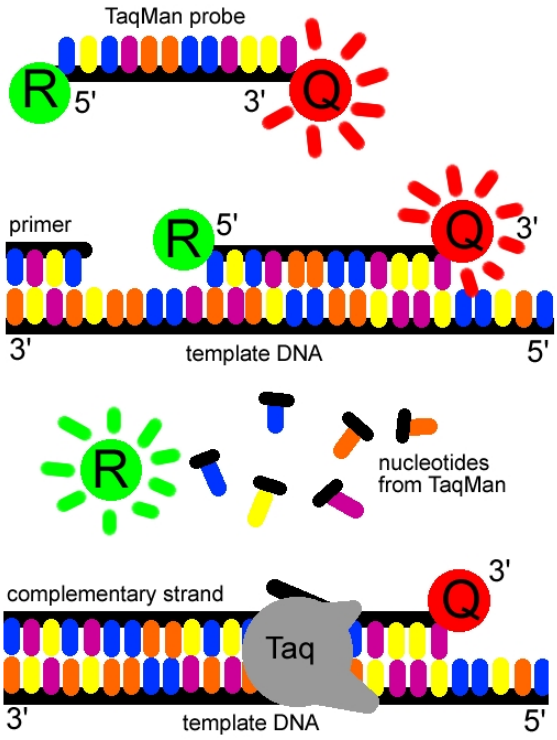

Figure 4.2 Real time RT-PCR with TaqMan probe (from ref[86])

While the probe is intact, the close proximity of the reporter and quencher prevents the emission of fluorophore via fluorescence resonance energy transfer (FRET). During the primer extension

step, the 5' exonuclease activity of Taq polymerase cleaves the 5’ end of probe which contains the reporter dye. This separates the reporter from the quencher and the reporter starts to emit fluorescence. The flurescence intensity increases in each cycle and is proportional to the amount of amplified DNA (Figure 4.2). The rRT-PCR assay is characterized by a wide dynamic range of quantification of 7 to 8 logarithmic decades, a high technical sensitivity (< 5 copies) and a high precision (< 2% standard deviation)[87;88]. A single-step RT-PCR method also greatly reduces the risk of cross contamination since it is a closed system once the template is added.

The application of real-time RT-PCR detection for identifying the AIV based on TaqMan probe chemistry was first described by Spackman et al.,(2002) [89]. The limit of detection in the assay is 1000 copies of target RNA, which is equivalent to 0.1 EID_{50} of virus. The matrix gene rRT-PCR was evaluated as highly sensitive, specific for AIV and selected as a method for surveillance by Avian influenza reference laboratories [90].

4.3 Subtyping AIV by RT-PCR

The molecular basis for subtyping of AIV is the antigenic differences of HA and NA. The amino acid sequence between H1 and H12 subtypes varies from 20% to 74% compared to 0-9% variation among the same subtypes [91]. As the amino acid sequences are determined by the nucleotide sequences, the presence of wobble in the codon usage (for e.g., Arginine can be CGU, CGC, CGA, CGG, AGA or AGG) will increase the difference in nucleotide sequences between HA subtypes to more than 20–74% [83]. Using conventional RT-PCR, Lee et al.,(2001)[83] designed the first subtype specific primers that were able to differentiate fifteen subtypes (H1–H15) of the AIV viruses. It has been showed that this method had a 100% correlation with the results of serological methods. The major advantage of this method is the reduction of testing time from one week (HI typing) to one day. Additionally, the PCR product could be used for sequence comparison and phylogenetic analysis which provide important information on the origin of the studied strain.

Among the sixteen HA subtypes of the AIV (H1-H16), H5 and H7 are the two known subtypes which are responsible for high pathogenicity. So the identification of these subtypes in the sample has been prioritised in AIV diagnosis. The detection and differentiation of H5 and H7 have been developed using both conventional RT-PCR (Starick et al.,(2000)[81], Munch et al.,

(2001))[84] and real-time RT-PCR (Spackman et al.,(2002) [92]. The developed rRT-PCR has been used for the quantification and competitive replication studies of AIV H5 and H7 subtypes [93]. The quantitative rRT-PCR demonstrated high correlation between the amount of viral RNA determined by quantitative rRT-PCR and the virus titre determined by virus isolation method using SPF eggs. The use of rRT-PCR for AIV quantification greatly reduces the risky handling of infectious materials. However, the rRT-PCR can only quantify the presence or absence but not the viability of the virus.

4.3.1 Primer/probe adaptation

The phylogenetic analysis of HPAI viruses of H5 and H7 subtype showed two geographically distinct lineages of North American and Eurasian viruses[94;95]. The primers and probe sequences designed by Spackman et al., (2002) were optimally designed to detect North American H5 and H7 and failed to detect some of Eurasian H5 and H7 subtypes[90]. So modifications have been made to originally design, validate and shown to sensitively detect all H5 Eurasian lineages[96]. Adaption of primers and probe are also needed if some new AIV's emerge with genetic variation that could affect the primer and/or probe binding sequences[97]. Such a case has been observed with H7 American lineage, when the 2002 H7 test does not have adequate specificity [98]. So a new test, the 2008 Pan-American H7 test, was developed by using recently available H7 nucleotide sequences. These data highlight the importance of continued monitoring of rRT-PCR primers and probes to ensure that sensitivity and specificity are maintained. It is important to employ validated and updated methods from the OIE (world organisation for animal health) reference laboratories in the diagnosis of a HPAI outbreaks[97].

4.4 Multiplex-RT-PCR

Multiplexing RT-PCR consists of simultaneous amplifications of more than one target using multiple primer sets in a single reaction. The produced RT-PCR amplicons vary in sizes that are specific to different DNA sequences. The advantages of the multiplex RT-PCR are rapid, sensitive, specific, and cost effective detection. Several multiplex RT-PCRs have been developed in the past decade. A two step reaction of a multiplex conventional RT-PCR for identification of influenza AIV and simultaneous subtyping of H1N1 and H3N2 subtypes were developed

(Stockton et al.,1998) [99] and further utilized for a one step detection of H1N1, H3N2 and H5N1 subtypes (Poddar et al. 2002) [100]. Other multiplex conventional RT-PCR for subtyping of H5, H7 and H9 subtypes have been reported[101;102].

The multiplex rRT-PCR assay using TaqMan probes labelled with two or three different reporter dyes for the simultaneous detection of combination of H5-H7[103], Matrix-H5-H9 [104] and Matrix-H5-N1 [105;106] genes have been developed. Recently, Hoffmann et al., (2008) developed a new rRT-PCR for rapid detection of H5 specific subtype and also for pathotyping of HPAI H5N1 of the Qinghai lineage[107]. In that study, a set of primers and two probes were designed for the amplification and detection of a fragment spanning the cleavage site HA0 sequence of the HA gene of H5 subtype. One probe was designed to target a sequence reasonably conserved among various H5 strains and the second probe was specific for the cleavage site sequence of H5N1 isolates of the Qinghai lineage. This assay offers an alternative method to conventional sequencing for identifying HPAI H5 virus.

Overall the methods based on rRT-PCR multiplexing offer rapidity and accuracy and are therefore attractive for large-scale screening of suspected cases of influenza A virus subtype of H5, H7 or H9 in order to control potential outbreaks. However, the use of two or three fluorophore dyes increases the complexity in the detection system and it become more expensive[108].

4.5 DNA Microarray

The molecular detection of AIV by RT-PCR always needs an extra step to confirm the desired target, which has been amplified, by methods such as gel electrophoresis, fluorogenic PCR or DNA sequencing. However, such methods are difficult to use for multiplex purposes [109]. Another approach for identification of PCR amplicon in multiplex assays is the use of DNA microarray. It consists of a solid support onto which arrays of spots from hundred to many thousands of oligonucleotides or capture-probes are fixed in an area of 1–2-cm^2[110]. These spots contain multiple copies of capture-probes (CP) and the spots can range in size from 10 to 500 microns. The CP can bind specifically to the target and the binding is detected using a

reporter molecule (e.g. fluorescent dye) of the target DNA sequence (Figure 4.3). The successful implementation of microarray technologies has required the development of many methods and techniques for fabricating the microarrays and spotting the CP, target preparation, hybridization reactions, and data analysis [110]. The DNA microarray enhances the assay capabilities by detecting multiple targets in parallel, and being more sensitive and specific.

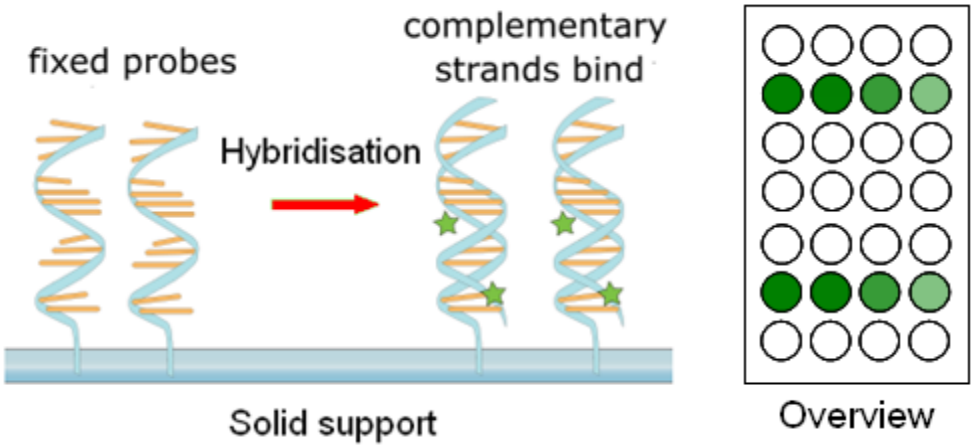

Figure 4.3 DNA microarray (reproduced from ref[111])

The first study on microarray for AIV detection was reported by Wang et al.,(2008) [112]. In that method the detection of H5 and H7 of AIV and NewCastle Disease virus (NDV) was made using PCR products of a multiplex RT-PCR. Using this method, the viruses were both detected and type classified. No cross-reactions were found and the sensitivity of the oligonucleotide microarray was ten to 100 times higher than the PCR end-point analysis by agarose gel electrophoresis. The hybridization signals on the microarrays were determined by colorimetry and identified using the naked eyes without any additional imaging equipment. Using DNA microarrays, Han et al., [113] reported simultaneous subtyping of all influenza A viruses i.e., sixteen serotypes of HA (H1–16) and nine (N1–9) of NA that have been identified in mammalian and avian species. In that study, an asymmetric multiplex PCR with 25 sets of primers was carried out in four separate reactions (50 µl each) and the amplified target cDNA's (fluorophore labelled) were hybridized over the immobilized capture-probes. By this approach, all subtypes were identified with high sensitivity (2.47 PFU/ ml) and the results were consistent with that of the virus isolation method. However, the hybridization procedure used in that method involved several steps and it was time consuming (3h)[114]. Moreover, considering the variability

between and within different HA and NA gene subtypes among the lineages, the designed capture-probe and oligonucleotide needs further optimization.

Recently, an electronic DNA microarray system (NanoChip 400 system (Nanogen Inc.)) San Diego, USA) has been used for fast detection of AIV as well as HA subtyping, and pathotyping [115]. In the assay, one-step amplification of HA0 cleavage site of all the 16 HA subtypes and matrix gene-specific of AIV were performed. The developed microarray comprised of 97 CP designed for HA subtyping. These CP targeting the HA0 cleavage site are conserved within a given subtype and have variation between subtypes. These CP can also distinguish between HPAI and LPAI viruses. One CP was designed to target the M-gene to identify AIV. The method was extensively validated with a high specificity and a high sensitivity (of 10^1 to 10^2 copies). This low-density microarray can be an approach to the problem of AIV classification and could be used as a diagnostic tool for the detection and typing of AIV. However, the method uses expensive equipment and it involves long processing steps. So far there had been no rapid, and inexpensive assay reported for subtyping using microarray.

4.6 Sample preparation

Nucleic acid amplification methods based on RT-PCR need a preparation of AI viral RNA from clinical samples suitable for detection. The different types of samples used for AIV diagnostics is mentioned earlier (Section 3.1) which includes swab, either oropharyngeal or cloacal, and faecal dropping. Among them, faeces are more accessible and often the only specimens available for routine surveillance work[116]. The faecal sample contain complex mixtures of host cells, microflora, bile salts, complex polysaccharides and other materials that have been show to be PCR inhibitors[117;118]. The presence of these inhibitors that either inactivates the Taq polymerase or degrades the nucleic acid in the sample limits the detection and the efficiency of the test [119;120]. Sample preparation is therefore an important step which is always required for removing inhibitors and to obtain reliable diagnosing results. Other important objectives of sample preparation are to reduce the sample volume, to concentrate the total RNA into a workable volume and to homogenize sample for a reproducible and repeatable test[118].

The extraction of RNA from samples is more difficult than that of DNA, as RNA is considerably less stable than DNA. Samples such as tracheal/oropharyngeal swabs contain low cellularity and RNA can easily be extracted. In contrast, cloacal swabs, tissue and faecal samples contain higher level of organic materials, cells, bacteria and tissues containing ribonuclease (RNase) enzymes that can rapidly degrade RNA into smaller components [121;122].

The most widely used method for extraction of RNA from AIV is based on a silica column extraction kits that are commercially available as shown in Figure 4.4. The advantages of column based extraction are removal of PCR inhibitors and a homogenous RNA with high quality. The drawback of the method however, is laborious and has a limited throughput capacity and batch-to-batch variation may exist in quality and quantity of the template[118].

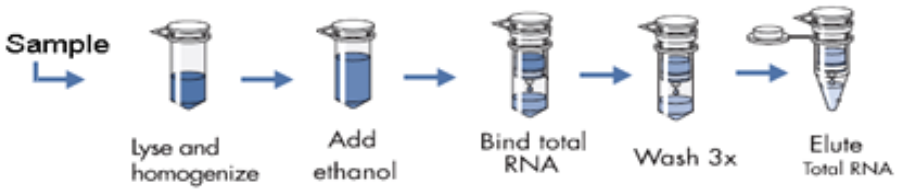

Figure 4.4 Scheme representing RNA extraction using RNeasy Kit, Qiagen [123]

A magnetic bead based RNA extraction has been introduced with automated platforms for pathogen detection[124;125]. Magnetic carriers prepared from a biopolymer exhibiting affinity to the target nucleic acid are used for the extraction process as shown in Figure 4.5. The magnetic bead based extraction method is a simple and efficient way to separate the RNA from PCR inhibitors. It also takes less time compared to column based extraction method due to the fewer manipulation steps and no centrifugation. Magnetic beads can be used for larger volume of sample up to 10 ml (with working volume upto 50 ml) and the purified RNA can be down scaled to 5 to 50µl.

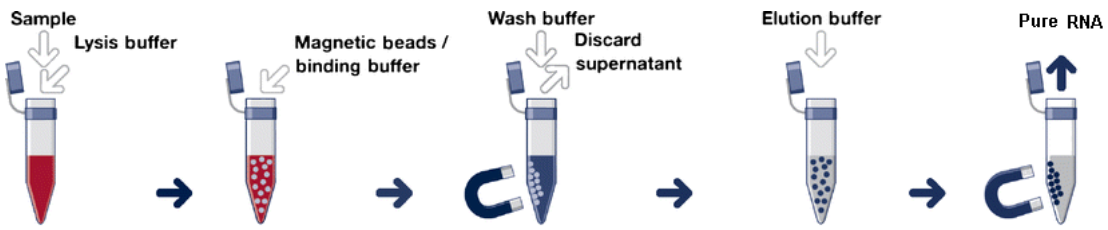

Figure 4.5 Magnetic bead based extraction method (reproduced from ref[126])

Tewari et al., (2007) used silica-based magnetic beads with robotics for extraction of RNA from AIV and obtained a sensitivity and specificity comparable to virus isolation and manual silica column extractions[127]. The main advantages of the automated robotic viral nucleic acid extraction are high throughput processing; hands-free operation; and reduction in human and technical errors. However, the robotic system is expensive and for laboratories with limited resources and/or lower sample volumes, the column extraction kits are required. The robotic method was only demonstrated for easily extractable sample such as tracheal swabs and allantoic fluid (virus isolation) and not for faecal sample.

Chapter 5

Point-of-care diagnosis

In both classical and molecular diagnosis, transportation of sample to the nearest reference or diagnostic laboratory is needed, and this will increases the time for diagnostic result. The continuing spread of Asian avian influenza H5N1 since 2003 highlights the need for a point-of-care (POC) diagnosis. The POC is defined as a diagnostic testing at or near the site of patient, and the test results will be available instantly or in a very short time that can improve medical decision-making[128]. A list of commercially available POC tests for influenza virus is shown in Table 5.1[129]. These tests are largely immunoassays which detect influenza viral antigen and are used for screening of influenza A and B virus infections within 5-30minutes. The accuracy of these POC test is determined by the sensitivity and specificity which is percentage of "true influenza cases" and "true non-influenza cases" detected as positive and being negative by a test respectively. In general, the sensitivity of POC tests is variable (29 -100 %) and in some cases the sensitivity is lower than that of the cell culture, while their specificity is a little higher (80%). A major concern for using these tests is the possibility of false negative results due to the low sensitivity of the tests [68;69]. Miniaturization of the molecular diagnostics using Lab-on-a-chip'(LOC) systems could provide the next-generation point-of-care diagnosis with a high sensitivity and specificity [128;130;131].

Table 5.1 A list of commercially available point-of-care test for influenza virus[129]

Test Name*	**Manufacturer**	**Influenza Type**	**Differentiate Between A and B?**	**Storage Requirement; Storage Life**	**Acceptable Specimens**	**Assay Time**	**General Ease of Use**	**Sensitivity**	**Specificity**
Binax NOW Flu A and Flu B	Binax Inc., Portland, ME. www.binax.com	A and B	Yes	15-30 º C, 1 year	Nasal wash, nasal aspirates, nasopharyngeal swabs	15 min	Easy	A: 52-82% B: 54-100%	A:92-94% B: 58-71%
Binax Now Influenza A & B	Binax Inc., Portland, ME.	A and B	Yes	15-30 º C, 1 year	Nasal wash, nasal aspirates, nasopharyngeal swabs	15 min	Easy	A: 100% B:92-100%	A: 92-93% B:94-99%

Directigen Flu A	Becton Dickinson, Franklin Lakes, NJ. www.bd.com	A	Detects A only	15-30 dgrs C, twelve months	Naso-pharyngeal wash, nasopharyngeal aspirate, nasopharyngeal swab, pharyngeal swab	15 min	Moderate	67- 100%	88-100%
Directigen Flu A+B	Becton Dickinson, Franklin Lakes, NJ. www.bd.com	A and B	Yes	2-25 º C, twelve months	Naso-pharyngeal wash, nasopharyngeal aspirate, nasopharyngeal swab, lower nasal swab, throat swab, bronchoaveolar lavage	15 min	Moderate	A: 55-100% B: 29-88%	A: 99.6% B:93100%
Flu OIA	Biostar, Inc., Boulder, CO www.biostar.com	A and B	No	2-8 º C, 1 year	Throat swabs, nasopharyngeal swabs, nasal aspirates, sputum	20 min	Moderate	46-100%	52-97%
QuickVue Influenza Test	Quidel, San Diego,CA. www.quidel.com	A and B	No	15-30 º C, 2 years	Nasal swab, nasal wash, nasal aspirate	10 min	Easy	AB:55-91%	AB:83-99%
QuickVue Influenza A+B	Quidel, San Diego, CA. www.quidel.com	A and B	Yes	15-30 º C, 2 years	Nasal swab, nasal wash, nasal aspirate	10 min	Easy	A:72-77%. B: 73-82%	A: 96-99%. B: 96-99%.
Influ AB Quick	,Denka Seiken Co., Ltd Japan www.denkaseiken.co.jp	A and B	Yes	2-30 º C, 10 months	Nasal swab, nasal aspirate	15 min	Easy	A:55-93%. B: 63-93%	A: 98-99%. B: 98-99%.
Quick S-Influ A/B "Seiken"	,Denka Seiken Co., Ltd Japan www.denkaseiken.co.jp	A and B	Yes	2-30 º C, 10 months	Nasal swab, nasal aspirate	25 min	Easy	A: 81-93%. B: 88-93%.	A: 96-99%. B: 98-99%..
Xpect Flu A & B	Remel Inc., Lenexa, KS, USA www.remelinc.com	A and B	Yes	2-25 º C, 12 months	Nasal wash, Nasopharyngeal swabs, throat swabs, tracheal aspirates, sputum,	15 min	Moderate	A: 89-100% B: 93-100%	A: 100% B: 100%
Wampole Clearview Flu A/B	Fisher Scientific, USA www.fishersci.com	A and B	Yes	2-25 º C, 12 months	(1) Nasal wash, Nasopharyngeal swabs, throat swabs	15 min	Easy	A:92% B:98%	A:100% B:100%
ZstatFlu-II test	Zyme Tx, Inc., Oklahopma City, OK. www.zymetx.com	A and B	No		Throat swab	30 min	Easy	A:76% B: 41%	7798%
Influ-A Respi-Strip	Coris BioConcept, Belgium www.corisbio.com	A	No	4-37 º C, 12 months	Nasopharyngeal swabs	5-15 min	Moderate	A: 91%	A: 86%
Influ-A&B Respi-Strip	Coris BioConcept, Belgium	A and B	Yes	4-37 º C	Nasopharyngeal aspirates, washings or	5-15 min	Moderate	A: 99% B: 72.2%	A:88% B:100%

	www.coris bio.com				swabs				
Espline Influenza A&B-N	Fujirebio Inc., Tokyo, Japan www.fujire bio.co.jp	A and B	Yes		Nasal aspirates/ swabs, Throat swabs	15 mins	Moderat e	A:85100% B:72-91	A/B:98-100%
Capila FluA,B	Tauns Co., Ltd., Japan	A and B	Yes		Nasal aspirate/swab, pharyngeal swab	15 mins	Easy	A:69-94% B: 81-96%	A:93-95% B: 96-99%
RapidTesta FLU AB	Daiichi Pure Chemicals Co., Tokyo, Japan	A and B	Yes	2-30 º C, 12 months	Nasal aspirates/ swabs	10 mins	Easy	A:82-83% B:80-83%	A:98-99% B:98%
SAS Influenza A Test	SA Scientific Inc, USA	A and B	Yes		Nasal wash/aspirate	30 mins	Easy		
Immuno*Card* STAT! Flu A&B	Meridian Bioscience, Inc	A and B	Yes	2-25 º C, 12 months	Nasal wash, Nasopharyngeal aspirate/swabs, nasal swabs	15-20 min	Easy	A:83% B:100%	A:98% B:100%
Wampole Clearview Flu A/B	Fisher Scientific, USA www.fisher sci.com	A and B	Yes	2-25 º C, 12 months	(1) Nasal wash, Nasopharyngeal swabs, throat swabs	15 min		A:92% B:98%	A:100% B:100%
ZstatFlu-II test	Zyme Tx, Inc., Oklahopma City, OK. www.zyme tx.com	A and B	No		Throat swab	30 min	Easy	A:76% B: 41%	77-98%
Influ-A Respi-Strip	Coris BioConcept , Belgium www.coris bio.com	A	No	4-37 º C, 12 months	Nasopharyngeal swabs	5-15 min	Easy	A: 91%	A: 86%
Influ-A&B Respi-Strip	Coris BioConcept , Belgium www.coris bio.com	A and B	Yes	4-37 º C	Nasopharyngeal aspirates, washings or swabs	5-15 min	Easy	A: 99% B: 72.2%	A:88% B:100%
Espline Influenza A&B-N	Fujirebio Inc., Tokyo, Japan www.fujire bio.co.jp	A and B	Yes		Nasal aspirates/ swabs, Throat swabs	15 mins		A:85100% B:72-91	A/B:98-100%
Capila FluA,B	Tauns Co., Ltd., Japan	A and B	Yes		Nasal aspirate/swab, pharyngeal swab	15 mins	Easy	A:69-94% B: 81-96%	A:93-95% B: 96-99%
RapidTesta FLU AB	Daiichi Pure Chemicals Co., Tokyo, Japan	A and B	Yes	2-30 º C, 12 months	Nasal aspirates/ swabs	10 mins		A:82-83% B:80-83%	A:98-99% B:98%
SAS Influenza A Test	SA Scientific Inc, USA	A and B	Yes		Nasal wash/aspirate	30 mins	Moderat e		
Immuno*Card* STAT! Flu A&B	Meridian Bioscience, Inc	A and B	Yes	2-25 º C, 12 months	Nasal wash, Nasopharyngeal aspirate/swabs, nasa l swabs	15-20 min	Easy	A:83% B:100%	A:98% B:100%

5.1 Lab-on-a-chip

Lab-on-a-chip (LOC) is an integrated microfluidic device that contains one or several laboratory functions on a single chip of only millimetres to a few square centimetres in size. The integrated microfluidic system with active or passive fluid control components for sample valving, pumping, mixing, etc., improves the functionality and reliability of LOC devices. The ability of these devices to conduct measurements from small volumes of complex fluids with efficiency and speed, without the need for a skilled operator, has been regarded as the most powerful application of LOC technologies[131].

The different steps of a molecular diagnostic LOC device are sample preparation, amplification and detection. Conventional PCR amplification is performed in a thermocylers that is based on Peltier element technology (Figure 5.1a). A 96- or 384-well plastic PCR plate is thermally cycled in a heating block made of thermal conductive metals and the reaction volume is between 10 and 50µl. Cycling is achieved by heating and cooling the massive metal block with a maximum temperature ramp of 1–3 ^{o}C/s. A large heat capacitance is required for homogeneity across the whole plate, resulting in slow PCR cycles.

a) b)

:

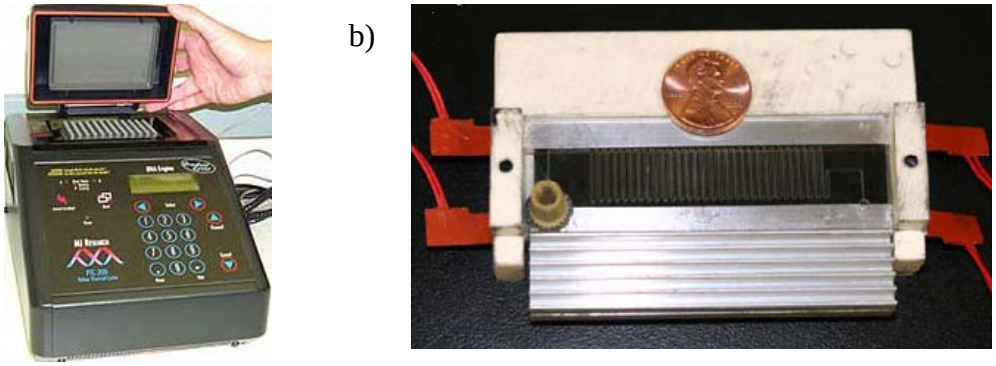

Figure 5.1: PCR thermocyclers a) A conventional PCR thermocyclers (MJ Research Inc., Waltham, MA, USA) and b) A miniaturized PCR thermocyclers[132].

By shrinking the sample volume, the over all heating and cooling rate becomes faster [133]. A variety of miniature PCR systems have been developed with fast heating (>10 ^{o}C/s) for efficient

amplification [134]. These miniaturized devices (Figure 5.1b) have the following advantages[135]:

- Shorter diagnosis times due to faster heating/cooling times, a high surface-to-volume ratio and a smaller thermal capacitance.
- Lower sample and reagent consumption (usually <10 μl)
- Improved resolution and higher sensitivity: massively parallel processing steps can be integrated into a microchip, which allows high-throughput analysis and more sensitive analytical results at the molecular level.
- Lower per unit cost: lower fabrication cost based on mass production allowing for cost-effective, disposable chips (single-time use).
- High-throughput automated analysis
- Minimum variability

Several comprehensive reviews were made on miniaturized PCR devices covering the fabrication techniques, PCR reaction speed, PCR inhibition and carryover contamination [134;136-138]. Over the years the fabrication material for PCR chambers or channel has been changing from glass and silicon to polymers due to the effort to minimize the fabrication cost (disposable chips). The commonly used polymers are SU-8, polydimethylsiloxane (PDMS), polycarbonate (PC) and polymethylmethacrylate (PMMA) and cyclic olefin copolymer (COC).

5.1.1 Microfluidics

Microfluidics deals with the behaviour, precise control and manipulation of fluids that are geometrically constrained to a small, typically sub-millimetre scale. The down scaling of the dimensions in the fluidic system increases the surface-to-volume ratio (SVR) and changes the behaviour of the fluids. The large SVR of a microfluidic chip permits rapid thermal cycling and also increases the interaction possibility between the analyst molecules and the surface of receptor molecules. The large SVR also increseases the non-specific binding and often causes inhibition of PCR reaction[139].

In microfluidic channels, mass transport is dominated by viscosity with inertial effects becoming negligible. As inertia is responsible for most of the instabilities and chaotic behaviour observed

in fluids, its reduced influence within micron scale systems leads to a simplified flow regime. The Reynolds number (Re), defined as the ratio of the inertial properties of the fluid to the viscous (**η**) properties of a fluid flow describes the flow regime as either laminar or turbulent.

$$Re = \frac{\rho \nu D}{\eta}$$

where **ρ** is the density of the fluid, **ν** is the velocity of the fluid and **D** is the hydraulic diameter of the flow channel. Re < 2300, as calculated by the above formula, generally indicates a laminar flow. As Re approaches 2300, the fluid begins to show signs of turbulence, and at Re greater than 2300 the flow is considered to be turbulent. For the microfluidic channel, with at least one characteristic dimension in the micrometer range and with fluid flow velocities in the millimetre to centimetre per second, the flow is generally in the low Reynolds number regime (Re <<1). The laminar flow provides a means by which molecules can be transported in a relatively predictable manner i.e., the position of a particle in the fluid stream as a function of time[140].

The common method used for fluid actuation through microfluidic channel is pressure driven flow. This is done via positive displacement pumps, such as syringe pumps. The pressure driven laminar flow produces a no-slip boundary condition where the fluid velocity at the walls is zero and a maximum flow velocity at the channel centre. This condition results in Poiseuille-type flow, characterised by a parabolic velocity profile across the channel (Figure 5.2)[141].

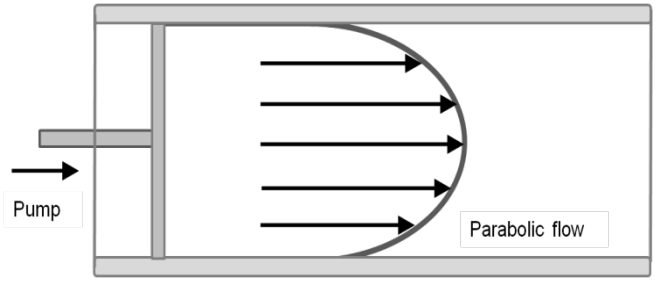

Figure 5.2 A parabolic fluid velocity profile in a microfluidic channel resulting from pressure-driven fluid[141].

Pressure driven flow can be a relative inexpensive and quite reproducible approach to pumping fluids through microdevices.

5.1.2 Integrated system

Although partially integrated PCR chips have been successfully developed, the total integrated PCR-based LOC still requires further development. Two main challenges that delay the realization of a truly and highly integrated PCR chip are on-chip sample preparation and on-chip detection steps. The on-chip sample preparation with crude sample such as faeces is more complex than for detecting purified analytic targets, because of the multiple preparing steps that should be required for complex crude sample. The miniaturization of sample preparation and functionalities on a chip remain a challenge in the development of point-of-care nucleic acid based assay for resource limited settings[137;142;143]. Many PCR chips have been developed for rapid amplification but in most of those studies the PCR product were analyzed off-chip by gel electrophoresis or fluorescence microscopes [144]. Although few reports on miniature real time PCR on chip have been made, significant advances are needed to reduce the cost, physical size and power requirement of the conventional detector suitable for integration and multiplex detection.

5.1.3 Magnetic beads

The challenge in the integration of sample preparation has been addressed using magnetic bead-labelled with biomolecules to enhance the specific separation and purification of the target [145]. In molecular diagnostics, magnetic beads have been applied in sample preparation and nucleic acid purification for PCR. The benefits of using magnetic beads in these steps are the removal of PCR inhibitors and concentration of target pathogen from a large sample volume (up to 10 ml) to workable volume (10-50μl)[146]. The use of magnetic beads allows high sample throughput and automation with reduced reagent costs and elimination of labour intensive steps. Magnetic beads have several advantages that include, simple and fast with only a few handling steps in comparison with standard separation procedures.

A number of magnetic beads are commercially available on the market with different characteristics such as surface chemistry, size, and the binding properties to ligands and target molecules [126;147]. The magnetic bead consists of a magnetic core (single or multiple) encapsulated in a polymer shell (Figure 5.3a and b). The core provides the magnetic

characteristics of the bead while the polymer (typically polystyrene) prevents the direct contact of biomolecules with the magnetic material and provides the beads with a biocompatible surface.

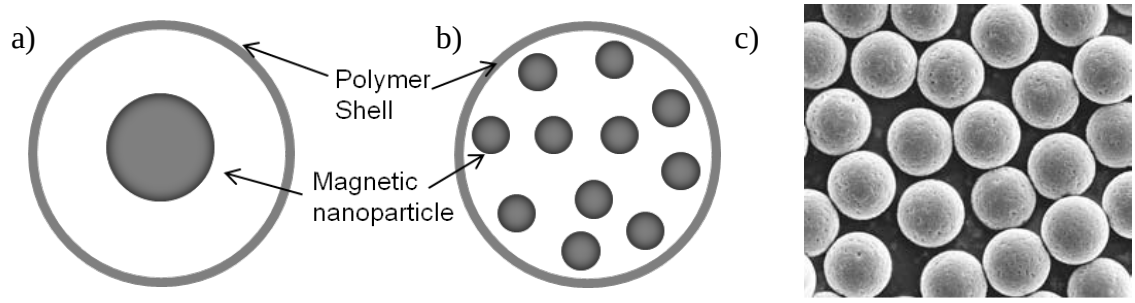

Figure 5.3 Configuration of magnetic beads: a) single-core and b) multi-core (reproduced from ref[148]). (c) Scanning electron microscopy picture of magnetic beads from Dynabeads, Invitrogen [149].

The commonly used magnetic cores are inorganic nanoparticles such as iron oxide (maghemite or magnetite) or other more complex metal-iron oxide alloys (e.g. Nicol or Cobalt-iron-oxide). The diameter of these nanoparticles (magnetic core) varies between 20nm to 200nm. There are different functional groups such as -COOH, -OH or $-NH_2$ available on the surface of magnetic particles (polymer shell). These functional groups are used for immobilization of ligand such as antibody, protein or antigen, and DNA/RNA capture-probe to capture the desired target. In some cases, the magnetic beads are available in the activated form (e.g., tosylactivated, carboxyl, epoxy, amine)[150].

A response of magnetic beads to an external magnetic field is characterized by hysteresis loop. A typical hysteresis loop of a ferromagnetic material is shown in Figure 5.4a [151]. In the presence of an external magnetic field (**H)**, the material exhibits a magnetic moment or magnetization (**M)**.The magnetization of the material increases the total induced magnetic flux density (**B)**, which is expressed as:

$$\mathbf{B = \mu_0 (M + H)}$$

where μ_0 is the permeability of a free space or vacuum. An increase in external magnetic field increases total flux density and reaches a saturation value $\mathbf{B_s}$. The material will retain the magnetic moment (remanence **R**) even in the absence of the external field. After the application of a coercitive field $\mathbf{H_C}$, the net magnetic moment of the material will return to zero.

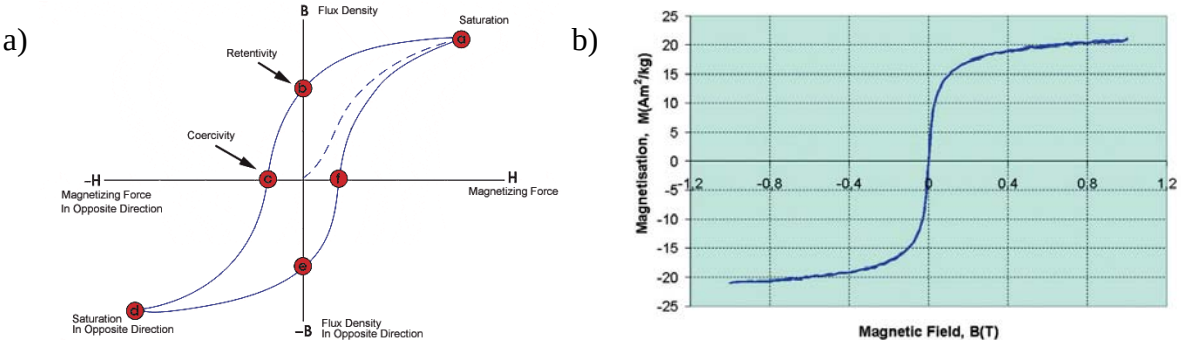

Figure 5.4 Hysteresis curve for the bead platform: magnetization as a function of magnetic field strength. The loop is generated for a) ferromagnetic or ferrimagnetic material [151] and b) super-paramagnetic beads (Myone Dynabeads (Invitrogen)) [152].

When the diameter of magnetic core decreases (<25 nm), the magnetic moment is increasingly affected by thermal fluctuations and the system becomes superparamagnetic[153]. The hysteresis curve for the superparamagnetic beads such as MyOne Dynabeads (Invitrogen) is shown in Figure 5.4b, where the magnetisation is linear with both increasing and decreasing the external magnetic fields[152]. The total magnetic field increases at the bead position as the bead is attracted towards the external field. When the external magnet is removed, the beads immediately lose all their magnetic remanence ($\mathbf{H_C}$ = 0 and so **B**=0) and are easily resuspended. The prevention of aggregation and clumping of the magnetic particles during the reaction results in a monodispersity and ensures a uniform reproducibility.

Using magnetic beads for sample preparation, an integrated RT-PCR microfluidic system has been developed for Dengue fever viruses [154-157]. Figure 5.5 shows such approach using immunomagnetic separation and amplification of target in microfluidic environment[157]. The sensitivity of the system for detection of dengue-virus serotype-2 is 10^2 PFU/ ml. However, in this case, the samples were purified dengue-virus serotype-2 and not a crude sample such as faeces. The RT-PCR product was also analyzed off-chip using gel-electrophoresis.

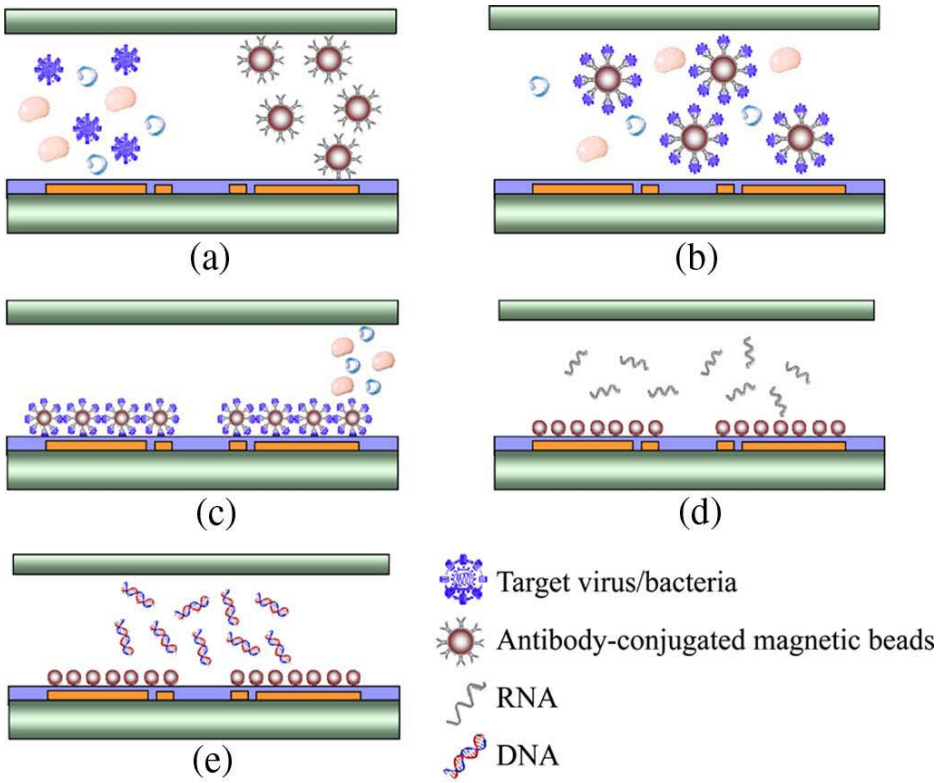

Figure 5.5 Schematic illustration of an operating process of a miniature RT-PCR system with sample preparation. (a) Mixing clinical biosamples with the antibody-conjugated magnetic beads. (b) Binding of the targeted analyte on the surfaces of the beads by specific antibodies. (c) Magnetic separation of the beads and the targeted analyte conjugates and washing of the non-target entities (d) Release of RNA by thermal lysis is performed by the on-chip microheaters. (e) Synthesizing and amplification of cDNA by the RT-PCR process [157].

Chapter 6

Sample preparation for RT-PCR

This chapter focuses on the development of an immunomagnetic bead-based assay for rapid sample preparation that could be used for on chip RT-PCR to detect AIV. The developed method was further investigated in a magnetic microfluidic system for high throughput. In the later part of this chapter, the experimental results for on chip sample preparation using SU-8 chip and on chip RT-PCR for rapid detection of AIV using SU-8 and COC chips are highlighted.

6.1 Rapid detection of avian influenza virus in chicken faecal samples by immunomagnetic capture RT-PCR assay

Manuscript published in Diagnostic Microbiology and Infectious Diseases (2011), 69, 258-265.

Available online at www.sciencedirect.com
ScienceDirect
Diagnostic Microbiology and Infectious Disease 69 (2011) 258–265
DIAGNOSTIC MICROBIOLOGY AND INFECTIOUS DISEASE
www.elsevier.com/locate/diagmicrobio

Virology

Rapid detection of avian influenza virus in chicken fecal samples by immunomagnetic capture reverse transcriptase–polymerase chain reaction assay ☆

Raghuram Dhumpa[a], Kurt Jensen Handberg[b,1], Poul Henrik Jørgensen[b], Sun Yi[c], Anders Wolff[c], Dang Duong Bang[a,*]

[a]Laboratory of Applied Micro and Nanotechnology (LAMINATE), National Veterinary Institute, Technical University of Denmark (DTU-Vet), Hangøvej 2, Dk-8200, Aarhus N, Denmark
[b]Avian Virology, National Veterinary Institute Technical University of Denmark (DTU-Vet), Hangøvej 2, Dk-8200, Aarhus N, Denmark
[c]BioLabChip group, Department of Micro and Nanotechnology, Technical University of Denmark (DTU-Nanotech), DK-2800 Lyngby, Denmark

Received 11 June 2010; accepted 29 September 2010

Abstract

Avian influenza virus (AIV) causes great economic losses for the poultry industry worldwide and threatens the human population with a pandemic. The conventional detection method for AIV involves sample preparation of viral RNA extraction and purification from raw sample such as bird droppings. In this study, magnetic beads were applied for immunoseparation and purification of AIV from spiked chicken fecal sample. The beads were conjugated with monoclonal antibodies against the AIV nucleoprotein, which is conserved in all the AIV. The bead-captured virus was detected by reverse transcriptase–polymerase chain reaction (RT-PCR) without RNA extraction because of effective removal of RT-PCR inhibitors. The developed bead-based assay showed a similar detection limit comparable to the RNA extraction and the classic virus isolation method. Using ready-to-use antibody-conjugated bead, the method requires less than 5 h. Furthermore, the method has potential to integrate into a Lab-on-a-chip system for rapid detection and identification of AIV.

Keywords: Avian influenza virus; Magnetic beads; Fecal sample; Immunoassay; Real-time RT-PCR

1. Introduction

Avian influenza is a disease caused by influenza A virus. Outbreaks of Avian influenza virus (AIV) caused great economic loss in the poultry industry and are threats to human health (IMF Report, 2006; Peiris et al., 2007). To prevent the emergence of a human pandemic, improved measures for controlling of AIV are crucial (de Wit and Fouchier, 2008; Editorial, 2008).

AIV belongs to the Orthomyxoviridae family—an enveloped and negative-sense single-stranded RNA virus. On the AIV surface, 2 glycoproteins [hemagglutinin (H) and neuraminidase (N)] are presented, and these have been used to classify the AIV into 16 H subtypes (H1–H16) and 9 N subtypes (N1–N9), respectively (Alexander, 2007). Based on the ability to cause disease and mortality of the virus in experimental infection of 4 to 8 week-old chickens, the AIV is classified as either highly pathogenic avian influenza (HPAI) or low pathogenic avian influenza (LPAI) [Alexander, 2007; World Organization for Animal Health (OIE), 2009].

Classic method for detection and identification of AIV is the isolation of virus in embryonated specific pathogen-free (SPF) chicken eggs. If successful, the virus is used for further typing (Charlton et al., 2009), but the method is time-consuming (3–10 days), laborious, expensive, and requires special laboratory facilities and trained staff. A faster method

☆ A part of this work was presented as oral and poster presentation at the International Lab-on-a-chip World Congress 2008, May 7–8, Barcelona, Spain.

* Corresponding author. Tel.: +45-3588-6892; fax: +45-3588-6901.
E-mail address: ddba@vet.dtu.dk (D.D. Bang).
[1] Present address: Department of Clinical Microbiology, University Hospital of Aarhus, Brendstrupgaardsvej 100, DK-8200, Aarhus N, Denmark.

0732-8893/$ – see front matter.
doi:10.1016/j.diagmicrobio.2010.09.022

for detecting AIV based on reversed transcriptase–polymerase chain reaction (RT-PCR) was developed (Fouchier et al., 2000). Although RT-PCR is a sensitive method for detection of AIV, the presence of any inhibitors in the sample limits the detection and the efficiency (Ginny and Helen, 1999; Peter et al., 2004). A sample preparation step for removing inhibitors is therefore always required to obtain reliable diagnosis results.

A number of commercial kits, especially column-based nucleic acid purification, are available for viral RNA extraction from raw samples such as feces. Recently, magnetic microspheres (beads) have been introduced to enhance AIV viral RNA extraction and purification (Tewari et al., 2007), and to detect antibodies against AIV in immunoassays (Deregt et al., 2006). Magnetic beads conjugated with anionic polymer have been utilized to capture H5 AIV from allantoic fluid sample (Sakudo and Ikuta, 2008). The beads can be used to catch H5 AIV strain from allantoic fluid or other virus suspension but cannot be used to catch the virus from raw samples because of the lack of specificity that may be due to unspecific hydrophobic interaction. Silica-based magnetic beads have been applied to extract AIV viral nucleic acid using robotics (Tewari et al., 2007). This method is sensitive, specific, and comparable to the conventional RNA extraction method. However, the method can isolate total RNA only from a small sample volume (up to 400 μL); therefore, it can be cumbersome pre-processing step for larger volumes of samples (up to 1 mL). Moreover, the robotic system is also very expensive.

In this study, a novel method for selective separation and purification of AIV from chicken fecal sample using monoclonal antibody (mAb)-conjugated magnetic beads without RNA extraction step is described. The applied mAb interacts with a protein conserved in all AIV strains. Subsequently, the AIV-captured mAb-conjugated magnetic beads were identified by RT-PCR. The method was evaluated using chicken fecal samples spiked with 16 different AIV subtypes and compared to the RNA extraction method and the virus isolation (VI) method.

2. Materials and methods

2.1. Viruses

Sixteen different AIV strains that belong to 16 H and 9 N subtypes were used to evaluate the method, and a Newcastle disease virus (NDV) was used to check the specificity of the AIV mAb. Table 1 shows a list of the AIV strains with different phenotypes, sources of isolation, and HA titers. All the strains except the H16N3 were kindly supplied by the Veterinary Laboratories Agency (VLA, Weybridge, UK). The viruses were prepared by propagation in 9- to 11-day-old embryonated chicken SPF eggs. The allantoic fluid containing the viruses was harvested from the eggs and kept at −80 °C until testing. The HPAI viruses (H5 and H7) were inactivated using β-propiolactone at a concentration of 1:1200. To determine the antigenic titer value for the viruses, hemagglutination (HA) test was performed using a 96-well microtiter V-bottomed plate according to standard method (OIE, 2009).The HA titer value is represented in HA unit (HAU), which is the reciprocal of the highest dilution causing complete HA per 50 μL. The 50% egg infectious dose (EID_{50}) was calculated for H16N3 strain using Reed–Muench formula (Reed and Muench, 1938).

Table 1
List of different strains used in this study and their HAU titer value

No.	AIV strains	Titer (HAU)	Limit of detection	
			A	B
1.	H1N1 A/Duck/Alberta 35/76	16	10^{-6}	10^{-5}
2.	H2N3 A/Duck/Germany/1215/73	64	10^{-5}	10^{-5}
3.	H3N2-A/Turkey/England/384/79	256	10^{-5}	10^{-5}
4.	H4N6 A/Duck/Czech/56	512	10^{-6}	10^{-6}
5.	H5N1 A/Chicken/Scotland/ 59 06.04.67	256	10^{-4}	10^{-4}
6.	H6N8 A/Turkey/Canada/63	256	10^{-5}	10^{-5}
7.	H7N7-2 A/Chicken/Netherland/2993/03	128	10^{-4}	10^{-4}
8.	H8N4 A/Turkey/Ontario/6118/68	128	10^{-6}	10^{-6}
9.	H9N2 A/Turkey Wisconsin/66/3577	64	10^{-7}	10^{-7}
10.	H10N4-A/Turkey/England/384/79	512	10^{-5}	10^{-5}
11.	H11N6 A/Duck/England./56	1024	10^{-6}	10^{-6}
12.	H12N5 A/Duck/Alberta/60/76	1024	10^{-5}	10^{-5}
13.	H13N6 A/Gull/Maryland/704/77	256	10^{-5}	10^{-5}
14.	H14N5 A/Mallard/Gurjev/263/82	256	10^{-5}	10^{-5}
15.	H15N9 A/Shearwater/Australia/2576/1979	256	10^{-6}	10^{-6}
16.	H16N3-A/Gull/Denmark/68110/02	128	10^{-5}	10^{-5}
17.	Newcastle diseases, Ulster strain	128		

All strains except H16N3 virus were supplied by VLA. The end-point dilution of each strain detectable by both (A) RNA extraction and (B) bead-based method is mentioned.

2.2. Antibody

Monoclonal antibody against the nucleoprotein (NP) of AIV was selected for conjugation onto the surface of the beads. The NP is conserved in different AIV strains, and different detection methods targeting NP have been developed successfully (Jin et al., 2004; Yang et al., 2008). The mAb (HYB 340-05) was purchased from Statens Serum Institut (Copenhagen, Denmark). The mAb was obtained in a purified solution with a concentration of 1 mg/mL.

2.3. Conjugation of antibody to magnetic beads

A number of magnetic beads are commercially available in the market with different characteristics such as surface chemistry, size, and the binding properties to the ligand and target molecules. Super-paramagnetic polystyrene beads were selected for the bead-based assay as it has a large surface, high capacity for target isolation, and excellent properties for automation (Andreassen, 2005). Super-paramagnetic polystyrene beads with a diameter of 1.08 μm (Dynabeads, MyOne-Tosylactivated; Invitrogen, Copenhagen, Denmark) were used for the assay. The beads were supplied in a concentration of 100 mg beads/mL. The mAb was conjugated

Table 2
List of primers and probes for RT-PCR and rRT-PCR used in this study

Description	Sequence (5′ to 3′)	Reference
RT-PCR forward (M52C)	CTTCTAACCGAGGTCGAAACG	Fouchier et al. (2000)
RT-PCR reverse (M253R)	AGGGCATTTTGG ACAAAKCGTCTA	
rRT-PCR forward (M+25)	AGATGAGTCTTCTAACCGAGGTCG	Spackman et al. (2002)
rRT-PCR reverse (M-124)	TGCAAAAACATCTTCAAGTYTCTG	
rRT-PCR probe (M+64)	FAM-TCAGGCCCCCTCAAAGCCGA-TAMRA	
NDV-2	CTGCCACTGCTAGTTGBGATAATCC	Jørgensen et al. (1999)
NDV-3	GTYAAYATATACACCTCATCYCAGACWGG	

covalently to magnetic beads according to manufacturer's instructions. Briefly, 3 mg (30 μL) of beads were suspended in 1 mL of coating buffer (0.1 mol/L sodium borate buffer). The beads were mixed by vortex and placed on a magnetic separator (Dynal MPC, Invitrogen) to separate the beads from the suspension. The supernatant (1.2 mL) was removed and the beads were washed once in coating buffer. The mAb was conjugated to the beads by adding 100 μg of immunoglobulin G (IgG) mAb in 685 μL of the coating buffer and 415 μL of 3 mol/L ammonium sulfate. The mixture was incubated at 37 °C for 24 h on a slow mixing rotor. Later, the supernatant was removed and saved for determination of the efficiency of antibody conjugation. The beads were resuspended in 1.2 mL of blocking buffer containing phosphate-buffered saline (PBS) with 0.5% bovine serum albumin (BSA) and 0.05% Tween 20 and incubated overnight at 37 °C. After the incubation, the mAb-conjugated beads were washed 3 times with 1 mL of storage buffer containing PBS with 0.1% BSA and 0.05% Tween 20 and finally resuspended in 300 μL of the storage buffer and stored at 4 °C for up to 3 months without loss of activity.

2.4. Antibody conjugation determination

The conjugation of antibodies to the surface of the beads was verified by 2 methods: enzyme-linked immunosorbent assay (ELISA) to determine the presence of mAbs on the bead surface and UV spectrophotometric method to measure the amount of mAbs in the liquid phase before and after conjugated to beads. The ELISA was performed according to the method described previously (Sakhalkar et al., 2005) with modification. Briefly, a 96-microwell plate was coated with blocking buffer to reduce the background signal. Fifty micrograms of either mAb-conjugated or unconjugated beads were placed in separate wells and 45 ng of horseradish peroxidase-conjugated rabbit antimouse IgG (Dakocytomation, Glostrup, Denmark) was added to each well and incubated for 1 h. For washing, magnets (IKEA, Aarhus, Denmark) were placed beneath the microwell plate to immobilize the beads on the bottom of the wells. The beads were washed 3 times with 300 μL of washing buffer (PBS 10 mmol/L and 0.05% Tween 20). After the washing steps, 100 μL of substrate solution (hydrogen peroxide) was added to each well. The plate was wrapped with aluminum foil and kept at room temperature for 20 min. Finally, 100 μL of 0.5 mol/L sulfuric acid was added to each well to stop color procedure. The optical density (OD) was measured using ELISA plate reader (MTX Lab Systems, Vienna, VA) by dual wavelength mode at 492 nm and reference wavelength at 620 nm. In the latter method, the amount of mAb conjugated to beads was determined by calculating the difference between total mAbs applied (100 μg) and the free remaining mAbs after conjugation by UV-visible spectrophotometer (Pharmacia Biotech, Uppsala, Sweden). The concentration was calculated using an extinction coefficient of 1.4 for IgG (A280/1.4 = concentration in milligrams per milliliter).

2.5. Preparation of chicken fecal sample

A fresh chicken fecal stock was prepared by suspending 1 g of chicken feces in 1 mL of PBS (10 mmol/L). The fecal mixture was homogenized by vortex. To prepare the AIV-spiked chicken fecal sample for testing, a sterilized cotton swab was dipped into the chicken fecal stock sample and approximately 235 mg was introduced into 2 mL of PBS to release fecal material. The solid fecal content was removed by centrifugation at 13 000 rpm for 5 min at room temperature and the supernatant was tested for the presence of AIV by RT-PCR (Fouchier et al., 2000). The AIV RT-PCR negative fecal suspension was used to prepare the AIV-spiked fecal sample for the assays. To mimic the natural AIV infectious fecal sample, 100 μL of each AIV virus (listed in Table 1) diluted at 1:100 in PBS was spiked and mixed with 900 μL of the prepared feces and used as AIV-spiked samples for the assays. AIV was spiked into the sample after centrifugation to ensure a uniform starting material for both the RNA extraction and the bead-based assay.

2.6. Bead-based assay

For the bead-based assay, 3 different volumes (5, 25, and 50 μg) of the beads were tested and evaluated. Fifty micrograms of beads were selected for the assay to have an efficient capturing. Fifty micrograms of mAb-conjugated magnetic beads were added to each of the 16 AIV subtypes spiked fecal samples. The mixture was mixed by slow rotation for 30 min at room temperature. The mixture was then placed in a magnetic particle concentrator (MPC-1, Invitrogen) to separate the bead-captured virus from the

solution containing potential PCR inhibitors in feces and unbound virus. The supernatant was removed and the beads were washed 5 times with 1 mL of washing buffer (PBS 10 mmol/L and 0.05% Tween 20). Finally, the beads (with captured virus) were resuspended in 50 μL of washing buffer to have same volume with the RNA extraction method and 5 μL of the bead suspension was used as template for RT-PCR. To study whether lysis of AIV by heat has any influence on the efficiency of the bead-based assay, the bead-captured AIV suspension was tested by both nonheating and preheating at 95 °C for 5 min and was chilled to 5 °C before the addition of RT-PCR mixture.

Pilot experiments for bead-based assays were conducted with H5N1 virus in feces suspension to verify the washing procedure. In these experiments, the fraction of each wash was collected and tested for the presence of unbound free virus after each wash by RT-PCR.

2.7. RNA extraction

Extraction of RNA from allantoic fluid and spiked fecal sample was performed using the RNeasy Kit (Qiagen, Copenhagen, Denmark) according to the manufacturer's instruction. RNA was also extracted from bead-captured virus to observe any loss of signal after the washing steps. The RNA was finally eluted using 50 μL of RNase-free water. All the extraction steps were performed in biosafety level 3 laboratory facilities.

2.8. RT-PCR reaction

Both conventional RT-PCR and real-time RT-PCR (rRT-PCR) were performed using one-step RT-PCR kit (Qiagen). All the primers and probes were synthesized by DNA technology A/S (Aarhus, Denmark). The sequences of primers, probes, and references used in this study are shown in Table 2. The RT-PCR was performed according to the manufacturer's instruction with minor modification. Briefly, 5 μL of template was used in 25 μL of RT-PCR reaction mixture with 2 primers, namely, M52C and M253R, targeting the matrix gene of AIV (Fouchier et al., 2000). The RT-PCR conditions consist of a reverse transcription at 56 °C for 30 min and an enzyme activation step at 95 °C for 15 min, 40 cycles of 94 °C for 30 s, 58 °C for 1 min, and 72 °C for 1 min, and finally, a primer extension step at 72 °C for 7 min using a thermal cycler (Biometra, Goettingen, Germany). The obtained PCR product was analyzed using agarose gel (1.5%) electrophoresis and a 100-bp DNA ladder (Invitrogen, Taastrup, Denmark) was used as a marker. The rRT-PCR was performed according to a method described previously (Spackman et al., 2002) with 2 μL of template in 20 μL master mix using a Stratagene Mx 3000 real-time PCR machine (AH-Diagnostics, Aarhus, Denmark). The RT-PCR for NDV virus was performed using 2 primers specific for NDV, namely, NDV-2 and NDV-3, as reported previously (Jørgensen et al., 1999).

2.9. Agglutination test

The HA test and the latex (LAT)-based agglutination test were performed to detect AIV. The HA test was performed by mixing 20 μL of 0.5% chicken red blood cells (CRBC) with 20 μL of the bead-captured virus on a white ceramic tile. Two minutes after the mixing, the agglutination was observed. The LAT-based agglutination test is a technique to detect antibodies that are capable to react with antigen coated on latex bead. The reaction of antibodies and antigen forms an agglutination that can clearly be seen with naked eye. When no specific antibodies are present, the latex suspension will remain homogeneous (negative result). In this study, the LAT-based agglutination test was performed to detect AIV as described by Chen et al. (2007), with modification by using magnetic beads conjugated with mAb instead of latex beads. Briefly, 10 μL of mAb beads was placed on a microscopic glass slide and 10 μL of virus (allantoic fluid)

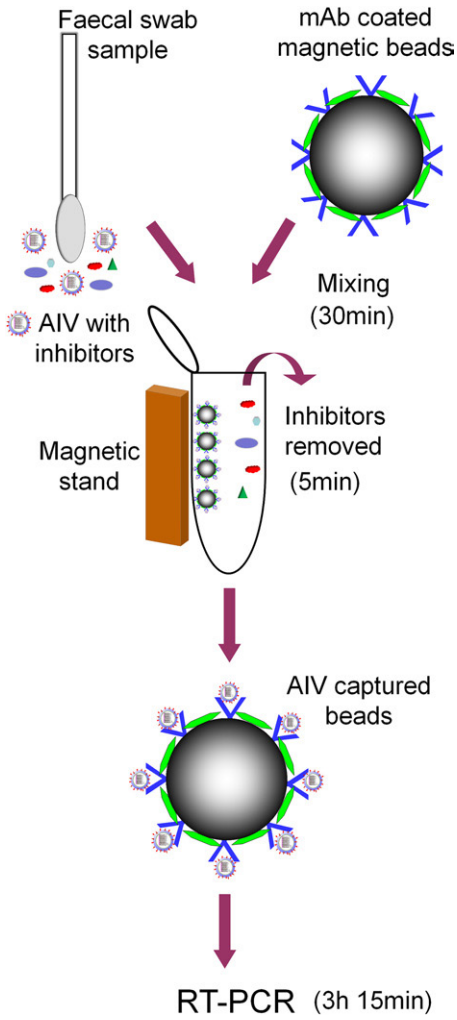

Fig. 1. A schematic representation of sample preparation of AIV using mAb-conjugated magnetic beads. The magnetic beads and fecal sample are mixed in a tube. The beads were separated using a magnetic stand and the inhibitors were removed. The AIV-captured beads were used for RT-PCR directly without further treatment.

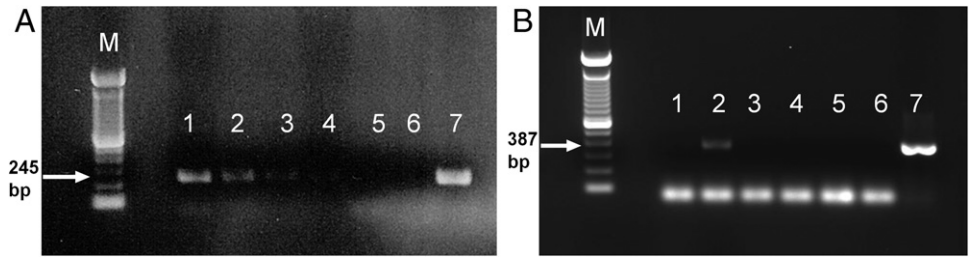

Fig. 2. Agarose gel electrophoresis images of the bead-based assay to determine (A) the optimal washing steps for the assay. On gel: lane 1, the bead-captured virus (H5N1); lanes 2–4, washing steps 1, 3, and 5, respectively. Controls: master mix (5), negative control (H_2O) (6), and positive control (AIV) for RT-PCR (7). (B) The specificity of the mAb-conjugated beads using NDV. On gel: Lane 1 shows no signal from the beads used to capture NDV virus. Lane 2, 3, and 4 represent supernatant washing numbers 1, 3, and 5. Lane 5 represents master mix, and 6 and 7 are the negative (H_2O) and positive control for NDV virus, respectively.

was added. The slide was then manually rotated for 30 s and agglutination event was observed.

2.10. Sensitivity

The sensitivity of the bead-based assay was determined and compared with the viral RNA extraction method and the VI method. Both the AIV-infected allantoic fluid and the AIV-spiked fecal samples were used. A 10-fold serial dilution of an AIV H16N3 strain (allantoic fluid) was made and 200 μL of each dilution was used as starting material for the 3 different methods: (1) For the VI method, 200 μL of each virus dilution was injected into the allantoic cavity of 9 to 11 day-old SPF eggs according to a standard method (OIE, 2009). The allantoic fluid was harvested from the eggs after 5 days of inoculation and the HA agglutination test was carried out to observe the agglutination. (2) For the viral RNA extraction method, the RNA was extracted from 200 μL of virus dilution series and 5 μL was used as template for RT-PCR. (3) For the bead-based method, 50 μg of bead was added to 200 μL of each virus dilution and the assay was performed as described in the earlier section. To determine the sensitivity of the bead-based assay, the H16N3 virus was spiked, chicken fecal sample was prepared by mixing 20 μL of virus with 180 μL of fecal suspension, and 50 μg of beads was added. The sensitivity of the bead-based assay was determined for all the 16 AIV viruses using 1 mL spiked sample and compared with the RNA extraction method.

The limit of detection of the bead-based method was determined by rRT-PCR and was compared to the RNA extraction method. In rRT-PCR, the bead-captured virus was heated at 95 °C for 5 min to separate the virus from the beads before used as a template. This heat step was performed to avoid the possible light scattering from the beads in rRT-PCR. The rRT-PCR was performed in duplicates.

2.11. Specificity

The specificity of the bead-based assay to capture AIV was tested using NDV. The assay was performed similar to the bead-based assay for AIV, except that the sample in this case was allantoic fluid containing NDV virus. After the assay, the presence of virus in beads and supernatant of each wash was tested by RT-PCR with NDV-specific primers.

3. Results

3.1. HA titer value

HA test was performed on allantoic fluid, and the titer value for the 17 viruses varied from 16 to 1024 HAU (Table 1). The EID_{50} for the AIV H16N3 was 6.7 $\log_{10}$ EID_{50}/mL.

3.2. Conjugation of mAb to magnetic beads

The efficiency of the conjugation of the antibody on the surface of the beads was determined by ELISA and UV spectrophotometer. Using ELISA, the OD values of the unconjugated and the mAb-conjugated beads were 0.37 (±0.347) and 2.73 (±0.063), respectively, while using UV spectrophotometer of 100 μg of mAb used for conjugation, approximately 80 μg (80%) was conjugated to 3 mg of beads.

3.3. Development of a bead-based method

Fig. 1 shows a schematic of sample preparation of AIV using the mAb-conjugated magnetic beads. Pilot experiments were performed to determine the optimal washings for the assay. Fig. 2A shows the results of one of such experiments. A positive RT-PCR was observed for the bead-captured virus (Fig. 2A, lane 1), while a negative RT-PCR was observed at the wash 5 (Fig. 2A, lane 4). Positive RT-PCRs were also seen at the first to the third wash with reduction in intensity (Fig. 2A, lanes 2–3). No signal was observed when the bead-based system was performed using NDV and tested by RT-PCR (Fig. 2B, lane 1). To test the ability of mAb-conjugated beads to catch different AIV subtypes (Table 1), chicken fecal samples spiked with 16 different AIV subtypes were tested twice with the bead-based assay, and all subtypes were detected from the spiked fecal sample using the assay. No significant difference was observed when the beads (with captured virus) were used

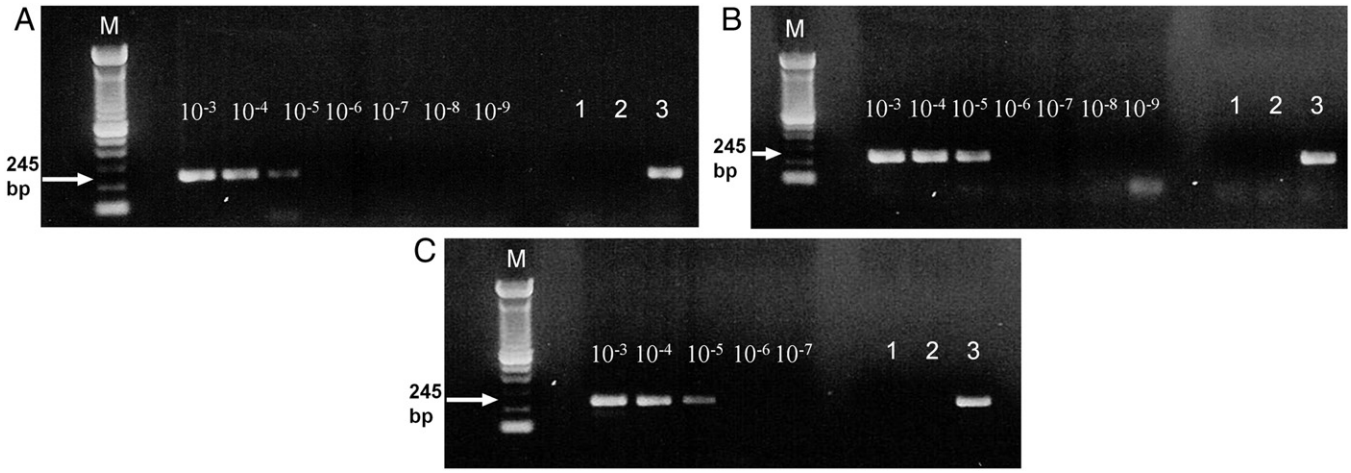

Fig. 3. The sensitivity of RT-PCR with H16N3 virus as target purified by RNA extraction method for allantoic sample (A), by bead-based method using allantoic sample (B) and spiked fecal sample (C). On gel, the number above each lane corresponds to the AIV dilutions. Lanes marked with 1, 2, and 3 represent master mix, negative, and positive PCR controls, respectively.

directly for RT-PCR, or preheat and lysis using a lysis buffer from RNA extraction kit (data not shown).

3.4. Agglutination test

Detection of AIV by agglutination was performed with HA- and LAT-based tests. No agglutination was observed with the HA test, whereas the LAT-based test clearly showed agglutination.

3.5. Sensitivity for the bead-based system

The sensitivity of bead-based system was determined and compared with both the VI and viral RNA extraction methods. The VI method showed a positive HA test for virus (H16N3) dilution up to 10^{-5} or equivalent to 1 $\log_{10}$ EID_{50}/mL. Similar detection limit was obtained for viral RNA extraction method (Fig. 3A) and the bead-based method for both allantoic fluid (Fig. 3B) and AIV-spiked fecal sample (Fig. 3C). A similar limit of detection was achieved when rRT-PCR was used to detect AIV from both the bead-based assay and the RNA extraction method with end-point Ct value of 36.21 ± 0.92 and 35.28 ± 0.62, respectively. The detection limits of all the 16 viruses for both the bead-based assay and the RNA extraction method are listed in Table 1.

4. Discussion

Detection and identification of AIV by RT-PCR is a faster method recommended by OIE for AIV diagnosis, and it has replaced the VI method (OIE, 2009). Conversely, the PCR-based approaches require sample pretreatment and enrichment, which is time-consuming and laborious. The approach to use magnetic beads for sample preparation in rapid assays has not only removed inhibitors from the sample but also concentrated the pathogen from a large sample volume (Bidawid et al., 2000; Gilpatrick et al., 2000). A number of immunomagnetic capture RT-PCR assays for the viral detection have been reported for hepatitis A virus (López-Sabater et al., 1997), ampeloviruses (Gambley et al., 2009), and Norwalk virus (Gilpatrick et al., 2000). In this study, a rapid bead-based method was developed to catch, to concentrate, and to purify the AIV from feces for detection by RT-PCR.

Two different agglutination tests, the HA and the LAT-based, were performed to confirm the presence of AIV on the surface of the beads. Using the HA test, no agglutination was observed. This could be due to the steric hindrance of beads, which was not able to provide enough room for the virus particles to agglutinate with other CRBCs. However, agglutination was observed through LAT-based test that confirmed the presence of AIV virus on the surface of the beads. The virus and beads contain multiple binding sites for each other that forms lattice (agglutination). The LAT-based test has been reported as a detection method for H5N1 subtype (Chen et al., 2007).

The development of the bead-based assay revealed that washing step is one of the factors that influence the performance of the bead-based system. In another study, it has shown that washing is an important step to remove PCR inhibitors (Nilsson et al., 1996). In this study, when the AIV-spiked sample was used directly as a template for RT-PCR, great inhibitions were observed, whereas positive RT-PCRs were obtained when purified RNA or purified AIV-captured beads were used (data not shown). Furthermore, the pilot experiments to define the optimal washing step for the assay revealed that no unbound virus was detected after 5 times of washing (Fig. 2A, lane 4); therefore, at least 5 times of washing was included in the bead-based method. Because of the effective removal of inhibitors during the bead-based assay, the AIV-captured beads were used directly as template for the RT-PCR without RNA extraction step and no preheat step

before RT-PCR was required to release the RNA as reported earlier with Chikungunya virus (Pastorino et al., 2005), which is advantageous compared to RNA extraction method.

A number of different methods such as ELISA (Jin et al., 2004; Velumani et al., 2008; Yang et al., 2008), microsphere immunoassay (Deregt et al., 2006), and anionic magnetic beads (Sakudo and Ikuta, 2008) have been developed to detect AIV in allantoic fluid. Although these immunocapture assays are simple and quick, these methods were not able to apply for the fecal material. Furthermore, these methods posed a lower sensitivity in comparison to the RT-PCR assay and the use of VI method to prepare allantoic fluid introduces tediousness.

The detection limit of all the AIV strains except H1N1 achieved in this study is comparable to the RNA extraction method. The strain H1N1 that exhibited 10 times low detection limit (10^{-5} dilution) also demonstrated a low HA titer value (16 HAU) indicating that presence of incomplete AIV (Carter and Mahy, 1982) was detected by extraction method (10^{-6} dilution). The immunomagnetic capture RT-PCR assays have been reported in previous studies (Gambley et al., 2009; Gilpatrick et al., 2000); however, data on the specificity of the assays were not reported. In this study, NDV virus is used to confirm the specificity of the bead-based system, and the use of NDV for testing the specificity of the assays has been described previously (Chen et al., 2009; Deregt et al., 2006).

The developed bead-based system was able to capture, concentrate, and purify AIV from 16 different AIV-spiked fecal samples, demonstrating the efficiency of mAb-conjugated beads. As the bead-based system separates the AIV virus rather than the viral RNA from samples, the attack of nucleases leading to false-negative results can be avoided as long as the protein (+/− lipid) coat is not disrupted (Anderson et al., 2003). The time required for sample preparation by the bead-based system (35 min) is similar to that for the RNA extraction method (45 min) with the advantage of fewer manipulation steps, which reduces the probability of obtaining false-positive result. Other obvious advantages are (i) the bead-based method works with higher volume (1 mL in this study), (ii) the method eliminates the use of hazardous chemical involved in the extraction method, and (iii) the cost of analysis for each sample preparation for the bead-based assay without considering the labor charge (€1.46) is less than half of that for the RNA extraction method (€3.97).

A big challenge for applying the bead-based system to clinical sample could be the variation and uncertainty of the concentration of AIV in the clinical samples and the degradation of the sample, which can affect the sensitivity of the assay. These depend on how the sample is treated while transportation to the reference laboratory (Forster et al., 2008). For safety reasons, if the sample is inactivated without destroying the RNA, it can be detected by the bead-based assay as observed in this study with the HPIV strains such as H5 and H7. It has been reported that AIV-infected feces may contain virus up to concentrations of 8.8 $\log_{10}$ EID_{50} infectious particles per gram and the virus can remain active over 30 days at 0 °C with decrease in mean EID value by 5-fold (Webster et al., 1978). At this AIV concentration, the developed bead-based assay may able to detect as demonstrated in this study with a number of AIV-spiked fecal samples.

In conclusion, the bead-based system presented in this study is a simple and powerful technique for immunoseparation and identification of AIV virus directly in fecal sample using RT-PCR. This AIV bead-based system could be potentially further integrated into a microsystem to obtain a rapid automated detection system with a high sensitivity. Moreover, using antibody-conjugated bead as ready to use, the entire detection required less than 5 h. The bead-based system has a potential to be an alternative sample preparation for surveillance of epidemic outbreaks caused by AIV in wild bird and poultry production.

Acknowledgment

The authors would like to thank Jonas Høgberg, Zohreh Ghavifekr, Hanne Røigaard-Petersen, and Susanne Jespersen for their experimental support. This study was financially supported by the Technical University of Denmark (DTU), food pathogen project no. 8 and grant no. 150627.

References

Alexander DJ (2007) An overview of the epidemiology of avian influenza. *Vaccine* 25:5637–5644.

Anderson NG, Gerin JL, Anderson NL (2003) Global screening for human viral pathogens. *Emerg Infect Dis* 9:768–774.

Andreassen J (2005) One micron magnetic beads optimised for automated immunoassays. *Clin Lab Int* in: April ed. Retrieved October 28, 2010 from http://www.cli-online.com/uploads/tx_ttproducts/datasheet/one-micron-magnetic-beads-optimised-for-automated-immunoassays.pdf.

Bidawid S, Farber JM, Sattar SA (2000) Rapid concentration and detection of hepatitis A virus from lettuce and strawberries. *J Virol Methods* 88:175–185.

Carter MJ, Mahy BWJ (1982) Incomplete avian influenza virus contains A defective non-interfering component. *Arch Virol* 71:13–25.

Charlton B, Crossley B, Hietala S (2009) Conventional and future diagnostics for avian influenza. *Comp Immunol Microbiol Infect Dis* 32:341–350.

Chen HT, Zhang J, Ma LN, Ma YP, Ding YZ, Wang M, Liu XT, Zhang YG, Liu YS (2009) Rapid subtyping of H9N2 influenza virus by a triple reverse transcription polymerase chain reaction. *J Virol Methods* 158:58–62.

Chen J, Jin M, Yu Z, Dan H, Zhang A, Song Y, Chen H (2007) A latex agglutination test for the rapid detection of avian influenza virus subtype H5N1 and its clinical application. *J Vet Diagn Invest* 19:155–160.

de Wit E, Fouchier RAM (2008) Emerging influenza. *J Clin Virol* 41:1–6.

Deregt D, Furukawa-Stoffer TL, Tokaryk KL, Pasick J, Hughes KMB, Hooper-McGrevy K, Baxi S, Baxi MK (2006) A microsphere immunoassay for detection of antibodies to avian influenza virus. *J Virol Methods* 137:88–94.

Editorial (2008) The long war against flu. *Nature* 454:137.

Forster JL, Harkin VB, Graham DA, McCullough SJ (2008) The effect of sample type, temperature and RNAlater(TM) on the stability of avian influenza virus RNA. *J Virol Methods* 149:190–194.

Fouchier RAM, Bestebroer TM, Herfst S, Van Der Kemp L, Rimmelzwaan GF, Osterhaus ADME (2000) Detection of influenza A viruses from different species by PCR amplification of conserved sequences in the matrix gene. *J Clin Microbiol* 38:4096–4101.

Gambley CF, Geering ADW, Thomas JE (2009) Development of an immunomagnetic capture-reverse transcriptase-PCR assay for three pineapple ampeloviruses. *J Virol Methods* 155:187–192.

Gilpatrick SG, Schwab KJ, Estes MK, Atmar RL (2000) Development of an immunomagnetic capture reverse transcription-PCR assay for the detection of Norwalk virus. *J Virol Methods* 90:69–78.

Ginny CS, Helen CP (1999) UK: RSC, pp. 91–96.

IMF Report (2006) The global economic and financial impact of an avian flu pandemic and the role of the IMF. Washington DC: International Monetary Fund.

Jin M, Wang G, Zhang R, Zhao S, Li H, Tan Y, Chen H (2004) Development of enzyme-linked immunosorbent assay with nucleoprotein as antigen for detection of antibodies to avian influenza virus. *Avian Dis* 48:870–878.

Jørgensen PH, Handberg KJ, Ahrens P, Hansen HC, Manvell RJ, Alexander DJ (1999) An outbreak of Newcastle disease in free-living pheasants (*Phasianus colchicus*). *J Vet Med, Ser B* 46:381–387.

López-Sabater EI, Deng M-Y, Cliver DO (1997) Magnetic immunoseparation PCR assay (MIPA) for detection of hepatitis A virus (HAV) in American oyster (*Crassostrea virginica*). *Lett Appl Microbiol* 24:101–104.

Nilsson H-O, Aleljung P, Nilsson I, Tyszkiewicz T, Wadström T (1996) Immunomagnetic bead enrichment and PCR for detection of *Helicobacter pylori* in human stools. *J Microbiol Methods* 27:73–79.

OIE (2009) Avian influenza. Chapter 2.3.4. OIE (World Organization for Animal Health) terrestrial manual; 2009.

Pastorino B, Bessaud M, Grandadam M, Murri S, Tolou HJ, Peyrefitte CN (2005) Development of a TaqMan RT-PCR assay without RNA extraction step for the detection and quantification of African Chikungunya viruses. *J Virol Methods* 124:65–71.

Peiris JSM, de Jong MD, Guan Y (2007) Avian Influenza Virus (H5N1): a threat to human health. *Clin Microbiol Rev* 20:243–267.

Peter R, Rickard K, Petra W, Maria L, Charlotta L (2004) Pre-PCR processing: strategies to generate PCR-compatible samples. *Mol Biotechnol* 26:133–146.

Reed LJ, Muench H (1938) A simple method of estimating fifty per cent endpoints. *Am J Epidemiol* 27:493–497.

Sakhalkar HS, Hanes J, Fu J, Benavides U, Malgor R, Borruso CL, Kohn LD, Kurjiaka DT, Goetz DJ (2005) Enhanced adhesion of ligand-conjugated biodegradable particles to colitic venules. *FASEB J* 19:792–794.

Sakudo A, Ikuta K (2008) Efficient capture of infectious H5 avian influenza virus utilizing magnetic beads coated with anionic polymer. *Biochem Biophys Res Commun* 377:85–88.

Spackman E, Senne DA, Myers TJ, Bulaga LL, Garber LP, Perdue ML, Lohman K, Daum LT, Suarez DL (2002) Development of a real-time reverse transcriptase PCR assay for type A influenza virus and the avian H5 and H7 hemagglutinin subtypes. *J Clin Microbiol* 40:3256–3260.

Tewari D, Zellers C, Acland H, Pedersen JC (2007) Automated extraction of avian influenza virus for rapid detection using real-time RT-PCR. *J Clin Virol* 40:142–145.

Velumani S, Du Q, Fenner B, Prabakaran M, Wee LC, Nuo LY, Kwang J (2008) Development of an antigen-capture ELISA for detection of H7 subtype avian influenza from experimentally infected chickens. *J Virol Methods* 147:219–225.

Webster RG, Yakhno M, Hinshaw VS, Bean WJ, Copal Murti K (1978) Intestinal influenza: replication and characterization of influenza viruses in ducks. *Virology* 84:268–278.

Yang M, Berhane Y, Salo T, Li M, Hole K, Clavijo A (2008) Development and application of monoclonal antibodies against avian influenza virus nucleoprotein. *J Virol Methods* 147:265–274.

6.2 Rapid sample preparation for detection and identification of avian influenza virus from chicken faecal samples using magnetic bead microsystem

Manuscript published in Journal of Virological Methods (2010), 169, 228–231.

Journal of Virological Methods 169 (2010) 228–231

Contents lists available at ScienceDirect

Journal of Virological Methods

journal homepage: www.elsevier.com/locate/jviromet

Short communication

Rapid sample preparation for detection and identification of avian influenza virus from chicken faecal samples using magnetic bead microsystem

Raghuram Dhumpa[a], Minqiang Bu[b], Kurt Jensen Handberg[c], Anders Wolff[b], Dang Duong Bang[a,*]

[a] Laboratory of Applied Micro and Nanotechnology (LAMINATE), National Veterinary Institute (VET), Technical University of Denmark (DTU), Hangøvej 2, DK-8200 Aarhus N, Denmark
[b] BioLabChip Group, DTU-Nanotech (Department of Micro and Nanotechnology), Technical University of Denmark (DTU), Building 345 East, DK-2800 Kgs Lyngby, Denmark
[c] Avian Virology, National Veterinary Institute (VET), Technical University of Denmark (DTU), Hangøvej 2, DK-8200 Aarhus N, Denmark

Article history:
Received 17 February 2010
Received in revised form 15 July 2010
Accepted 20 July 2010
Available online 27 July 2010

Keywords:
Avian influenza virus
Sample preparation
Magnetic beads
Faecal sample
Magnetic microsystem

A B S T R A C T

Avian influenza virus (AIV) is an infectious agent of birds and mammals. AIV is causing huge economic loss and can be a threat to human health. Reverse transcriptase polymerase chain reaction (RT-PCR) has been used as a method for the detection and identification of AIV virus. Although RT-PCR is a sensitive method for detection of AIV, it requires sample preparation including separation and purification of AIV and concentrate viral RNA. It is laborious and complex process especially for diagnosis using faecal sample. In this study, magnetic beads were used for immunoseparation of AIV in chicken faecal sample by a magnetic microsystem. Using this system, all the 16 hemagglutinin (H) and 9 neuraminidase (N) subtypes of AIV were separated and detected in spiked faecal samples using RT-PCR, without an RNA extraction step. This rapid sample preparation method can be integrated with a total analysis microsystem and used for diagnosis of AIV.

Avian influenza virus (AIV) in wild and domestic birds, causes an abundant economic loss and continues to threat a pandemic in human (Peiris et al., 2007; Subbarao and Katz, 2000). AIV is an enveloped RNA virus with eight-segmented single-stranded, negative-sense genome that belongs to the family *Orthomyxoviridae*. The virus is classified into 16 H and 9 N types based on the antigenic properties of two surface glycoproteins; the hemagglutinin (H) and the neuraminidase (N) (Alexander, 2007). The gold standard method used for diagnosis of AIV is virus inoculation. In this method, the sample is inoculated into specific pathogen free (SPF) eggs and incubated for a week or two (Charlton et al., 2009). Conventional RT-PCR (Fouchier et al., 2000) and real-time RT-PCR (Spackman et al., 2002) have been used for amplification and detection of AIV viral RNA. These methods are more rapid and more sensitive than virus inoculation. However, RT-PCR requires sample preparation that involves isolation of virus and extraction of RNA. This sample preparation is a crucial step for removing substances that cause the inhibition of RT-PCR (Peter et al., 2004). To avoid inhibition, extraction of AIV RNA from samples can be performed using commercial kits.

The micro electro mechanical system (MEMS) has been applied at different stages of sample preparation that added in miniaturization and automation of the sample preparation unit (Huang et al., 2002). The application of magnetic bead-labeled biomolecules inside the microfluidics system enhanced the target specific separation (Gijs, 2004). Different approaches have been applied for the automation of sample preparation using magnetic beads. One such system has been developed to purify and concentrate Dengue viruses and detected using RT-PCR (Lien et al., 2007). Conversely, the system was used only for purified analytic target and not a crude sample such as faeces. Faecal sample contains a mixture of complex components which could inhibit the detection of virus if used directly in RT-PCR. A magnetic bead based microsystem is described for rapid sample preparation and purification of AIV from chicken faecal samples and was used directly for RT-PCR.

For immunoassay separation, magnetic beads were coated with monoclonal antibody (mAb) raised against the nucleoprotein of AIV, which is a conserved part in all AIV subtypes. The protein A purified mAb was purchased from Staten Serum Institute (Copenhagen, Denmark). The mAb was conjugated to the magnetic beads covalently, according to the manufacturer's instructions. Briefly, 3 mg of super-paramagnetic polystyrene beads (Ø1.08 μm) (MyOne™ Tosylactivated, Invitrogen, Taastrup, Denmark) were washed twice with 1 ml of 0.1 M sodium borate (coating buffer) using a magnetic separator (Dynal MPC, Invitrogen, Taastrup, Denmark). The beads were re-suspended in a mixture of 685 μl of coating buffer, 415 μl of 3 M ammonium sulphate and 100 μg of mAb (1 mg/ml). The bead suspension was incubated at 37 °C for 24 h using a slow mixing rotor. Later, the beads were blocked by incubation overnight at 37 °C in a blocking buffer of phosphate

* Corresponding author. Tel.: +45 35886892; fax: +45 35886901.
E-mail address: ddba@vet.dtu.dk (D.D. Bang).

0166-0934/$ – see front matter © 2010 Elsevier B.V. All rights reserved.
doi:10.1016/j.jviromet.2010.07.017

Table 1
List of different subtypes of AIV used for the bead based assay.

No.	AIV strains	HA titre
1.	H1N1 A/Duck/Alberta 35/76	1:16
2.	H2N3 A/Duck/Germany/1215/73	1:64
3.	H3N2 – A/Turkey/England/384/79	1:256
4.	H4N6 A/Duck/Czech/56	1:512
5.	H5N1 A/Chicken/Scotland/ 59/67	1:256
6.	H6N8 A/Turkey/Canada/63	1:256
7.	H7N7-2 A/Chicken/Netherland/2993/03	1:128
8.	H8N4 A/Turkey/Ontario/6118/68	1:128
9.	H9N2 A/Turkey wisconsin/3577/66	1:64
10.	H10N4 – A/Turkey/England/384/79	1:512
11.	H11N6 A/Duck/England./56	1:1024
12.	H12N5 A/Duck/Alberta/60/76	1:1024
13.	H13N6 A/Gull/Maryland/704/77	1:256
14.	H14N5 A/Mallard/Gurjev/263/82	1:256
15.	H15N9 A/Shearwater/Australia/2576/79	1:256
16.	H16N3 – A/Gull/Denmark/68110/02	1:128

based saline (PBS) with 0.5% bovine serum albumin (BSA) and 0.05% Tween 20. Finally, the beads were captured and re-suspended in 300 μl of storage buffer containing PBS with 0.1% BSA and 0.05% Tween20 and used for the assay. The presence of mAb on the surface of magnetic beads was tested by enzyme linked immunosorbant assay (ELISA) as described by Sakhalkar et al. (2005) and confirmed (unpublished data).

A microfluidic magnetic microsystem was used for the bead based sample preparation. The design and the manufacture details of the microsystem was described previously (Bu et al., 2007; Smistrup et al., 2008). The microsystem consists of a 200 μm high SU-8 separation chamber with a volume of 10 μl. The magnetic system beneath the separation chamber consists of two parts: The first part is an array of external Nd–Fe–B permanent magnets each with a dimension of 2 mm × 2 mm × 2 mm and a flux density of about 0.3 T at the surface. The second part is an array of integrated permalloy soft magnetic elements buried at the bottom of the separation chamber. These elements are magnetized by the external permanent magnet and the total magnetic force increases up to two orders of magnitude (Smistrup et al., 2008).

To mimic the natural AIV infectious faecal sample, 100 μl of avian influenza virus diluted at 1:100 in PBS was spiked to 900 μl of chicken faecal swab sample that was tested negative for AIV by RT-PCR. Table 1 shows a list of 16 different AIV strains with all AIV subtypes (from H1 to H16 and N1 to N9) that were used for the assays. The list includes both AIV high and low pathogenic viruses. The titres of the 16 viruses using hemagglutination assay (HA) varied from 1:16 to 1:1024 HA units. Fifty μg of magnetic beads coated with mAb was added into 1 ml of the AIV-spiked-faecal sample and the mixture was mixed at room temperature for 30 min.

The magnetic microsystem (Fig. 1) consists of two inlets connected to syringe pumps (model 540060, TSE Systems, Bad Homburg, Germany) and an outlet. For the bead based assay, 1 ml mixture of the bead and faecal sample was introduced into the chip through the inlet 1 at a flow rate of 0.5 ml/min. As the liquid passes through the chamber, the magnetic beads were captured by the magnetic field created in the magnetic microsystem. Fig. 1B shows the microscopic image of the microsystem after magnetic beads were introduced. Three ml of washing buffer (PBS and 0.05% Tween 20) were introduced into the microchamber via inlet 2 at 0.5 ml/min to remove PCR inhibitors and other complex material that were in the faecal sample (Fig. 1A). Finally, the microsystem was de-magnetised by removing the permanent magnets. The removal of the permanent magnets reduced the total magnetic force of attraction to the beads to a great extend. The magnetic beads were collected in 50 μl of washing buffer by pumping out at a flow rate of 1 ml/min (Fig. 1C).

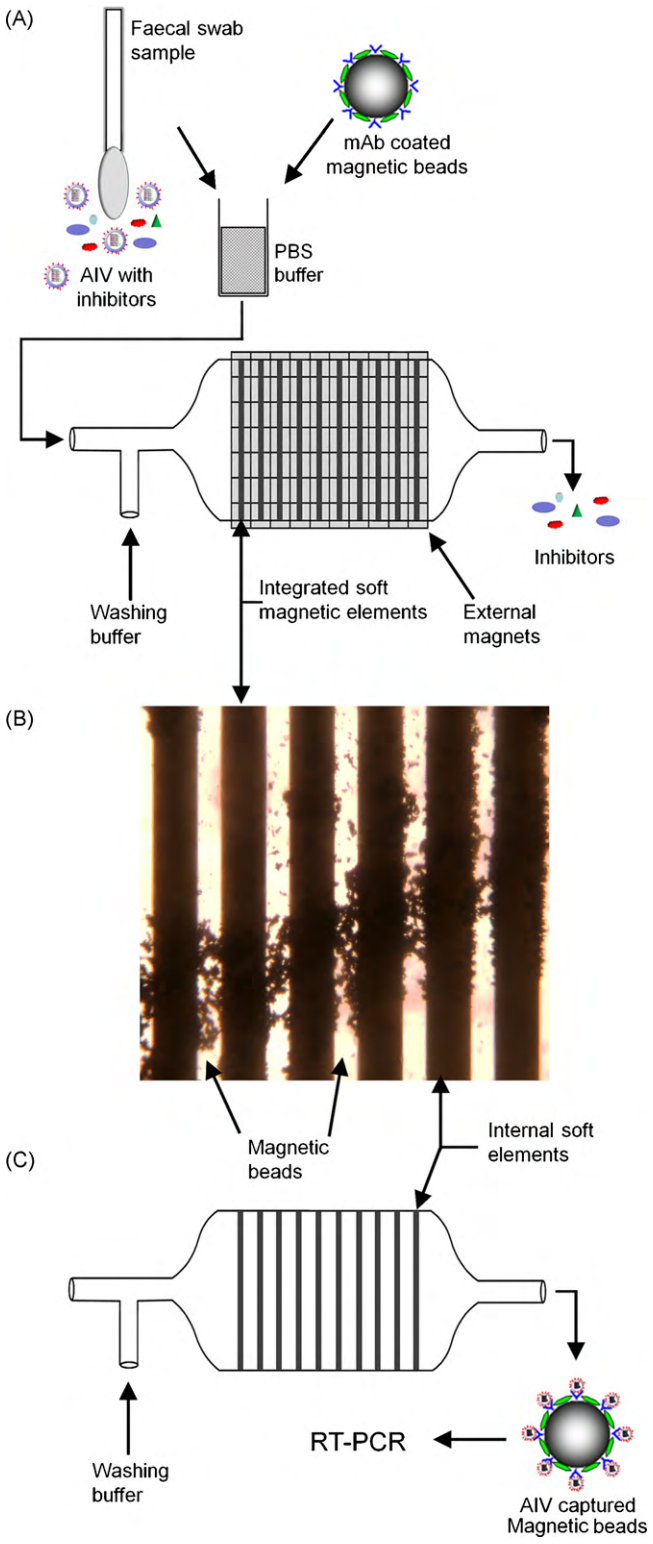

Fig. 1. Sample preparation of AIV using magnetic microsystem. (A) Faecal swab sample was mixed with monoclonal antibody coated magnetic beads and introduced into the chip and later washing buffer used to remove inhibitors. (B) Microscopic image showing internal permalloy magnets and the captured magnetic beads. (C) External magnet was removed and beads were eluted using washing buffer.

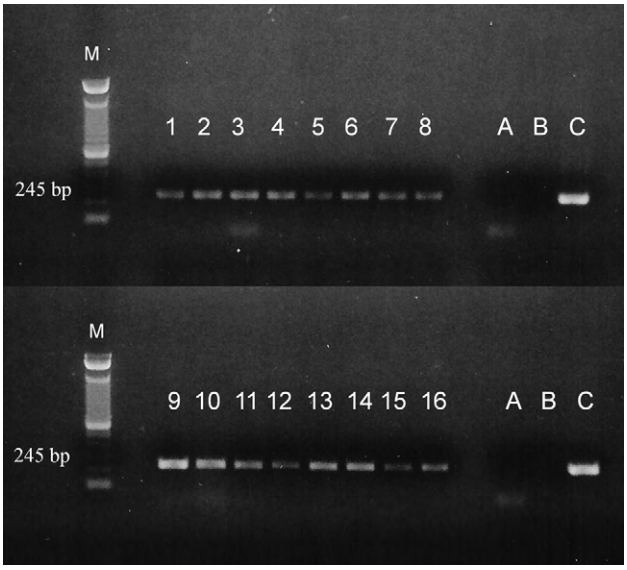

Fig. 2. RT-PCR results for 16 different strains of AIV performed using magnetic bead based microsystem. Lanes 1–16 (number corresponds to Table 1). A, B and C are RT-PCR's master-mix, negative and positive controls, respectively. Marker (M) is a 100 bp DNA ladder (Invitrogen, Taastrup, Denmark).

To avoid cross-contamination after each assay, the microsystem was washed by pumping 4 ml of washing buffer into the chamber at a flow rate of 2 ml/min. The last 50 μl of the washing liquid was collected and tested for the presence of AIV using RT-PCR.

A 25 μl AIV specific RT-PCR with 5 μl of template was used to perform with one step RT-PCR kit (Qiagen, Copenhagen, Denmark). Two primers; the forward primer M52C with sequence 5′-CTTCTAACCGAGGTCGAAACG-3′ and the reverse primer M253R with sequence 5′-AGGGCATTTTGGACAAAKCGTCTA-3′ specific for the matrix gene of AIV reported previously (Fouchier et al., 2000). The templates used for RT-PCR include AIV-captured collected beads; collected washing liquid as well as RNA extractions. The RT-PCR program: 56 °C for 30 min, 95 °C for 15 min, following 40 cycles of 94 °C for 30 sec, 58 °C for 1 min and 72 °C for 1 min and final extension step at 72 °C for 7 min was performed on a thermal cycler (Biometra, Goettingen, Germany). The RT-PCR product was analysed using agarose gel (1.5%) electrophoresis.

The limit of detection for sample preparation of AIV-spiked faecal was determined using magnetic bead based microsystem method and compared with RNA extraction method. A 10-fold serial dilution of H16N3 virus spiked faecal sample was prepared and the dilutions were used for sample preparation in the tube (RNA extraction) and in the magnetic microsystem. The RNA extraction was performed using an RNeasy Kit (Qiagen, Copenhagen, Denmark) in accordance with manufacturer's instruction. Purified RNA was eluted using 50 μl of RNase free water and used as a template for RT-PCR. The RT-PCR results of the assays performed with 16 different AIV strains using the magnetic bead based microsystem method are shown in Fig. 2. The detection limit of sample preparation was determined using the bead based microsystem method as 10^{-3} dilution of H16N3 virus (Fig. 2, lane 16) and it was 100 times lower than the RNA extraction method (10^{-5} dilution).

The bioanalytical microsystems with microfluidics have been developed more than a decade ago but have not yet been successfully applied to the clinical sample due to the requirement of multiple preparing steps (Chen and Cui, 2009). The clinical sample for example, a faecal swab, consists of complex faecal composition, with a fragile target (virus particles) which sometimes insufficient for detection. The extraction and purification of viral RNA of such sample is a big challenge. Tewari et al. (2007) described an automation method for extraction and purification of AIV viral RNA from treacle swab samples using a commercial robotic system (BioRobot M48, Qiagen; Valencia CA) with magnetic beads. Although the use of the robotic system for AIV sample preparation is rapid with no cross-contamination and as good as the use of commercial RNA kit method; the commercial robotic system is expensive (approximately €50,000). In this study, a simple and portable microsystem made by photoresist SU-8 was used with magnetic beads coated with mAb to separate and concentrate AIV in faecal samples.

Nilsson et al. (1996) reported that washing step plays an important role for the effective removal of PCR inhibitor in the bead based assay. In this study, three different flow rates of 0.5, 2 and 4 ml/min were selected for washing. The flow rate of 0.5 ml/min was determined as optimal flow rate and was selected for the assay. At this flow rate the loss of magnetic beads due to the shear force was minimized, while a higher flow rate of 1 ml/min was used for eluting the beads from the chip chamber. Using the magnetic microsystem described in this study, all the subtypes of AIV were separated, concentrated and purified from chicken faecal samples.

The AIV-captured magnetic beads was detected using RT-PCR, without using a viral RNA extraction step (Noroozian et al., 2007) or a pre-heat step to release the viral RNA (Gambley et al., 2009). This could due to the low thermal stability of AIV (Shahid et al., 2009) or the presence of non-ionic detergent (Tween20) which may further enhanced the released of the viral RNA (Singh, 1999). Similar results have been observed with Chikungunya virus (Pastorino et al., 2005).

The specificity of the monoclonal antibody was determined with two viruses which are infectious to avian species: Infectious bursal disease virus (IBDV) and Newcastle disease virus (NDV). In both cases no RT-PCR signal was observed (unpublished data). The robustness of the method was demonstrated by assays with 16 different AIV strains which cover all the 16 H and 9 different N subtypes with varying HA titre. In all cases, the method was completed within 5 h without RNA extraction and purification steps. The microsystem was reused for all the viruses and no cross-contamination occurred after each assay, when a washing step combined with the RT-PCR was performed as control test.

The sensitivity of sample preparation step using the magnetic microsystem is 10^{-3} dilution of the virus (H16N3) for both faecal and allantoic fluidic samples and is lower than the RNA extraction method for faecal sample (in this study) and for allantoic fluid (Cao et al., 2010). Recently, Lien et al. (2007) developed an integrated microRT-PCR system using magnetic beads coated with monoclonal antibody for rapid detection of Dengue virus. Using that system, a sensitivity limit of 10^2 plaque forming unit was obtained for Dengue virus and was comparable to conventional RNA extraction kit. The magnetic bead based microsystem used in this study for virus separation and concentration showed a lower sensitivity than the RNA extraction method. This could be due two reasons (i) after the immuno-magnetic capture step the bead was collected and transferred to the tube to perform RT-PCR, which could have caused the loss of targets during the transportation and (ii) free RNA from disrupted virus in the sample may have contributed to a higher detection limit by the RNA extraction method and might not have been captured in the magnetic bead based method. Therefore, an alternative to increase the detection limit could be to integrate the RT-PCR step in the sample preparation platform and research is in progress.

In conclusion, a rapid, robust and simple method developed for the sample preparation of AIV from chicken faecal samples using a magnetic bead microsystem. The method tested and evaluated with 16 different AIV strains and the microsystem can be reused without cross-contamination. A higher detection limit could be achieved by sample preparation and RT-PCR inside the microsystem. The method can be integrated in a total analysis microsystem and used for diagnosis of AIV.

Acknowledgements

This work was supported by Technical University of Denmark (DTU), food pathogen project no. 8 and grant no. 150627, EU sixth framework program OPTOLABCARD (contract no. 016727) and EU seventh framework LABONFOIL (contract no. 224306) projects.

References

Alexander, D.J., 2007. An overview of the epidemiology of avian influenza. Vaccine 25, 5637–5644.

Bu, M., Christensen, T.B., Smistrup, K., Wolff, A., Hansen, M.F., 2007. Characterization of a microfluidic magnetic bead separator for high-throughput applications. Sens. Actuators A 145–146, 430–436.

Cao, C., Dhumpa, R., Bang, D.D., Ghavifekr, Z., Hogberg, J., Wolff, A., 2010. Detection of avian influenza virus by fluorescent DNA barcode-based immunoassay with sensitivity comparable to PCR. Analyst 135, 337–342.

Charlton, B., Crossley, B., Hietala, S., 2009. Conventional and future diagnostics for avian influenza. Comp. Immunol. Microbiol. Infect. Dis. 32, 341–350.

Chen, X., Cui, D.F., 2009. Microfluidic devices for sample pretreatment and applications. Microsyst. Technol. 15, 667–676.

Fouchier, R.A.M., Bestebroer, T.M., Herfst, S., Van Der Kemp, L., Rimmelzwaan, G.F., Osterhaus, A.D.M.E., 2000. Detection of influenza A viruses from different species by PCR amplification of conserved sequences in the matrix gene. J. Clin. Microbiol. 38, 4096–4101.

Gambley, C.F., Geering, A.D.W., Thomas, J.E., 2009. Development of an immunomagnetic capture-reverse transcriptase-PCR assay for three pineapple ampeloviruses. J. Virol. Methods 155, 187–192.

Gijs, M.A.M., 2004. Magnetic bead handling on-chip: new opportunities for analytical applications. Microfluid Nanofluid 1, 22–40.

Huang, Y., Mather, E., Bell, J., Madou, M., 2002. MEMS-based sample preparation for molecular diagnostics. Anal. Bioanal. Chem. 372, 49–65.

Lien, K.Y., Lin, J.L., Liu, C.Y., Lei, H.Y., Lee, G.B., 2007. Purification and enrichment of virus samples utilizing magnetic beads on a microfluidic system. Lab. Chip 7, 868–875.

Nilsson, H.-O., Aleljung, P., Nilsson, I., Tyszkiewicz, T., Wadström, T., 1996. Immunomagnetic bead enrichment and PCR for detection of Helicobacter pylori in human stools. J. Microbiol. Methods 27, 73–79.

Noroozian, H., Vasfi Marandi, M., Razazian, M., 2007. Detection of avian influenza virus of H9 subtype in the faeces of experimentally and naturally infected chickens by reverse transcription-polymerase chain reaction. Acta Vet. BRNO 76, 405–413.

Pastorino, B., Bessaud, M., Grandadam, M., Murri, S., Tolou, H.J., Peyrefitte, C.N., 2005. Development of a TaqMan RT-PCR assay without RNA extraction step for the detection and quantification of African Chikungunya viruses. J. Virol. Methods 124, 65–71.

Peiris, J.S.M., de Jong, M.D., Guan, Y., 2007. Avian influenza virus (H5N1): a threat to human health. Clin. Microbiol. Rev. 20, 243–267.

Peter, R., Rickard, K., Petra, W., Maria, L., Charlotta, L., 2004. Pre-PCR processing: strategies to generate PCR-compatible samples. Mol. Biotechnol. 26, 133–146.

Sakhalkar, H.S., Hanes, J., Fu, J., Benavides, U., Malgor, R., Borruso, C.L., Kohn, L.D., Kurjiaka, D.T., Goetz, D.J., 2005. Enhanced adhesion of ligand-conjugated biodegradable particles to colitic venules. FASEB J., 04-2668fje.

Shahid, M., Abubakar, M., Hameed, S., Hassan, S., 2009. Avian influenza virus (H5N1); effects of physico-chemical factors on its survival. Virol. J. 6, 38.

Singh, R.P., 1999. A solvent-free, rapid and simple virus RNA-release method for potato leafroll virus detection in aphids and plants by reverse transcription polymerase chain reaction. J. Virol. Methods 83, 27–33.

Smistrup, K., Bu, M., Wolff, A., Bruus, H., Hansen, M., 2008. Theoretical analysis of a new, efficient microfluidic magnetic bead separator based on magnetic structures on multiple length scales. Microfluid Nanofluid 4, 565–573.

Spackman, E., Senne, D.A., Myers, T.J., Bulaga, L.L., Garber, L.P., Perdue, M.L., Lohman, K., Daum, L.T., Suarez, D.L., 2002. Development of a real-time reverse transcriptase PCR assay for type A influenza virus and the avian H5 and H7 hemagglutinin subtypes. J. Clin. Microbiol. 40, 3256–3260.

Subbarao, K., Katz, J., 2000. Avian influenza viruses infecting humans. Cell. Mol. Life Sci. 57, 1770–1784.

Tewari, D., Zellers, C., Acland, H., Pedersen, J.C., 2007. Automated extraction of avian influenza virus for rapid detection using real-time RT-PCR. J. Clin. Virol. 40, 142–145.

6.3 On-chip sample preparation and RT-PCR for detection of avian influenza virus from chicken faecal sample

6.3.1 Introduction

The magnetic bead based sample preparation has been developed successfully both in-tube and in a magnetic microsystem. However, the RT-PCR amplification steps are performed using a conventional thermocycler which is time consuming (3h 15min). This project aimed to reduce total amplification time by using integrated microfluidic devices for both sample preparation and RT-PCR amplification (Figure 6.3.1). As discussed in Chapter 5, there is an expanding use of polymers in microfabrication, due to its simplicity in fabrication methods and low cost, making it popular for various applications.

In this project, two microfluidic chips made of a) SU-8 and b) Cyclic olefin copolymers (COC) were tested for RT-PCR amplification of the AIV. The SU-8 chip was also tested for sample preparation. These chips were from the EU projects, OPTOLABCARD [158] and LABONFOIL [159]. The performance of a miniaturized RT-PCR was first developed in-tube and later transferred to the chips. The biocompatible effects of the surface of the SU-8 chips on RT-PCR reaction have been addressed and characterized.

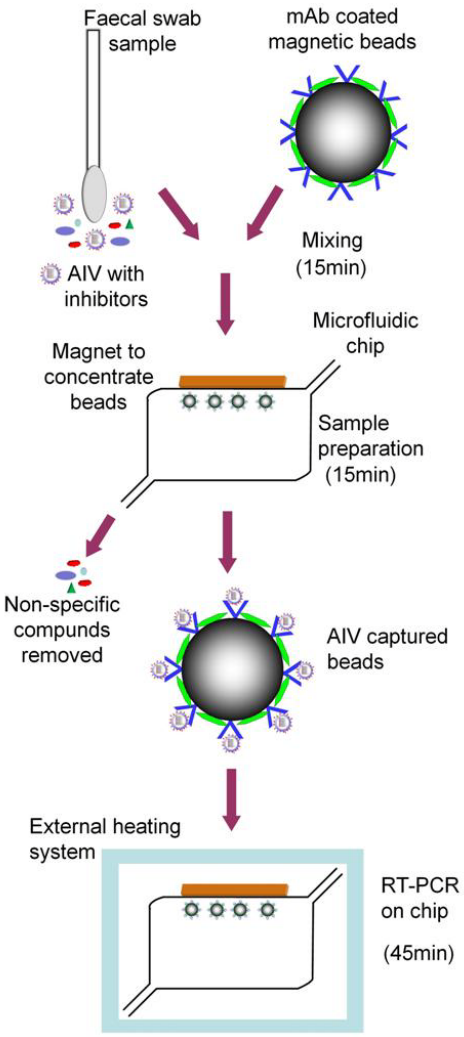

Figure 6.3.1 Scheme of integrated microfluidic system for sample preparation of AIV from chicken faecal swab sample using magnetic beads followed by RT-PCR on chip.

6.3.2 SU-8 Chip

SU-8 is an epoxy-based negative photoresist polymer that has been commonly used to transfer a pattern in a thin film during photolithography. It is also being used recently as structural materials in micro and nanotechnologies[160]. The SU-8 chip used in this study was fabricated based on a method applying bonding and releasing of photo-patterned SU-8 layer that creates multilayer microfluidic structures [161]. The microfluidic or PCR chamber is 3x5.4x0.2 mm (WxLxH) and has a chamber volume of 3 µl. The chamber was bonded on a Pyrex substrate which consists of an integrated resistive Ti/Pt sensor and heaters with parallel heat elements (Figure 6.3.2 right).

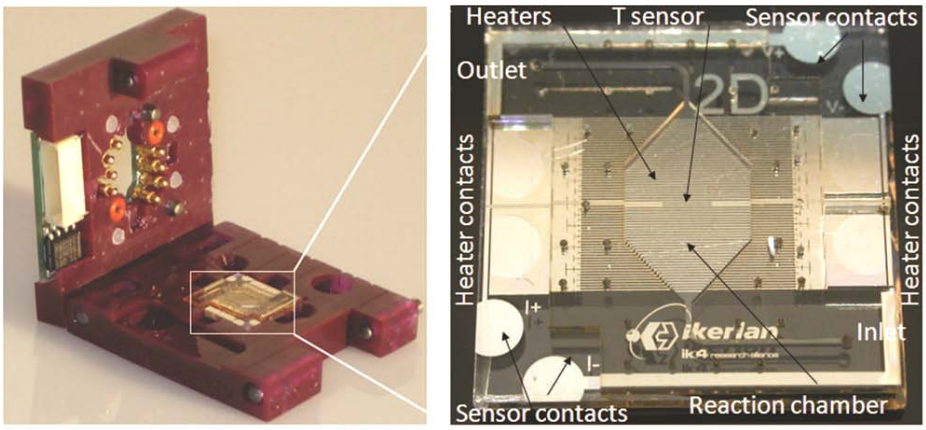

Figure 6.3.2 Pictures of the OPTOLABCARD LOC system; capsule (left) and the SU-8 PCR chip (right)[162]

The PCR chip is placed into a reusable package or capsule establishing full electric and fluidic connections to the macro world without the need of adhesives or wirebonding. This allows an easy replacement of the used chips, forming a disposable portable LOC device. The package is connected to a PCR controller, which acts as a data acquisition system, and the controller is connected to a computer. The computer with specific software controls the parameters of the thermocycling on the chip.

6.3.2.1 Materials and Methods

Sample preparation on SU-8 chip: The sample preparation step was performed using magnetic beads(1 µm) coated with mAb as described previously (See section 6.2 *Conjugation of antibody to magnetic beads*). To 100 µl of allantoic fluid containing H16N3 virus, 50 µg magnetic beads coated with mAb were added and mixed for 30 min at room temperature using a rotor. The magnetic particles in the mixture were concentrated to 5 µl volume using a magnetic particle concentrator (MPC-1, Invitrogen, Taastrup, Denmark). The mixture of beads and viruses were transferred into the chamber of the chip by a pipette. Magnetic elements were placed at the top and bottom of the chip. The chip was placed into the chip holder (fig 6.3.3 a) with an inlet connected to a syringe pump containing washing buffer (10 mM PBS and 0.05% Tween 20) (Figure 6.3.3.b).

a) 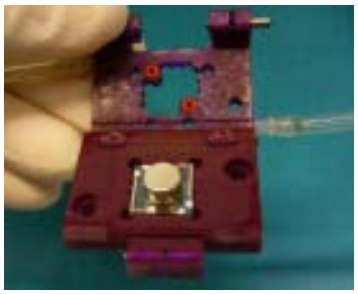 b) 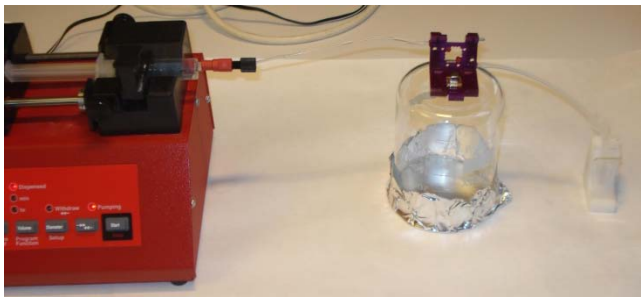

Figure 6.3.3 Set up for sample preparation using SU-8 chip a) SU-8 placed in a chip holder with a magnet placed on top to capture magnetic beads[158]. b) The chip holder was connected to a syringe pump system for the washing step.

For the SU-8 chips; optimal flow rate of washing step for removing unbounded virus and other PCR inhibitors was determined. Three different flow rates of 0.25 ml/min, 0.5 ml/min and 1 ml/min were tested. For each wash, a total of 2 ml of the washed buffer was collected in 8 aliquots of 250 µl each. After the wash, the magnetic elements were removed. The mixture of liquid containing beads inside the chamber was collected and tested for AIV using RT-PCR in-tube.

RT-PCR reaction: A one-step RT-PCR mixture of 25 µl with 5 µl of template was used as described in Section 6.2. A primer set namely M2 consisting of a forward primer with sequences 5'-CY5-AGA TGA GTC TTC TAA CCG AGG TCG-3' and a reverse primer with

sequence 5'-TGC AAA AAC ATC TTC AAG TCT CTG-3' specific for the matrix gene of the AIV was used.

Miniaturization in-tube: For miniaturization of the RT-PCR, a commonly used RT-PCR volume of 25 µl containing 5 µl of AIV RNA (H16N3) was reduced to 3 µl volume and tested for in-tube RT-PCR amplification using conventional thermal cycler (Biometra, Goettingen, Germany). The required time for each step in the PCR thermocycler was reduced and tested for the performance of the miniaturization. The miniaturization was first tested with RNA (AIV) and later with the magnetic bead captured virus. The sensitivity of the in-tube miniaturized RT-PCR (3 µl) was determined using a 10-fold serial dilutions of the AIV. Due to the small volume of the RT-PCR amplified products, the end point analysis of the RT-PCR was performed on a Bioanalyzer 2100 (Santa Clara, CA, USA) using DNA1000 chip.
In addition, different final volumes of 50 µl to 25 µl and 5 µl of the bead suspension in the sample preparation step were also tested for RT-PCR in 3 µl in-tube.

RT-PCR on SU-8 chip

The SU-8 chip was loaded with RT-PCR reaction mixture with template (RNA from H16N3 virus) and introduced into a capsule. This capsule is connected to a small device capable of generating the thermocycling steps (Figure 6.3.4).

a) b)

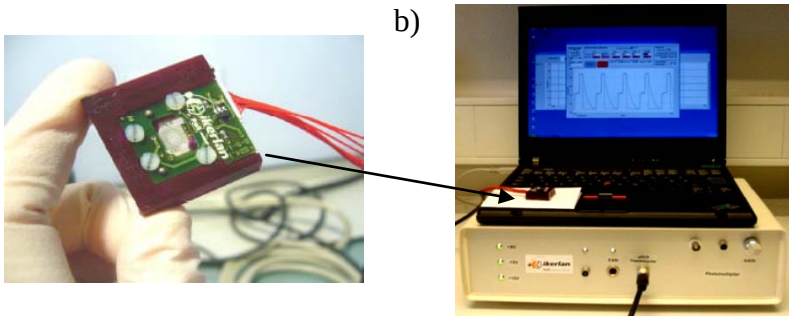

Figure 6.3.4 The experimental setup for RT-PCR. a) SU-8 chip in a capsule[158] and (b) the capsule connected to a computer controlled thermocycling system.

Preliminary results for RT-PCR on-chip showed no PCR amplification (inhibition) while the same reaction mixture was amplified in-tube. To address this inhibition effect the following studies were performed.

Surface treatment: The surface of SU-8 chip was treated with BSA before RT-PCR reaction. BSA solution (10 mg/ml) was made from crystallized BSA dissolved in PBS buffer and filtered using 0.22µm filter. Two approaches: static and dynamic were performed to reduce the effect of inhibition. In the static approach, various concentrations of BSA solution of 10 mg/ml, 1 mg/ml and 0.1 mg/ml were prepared. The BSA was introduced into the chip and incubated at room temperature for 1 h. The BSA was removed and the chip was dried at 37^{o}C for 1h. Later the chip was used for RT-PCR. In the dynamic approach, 1 µl of BSA (1 mg/ml) was added to the RT-PCR reaction mixture and tested.

RT-PCR conditions: The concentration of enzyme mix for RT-PCR was doubled in the RT-PCR reaction mixture and tested for amplification on both tube and chip. To test the inhibition by ribonucleases, 1 µl of RNAse inhibitor (Invitrogen, Taastrup, Denmark) was added to the reaction mixture of RT-PCR and tested.

To further investigate the mechanism by which RT-PCR amplification was inhibited, the components of the RT-PCR reaction such as RNA and enzyme mix (RT & TAQ) were tested individually. Chip control:

a) RT-PCR reaction mixture was incubated inside the chip for 1min at room temperature and the mixture was transferred to a tube and RT-PCR amplification was performed in-tube.
b) RNA from H16N3 virus was incubated inside the chip for 1 min at room temperature and used as a template for RT-PCR.
c) RT-PCR enzyme mix (without template) was incubated inside the chip for 1 min at room temperature and RNA was added later and tested for amplification

6.3.2.2 Results and discussions

Sample preparation on SU-8 chip

Figure 6.3.5 shows results for sample preparation on SU-8 using three flow rates a) 0.25 ml/min, b) 0.5 ml/min and c) 1 ml/min. The RT-PCR signals for the aliquots collected from the washing step shows a decrease in the intensity of signals indicating the efficient removal of unbounded

virus from the chip, while a positive signal was observed from the elution of beads (Figure 6.3.5 a, b, c lane 6). The rate at which the unbound viruses were removed was dependent upon the flow rate of the washing buffer. At the flow rate of 0.25 ml/min (Figure 6.3.5 a, lane 6), there were still some unbound viruses present in the final washing aliquot, indicating the need for additional washing step where as at the higher flow rate of 1 ml/min (Figure 6.3.5 c) the unbound viruses were totally removed after a few washing steps (Figure 6.3.5 c lane 3, 4). Similar with the flow rate of 0.5 ml, the unbound viruses were totally removed after 7 washing steps (Figure 6.3.5 b lane 5).

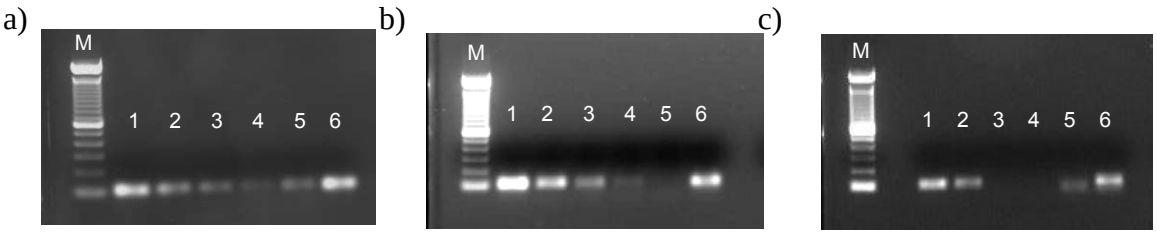

Figure 6.3.5 RT-PCR results for sample preparation on SU-8 using three flow rates a)0.25 ml/min, b) 0.5 ml/min and c) 1 ml/min. Lanes number 1 to 5 represent the washed buffer aliquot (250 µl) of 1, 3, 5, 7 and 8. Lane 6 corresponds to extracted beads from the chip. Marker (M) is a 100 bp DNA ladder (Invitrogen, Taastrup, Denmark).

Determination of shear forces in SU-8 Chamber

The fluidic flow inside the chamber generates a parabolic laminar flow profile which removes inhibitors and unbound virus in the sample and also creates a fluidic drag forces on the virus-bound bead (Figure 6.3.6). In the parabolic flow profile, the flow velocity (V_f) is characterized by a parabolic velocity distribution where the centerline velocity is 1.5 x the linear flow velocity:

$$V_f = 1.5\frac{Q}{wh}\left(1 - \left(\frac{d-h/2}{h/2}\right)^2\right) \qquad (1)$$

where Q is the volumetric flow rate, w and h are the width (3mm) and height (0.2 mm) of flow chamber, d distance(1.05µm) between the center of the virus particle to the wall of the chamber. As the magnetic bead are close to the channel wall (d<<h) the quadratic term in Eqn (1) can be linearly approximated[163;164], resulting a velocity profile known as plane shear flow:

$$V_f = 1.5\frac{Q}{wh}\left(4\frac{d}{h}\right) = 6\frac{Q}{wh}\frac{d}{h} \qquad (2)$$

For the three flow rates of 0.25, 0.5 and 1 ml/min, the flow velocities inside the chamber at the virus-bead position were 0.88, 1.75 and 3.5, mm/sec.

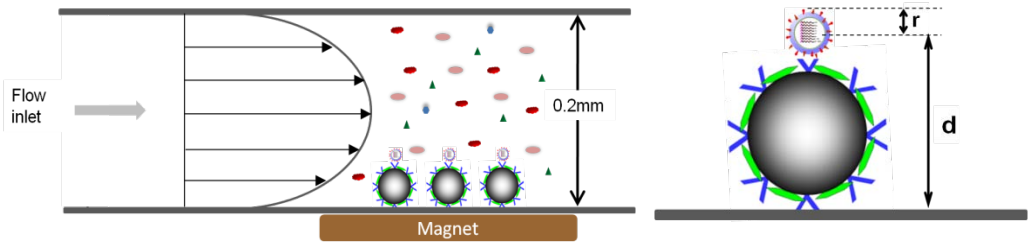

Figure 6.3.6 shows the cross section side view of the flow channel (not to scale).

The shear force on the virus particle can be calculated with equation (2) according to a model by Goldman and co-workers[165]. The force depends on the viscosity (η) of the buffer (1mPa s), radius(r) of virus particle (0.05µm) and the flow velocity (V_f) at the level of the particle center.

$$Fs=Fs*6\pi\eta r\, V_f \qquad (3)$$

Fs* is a function (Tabulated in [165]) of the ratio of distance between the center of the virus particle above the wall(d) and the radius of the particle. Since the ratio is high (21), the Fs* value taken as 1 for the calculation. The shear force on the virus-bead bound for the three flow rates of 0.25, 0.5 and 1 ml/min were 0.85, 1.7 and 3.4 pN respectively. Although the calculated shear force (3.4pN) for the highest flow rate (1ml/min) was approximately 10times lower than the single-bond rupture forces for IgG and protein (35pN)[166], the effective bond strength of virus on the surface of bead can be much lower (56 times) due to the applied tangential or shear forces[167]. So an optimal flow rate of 0.5 ml/min was selected for the sample preparation to minimize the shear force on the virus-bound bead.

In-tube RT-PCR miniaturization

Figure 6.3.7 shows the result of 3 µl RT-PCR reaction. The quantity of PCR product for the 3 µl volume was determined as 14.12±1.83 ng/µl and that was similar to the result (14.41±3.1 ng/µl)

of the RT-PCR 25 µl volume. Two peaks (double band)of PCR products of 107 bp and 116 bp were observed in the Bioanalyzer graph probably due to CY5 (dye) conjugation to the DNA and this effect was studied earlier by Carisson et al. 1995[168] by gel electrophoresis and later by Tu et al. 1998[169] by capillary electrophoresis.

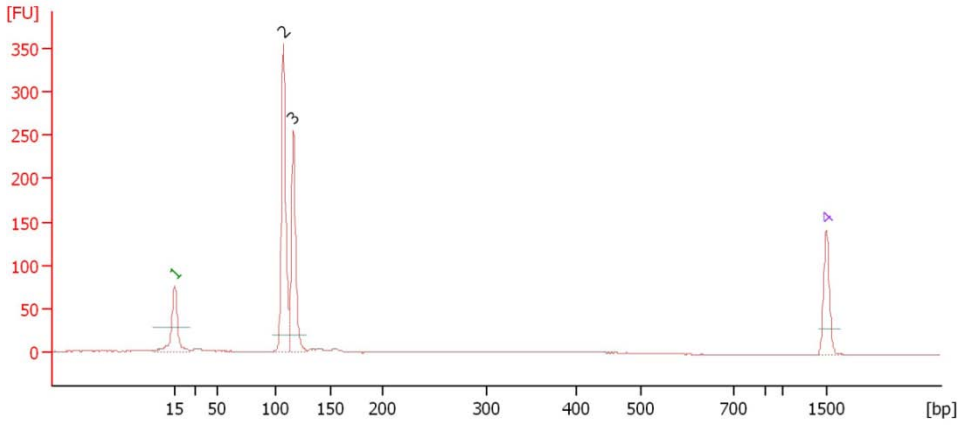

Peak table for sample : H16N3 RNA

Peak	Size [bp]	Conc. [ng/µl]	Molarity [nmol/l]	Observations
1	15	4.20	424.2	Lower Marker
2	107	9.09	128.9	
3	116	6.61	86.6	
4	1,500	2.10	2.1	Upper Marker

Figure 6.3.7: Bioanalyzer graph of RT-PCR amplification of 3 µl reaction volume

In-tube miniaturized RT-PCR with magnetic bead captured virus

As a first step toward on-chip RT-PCR, the developed miniaturized RT-PCR with magnetic bead captured virus as template was performed in-tube. Although with a high volume of the magnetic beads in the RT-PCR reaction mixture, a PCR amplicon of 110bp was observed. Furthermore, there is no significant difference in the RT-PCR amplification efficiency when the miniaturized RT-PCR performing with the three different re-suspension volumes of 5 µl, 25 µl and 50 µl of the beads.

Table 6.3.1 shows a comparison of the required time of a conventional RT-PCR and the miniaturized RT-PCR using one-step RT-PCR kit from Qiagen (Germany). Using the miniaturized RT-PCR, the total time was reduced from 3h 15min to 1h 20min (Table 6.3.1). The fast thermocycling was possible because of the low reaction volume (3 µl) and thus better heating/cooling rates. During this process, the time required for the activation step was critical

since a decrease of 5 min in this step was drastically reduced the amplification efficiency up to 20%.

Table 6.3.1: Comparison of amplification time required for RT-PCR using one-step Qiagen kit with conventional and miniaturized.

	Conventional		**Miniaturized**	
	Temperature	Time	Temperature	Time
RT	56^{o}C	30min	56^{o}C	15min
Activation	95^{o}C	15min	95^{o}C	15min
Denature	94^{o}C	30sec	94^{o}C	1sec
Annealing	58^{o}C	1min	54^{o}C	5sec
Extension	72^{o}C	1min	72^{o}C	5sec
Number of cycles	40			
Final extension	72^{o}C	7min	72^{o}C	3min
Total time		3h 15min		1h 20min

A sensitivity test of the miniaturized RT-PCR (3 µl) in-tube was performed with the miniaturized thermocycling time and the results are shown in Figure 6.3.8. The sensitivity for the 3 µl miniaturized RT-PCR was determined as low as 10^{-5} dilution corresponding to H16N3 virus and was found to be similar to the larger volume (25 µl).

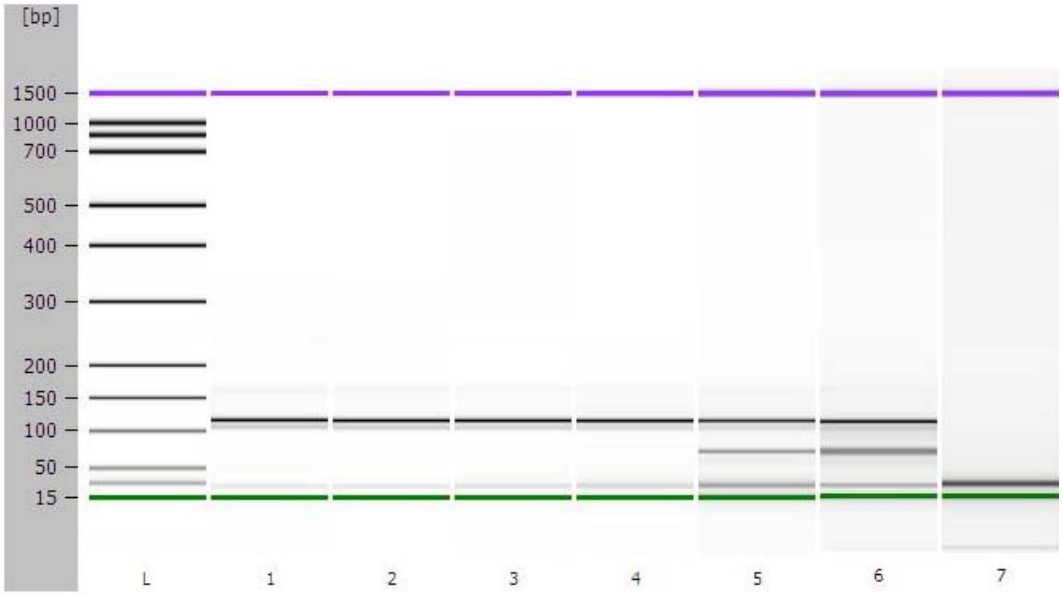

Figure 6.3.8: The sensitivity of RT-PCR with RNA from H16N3 virus as template. Lanes number 1 to 7 represent dilution of series of virus from 10^0 to 10^{-6} of virus and 'L' corresponds to the ladder.

RT-PCR on SU-8 chip

Figure 6.3.9 shows a measured temperature profile of a SU-8 chip during the PCR cycles using the OPTOLABCARD Lab-on-a-chip system. It took 4 s for heating from 54°C to 72°C with a 4.5°C /s heating rate. For raising temperature from 72 °C to 94 °C, generally 6 s are needed, with a rate of 3.66°C /s. Thus, the average heating rate for the two steps was 4.08°C/s while the cooling rate from 94 °C to 54°C was 1.52°C/s. The cooling rate of the chip was slower than the heating rate due to passive cooling process, and can be improved by connecting an additional cooling fan to the microcontroller.

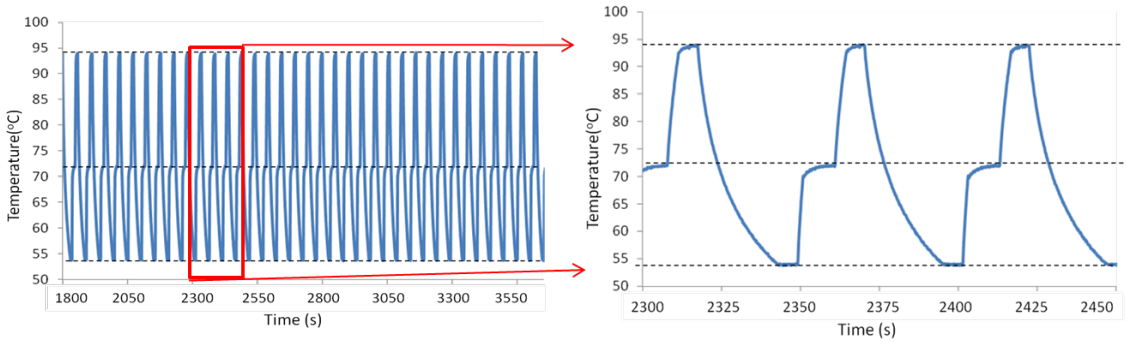

Figure 6.3.9: Measured temperature profile of the RT-PCR during the PCR thermocycles using OPTOLABCARD lab-on-a-chip system.

The entire RT-PCR amplification was performed within 45 min. However, preliminary results of on-chip RT-PCR amplification showed PCR inhibition effects i.e., no PCR amplification product was observed. It has been shown that miniaturization of RT-PCR or PCR often causes PCR inhibition due to the high surface-to-volume ratio (SVR) that increases the significance of the surface chemistry in RT-PCR[139]. In addition, the components of RT-PCR such as Taq polymerase often adsorb non-specifically on the surface of the chip and cause no amplification[170]. To avoid the PCR inhibition effects, the chip surface is treated chemically or pre-coated with a bio-compatible substance during fabrication process or immediately before use [134] . The substances such as bovine serum albumin (BSA), polyethylene glycol (PEG) or

silanizing agents (for example dichlorodimethy-lsilane (DCMDS), or trimethylchlorosilane) [139;171] are the most common substances that were used to obtain the bio-compatible of the chips. In this study, BSA was selected for the surface treatment as it has been proved to significantly improving the PCR efficiency for SU-8 material [171].

Figure 6.3.10 shows the results for different approaches (see Materials and Methods) used to study the PCR inhibition effect. PCR inhibitions were observed when an untreated surface SU-8 chip was used and also when increasing the concentration of enzyme mix (2X) to encounter its adsorption on the chip surface. Similar PCR inhibition effects were observed when the surface was treated with BSA according to the static approach where three different concentrations of 10 mg/ml, 1 mg/ml and 0.1 mg/ml and as well as the dynamic approach was applied. A total number of 6 SU-8 chips tested and 3 chips (50% 3/6) showed primer dimmer (PD) (Figure 6.3.10, lane 4).

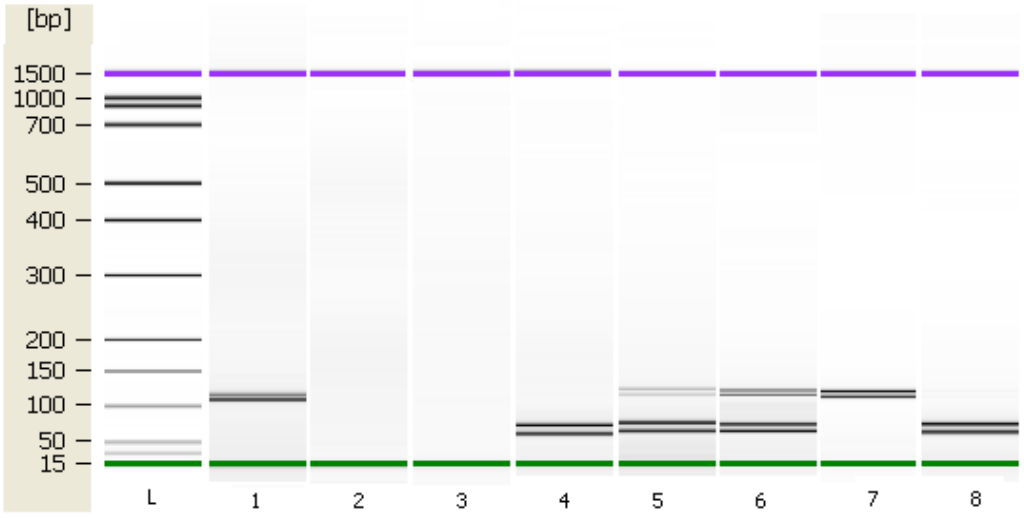

Figure 6.3.10: Gel Chart of Bioanalyzer showing the different approaches used to study RT-PCR inhibition study. Lane 1 positive control (in-tube). RT-PCR performed on SU-8 chip 2) untreated surface, 3) untreated surface with 2X enzyme mix, 4) BSA treated, 5) RT-PCR reaction with RNase inhibitor and BSA (1 mg/ml) and 6) chip control. RT-PCR in-tube with 7) RNA incubated on-chip and 8) RT-PCR master mix incubated on-chip. ‘L’ corresponds to the marker.

The PD's are formed due to the weak interactions occurring between the primers and in the absence of template (cDNA), the inter-primer extension takes place due to the highly processivity of Taq polymerase[172;173]. The formation of PD is used as an internal control of amplification[174] and the failure to amplify the PD have been identified as the presence of inhibitors[175]. This phenomenon of PD formation was observed when chips were treated with BSA indicating the existence of amplification step and the presence of cDNA synthesis. When further testing was made by adding RNase inhibitor to the PCR mixture a weak PCR positive signal with a reduction of PCR efficiency (Figure 6.3.9 lane 5) compared to the positive control (Figure 6.3.10 lane 6) was observed. This indicates that the RT-PCR reaction mixture inside the SU-8 chip chamber quickly deteriorates by an unknown factor.

Since RT-PCR giving a positive band when performed with RNA as template pre-incubated inside the chip and a negative band (only PD) while using the RT-PCR master mix pre-incubated inside chip, this results confirms the instability of RT enzyme presence inside the SU-8 chip.

6.3.2.3 Conclusion

The miniaturization of RT-PCR in-tube to detect AIV has been performed successfully. However, the attempt to miniaturize on SU-8 chip using OPTOLABCARD lab-on-a-chip system has failed due to the PCR inhibition that caused by the SU-8 chip surface-effect. The efforts to address the inhibition for improving the RT-PCR efficiencies were often inconsistent and not always comparable to those of conventional in-tube RT-PCR. Conversely, the same system has been applied for PCR rapid detection of *Campylobacter* spp. directly from chicken faeces with high sensitivity (0.7 – 7 pg DNA /µl)[176]. An improvement in the system can be made with the availability of sufficient information on chip fabrication chemical materials and the reduction of the batch-to-batch variation.

6.3.3 RT-PCR to detect AIV using COC-chip

Cyclic-Olefin-Copolymer is a new group of polymers that has been introduced as a promising plastic substrate for microfluidic devices[177]. The fabrication of COC devices is inexpensive and compatible with mass production. In this study, COC chips were fabricated by milling and thermal bonding. The chips were used to test the ability of the chip for performing AIV RT-PCR amplification steps. The chip has dimensions of 4x6x0.42mm (WxLxH) with a volume capacity of 10 µl. For thermocycling, the chip was placed on the miniaturized thermocycler-chip holder made of Pyrex substrate with integrated resistive Ti/Pt sensor and heat elements (Figure 6.3.11).

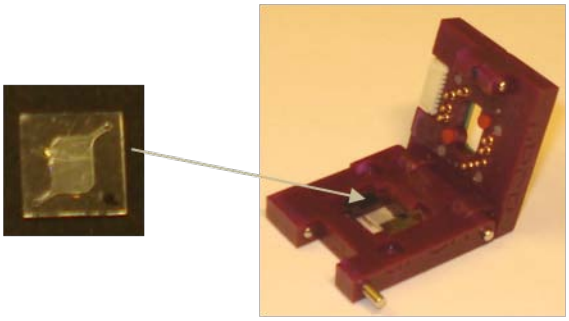

Figure 6.3.11 Pictures of COC PCR chip (left) and the capsule (right).

6.3.3.1 Materials and Methods

RT-PCR reaction

The one-step RT-PCR reactions were carried out using SuperScript III Platinum One-Step-PCR (Inivtrogen, Taastrup, Denmark). A 20 µl reaction mixture was prepared containing 6 µl of nuclease-free water, 12.5 µl of RT-PCR buffer, 0.5 µl of each primer (50 pmole) and 0.5 µl of Superscript III/Platinum *Taq* enzyme mix. To the reaction mixture 5 µl of RNA extracted from H16N3 was added. The primer set M1 targeting matrix gene of AIV that was described previously in section 6.2 was used. The RT-PCR cycling conditions were: 56°C for 15min, 95°C for 2 min followed by 40 cycles of 94°C for 2 s, 58°C for 5 s, and 72°C for 5s and finally 72°C for 3min. The RT-PCR product was analyzed with 1.5% (w/v) agarose gel electrophoresis.

RT-PCR on COC chip

The RT-PCR reaction was performed on COC chips using the miniaturized thermocycler-chip holder with integrated heaters and microcontroller (see figure 6.3.4) and compared with COC chips using a flat-bed thermocycler (MJResearch, MA, USA). The inlet/outlet of the COC chips used in flat-bed was sealed with PCR-tape (Abgene House, Surrey, UK). For positive control, a miniature in-tube (10µl) RT-PCR was used.

6.3.3.2 Results and discussions

The RT-PCR on COC-chip using miniaturized thermocycler-chip holder showed a heating/cooling rate similar to that of the SU-8 chip. The RT-PCR reaction was completed in 45 min using miniaturized thermocycler and the results are shown in Figure 6.3.12.

.

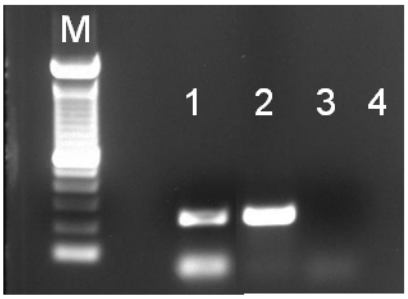

Figure 6.3.12: Gel electrophoresis image of RT-PCR performed with RNA (H16N3) as template. On gel: lane 1) RT-PCR on-COC chip using miniaturized thermocycler, lane 2) chip control; lane 3) positive control miniaturized in-tube and lane and lane 4) Negative control (tube). Marker (M) is a 100bp DNA ladder

The RT-PCR was performed successfully on COC chip (Figure 6.3.12, Lane 1). To compare the efficiency of RT-PCR amplification on-COC chip and in tube, their fluorescent intensity was quantified using ImageJ software (National Institute of Health, USA). The on-chip RT-PCR showed a weak signal 43.52%, (6812.64) compared to positive control (15652).

To investigate the reason for the weak signal from the on chip RT-PCR using the miniaturized thermocycler, the on COC chip RT-PCR was performed using flat-bed thermocycler and the results of this test are shown in Figure 6.3.13.

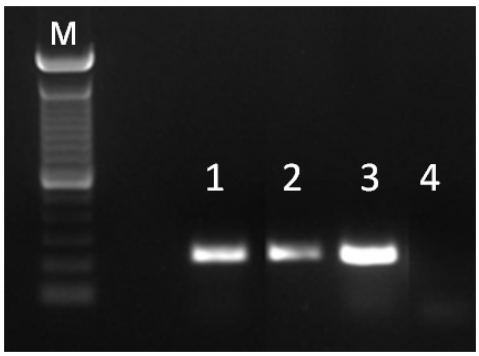

Figure 6.3.13: Gel electrophoresis of on COC chip RT-PCR results. On gel: Lane 1)on COC chip RT-PCR using flat bed thermocycler, Lane 2) on COC chip RT-PCR using miniaturized thermocycler 3) RT-PCR positive control (in-tube) and 4) negative control (in-tube).

For the same RT-PCR reaction mixture, the COC chip on flat-bed showed stronger signal 72.71% (12671.95) than miniaturized thermocyler 50.87% (8865.30) and in all cases the RT-PCR in-tube showed superior results (17425.05). The difference in the efficiency of RT-PCR could be due to the low thermal conductivity of COC material and the heating system.

6.3.3.3 Conclusion

The preliminary results of on COC chip RT-PCR show the possibility of using the system for rapid detection of AIV in less than two hours. However the system needs to be optimized further for efficient amplification and integration of sample preparation.

Chapter 7

Solid-phase DNA microarray

This chapter focuses on the development of a DNA microarray based solid-phase PCR platform for sub-typing of AIV. This approach overcomes a limitation of real-time RT-PCR in sub-typing a number of targets, e.g. H5&H7 subtypes of the AIV, simultaneously. The developed solid-phase RT-PCR method was incorporated into a microchip to reduce the sample volume and detection time from 2h to 1h. Subtyping of all the 16 HA types of the AIV is essential for identification of circulating AIV strains that have recently emerged as a pandemic influenza virus. The development of a method for sub-typing of all the 16 HA types of the AIV is presented in the last part of this chapter where preliminary results in designs of primers and probes for simultaneous HA subtyping (H1-H16) and the use of the designed probes and primers for AIV subtyping are presented and discussed.

7.1 DNA Microarray Based Solid Phase RT-PCR for Rapid Detection and Identification of Avian Influenza Virus

Manuscript published in Diagnostic Microbiology and Infectious Diseases (2011), 69, 432–439.

Available online at www.sciencedirect.com
ScienceDirect
Diagnostic Microbiology and Infectious Disease 69 (2011) 432–439
DIAGNOSTIC MICROBIOLOGY AND INFECTIOUS DISEASE
www.elsevier.com/locate/diagmicrobio

DNA microarray-based solid-phase RT-PCR for rapid detection and identification of influenza virus type A and subtypes H5 and H7☆

Yi Sun[a], Raghuram Dhumpa[b], Dang Duong Bang[b], Kurt Handberg[c], Anders Wolff[a,*]

[a]DTU Nanotech, Department of Micro- and Nanotechnology, Technical University of Denmark, Ørsteds Plads, DK-2800 Kgs. Lyngby, Denmark
[b]Laboratory of Applied Micro-Nanotechnology, Department of Poultry, Fish and Fur Animals, National Veterinary Institute, Technical University of Denmark, Aarhus, Denmark
[c]Laboratory of Avian Influenza Virus, National Veterinary Institute, Technical University of Denmark (DTU), Aarhus, Denmark

Received 28 September 2010; accepted 12 November 2010

Abstract

Endemic of avian influenza virus (AIV) in Asia and epizootics in some European regions have caused considerable public concern on a possible pandemic of AIV. A rapid method for virus detection and effective surveillance in wild avian, poultry production as well as in humans is required. In this article, a DNA microarray-based solid-phase polymerase chain reaction (PCR) approach has been developed for rapid detection of influenza virus type A and for simultaneous identification of pathogenic virus subtypes H5 and H7. This solid-phase RT-PCR method combined reverse-transcription amplification of RNA extract in the liquid phase with sequence-specific nested PCR on the solid phase. A simple ultraviolet cross-linking method was used to immobilize the DNA probes over an unmodified glass surface, which makes solid-phase PCR a convenient possibility for AIV screening. The testing of 33 avian fecal and tracheal swab specimens was completed in less than 2 h with 94% accuracy.

Keywords: Avian influenza virus; Solid-phase RT-PCR; DNA microarray

1. Introduction

Avian influenza virus (AIV) belongs to the virus family Orthomyxoviridae. It is an infectious disease and has caused great economic losses in poultry and started to threaten human life (WHO, 2010). The AIV genome consists of 8 segments of negative-sense single-stranded RNA. Based on antigenic differences in the hemagglutinin (HA) and neuraminidase (NA) proteins, AIV is divided into 16 HA and 9 NA subtypes, and is classified as either highly pathogenic avian influenza virus (HPAIV) or low pathogenic avian influenza virus (LPAIV) based on the ability to cause disease and mortality (Alexander, 2007).

Although virus cultivation combined with hemagglutination inhibition (HI) and neuraminidase inhibition (NI) tests is still the standard for influenza virus detection (Knipe and Howley, 2001), many nucleic acid amplification techniques, such as reverse transcriptase PCR (RT-PCR) (Lee et al., 2001), real-time RT-PCR (Spackman et al., 2002), and real-time NASBA (van Aarle et al., 2006), have been developed for more sensitive and rapid diagnosis.

PCR amplification products can be analyzed in parallel by using high-density oligonucleotide microarrays. Several studies about microarray for AIV identifications have been reported (Gall et al., 2009a; Han et al., 2008; Kessler et al., 2004; Li et al., 2001; Wang et al., 2008). In these studies, the AIV viral RNA was amplified through RT-PCR and the resulting product was hybridized on the spotted probes and detected through fluorescent labeling. Although differentiation of all 16 HA subtypes of AIV has been demonstrated (Gall et al., 2009b), hybridization as a post-PCR process inevitably increased the complexity of the assay.

To enable multiplex amplification and sequence detection done in one step, microarray-based solid-phase PCR was developed (Huber et al., 2001). This approach combined

☆ This work is financially supported by the Technical University of Denmark(DTU), Food Pathogen Project No. 8, Grant No. 150627.
* Corresponding author. Tel.: +45-4525-6305; fax: +45-45887762.
E-mail address: anders.wolff@nanotech.dtu.dk (A. Wolff).

0732-8893/$ – see front matter © 2011 Published by Elsevier Inc.
doi:10.1016/j.diagmicrobio.2010.11.008

liquid-phase PCR with simultaneous nested amplification using oligonucleotide primers attached to a glass slide. The PCR amplicons remained covalently bound to the solid surface and could be identified by fluorescence scanning. This method was further applied for single nucleotide polymorphism detection (Huber et al., 2002; Pemov et al., 2005; Shapero et al., 2001), bacteria identification (Mitterer et al., 2004), and disease genotyping (Khodakov et al., 2008). Solid-phase PCR has shown its advantages of high throughput, ease of operation, and specific detection; however, protocols for attaching probes on the glass surface were complicated and the method has never been applied for a fragile material like viral RNA.

In this article, we extended the strategy and developed a DNA microarray platform where RT-PCR of viral RNA occurred in the liquid solution and nested amplification occurred on the microarray elements with specific oligonucleotide probes for interrogating different influenza types. A very simple ultraviolet (UV) cross-linking immobilization procedure was used to immobilize TC-tagged oligonucleotide probes on a bare glass slide. With this method, AIV can be quickly detected with subtypes of H5 and H7 simultaneously identified. Thirty-three specimens from wild birds and experimentally infected chicken were tested. The microarray-based platform can be a good tool for rapid detection of AIV and could be widely employed for on-site screening of potential AIV carriers in wild and domestic poultry.

2. Materials and methods

2.1. Virus strains

Four inactivated AIV strains, namely, H1N1 A/DK/ALB 35/76, H5N1 A/CK/Scotland/59 06.04.67, H16N3-A/Gull/Denmark/68110/02, and H7N5 A/Chick/Nether/2993–17/03 AV 506/03, were used in this study. Two strains, a Newcastle diseases virus and an infectious bursal disease virus (IBDV), were used to check the specificity of the PCR. All the strains were kindly supplied by the National Veterinary Institute, Technical University of Denmark.

2.2. Sample collection from wild birds for method validation

A total of 33 samples which include cloacal ($n = 24$) and tracheal ($n = 9$) swabs were collected and used to validate the solid-phase RT-PCR method. The samples were originating from a national surveillance program for AIV in wild birds ($n = 20$) and chickens experimentally infected with AIV ($n = 13$). The swabs were dipped in 2 mL phosphate-buffered saline to release the fecal or tracheal materials from the swabs. Nine hundred microliters of the mixture sample was subjected to a centrifugal force of 18,894×g for 5 min (Eppendorf, Hamburg, Germany) to remove debris, and the supernatant was collected for isolating viral RNA.

2.3. Isolation of RNA from AIV virus

Isolation of RNA from AIV virus was performed using the RNeasy Kit (Qiagen, Hilden, Germany) according to the manufacturer's instruction. The RNA was eluted using 50 μL of RNase-free water. The isolated RNA was used as a template for evaluation of the solid-phase RT-PCR.

2.4. Primers and probes

Table 1 shows a list of primers and probes used for amplification. The matrix (M) gene was selected for AIV screening as it has been found to be conserved across all type A influenza viruses (Starick et al., 2000). Primers and probes for H5 and H7 subtypes were targeted at the HA gene of the influenza virus with avian origin. Each forward primer was Cy5 labeled at the 5′ end so that the solid-phase RT-PCR results could be directly visualized on the microarray. The probes (immobilized primers) were modified at the 5′ end with a poly(T)10-poly (C)10 tail to facilitate the attachment to the solid substrate as previously described (Gudnason

Table 1
List of specific primers and probes used in this study

Type or subtype	Target gene	Primers and probes	Sequences (5′–3′)	Amplicon (bp)
A	Matrix	Forward DB-MF (24–47, sense) Reverse DB-MR (101–124, antisense) M gene probe (74-93, sense)	CY5-AGA TGA GTC TTC TAA CCG AGG TCG TGC AAA AAC ATC TTC AAG TCT CTG TTTTTTTTTTCCCCCCCCCC TCA GGC CCC CTC AAA GCC GA	100[a]
H5	HA	Forward DB-H5LH1 (1508-1532, sense) Reverse DB-H5RH1 (1640-1659, antisense) H5 Probe (1613-1636, sense)	CY5-ACA TAT GAC TAC CCA CAR TAT TCA G AGA CCA GCT AYC ATG ATT GC TTTTTTTTTTCCCCCCCCCC TCW ACA GTG GCG AGT TCC CTA GCA	151[b]
H7	HA	Forward DB-LH6H7 (1477-1503, sense) Reverse DB-R4H7 (1586-1608, antisense) H7 Probe (1545-1574, sense)	CY5-GGC CAG TAT TAG AAA CAA CAC CTA TGA GCC CCG AAG CTA AAC CAA AGT AT TTTTTTTTTTCCCCCCCCCC CCG CTG CTT AGT TTG ACT GGG TCA ATC T	131[c]

[a] Based on GenBank accession no. CY015082 (A/chicken/Scotland/1959 [H5N1]).
[b] Based on GenBank accession no. CY015081 (A/chicken/Scotland/1959 [H5N1]).
[c] Based on GenBank accession no. AB438941 (A/chicken/Netherlands/2586/2003 [H7N7]).

et al., 2008). All the oligonucleotide primers and probes were synthesized at DNA Technology, Denmark.

2.5. In-tube RT-PCR conditions

The in-tube multiplex RT-PCR was performed using a RT-PCR kit (Qiagen). The RT-PCR conditions were based on the manufacturer's instruction with minor modifications. Briefly, a 25-μL RT-PCR reaction mixture contained 5 μL of 5 × RT-PCR buffer, 1 μL of 10 mmol/L DNTP mix, 1 μL of enzyme mix, 5 μL of RNA sample, and three pairs of primers, each at a final concentration of 0.2 μmol/L. RT-PCR was carried out in a thermal cycler (MJ Research, Massachusetts, USA) and the cycling protocol consisted of reverse transcription for 30 min at 50 °C; enzyme activation for 15 min at 95 °C; followed by 40 cycles of 10 s at 95 °C, 30 s at 54 °C, and 10 s at 72 °C; and, finally, extension of 5 min at 72 °C. The PCR amplicons were analyzed quantitatively using the Agilent Bioanalyzer 2100 system (Agilent, California, USA) with a DNA 500 chip kit according to the manufacturer's instruction.

2.6. Preparation of DNA microarrays for solid-phase RT-PCR

Microarray was produced on the glass slides by a simple method using TC-tagged probes. Briefly, normal Super Frost glass microscope slides were purchased from Menzel (Braunschweig, Germany) and the glass slides were used without any pretreatment or modification. The three oligonucleotide probes with poly(T) 10-poly(C) 10 tails were diluted in 150 mmol/L sodium phosphate buffer (pH 8.5) to a final concentration of 50 μmol/L and spotted using a noncontact array, Nano-Plotter 2.1 (GeSim, Dresden, Germany). The array layout is shown in Fig. 1A. Spots had a diameter of 150 μm and the spot-to-spot distance was 300 μm. The spots were allowed to dry and the probes were immobilized by UV irradiation at 254 nm for 10 min using Stratalinker 2400 (Stragtagene, California, USA). Subsequently, the slides were washed under agitation in 0.1× standard saline citrate (SSC) with 0.1% (w/v) sodium dodecyl sulfate (SDS) (Promega, Wisconsin, USA) solution for 10 min and then rinsed in deionized water and dried by nitrogen.

2.7. On-slide solid-phase RT-PCR

The on-slide solid-phase RT-PCR method consists of two phases: liquid phase and solid phase. The extracted RNA of AIV strains was used directly on the array to develop the method. Briefly, 25 μL of reaction master mix for solid-phase RT-PCR containing 10 μL of 5× RT-PCR buffer, 1 μL of 10 mmol/L DNTP mix, 1 μL of enzyme mix, 5 μL of RNA sample, three pairs of primers each at a final concentration of 1 μmol/L, 2.5 μL of 2.5 μg/μL bovine serum albumin (BSA), and 6 μL self-sealing reagent (MJ Research). The self-sealing reagent polymerizes upon contact with air at high temperature and thereby seals the reaction mixture at the edges to prevent evaporation during

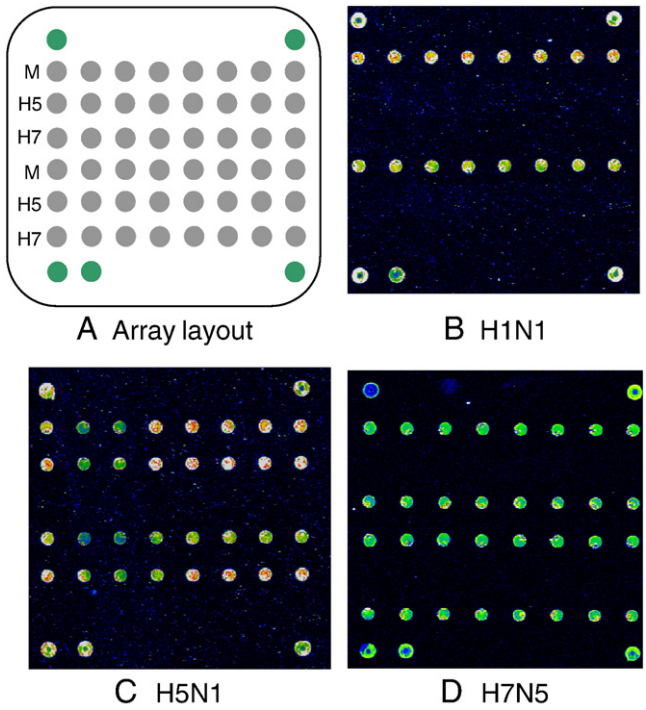

Fig. 1. (A) Microarray layout. The spotted solid-phase PCR probes for M, H5, and H7 are represented as gray circles. Each dot is 150 μm in diameter with a spot-to-spot distance of 300 μm. Green circles in the top and bottom corners are guide dots used for orientation and grid alignment during analysis. (B–D) Fluorescent images after 40 cycles of multiplex SP/RT-PCR amplification of three different viral RNA strains, (B) H1N1, (C) H5N1, and (D) H7N5.

RT-PCR. Immediately before use, the glass slides were rinsed in BSA (2.5 μg/μL) at room temperature. This step was to block the surface and reduce the absorption of enzymes during reaction. The slides were then washed with deionized water and dried using compressed air.

Ten microliters of the reaction master mix was loaded directly on the oligonucleotide microarrays and coverslips were mounted to seal the reaction droplets. The glass slides were transferred to a twin-tower PTC 200 slide thermocycler (MJ Research). PCR was carried out according to the following program: 15 min at 50 °C for reverse transcription, 10 min at 95 °C for enzyme activation, followed by 40 cycles of 10 s at 95 °C, 30 s at 54 °C, and 10 s at 72 °C, and, finally, 5 min at 72 °C for extension. After cycling, the slides were washed with agitation in 0.1× SSC/0.1% SDS for 10 min, followed by a short rinse in deionized water.

The microarrays were scanned by ScanArray Lite (Packard Bioscience, MA), with appropriate laser power and photomultiplier tube settings. ScanArray software (Packard Bioscience) was used to quantify the spots by calculating the average pixel intensity inside the defined spots.

2.8. Sensitivity of the solid-phase RT-PCR

The sensitivity of the solid-phase RT-PCR was evaluated and compared analytically with in-tube multiplex RT-PCR.

Ten-fold serial dilution of the AIV strain H16N3 ranging from 10^0 to 10^{-9} was prepared. The HA titre value for the AIV strains was measured to be 1:64. The 50% egg infectious dose (EID_{50}) calculated for the H16N3 strain was 6.7$\log_{10}$ EID_{50} per milliliter. RNA was isolated from the viral dilution series according to the method described above, and 5 μL of each dilution was used as a template for both in-tube RT-PCR and solid-phase PCR.

2.9. Specificity of the solid-phase PCR

The specificity for both the solid-phase RT-PCR and in-tube multiplex RT-PCR was tested using RNA extracts of avian pathogens with different subtypes, as well as RNA isolated from NDV and IBDV virus strains.

3. Results

3.1. Development of in-tube multiplex RT-PCR

With an aim to develop a solid-phase method for rapid detection and identification of AIV, an in-tube multiplex RT-PCR was first carried out. In this multiplex PCR, three pairs of primers were used to amplify the AIV conserved region on the M gene and H5 and H7 regions on the HA gene. In-tube RT-PCR was carried out to amplify three PCR amplicons with expected lengths of 100, 151, and 131 bp for the M, H5, and H7 fragments, respectively. Fig. 2 shows a bioanalyzer figure of the results of amplifications where the RNA of three AIV virus strains (H1N1, H5N1, H7N5), as well as of NDV and IBDV, was used as a template. A fragment of 100 base pairs (bp) from the M gene was detected in PCR products from all of the three AIV viral RNAs: H1N1, H5N1, and H7N5 (Fig. 2, lanes 1, 3, and 5). PCR amplicons with lengths of 151 and 131 bp were only observed from H5N1 and H7N5 viral RNA, respectively (Fig. 2, lanes 1 and 3). No PCR product was observed when the RNAs of other infectious viruses such as NDV and IBDV were used (Fig. 2, lanes 2 and 4).

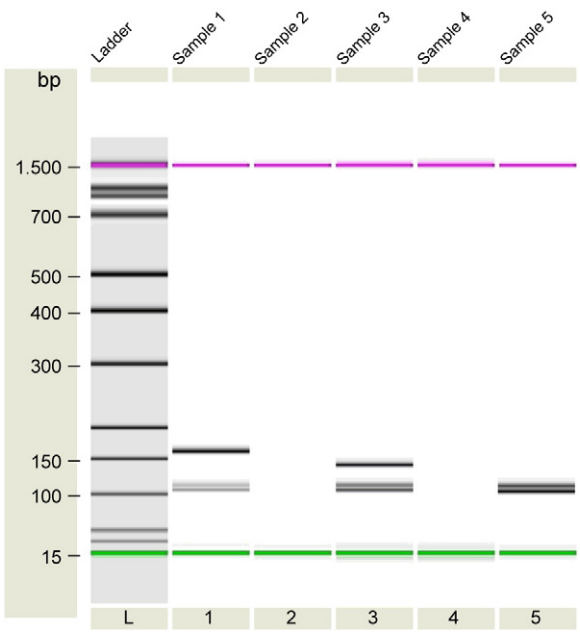

Fig. 2. In-tube multiplex RT-PCR for different virus strains. Three sets of primers specific to influenza virus type A and two important HA subtypes H5 and H7 were added into a single tube. Forty cycles of PCR were performed and the results were obtained using the bioanalyzer. Lane 1: H5N1; lane 2: NDV; lane 3: H7N5; lane 4: IBDV; lane 5: H1N1.

3.2. Solid-phase RT-PCR using RNA isolated from AIV virus

A microarray-based solid-phase multiplex PCR was developed to identify AIV at subspecies level as shown in Fig. 3. During the reaction, the RNA was firstly reverse transcribed to cDNA in the liquid sandwiched between the glass slide and the cover lid. cDNA was then amplified with three pairs of freely moving PCR primers as described above (Fig. 3A). Simultaneously, the newly amplified PCR amplicons in the liquid phase interacted with the nested probes immobilized in the solid phase (Fig. 3B). If the probes matched the bases in the template DNA, they were extended by the polymerase, which served as the template for the second-strand elongation primed by the liquid-phase primers, thus generating new templates for the solid-phase amplification. After the reaction, PCR products remained on the glass slide through covalent binding and could be directly visualized as the liquid-phase primer was labeled with Cy5 dyes.

Fig. 1B–D shows the fluorescent images of the microarray after the solid-phase RT-PCR using RNA templates from three different strains, H1N1, H5N1, and H7N5, respectively. The three types of viruses were unambiguously identified by the distinct patterns. For H1N1, only the probe for the M gene was amplified (Fig. 1B), while with RNA from the H5N1 strain, both the M and H5 probes were positive (Fig. 1C), indicating that the virus belonged to influenza type A and H5 subtype. With RNA from the AIV H7N5 strain, both the M and H7 probes lightened up (Fig. 1D). Despite the presence of all the primers and probes, nonspecific amplification was negligible.

3.3. Analytical sensitivity of solid-phase RT-PCR

The sensitivity of the solid-phase RT-PCR system was investigated and compared to multiplex RT-PCR in tubes. A 10-fold serial dilution (from 10^0 to 10^{-9}) of the AIV H16N3 strain (HA 1:64) was prepared and the extracted RNA was used as a template. For the multiplex RT-PCR in tubes, the 100-bp PCR amplicon of the M gene was observed up to 10^{-5} or equivalent to 1 $\log_{10}$ EID_{50}/mL (Fig. 4A). A similar detection limit was obtained for solid-phase RT-PCR on slides where the lowest concentration of template at which positive fluorescence signals could be detected was also 10^{-5} (Fig. 4B).

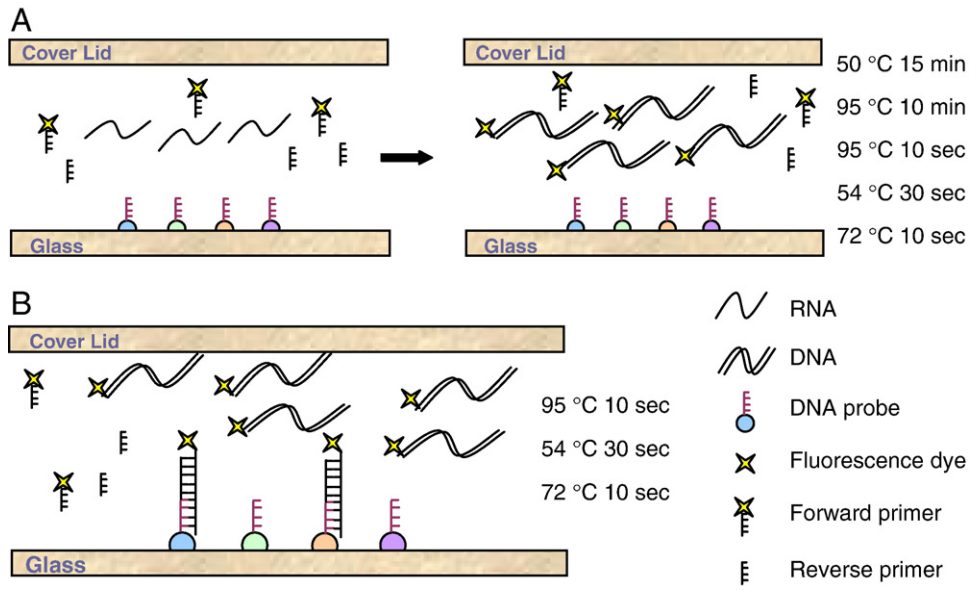

Fig. 3. DNA Microarray-based solid-phase RT-PCR. (A) In the liquid phase, the RNA is firstly reverse transcribed to cDNA and then amplified with freely moving PCR primers. (B) Simultaneously in the solid phase, the probes matched to the templates in solution are extended by the polymerase, which served as templates primed by the liquid-phase primers, thus generating strands complementary to the extended probes.

3.4. Validation of solid-phase RT-PCR using real samples

To validate the performance of the method, 33 samples from a national surveillance program for AIV in wild birds were analyzed both by solid phase RT-PCR on slides and by multiplex RT-PCR in tubes. Five microliters of the isolated RNA was used as templates and the results are compared in Table 2.

Of 33 samples, 14 (42.4%) were identified as AIV at subspecies level using conventional culture and the rest of the 19 samples (57.6%) were negative (Table 2, column 3). With the use of multiplex RT-PCR in tubes, 14 (42.4%) positive samples were recognized (Table 2, column 7), whereas for the solid-phase RT-PCR method, 12 (39.4%) samples were found to be AIV positive (Table 2, column 11). Two samples, namely, 063234C and 063234T [cloacal (C) and tracheal (T) swabs from the same bird], which were identified as AIV H5N3 by conventional culturing and inhibition tests as well as by RT-PCR in tubes, were shown to be negative using solid-phase RT-PCR. In contrast, two samples (0753794T and 0753594C) that could not be subtyped by RT-PCR in tubes were correctly identified as AIV H7 subtype by solid-phase RT-PCR. Four chicken samples that were experimentally infected with different non-AIV avian viruses (new cattle virus, IBD, and avian penury virus) were all correctly identified as negative by both methods. Overall, 31 (94%) of 33 samples were identified accurately using the solid-phase RT-PCR.

4. Discussion

In recent years, HPAIV has caused massive economic losses for the poultry industry and has been the cause of death for hundreds of millions of birds around the world (Rushton et al., 2005; WHO, 2005). Strong evidence suggests that all known outbreaks of HPAIV have been preceded by transmission of LPAIV of H5 or H7 subtypes that was circulating in feral birds and transmitted to domestic poultry (Ito et al., 2001). So far, RT-PCR has been applied for the regular diagnosis of AIV (WHO, 2007). Therefore, development of a mobile and automated method based on RT-PCR would be a great advantage for rapid detection and early warning of AIV infection.

Multiplex RT-PCR involves simultaneous amplification of several PCR products; however, the formation of primer dimers due to the presence of more than one primer pair in the multiplex PCR increases the chances of undesirable nonspecific RT-PCR products. Such products could be avoided by optimizing primer design and RT-PCR conditions. In this article, three sets of primers were carefully chosen to target general influenza virus type A and two highly pathogenic virus subtypes H5 and H7. Experiments performed in tubes show that the three sets of primers designed for the multiplex amplification were very specific and did not interfere with each other.

Using the specific primers and probes designed for multiplex RT-PCR, we developed a DNA microarray-based solid-phase PCR platform for rapid identification of AIV. Despite the great potential of solid-phase PCR, the widespread use of the technology is limited. One of the major causes lies in the tedious and time-consuming procedures for surface treatment and DNA immobilization. It took days to derivatize the glass surface and incubate the slides after spotting (Huber et al., 2001; Mitterer et al., 2004). In this study, a much faster and easier immobilization method was developed by us where DNA probes with poly

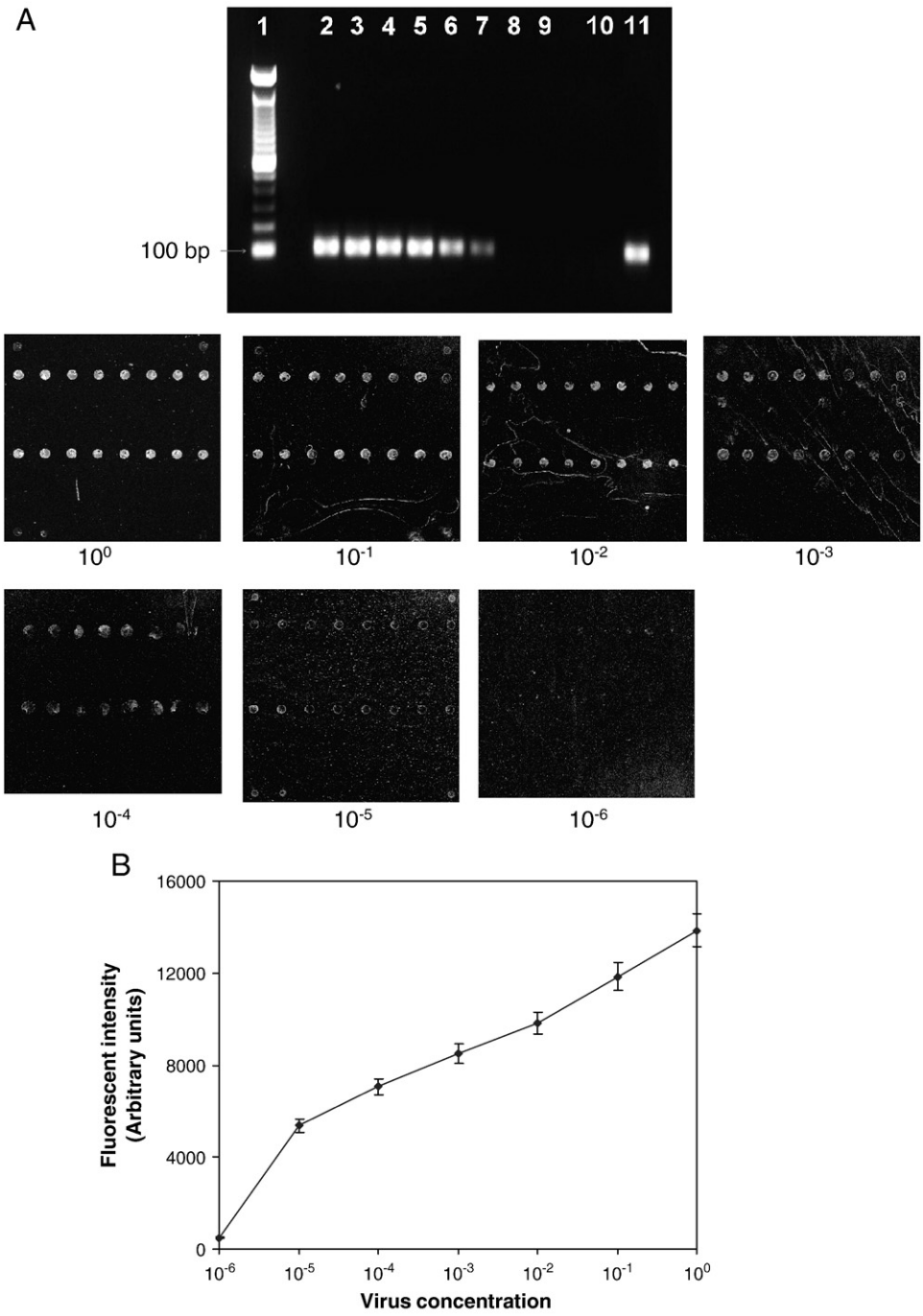

Fig. 4. Detection of H16N3 AIV by on-tube RT-PCR and solid-phase RT-PCR. Serial 10-fold dilutions of the extracted viral RNA templates, ranging from 10^0 to 10^{-9} were tested. (A) Sensitivity of on-tube RT-PCR. Amplified products (100 bp target for M gene) with different template concentrations are shown. One gel, lane 1: 100 bp DNA ladder; lanes 2–9: 10-fold dilutions of the virus pool ranging from the original HA titre to 10^{-7}, respectively; lane 10: negative control (virus free); lane 11: positive control. The virus strain was not recognized at dilutions higher than 10^{-5}. (B) Sensitivity of solid-phase RT-PCR. Fluorescence intensities of probes specific to the M gene were measured. The detection limit was 10^{-5}.

(T)10-poly (C)10 tails were immobilized over an unmodified glass surface by simple UV cross-linking. The probes modified with TC tails offer up to 70% cost reduction when compared to the commonly used amino group modifications of the probes and make solid-phase PCR a convenient possibility for AIV screening. Another advantage of our immobilization method is that the probes are thermally stable. For other immobilization methods, it can be a problem if the primer detaches during thermocycling. A 60% loss of grafted primers during thermocycling was reported (Fedurco et al., 2006). This is, however, not a problem with our method. No significant decrease in fluorescence signal was observed after 20 min of incubation in water at 100 °C (Gudnason et al., 2008).

Table 2
Detection and identification of AIV from 33 real samples by in-tube multiplex RT-PCR and solid-phase RT-PCR

No.	Specimen ID	Known subtype[a]	In-tube RT-PCR			Identification	Solid-phase RT-PCR			Identification
			M	H5	H7		M	H5	H7	
1	0853404T		−	−	−		−	−	−	
2	0853404C						−	−	−	
3	781347C	H5N2	+	+	−	AIV, H5 type	+	+	−	AIV, H5 type
4	0853405T		−	−	−		−	−	−	
5	0853405C		−	−	−		−	−	−	
6	7860366C	H6N8	+	−	−	AIV	+	−	−	AIV
7	065341T		−	−	−		−	−	−	
8	065393C		−	−	−		−	−	−	
9	0653130T	H5N3	+	+	−	AIV, H5 type	+	+	−	AIV, H5 type
10	0653234 T	H5N3	+	+	−	AIV, H5 type	−	−	−	False negative
11	0653234 C	H5N3	+	+	−	AIV, H5 type	−	−	−	False negative
12	0850406 T		−	−	−		−	−	−	
13	0850406 C		−	−	−		−	−	−	
14	0753594T	AIV	+	−	−	AIV	+	−	+	AIV, H7 type
15	0753594C	AIV	+	−	−	AIV	+	−	+	AIV, H7 type
16	0853407T		−	−	−		−	−	−	
17	0853407C		−	−	−		−	−	−	
18	7860295T	H5N1	+	+	−	AIV, H5 type	+	+	−	AIV, H5 type
19	H5N2	H5N2	+	+	−	AIV, H5 type	+	+	−	AIV, H5 type
20	0853408T		−	−	−		−	−	−	
21	0853408C		−	−	−		−	−	−	
22	H5N2	H5N2	+	+	−	AIV, H5 type	+	+	−	AIV, H5 type
23	Lasota NDV		−	−	−		−	−	−	
24	APV type C		−	−	−		−	−	−	
25	IBV m41		−	−	−		−	−	−	
26	Beijing 184/93		−	−	−		−	−	−	
27	H7N1	H7N1	+	−	+	AIV, H7 type	+	−	+	AIV, H7 type
28	H5N1	H5N1	+	+	−	AIV, H5 type	+	+	−	AIV, H5 type
29	IBV		−	−	−		−	−	−	
30	H7N7	H7N7	+	−	+	AIV, H7 type	+	−	+	AIV, H7 type
31	IBD Cux52/70		−	−	−		−	−	−	
32	H11N6	H11N6	+	−	−	AIV	+	−	−	AIV
33	NDV		−	−	−		−	−	−	

[a] Measured using conventional culturing and HI and NI test with reference antisera (Knipe and Howley, 2001).

The DNA microarray platform described in this article combines liquid-phase amplification and specific solid-phase PCR in 1 step. As probes are spatially separated, nonspecific amplification is minimized. Moreover, apart from array scanning, no other post-PCR steps are needed. Solid-phase PCR is also advantageous when compared to the more advanced real-time multiplex PCR as the latter suffers from the interference of absorption and fluorescence spectra and no more than four reactions can be reliably detected in one assay (Khodakov et al., 2008).

The solid-phase PCR method was used to test 33 cloacal and tracheal swabs samples collected from wild birds. Two (6%) of 33 samples showed a false-negative result. This is probably because of the insufficient binding of the probe and its target due to low viral concentration. However, two samples that were not able to be subtyped by in-tube RT-PCR were identified as AIV H7 subtype by solid-phase RT-PCR, showing that solid-phase PCR has higher specificity. In all, the testing of 33 avian fecal and tracheal swab specimens was completed in less than 2 h with 94% accuracy.

Last but not least, the small footprint of the microarray makes it easily adaptable to a microfluidic chip format. Various functional modules such as sample pretreatment (virus concentration and purification), on-chip virus lysis, and solid-phase RT-PCR typing array can be integrated on a single device so that detection of AIV can be obtained in a rapid and automated way. Research works in this direction are in progress.

5. Conclusion

We have developed a DNA microarray-based solid-phase RT-PCR method for rapid detection of AIV and simultaneous identification of the HA subtypes H5 and H7. Oligonucleotide probes were immobilized on bare glass surface by a much simpler and faster UV cross-linking method. This is an important step forward towards the development of a rapid and cost-effective test for AIV screening in the laboratory or on-site. Compared to in-tube multiplex PCR, the solid-phase PCR method involves fewer

steps, while comparable sensitivity and specificity have been achieved. The microarray-based platform can be widely employed for routine screening of potential carriers in wild birds and domestic poultries.

References

Alexander DJ (2007) An overview of the epidemiology of avian influenza. *Vaccine* 25:5637–5644.

Fedurco M, Romieu A, Williams S, Lawrence I, Turcatti G (2006) BTA, A novel reagent for DNA attachment on glass and efficient generation of solid-phase amplified DNA colonies. *Nucleic Acids Res* e22:34.

Gall A, Hoffmann B, Harder T, Grund C, Ehricht R, Beer M (2009a) Rapid haemagglutinin subtyping and pathotyping of avian influenza viruses by a DNA microarray. *J Virol Methods* 160:200–205.

Gall A, Hoffmann B, Harder T, Grund C, Hoper D, Beer M (2009b) Design and validation of a microarray for detection, hemagglutinin subtyping, and pathotyping of avian influenza viruses. *J Clin Microbiol* 47:327–334.

Gudnason H, Dufva M, Bang DD, Wolff A (2008) An inexpensive and simple method for thermally stable immobilization of DNA on an unmodified glass surface: UV linking of poly(T)10-poly(C)10-tagged DNA probes. *Biotechniques* 45:261–271.

Han X, Lin X, Liu B, Hou Y, Huang J, Wu S, Liu J, Mei L, Jia G, Zhu Q (2008) Simultaneously subtyping of all influenza A viruses using DNA microarrays. *J Virol Methods* 152:117–121.

Huber M, Losert D, Hiller R, Harwanegg C, Mueller MW, Schmidt WM (2001) Detection of single base alterations in genomic DNA by solid phase polymerase chain reaction on oligonucleotide microarrays. *Anal Biochem* 299:24–30.

Huber M, Mundlein A, Dornstauder E, Schneeberger C, Tempfer CB, Mueller MW, Schmidt WM (2002) Accessing single nucleotide polymorphisms in genomic DNA by direct multiplex polymerase chain reaction amplification on oligonucleotide microarrays. *Anal Biochem* 303:25–33.

Ito T, Goto H, Yamamoto E, Tanaka H, Takeuchi M, Kuwayama M, Kawaoka Y, Otsuki K (2001) Generation of a highly pathogenic avian influenza A virus from an avirulent field isolate by passaging in chickens. *J Virol* 75:4439–4443.

Kessler N, Ferraris O, Palmer K, Marsh W, Steel A (2004) Use of the DNA flow-thru chip, a three-dimensional biochip, for typing and subtyping of influenza viruses. *J Clin Microbiol* 42:2173–2185.

Khodakov DA, Zakharova NV, Gryadunov DA, Filatov FP, Zasedatelev AS, Mikhailovich VM (2008) An oligonucleotide microarray for multiplex real-time PCR identification of HIV-1, HBV, and HCV. *Biotechniques* 44:241–248.

Knipe DM, Howley PM, Eds. (2001) Fields Virology, 4th ed., vol. 1. Philadelphia, PA: Lippincott Williams & Wilkins.

Lee MS, Chang PC, Shien JH, Cheng MC, Shieh HK (2001) Identification and subtyping of avian influenza viruses by reverse transcription-PCR. *J Virol Methods* 97:13–22.

Li JP, Chen S, Evans DH (2001) Typing and subtyping influenza virus using DNA microarrays and multiplex reverse transcriptase PCR. *J Clin Microbiol* 39:696–704.

Mitterer G, Huber M, Leidinger E, Kirisits C, Lubitz W, Mueller MW, Schmidt WM (2004) Microarray-based identification of bacteria in clinical samples by solid-phase PCR amplification of 23S ribosomal DNA sequences. *J Clin Microbiol* 42:1048–1057.

Pemov A, Modi H, Chandler DP, Bavykin S (2005) DNA Analysis with multiplex microarray-enhanced PCR. *Nucleic Acids Res* 33:e11.

Rushton J, Viscarra R, Bleich EG, McLeod A (2005) Impact of avian influenza outbreaks in the poultry sectors of five South East Asian countries (Cambodia, Indonesia, Lao PDR, Thailand, Viet Nam) outbreak costs, responses and potential long term control. *World's Poultry Sci J* 61:491–514.

Shapero MH, Leuther KK, Nguyen A, Scott M, Jones KW (2001) SNP Genotyping by multiplexed solid-phase amplification and fluorescent minisequencing. *Genome Res* 11:1926–1934.

Spackman E, Senne DA, Myers TJ, Bulaga LL, Garber LP, Perdue ML, Lohman K, Daum LT, Suarez DL (2002) Development of a real-time reverse transcriptase PCR assay for type A influenza virus and the avian H5 and H7 hemagglutinin subtypes. *J Clin Microbiol* 40:3256–3260.

Starick E, Romer-Oberdorfer A, Werner O (2000) Type- and subtype-specific RT-PCR assays for avian influenza A viruses (AIV). *J Vet Med Ser B-Infect Dis Vet Public Health* 47:295–301.

van Aarle R, Brengel-Pesce K, Lefeuvre A, Touchard M, Jacobs E, van de Wiel R (2006) Real-time NASBA assay for the detection of influenza A and B. *J Clin Virol* 36:46–47.

Wang LC, Pan CH, Severinghaus LL, Liu LY, Chen CT, Pu CE, Huang D, Lir JT, Chin SC, Cheng MC, Lee SH, Wang CH (2008) Simultaneous detection and differentiation of Newcastle disease and avian influenza viruses using oligonucleotide microarrays. *Vet Microbiol* 127:217–226.

WHO (2005) Avian influenza: assessing the pandemic threat. http://www.who.int/csr/disease/influenza/H5N1-9reduit.pdf.

WHO (2007) Recommendations and laboratory procedures for detection of avian influenza A(H5N1) virus in specimens from suspected human cases. http://www.who.int/csr/disease/avian_influenza/guidelines/RecAIlabtestsAug07.pdf.

WHO (2010) Cumulative number of confirmed human cases of avian influenza A/(H5N1) reported to WHO. http://www.who.int/csr/disease/avian_influenza/country/cases_table_2010_02_17/en/index.html.

7.2 A lab-on-chip device for rapid identification of avian influenza virus by solid phase

Manuscript published in Lab chip journal (2011), 11, 1457-1463.

Lab on a Chip

View Online
Dynamic Article Links

Cite this: *Lab Chip*, 2011, **11**, 1457

www.rsc.org/loc

PAPER

A lab-on-a-chip device for rapid identification of avian influenza viral RNA by solid-phase PCR†

Yi Sun,[a] Raghuram Dhumpa,[b] Dang Duong Bang,[b] Jonas Høgberg,[b] Kurt Handberg[c] and Anders Wolff*[a]

Received 21st October 2010, Accepted 7th February 2011
DOI: 10.1039/c0lc00528b

The endemic of Avian Influenza Virus (AIV) in Asia and epizootics in some European regions have caused serious economic losses. Multiplex reverse-transcriptase (RT) PCR has been developed to detect and subtype AIV. However, the number of targets that can be amplified in a single run is limited because of uncontrollable primer–primer interferences. In this paper, we describe a lab-on-a-chip device for fast AIV screening by integrating DNA microarray-based solid-phase PCR on a microfluidic chip. A simple UV cross-linking method was used to immobilize the DNA probes on unmodified glass surface, which makes it convenient to integrate microarray with microfluidics. This solid-phase RT-PCR method combined RT amplification of extracted RNA in the liquid phase and species-specific nested PCR on the solid phase. Using the developed approach, AIV viruses and their subtypes were unambiguously identified by the distinct patterns of amplification products. The whole process was reduced to less than 1 hour and the sample volume used in the microfluidic chip was at least 10 times less than in the literature. By spatially separating the primers, highly multiplexed amplification can be performed in solid-phase PCR. Moreover, multiplex PCR and sequence detection were done in one step, which greatly simplified the assay and reduced the processing time. Furthermore, by incorporating the microarray into a microchamber-based PCR chip, the sample and the reagent consumption were greatly reduced, and the problems of bubble formation and solution evaporation were effectively prevented. This microarray-based PCR microchip can be widely employed for virus detection and effective surveillance in wild avian and in poultry productions.

Introduction

Avian influenza virus (AIV) or "bird flu" is an infectious disease caused by Influenza A virus. Based on antigenic differences in the hemagglutinin (HA) and neuraminidase (NA) proteins, AIV is divided into 16 HA and 9 NA subtypes.[1] The AIV is classified as either highly pathogenic avian influenza (HPAI) or low pathogenic avian influenza (LPAI) based on the ability to cause disease and mortality.[2] Reverse transcriptase PCR (RT-PCR) has been introduced as the most sensitive method for detection and pathotyping of AIV.[3] Identification and subtyping of HPAI virus by RT-PCR often involve multi-step amplifications, which make the assay complicated and time-consuming.[4] Multiplex RT-PCR was then developed by targeting multiple genes at once.[5,6] Detection and subtyping of AIV were gained from a single test run that otherwise would require several tests to perform. However, analysis using multiplex PCR is constrained by two main limitations: the formation of primer–dimers due to the uncontrollable primer–primer interferences and preferential amplification of one target sequence over another.[7] Moreover, identification of multiplex PCR amplicons typically requires a secondary method, such as slab gel, melting curve, microarray hybridization or capillary electrophoresis,[8] for size separation or sequence verification.

To minimize the interferences in multiplex PCR, a technique called solid-phase PCR has been developed by grafting one or both primers on a solid support while keeping other PCR components in the liquid phase.[9,10] The primers can be immobilized on microtiter plates,[11] flat surfaces,[12] or microbeads.[13] In each case, enzymatic extension of the primer produces a tethered amplicon. Solid-phase PCR on DNA microarray has become increasingly popular as highly multiplexed amplification could occur in a miniature space with hundreds or thousands of discrete immobilized primers.[14–16] The multiplexing capabilities are produced by spatially encoding the array, in which each spot on the array is used to target a specific analyte. As the primers are

[a]*DTU Nanotech, Department of Micro- and Nanotechnology, Technical University of Denmark (DTU), Ørsteds Plads, DK-2800 Kgs Lyngby, Denmark. E-mail: anders.wolff@nanotech.dtu.dk*
[b]*DTU Vet, Laboratory of Applied Micro-Nanotechnology, National Veterinary Institute, Technical University of Denmark, Hangøvej 2, DK-8200 Aarhus, Denmark*
[c]*Laboratory of Avian Influenza Virus, National Veterinary Institute, Technical University of Denmark (DTU), Hangøvej 2, DK-8200 Aarhus, Denmark*

† Electronic supplementary information (ESI) available: Information on sensitivity of two other AIV identification methods—multiplex solution-based RT-PCR and conventional solid-phase PCR with coverslip. See DOI: 10.1039/c0lc00528b

spatially separated, the interferences between various primers are minimized, and the number of different targets able to be amplified in a single PCR reaction is greatly improved. The technique has been applied for a variety of applications, including diagnosis of infectious diseases[16] and single-nucleotide polymorphism (SNP) analysis.[17] Solid-phase PCR has shown its advantages of high throughput, ease of operation and specific detection. However, protocols for attaching probes on the glass surface were complicated and the method has never been applied for a fragile material like viral RNA.

In conventional solid-phase PCR, a self-adhesive frame[7] or a glass coverslip[18] is mounted on the oligonucleotide array to seal the reaction mixture. In both cases, a large amount of PCR samples are required. Moreover, air bubbles are easily trapped in the aqueous phase and the solutions are subject to evaporation, which could adversely affect the efficiency of solid-phase PCR. The problems can be addressed by using lab-on-a-chip technology. Since the concept of lab-on-a-chip was proposed, PCR microchips have been rapidly developed.[19–21] The microfabricated chips have characteristic dimensions in the order of μm, and PCR samples could be processed in a much shorter time with a high degree of fluid control. With the advances of microfabrication techniques, DNA microarrays have been incorporated into PCR microchips to detect PCR products by hybridization where unique DNA sequences are recognized through base pairing.[22–24] However, PCR microchips with microarrays for solid-phase PCR have seldom been reported.

In this paper, we describe a lab-on-a-chip device for rapid AIV detection by integrating DNA microarray-based solid-phase PCR on microchip. A 2 μl hybrid PDMS–glass chamber-based PCR microchip was fabricated and a DNA microarray for interrogating different influenza types was integrated in the chip. A very simple UV cross-linking procedure was used to immobilize TC-tagged oligonucleotide probes on the glass surface without any surface modification. The immobilization method is fast and thermally stable, making it a convenient to integrate microarrays into microfluidic systems. The fragile viral RNA was used as templates. The on-chip solid-phase PCR combined reverse-transcription amplification of RNA extract in the liquid phase and the simultaneous sequence-specific enzymatic extension of probes on the solid phase. The amplicons remained covalently bound to the glass and could be directly detected after PCR by fluorescence scanning. Using the developed approach, AIV viruses and their subtypes were unambiguously identified by their distinct patterns. Parameters such as the ratio of aqueous primers and solid probe densities were optimized for the system to improve efficiency of solid-phase amplification. This is the first demonstration of incorporation of solid-phase PCR into PCR microchip. Highly multiplex PCR can be performed on chip for viral classification attributed to the high-throughput capabilities of microarrays. Amplification and sequence detection are done during solid-phase PCR in a single, valveless chamber, which eliminates the need for post-PCR step and greatly simplifies the assay. Moreover, despite the sample volume being at least ten times less than that in the literature, ten-fold increase in detection sensitivity has been achieved when compared to both solution-based multiplex PCR and standard microarray method. The device can be considered as a versatile tool for identification of other genetic targets or it can also be integrated with other functionalities such as sample preparation to develop an automated and fully integrated sample-in–answer-out system.

Experimental

Design of on-chip solid-phase PCR

Previous studies revealed that solid-phase PCR is generally less efficient than conventional solution-based reactions.[9,10] This inefficiency may be attributed to a low primer concentration, its inability to diffuse through solution or inefficient enzymatic extension. Huber *et al.* proposed a method to allow the reaction to proceed in the liquid phase and on the surface of the solid phase simultaneously, which dramatically increased the product yield on the solid support.[25] The liquid-phase amplification produced DNA templates to initiate amplification on the solid phase and the accumulation of targets in a solution also served to accelerate the solid-phase amplification. In this study, we extended this strategy and developed an approach where RT-PCR occurs in the liquid solution and nested amplification occurs on the microarray elements with specific oligonucleotide probes. For the liquid-phase PCR, three pairs of primers were designed to amplify AIV conserved region on the matrix (M) gene and H5 and H7 regions on the HA gene. For the solid-phase amplification, three nested probes were spotted on the glass surface to target the M, H5 and H7 templates generated in the liquid. Though a multitude of unbound primers were added to the liquid phase, the potential for primer interference is counteracted by the superior specificity of nested amplification on the solid surface.

The working model for on-chip solid-phase PCR is illustrated in Fig. 1. The viral RNA and RT-PCR mixture is pumped into the chamber. Subsequently, the chamber is sealed and RT-PCR is performed by temperature cycling (Fig. 1a). The RNA is first reverse transcribed to complementary DNA (cDNA) in the liquid (Fig. 1b). cDNA is then amplified with freely moving PCR primers (Fig. 1c). Simultaneously, the newly amplified PCR amplicons in the liquid phase interact with the nested probes immobilized on the solid phase (Fig. 1d). If the probes match the bases in the template DNA, they are extended by the polymerase (Fig. 1e). In the next cycle, the extended probe served as templates for the second strand elongation primed by the forward primers in the liquid phase (Fig. 1f), thus generating new templates for the solid-phase amplification (Fig. 1g). After the reaction, PCR products remain attached to the glass slide through covalent binding and could be directly visualized as the forward primers in the liquid phase were labelled with Cy5 dyes. Detection of influenza virus A and simultaneous identification of two highly pathogenic AIV subtypes H5 and H7 are achieved by examining the specific patterns of the microarray.

Viral strains

Four different inactivated AIV strains and one strain of Newcastle diseases virus (NDV) were used in this study. The phenotypes, sources of isolation and HA titres of the viral strains are listed in Table 1. They were provided by the National Veterinary Institute of Denmark.

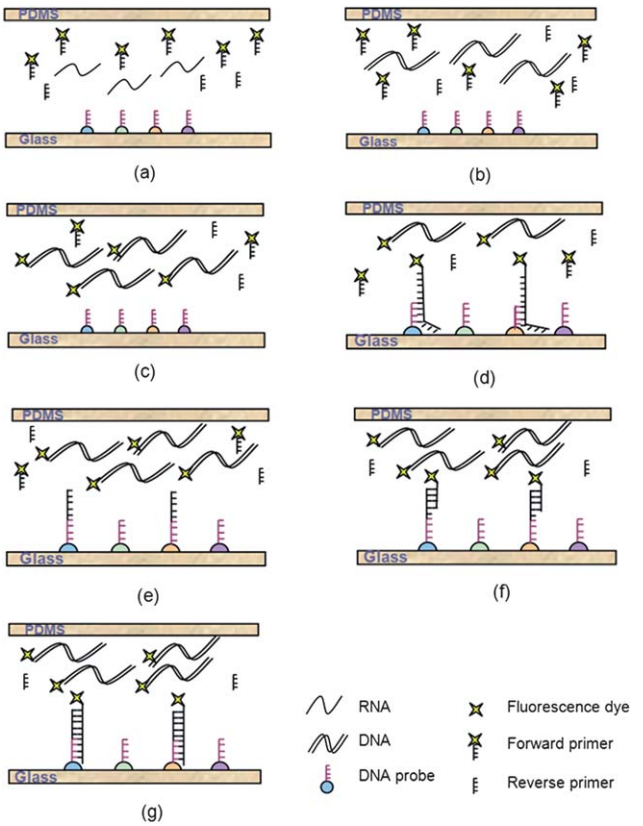

Fig. 1 The concept of on-chip solid-phase PCR for rapid AIV detection. (a) The viral RNA and RT-PCR mixture is pumped into the chamber. (b) The RNA is reverse transcribed to cDNA in the liquid. (c) cDNA is amplified with freely moving PCR primers. (d) The newly amplified PCR amplicons in the liquid phase interact with the nested probes immobilized on the solid support. (e) The matched probes are extended by the polymerase. (f) In the next cycle, the forward primers in the liquid phase are annealed to the extended probes. (g) Complementary strands are generated and serve as new templates for the solid-phase amplification. After the reaction, PCR products remain attached to the glass slide through covalent binding and could be directly visualized as the forward primers are labeled with Cy5 dyes.

Table 1 List of sources and hemagglutination titre (HA titre) of viral strains used in this study

No.	Viral strains and sources	Titre (HA)
1	H1N1 A/DK/ALB 35/76	1 : 16
2	H5N1 A/CK/Scotland/ 59 06.04.67	1 : 256
3	H7N5-2 A/Chick/Nether/2993—17/03 AV 506/03	1 : 128
4	Newcastle diseases, Ulster strain	1 : 128
5	H16N3—A/Gull/Denmark/68110/02	1 : 128

RNA extraction

Isolation of RNAs from virus strains was performed using the RNeasy Kit (Qiagen, Germany) according to the manufacturer's instruction. The RNAs were eluted using the RNase free water. The isolated RNAs were used as templates for evaluation of the solid-phase PCR.

Primer and probes

Table 2 shows a list of primers and probes used for AIV identification and subtyping. The M gene-specific primers and probes were designed for AIV screening as it has been found that the region on the M gene is conserved across all type A influenza viruses.[4] Primers and probes for H5 and H7 subtypes were designed to target the H5 and H7 regions on HA gene of Influenza virus with avian origin. Each forward primer was Cy5-labeled at the 5′ end so that the solid-phase PCR results could be directly visualized on the microarray. The probes (immobilized primers) were modified at the 5′ end with a poly(T)10–poly(C)10 tail to facilitate the attachment on the solid substrate. All the oligonucleotide primers and probes were synthesized at DNA Technology A/S, Denmark.

Preparation of DNA microarrays on glass substrate

Microarray was produced on an unmodified glass substrate by simple UV cross-linking according to a method developed in our lab.[26] Briefly, a glass chip of 10 mm × 10 mm was diced from a 0.5 mm glass wafer using a Dicing Saw (Disco, Japan) and was used without any pre-treatment or modification. The three oligonucleotide probes with poly(T)10–poly(C)10 tails were diluted in 150 mM sodium phosphate buffer (pH 8.5) to a final concentration from 5 to 50 μM and spotted using a non-contact array nano-plotter 2.1 (GeSim, Dresden, Germany). The layout is shown in Fig. 3a. The array was spotted at the centre of the glass chip and each probe was repeated four times for easy identification of the reaction products. The spot had a diameter of 150 μm and the spot-to-spot distance was 300 μm. The spots were allowed to dry and then exposed to UV irradiation at 254 nm with an energy of 0.3 J cm^{-2} for 10 min (Stratalinker 2400, Stratagene, CA, USA). Subsequently, the glass chip was washed under agitation in 0.1× standard saline citrate (SSC) with 0.1% (w/v) sodium dodecyl sulfate (SDS) (Promega, WI, USA) solution for 10 min, then rinsed in deionized water and dried under nitrogen.

Microfabrication

The PCR microchamber was fabricated in polydimethylsiloxane (PDMS) by rapid prototyping. The mask layout was designed using a CAD program. The master for molding was fabricated in SU-8 50 (MicroChem, MA, USA) by the standard photolithography. A 10 : 1 mixture of PDMS pre-polymer and curing agent (Sylgard 184, Dow Cornig, MI, USA) was stirred thoroughly and then poured onto the master and cured for 1 h at 65 °C. After curing, the 1 mm thick PDMS replica was peeled from the master. Inlet and outlet holes were punched by a needle. The PDMS substrate and the glass chip with DNA microarray were sealed by plasma bonding. Both PDMS and glass substrates were exposed to oxygen plasma for 30 s at 100 W with an oxygen flow rate of 240 ml min^{-1} (Plasma Processor 300, PVA TePla, Germany). Right after the removal from the plasma chamber, the substrates were brought into conformal contact where an irreversible seal formed spontaneously. Though the probe array was also exposed to oxygen plasma, test showed that the functionality of DNA as probes for PCR was not affected at such low power exposure. As shown in Fig. 2, the outer dimension of the

Table 2 List of primers and probes specific to the conserved region of M gene and H5 and H7 regions of HA gene

Type or subtype	Target gene	Primers and probes	Sequences (5′–3′)	Amplicon (bp)
A	Matrix	Forward DB-MF	CY5-AGA TGA GTC TTC TAA CCG AGG TCG	98
		Reverse DB-MR	TGC AAA AAC ATC TTC AAG TCT CTG	
		M gene probe	TTTTTTTTTTCCCCCCCCCC TCA GGC CCC CTC AAA GCC GA	
H5	HA	Forward DB-H5LH1	CY5-ACA TAT GAC TAC CCA CAR TAT TCA G	151
		Reverse DB-H5RH1	AGA CCA GCT AYC ATG ATT GC	
		H5 Probe	TTTTTTTTTTCCCCCCCCCC TCW ACA GTG GCG AGT TCC CTA GCA	
H7	HA	Forward DB-LH6H7	CY5-GGC CAG TAT TAG AAA CAA CAC CTA TGA	131
		Reverse DB-R4H7	GCC CCG AAG CTA AAC CAA AGT AT	
		H7 Probe	TTTTTTTTTTCCCCCCCCCC CCG CTG CTT AGT TTG ACT GGG TCA ATC T	

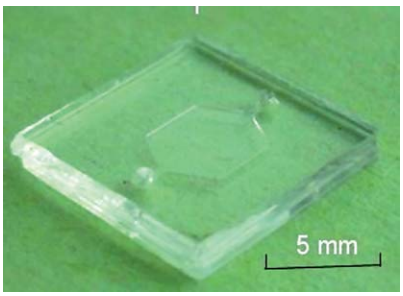

Fig. 2 Photograph of the hybrid PDMS–glass microchip. DNA microarray was spotted on the glass substrate. The outer dimension of the microchip was 10 mm × 10 mm and the volume of the microchamber was 2 μl.

microchip was 10 mm × 10 mm and the volume of the microchamber was 2 μl.

On-chip solid-phase PCR

25 μl PCR reaction mix was prepared which consisted of 10 μl of 5 x RT-PCR buffer, 1 μl of 10 mM DNTP mix, 1 μl of 2 μl /reaction enzyme mix, 2.5 μl of 2.5 μg μl^{-1} BSA (Onestep RT-PCR kit, Qiagen, Germany), three pairs of primers with a final concentration of 1 μM for forward primers and 0.5 μM for reverse primers, and 5 μl RNA sample. 2 μl of the mixture was loaded into the microchamber. The whole chip was placed in a homemade chip holder and the inlet and outlet were then sealed by pressing rubber plugs down on the holes. The chip holder was put on a flatbed thermocycler (MJ Research Inc., MA, USA). PCR was carried out according to the following program: 15 min at 50 °C for reverse transcription, followed by 40 cycles of 1 s at 95 °C, 5 s at 54 °C and 3 s at 72 °C, and finally 3 min at 72 °C for extension. After the cycling, the microchamber was washed with 0.1× SSC per 0.1% SDS and deionized water.

The microarray in the microchip was scanned by an array scanner (LaVision BioTec, Germany). Fluorescence imaging and processing software (LaVision BioTec, Germany) was used to quantify the spots by calculating the average pixel intensity inside the defined spots.

Sensitivity of solid-phase PCR

The sensitivity of the solid-phase PCR was evaluated. Ten-fold serial dilution of an AIV strain H16N3 ranging from 10^0 to 10^{-9} was made and the RNA was isolated from the virus dilution series according to the method described above. The hemagglutination titre (HA titre) value for the AIV strain was measured to be 1 : 64. The fifty percent egg infectious dose (EID_{50}) calculated for H16N3 strain was 6.7 $\log_{10}$ EID_{50} per ml. 5 μl of RNA was used as template and added to 20 μl PCR master mix.

Results and discussion

DNA immobilization on unmodified glass surface

Conventionally, fabrication of DNA microarrays on glass slides requires tedious and time-consuming procedures for surface treatment and DNA immobilization,[14,25] which seriously hinders the integration of microarrays into microfluidic systems. In this study, a much faster and easier immobilization method was developed by us where DNA probes with poly(T)10–poly(C)10 tails were immobilized on the unmodified glass surface by simple UV cross-linking. During UV exposure, covalent bonds are formed between the TC tag and the glass surface. The probes modified with TC tails offer up to 70% cost reduction when compared to the commonly used amino group modifications of the probes and make solid-phase PCR a convenient possibility for AIV screening. Another advantage of our immobilization method is that the probes are thermally stable. For other immobilisation methods it can be a problem that the primer detaches during thermo-cycling. A 60% loss of grafted primers during thermo-cycling was reported.[27] This is, however, not

a problem with our method. No significant decrease in fluorescence signal was observed after 20 min incubation in water at 100 °C.[26]

Specificity of on-chip solid-phase PCR

On-chip solid-phase amplifications were conducted with RNA extracts from four viral strains: H1N1, H5N1, H7N5, and NDV respectively. As shown in Fig. 3, with the developed microchip, three AIV viral strains were accurately identified by the distinct patterns of amplified products. No positive signal was obtained for the NDV. In particular, non-specific amplification was almost negligible as the probes in solid-phase PCR were spatially separated. The simple visual inspection of the fluorescence scan images suggested that the multiplex solid-phase amplification is an efficient and specific procedure. But it was also noticed that significant amounts of spot intensity variations were produced for different kinds of probes. As suggested by Huber *et al.*,[28] this was due to some inherent factors such as microarray substrate quality, template quality, and sequence properties of the analyzed DNA fragments. Nevertheless, all strains tested in this study were unambiguously distinguished from each other based on their specific combinations of fluorescence products. The number of solid-phase probes can be continually extended to include sequences for additional AIV subtypes.

Optimization of solid-phase amplification

In this study, parameters such as the ratio of aqueous primers and solid-phase probe density that are likely to affect solid-phase PCR were optimized to ensure efficient amplification. RNA extracted from 10^{-1} AIV H16N3 strain was used as template for the amplification.

As the aqueous forward primers were designed to bind to both templates in the solution and amplicons tethered on the solid support, the reverse primers were included at a limiting concentration to lower the competition with solid probes. The optimum primer ratios were identified by keeping the concentration of reverse primers at 0.5 μM while increasing the concentration of forward primers from 0.5 μM to 5 μM. When the forward primers in the liquid were doubled from 0.5 μM to 1 μM, 20% increase in the amount of immobilized amplicons was observed. Further increase in the concentration had no effect on the yield of solid-phase amplifications. Therefore, 1 μM forward primers were used to ensure amplification was not limited by the amount of aqueous primers in the reaction.

The probe density is another important factor that could limit the amount of amplicons. The density of probes immobilized on the glass substrate was changed by varying the spotting concentrations from 5 μM to 50 μM. As shown in Fig. 4, the amount of amplicons increased linearly when the probe concentration was raised from 5 μM to 20 μM. But increasing the concentration from 20 μM to 40 μM had no significant effect on the yield of the immobilized amplicons, while an excess number of probes reduced the yield of solid-phase amplifications, indicating that too high probe density negated amplification. The low amplification efficiency at high probe concentration may have several explanations. One explanation could be screening effect: when the probes are immobilized at high density, the high negative charges in close proximity to a solid support disturb polymerase functioning on the surface and repel of target DNA in solution, thus reducing the extension efficiency. Another explanation could be that abnormal target–probe and probe–probe interactions on planar microarrays are intensified at higher probe density, therefore decreasing the amount of accessible probes on the chip and reducing priming and amplification efficiency. For this system, the maximum amplification efficiency

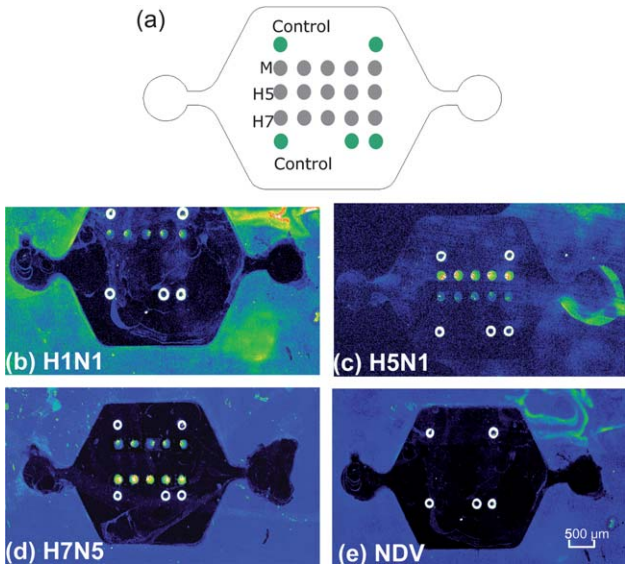

Fig. 3 Specificity of on-chip solid-phase PCR. (a) Microarray layout. The DNA probes for M gene and HA genes specific for H5 and H7 are represented as gray circles. Each dot is 150 μm in diameter with a center-to-center distance of 300 μm. Green circles are guiding dots used for orientation. Fluorescent images after 40 cycle amplification of four different viral RNA strains: (b) AIV H1N1, (c) AIV H5N1, (d) AIV H7N5 and (e) Newcastle disease virus (NDV). The strong fluorescence outside of the chip is due to the autofluorescence of PDMS residues.

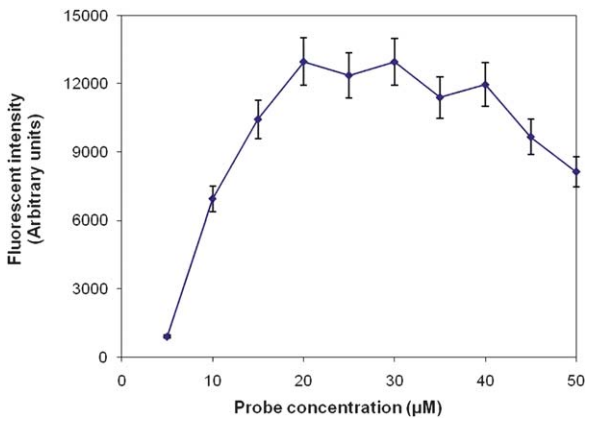

Fig. 4 Effect of probe concentration on solid-phase RT-PCR. Solid-phase amplification of 10^{-1} H16N3 viral RNA was performed in replicate reactions with probe concentration varied from 5 μM to 50 μM. 1 μM forward primers and 0.5 μM reverse primers were contained in the PCR solution. Fluorescence intensities of probes specific to M gene were measured. Values represent the mean fluorescence and the standard deviation of triplicate reactions for each probe concentration.

was achieved at the combined condition of 1 μM forward primers and 20 μM immobilized probes.

Detection limit of on-chip solid-phase PCR

The sensitivity of the on-chip solid-phase PCR was determined and compared analytically with solution-based multiplex RT-PCR. 10-Fold serial dilution (from 10^0 to 10^{-9}) of RNA extracted from AIV H16N3 strain was amplified in triplicate reactions. As shown in Fig. 5, the lowest concentration of template at which positive fluorescence signals could be detected for solid-phase PCR was 10^{-6}, or equivalent to 0.7 $\log_{10}$ EID_{50} per ml. The fluorescence increased with template concentration, suggesting that more amplification occurred on the surface at higher template concentration. The signal reached a plateau when the RNA template was present at 10^{-1}, indicating the surface became saturated with the PCR products. The coefficient of variation of the replicate reactions was 8% on average. The detection limit of the solution-based multiplex PCR using the same biological model was 10^{-5}, or equivalent to 1 $\log_{10}$ EID_{50} per ml, similar to that published in the literature[29] (see ESI†). Compared to liquid-based amplification, 10-fold improvement was achieved by on-chip solid-phase PCR.

Compared to solid-phase PCR using a coverslip or a self-adhesive frame

In conventional solid-phase PCR, a glass coverslip or a self-adhesive frame is mounted onto the oligonucleotide array to seal the reaction mixture. In both cases, a large amount of PCR samples (25 μl for standard Gene frame) are required.[7] The large sample mass requires lengthy time for denaturation and annealing, and total reaction times are typically in excess of 2 hours. In addition, air bubbles are easily trapped under the coverslip or in the frame even with very careful handling, which could adversely affect the efficiency of solid-phase PCR. Moreover, self-seal reagent is usually contained in the reaction mixture to prevent evaporation during PCR, which polymerizes upon contact with air at high temperature and thereby seals the reaction at the edges. While the effect of polymerization on solid-phase PCR is still under investigation, MJ Research Inc. has stopped the supply of the self-seal reagent and a substitute product has not appeared in the market. This poses a great challenge to solid-phase amplification.

In our approach, a 2 μl chamber-based PCR microchip was fabricated to replace the conventional coverslip or frame. As the sample volume was greatly reduced, the denaturation and annealing steps occurred as soon as the correct temperature was reached, and the process was only limited by the extension step. Consequently, the total reaction time was shortened by half. Furthermore, due to the micron sized feature dimension and the closed fluidic format of the microchip, the small amount of samples could be manipulated and processed with a high degree of control. Solution evaporation and bubble formation were effectively prevented. Compared to solid-phase PCR carried out using the coverslip or frame, the amplification in PCR microchip provided better performance as the detection limit achieved on-chip (10^{-6}) was 10-fold better than that obtained using the coverslip (10^{-5})[30] (see ESI†). PCR microchip and DNA microarray have been shown to be a perfect combination, which affords gains in terms of control, speed, efficiency and functionality.

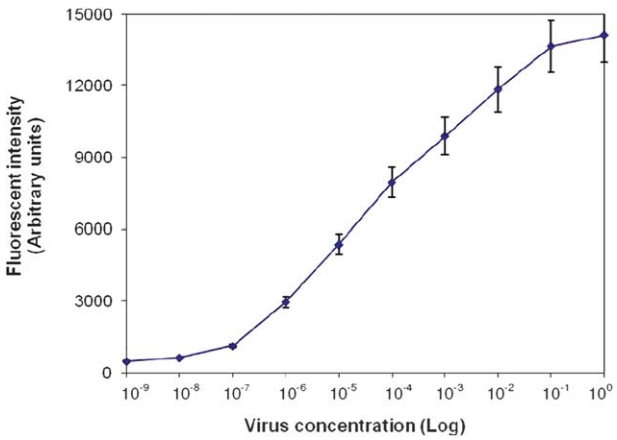

Fig. 5 Sensitivity of solid-phase RT-PCR. Serial 10-fold dilutions of viral RNA extracted from H16N3, ranging from 10^0 to 10^{-9}, were used as templates. Replicate solid-phase PCR was prepared each containing 1 μM forward primers and 0.5 μM reverse primers in solution, and 20 μM probes immobilized on glass surface. Fluorescence intensities of probes specific to M gene were measured. Values represent the mean fluorescence and the standard deviation of triplicate reactions for each template concentration. The detection limit was 10^{-6}, or equivalent to 0.7 $\log_{10}$ EID_{50} per ml.

Conclusions

In conclusion, we have developed a simple lab-on-a-chip device for rapid screening and subtyping AIV viral RNA based on on-chip solid-phase PCR. The platform combines RT-PCR in the liquid phase and simultaneous nested amplification with species-specific oligonucleotide probes on the solid surface. Different AIV viral strains were accurately identified by the distinct patterns of reaction products. By immobilizing probes on the glass surface, primer interference effects are minimized, such that the number of AIV subtypes to be identified can easily be extended by adding more species-specific oligonucleotides to the microarray. Moreover, no post-PCR step is needed apart from array scanning, which prevents potential cross-contamination and facilitates the process for AIV detection. By combining the superior specific multiplex format of solid-phase PCR with low reagent consumption and fast cycling provided by the PCR microchip, the platform can be widely employed by veterinarians for on-site rapid screening of AIV in wild and industrial domestic poultries.

Acknowledgements

This work is financially supported by Technical University of Denmark (DTU), Food Pathogen Project No. 8, Grant No. 150627, Forskningsrådet Teknologi og Produktion (FTP), Sagsnr. 09066477, and EU FP-7 IP LABONFOIL project, Grant No. 224306.

References

1 D. J. Alexander, *Vaccine*, 2007, **25**, 5637–5644.
2 D. J. Alexander, *Vet. Microbiol.*, 2000, **74**, 3–13.

3 M. S. Lee, P. C. Chang, J. H. Shien, M. C. Cheng and H. K. Shieh, *J. Virol. Methods*, 2001, **97**, 13–22.
4 E. Starick, A. Romer-Oberdorfer and O. Werner, *J. Vet. Med., Ser. B*, 2000, **47**, 295–301.
5 B. Chaharaein, A. R. Omar, I. Aini, K. Yusoff and S. S. Hassan, *Microbiol. Res.*, 2009, **164**, 174–179.
6 Z. X. Xie, Y. S. Pang, H. B. Uu, X. W. Deng, X. F. Tang, H. H. Sun and M. I. Khan, *Mol. Cell. Probes*, 2006, **20**, 245–249.
7 A. Pemov, H. Modi, D. P. Chandler and S. Bavykin, *Nucleic Acids Res.*, 2005, **33**, e11.
8 K. A. Hagan, C. R. Reedy, M. L. Uchimoto, D. Basu, D. A. Engel and J. P. Landers, *Lab Chip*, 2011, **11**, 957–961.
9 C. Adessi, G. Matton, G. Ayala, G. Turcatti, J. J. Mermod, P. Mayer and E. Kawashima, *Nucleic Acids Res.*, 2000, **28**, 87e.
10 M. H. Shapero, K. K. Leuther, A. Nguyen, M. Scott and K. W. Jones, *Genome Res.*, 2001, **11**, 1926–1934.
11 C. M. Niemeyer, M. Adler and R. Wacker, *Nat. Protoc.*, 2007, **2**, 1918–1930.
12 M. v. Nickisch-Rosenegk, X. Marschan, D. Andresen and F. F. Bier, *Anal. Bioanal. Chem.*, 2008, **391**, 1671–1678.
13 R. Palanisamy, A. R. Connolly and M. Trau, *Bioconjugate Chem.*, 2010, **21**, 690–695.
14 G. Mitterer, M. Huber, E. Leidinger, C. Kirisits, W. Lubitz, M. W. Mueller and W. M. Schmidt, *J. Clin. Microbiol.*, 2004, **42**, 1048–1057.
15 A. Suomalainen and A. C. Syvanen, *Mol. Biotechnol.*, 2000, **15**, 121–131.
16 D. A. Khodakov, N. V. Zakharova, D. A. Gryadunov, F. P. Filatov, A. S. Zasedatelev and V. M. mikhailovich, *BioTechniques*, 2008, **44**, 241–248.
17 H. N. Liu, S. Li, L. Liu, L. Tian and N. Y. He, *Anal. Biochem.*, 2009, **386**, 126–128.
18 G. Mitterer, O. Bodamer, C. Harwanegg, W. Maurer, M. W. Mueller and W. M. Schmidt, *Genet. Test.*, 2005, **9**, 6–13.
19 Y. Sun, M. V. D. Satya, Y. C. Kwok and N. T. Nguyen, *Sens. Actuators, B*, 2008, **130**, 836–841.
20 Y. Sun, Y. C. Kwok, F. P. Lee and N. T. Nguyen, *Anal. Bioanal. Chem.*, 2009, **394**, 1505–1508.
21 Y. H. Zhang and P. Ozdemir, *Anal. Chim. Acta*, 2009, **638**, 115–125.
22 Z. Guttenberg, H. Muller, H. Habermuller, A. Geisbauer, J. Pipper, J. Felbel, M. Kielpinski, J. Scriba and A. Wixforth, *Lab Chip*, 2005, **5**, 308–317.
23 M. Hashimoto, F. Barany and S. A. Soper, *Biosens. Bioelectron.*, 2006, **21**, 1915–1923.
24 D. Sabourin, J. Petersen, D. Snakenborg, M. Brivio, H. Gudnadson, A. Wolff and M. Dufva, *Biomed. Microdevices*, 2010, **12**, 673–681.
25 M. Huber, D. Losert, R. Hiller, C. Harwanegg, M. W. Mueller and W. M. Schmidt, *Anal. Biochem.*, 2001, **299**, 24–30.
26 H. Gudnason, M. Dufva, D. D. Bang and A. Wolff, *BioTechniques*, 2008, **45**, 261–271.
27 M. Fedurco, A. Romieu, S. Williams, I. Lawrence and G. Turcatti, *Nucleic Acids Res.*, 2006, **34**, e22.
28 M. Huber, A. Mundlein, E. Dornstauder, C. Schneeberger, C. B. Tempfer, M. W. Mueller and W. M. Schmidt, *Anal. Biochem.*, 2002, **303**, 25–33.
29 C. W. Lee and D. L. Suarez, *J. Virol. Methods*, 2004, **119**, 151–158.
30 Y. Sun, R. Dhumpab, D. D. Bang, K. Handberg and A. Wolff, *Diagn. Microbiol. Infect. Dis.*, 2011, **69**, 432–439.

Supplementary Information to paper "A lab-on-a-chip device for rapid identification of avian influenza viral RNA by solid-phase PCR"

The sensitivity of two other AIV identification methods - multiplex solution-based RT-PCR and conventional solid-phase PCR with cover slip, were determined. The limit of detection was compared to that achieved by on-chip solid-phase PCR as described in the paper.

Sensitivity of solution-based multiplex RT-PCR

10-fold serial dilution of AIV strain H16N3 ranging from 10^0 to 10^{-9} was prepared. Hemagglutination (HA) titre values for the AIV strains were measured to be 1:64. The fifty percent egg infectious dose (EID_{50}) calculated for H16N3 strain was $6.7\log_{10}$ EID_{50} per ml. RNA was isolated from the viral dilution series and 5µl of each dilution was used as template. The multiplex RT-PCR was performed using a RT-PCR kit (Qiagen, Hilden, Germany). The RT-PCR conditions were based on the manufacturer's instruction with minor modification. Briefly, a 25 µl reaction mixture contains 5 µl of 5× RT-PCR buffer, 1 µl of 10 mM DNTP mix, 1 µl of enzyme mix, 5 µl of RNA sample, and three pairs of primers, each at a final concentration of 0.2 µM. PCR was carried out in a thermal cycler (MJ Research Inc., MA, USA) and the cycling protocol consisted of 30 min at 50 ºC for reverse transcription, 15 min at 95 ºC for enzyme activation, followed by 40 cycles of 10 sec at 95 °C, 30 sec at 54 °C and 10 sec at 72 °C, finally 5 min at 72 °C for extension. The PCR amplicons were analyzed using slab gel. As shown in Fig. 1, the 100 bp PCR amplicon of M gene was observed up to 10^{-5} or equivalent to 1 $\log_{10}$ EID_{50}/ml.

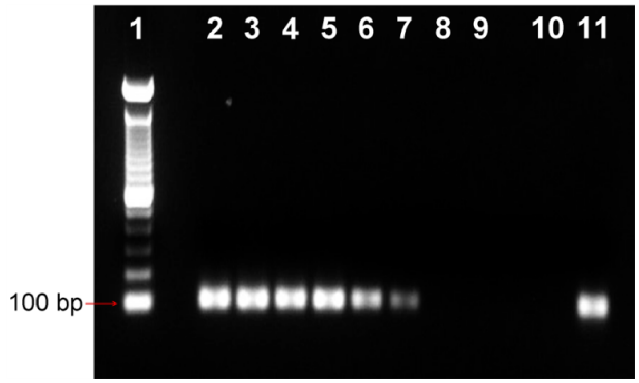

Fig. 1. Detection of H16N3 AIV by solution-based multiplex RT-PCR. Serial 10-fold dilutions of the extracted viral RNA templates, ranging from 10^0 to 10^{-9}, were tested. Amplified products (100 bp target for M gene) with different template concentrations are shown. Lane 1: 100 bp DNA ladder; Lane 2 – 9: 10-fold dilutions of the virus pool ranging from the original HA titre to 10^{-7}, respectively; Lane 10: Negative control (virus free); Lane 11: Positive control. The virus strain was not recognized at the dilutions higher than 10^{-5} or equivalent to 1 log10EID_{50}/ml.

Sensitivity of conventional solid-phase PCR with cover slip

10-fold serial dilution of AIV strain H16N3 ranging from 10^0 to 10^{-9} was prepared and RNA was isolated from the viral dilution series. Microarray was produced on the glass slides by using TC-tagged probes as described in the paper. 25 µl reaction master mix for solid phase RT-PCR contains

10 µl of 5× RT-PCR buffer, 1 µl of 10 mM DNTP mix, 1 µl of enzyme mix, 5 µl of RNA sample, three pairs of primers with each at a final concentration of 1 µM, 2.5 µl of 2.5 µg/µl BSA and 6 µl self sealing reagent (MJ Research, Inc., MA, USA).

10 µl master mix was loaded directly on the oligonucleotide microarrays and cover slips were mounted to seal the reaction droplets. The glass slides were transferred into a twin tower PTC 200 slide thermocycler (MJ Research Inc., MA, USA). PCR was carried out according to the following program: 15 min at 50 ºC for reverse transcription, 10 min at 95 ºC for enzyme activation, followed by 40 cycles of 10 sec at 95 °C, 30 sec at 54 °C and 10 sec at 72 °C, and finally 5 min at 72 °C for extension. After cycling, the slides were washed with agitation in 0.1× SSC/0.1% SDS for 10 min, followed by a short rinse in deionized water. The microarrays were scanned by ScanArray Lite (Packard Bioscience, MA, USA), with appropriate laser power and PMT settings. ScanArray software (Packard Bioscience, MA, USA) was used to quantify the spots by calculating the average pixel intensity inside the defined spots.

As shown in Fig. 2, similar detection limit was obtained for solid-phase RT-PCR with cover slips, where the lowest concentration of template at which positive fluorescence signals could be detected was also 10^{-5} or equivalent to 1 $\log_{10}$ EID_{50}/ml. In this paper, for solid-phase PCR performed in the microchamber, the lowest concentration of template at which positive fluorescence signals could be detected was 10^{-6}, or equivalent to 0.7 $\log_{10}$ EID_{50}/ml. Compared to both solution-based multiplex PCR and solid-phase PCR with cover slips, 10-fold improvement was achieved by on-chip solid-phase PCR.

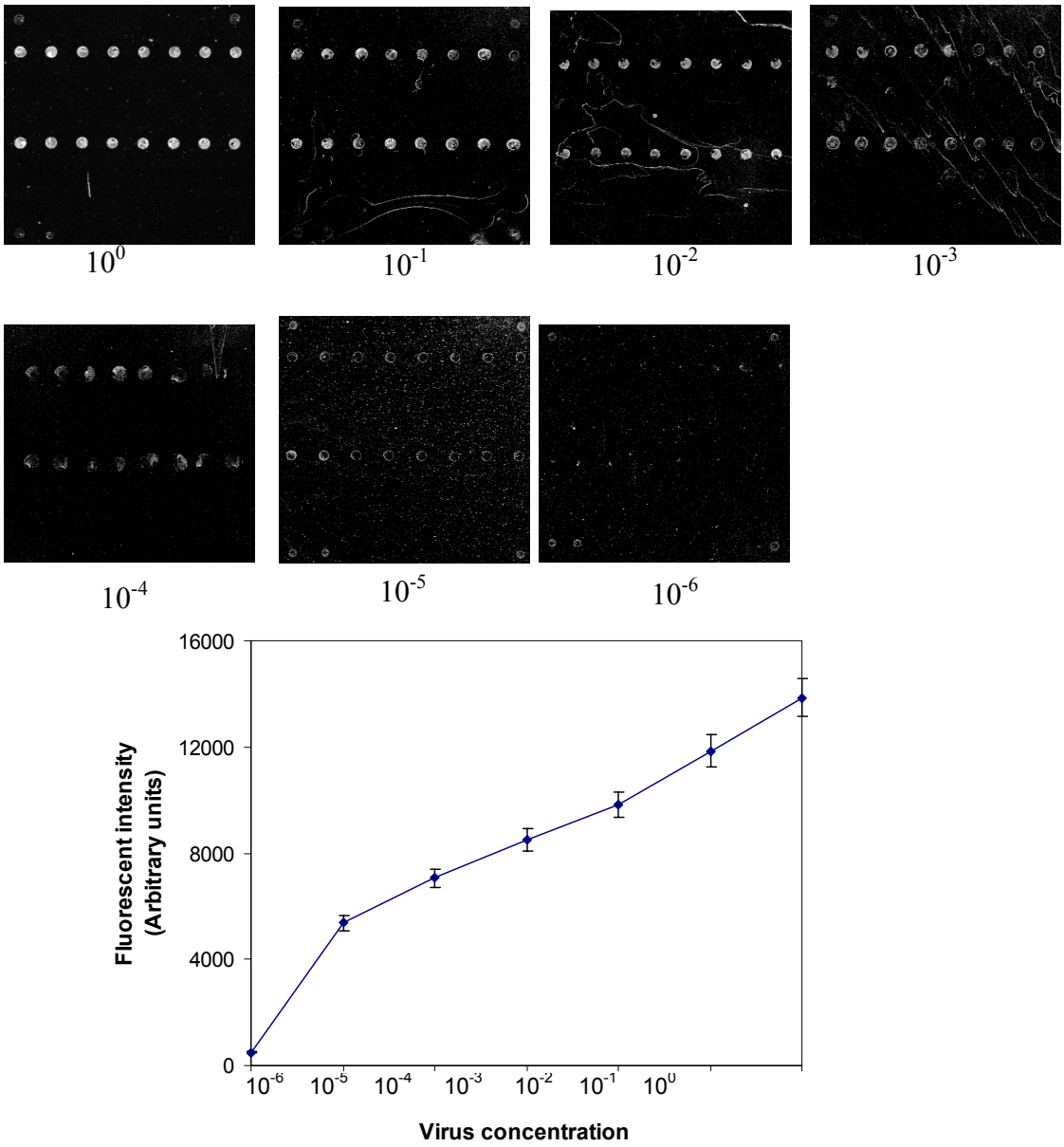

Fig. 2 Detection of H16N3 AIV by conventional solid-phase PCR with cover slip. Serial 10-fold dilutions of the extracted viral RNA templates, ranging from 10^{0} to 10^{-9}, were tested. Fluorescence intensities of probes specific to M gene were measured. The detection limit was also 10^{-5} or equivalent to 1 $\log_{10}$ EID_{50}/ml.

7.3 Development of simultaneous detection and haemagglutinin subtyping of Avian Influenza Viruses using solid-phase RT-PCR

7.3.1 Introduction

In section 7.1 and 7.2 solid-phase RT-PCR that combines multiplex reverse-transcription amplification of RNA target in the liquid-phase and sequence-specific nested PCR was developed successfully in both microscopic glass slide and PDMS chip. However, the developed method can only detect two subtypes H5 & H7 among 16 HA types. Subtyping of all the 16 HA types is essential for the identification of circulating AIV strains that could emerge as a pandemic influenza virus[44]. In this section, the research is therefore focused on development of simultaneous detection and haemagglutinin subtyping of all 16 HA subtypes of AIV.

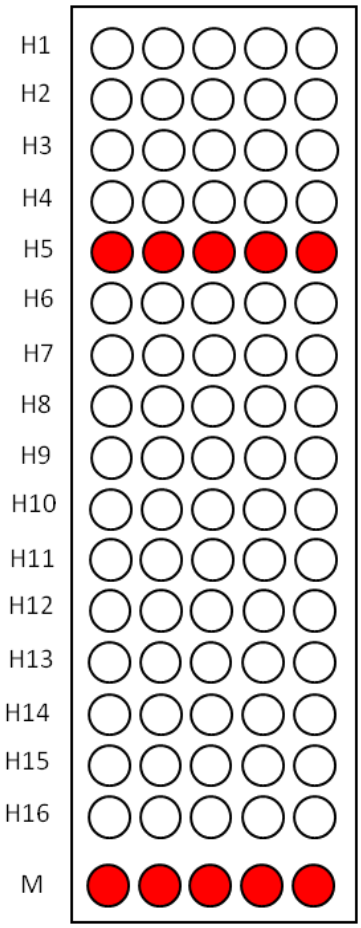

Figure 7.3.1 Scheme of simultaneous subtyping of all hemagglutinin types (H1-H16) using solid-phase RT-PCR.

The standard diagnostic method for HA subtyping is haemagglutinin inhibition (HI) test (See section 3.4). The HI test is performed only at reference laboratories due to the limited supply of antisera, the highly variation within a subtype, and the cross-reactivity among different subtypes [61]. Thus a reliable subtyping method that can be easily applied at most diagnostic laboratories is needed. Subtyping of AIV based on rRT-PCR has been considered as sensitive and specific methods (see section 4.3 to 4.4) that can be performed in normal diagnostic laboratories. However, rRT-PCR based on multiplexing has a limit for the number of targets that can be detected simultaneously because of the limit in availability of fluorescent dye combinations[108].

Microarrays provide an opportunity to detect many targets simultaneously. Recently, great efforts were made in utilizing a combination of RT-PCR and a microarray for not only subtyping

but also for pathotyping of AIV[112-115]. However, in those studies the combination of RT-PCR amplification and microarray detection has often been performed in multiple steps and the protocol is complicated. In this study, we aimed to develop a method that combines microarray and solid phase RT-PCR for AIV detection and simultaneous HA subtyping (H1-H16) (Figure 7.3.1). As a first step to develop such method, primers and probes were designed and tested.

7.3.2 Materials and Methods

Design of oligonucleotides

The RT-PCR capture-probes (CP) and primers were designed based on sequence information obtained from the NCBI Influenza Virus Resource Database (IVRD)[178]. A total of 200 AIV strains with at least 10 sequences of each of 16 HA that originated from different geographical (Europe and Asian) locations were selected for this study. These sequences were aligned using the "Alignment tool" of CLC Workbench program, version 5.0.2 (CLC bio, Aarhus, Denmark). On the alignment the conserved regions of HA1 and HA2 serve as annealing sites for a forward and a reverse primer to amplify the HA cleavage site [179] whereas the variable region (within the two primers region) was used to search for the sequences that could be used as probes for subtyping HA (H1 to H16) of AIV (Figure 7.3.2). The 16 HA CP were designed according to the similarities within the HA subtypes.

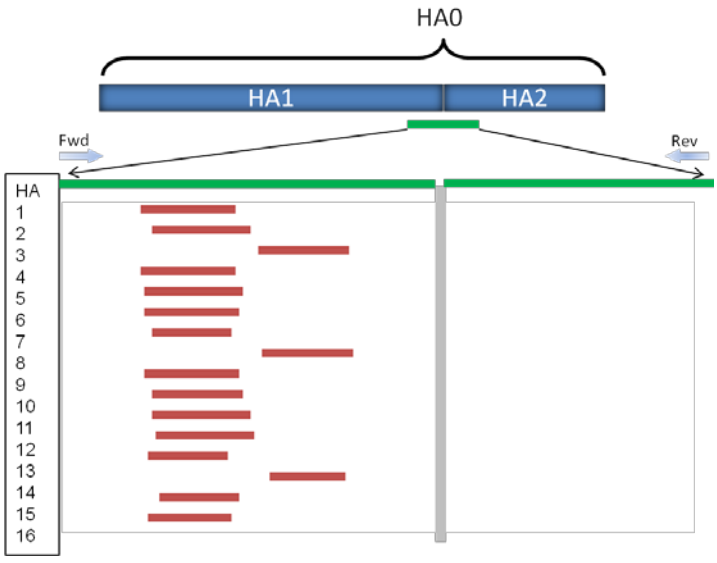

Figure 7.3.2 Scheme of HA subtyping to detect all 16 HA subtypes at the HA cleavage site (reproduced from ref [180]).

RT-PCR

A one-step RT-PCR was performed using One-Step RT-PCR kit (Qiagen, Copenhagen, Denmark). The RT-PCR mixture (10 µl per reaction) contained 2 µl of RNA, 0.4 µl of each primer (50 µM), 2 µl of RT-PCR buffer, 4.4 µl of RNase-free water, 0.4 µl of dNTP and 0.4 µl of enzyme mix. The RT-PCR cycling conditions were 50 °C for 30 min and 95 °C for 15 min followed by 40 cycles of 94°C for 10s , 50 °C for 30 s, and 72 °C for 10 s and finally 72 °C for 3 min. The results were analysed by electrophoresis on a 1.5% agarose gel.

AIV Subtyping

The designed probes for subtyping the 16 HA types were first tested using RT-PCR. Each probe was used as a forward primer in a HA primer set and tested by RT-PCR. The specificity of each HA probe was tested using RT-PCR with RNA isolated from other HA subtypes.

7.3.3 Results and Discussions

Design of primers and capture-probes for subtyping of 16 HA Subtypes of the AIV

Table 7.3.1 shows a list of primers and capture-probes that were designed in this study. Due to a high variation among the 16 HA subtypes, the consensus of HA primer includes some degenerate sequence with several bases that permit binding to all or most common known variants on the conversed region (Figure 7.3.3). These degenerated primers would also find genes or subtypes that would emerge by a change in the HA cleavage region. A number of publications have used degenerated primers for the amplification of HA or NA genes as well as for subtyping of AIV[179-182]. Our approach differs from these studies, since the use of solid-phase PCR that could provide a cost effective system needed in the future for fast and accurate identification of any emerging new AIV subtypes during large screening and surveillance[183]. The use of solid-phase PCR with several probes specific for each of HA subtype can be used and reduces the risk of non-specific amplification involved in degenerate primers.

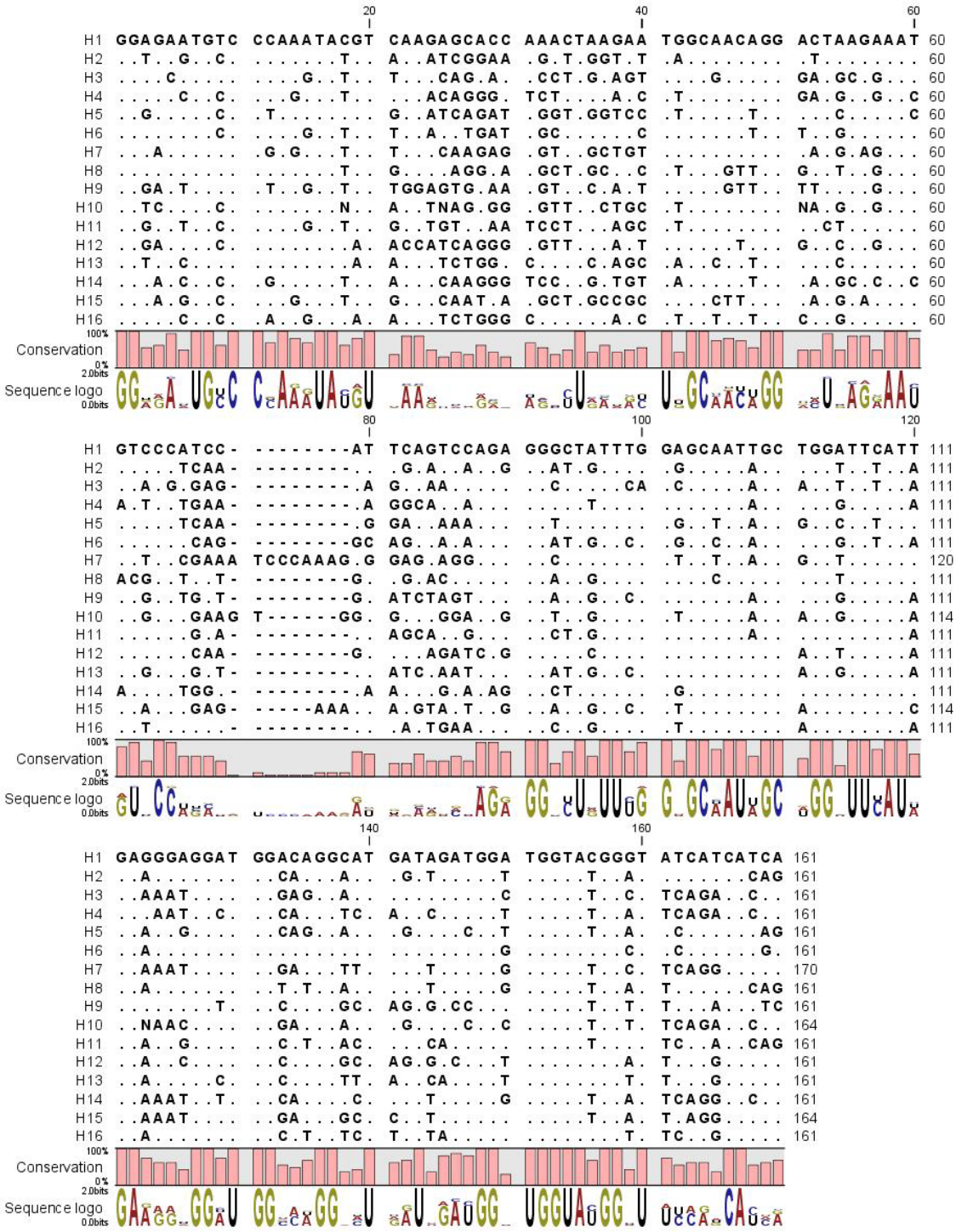

Figure 7.3.3 A simplified alignment of all 16HA subtypes of AIV. The big letter/bar in the sequence logo/conversation represents the consensus in all subtype.

Table 7.3.1 List of designed primers and probes for typing of 16 HA subtypes of AIV. The degenerate position are R:A+G, Y:C+T, M:A+C, K:G+T, W:A+T, H:A+T+C, D:G+A+T, N:A+G+C+T

Oligonucleotide	Sequence (5'-3')
HA_Fwd	GGD RMN TGY CCN ARR TAY RT
HA_Rev	GHY KRW ANC CRT ACC ANC C
H1 Probe	CAA GAG CAC CAA ACT AAG AAT GGC AA
H2 Probe	ATC GGA AAG ATT GGT ATT AGC AAC AGG
H3 Probe	AT GCG GAA TGT ACG AGA GAA GCA AA
H4 Probe	CAA ACA GGG CTC TCT AAA ACT TGC AA
H5 Probe	AA ATC AGA TAG GTT GGT CCT TGC AAC T
H6 Probe	AAA AGT GAT AGC CTA AGA CTG GCA AC
H7 Probe	GCA AGA GAG TCT GCT GTT GGC A
H8 Probe	T TAG GAA TAC GCC TTC TGT TGA ACC
H9 Probe	GGA GTG AAA AGT CTC AAA TTG GCA GT
H10 Probe	TMA GAR GAG TTT RMT GCT TGC AAC A
H11 Probe	TGT CAA ATC CTT AAA GCT TGC AAC AGG
H12 Probe	TC AGG GAG TTT AAA ATT GGC AAT AGG G
H13 Probe	A GTC TGG CCA ACT CAA GCT AGC
H14 Probe	CGC AAC ATC CCT GGC AAA CAG
H15 Probe	A ATC AAG CTT GCC GCT GGC CTT
H16 Probe	A GTC TGG GCA ACT AAA ACT TGC TAC T

HA primer set for detection of AIV

The designed HA primer set was tested and evaluated using RT-PCR with RNA from all 16 different HA subtypes (Table 1 of section 6.1). Figure 7.3.4 shows such results. Using, primer set namely HA_Fwd / HA_Rev (Table 7.3.1) all the 16 HA subtypes of the AIV were amplified successfully. A difference in the signal intensity of RT-PCR was observed that could be due to the differences in the binding energies and the preferential amplification of sequences containing G/C rich primer sites[184]. To determine the specificity of the HA primer set, RT-PCR was performed with RNA extracted from faecal sample as well as with RNA isolated from two

strains of NDV virus (La Sota and Ulster strains). Figure 7.3.5 shows the results of such experiment. Although the HA primers contain degeneracy, the specificity test showed no PCR amplification for both the RNA extracted from Chicken faecal (isolated from AIV-free Chicken) and the NDV virus strains were observed. This demonstrates the usefulness of the HA primer for amplification of HA cleavage region for further subtyping and pathotyping.

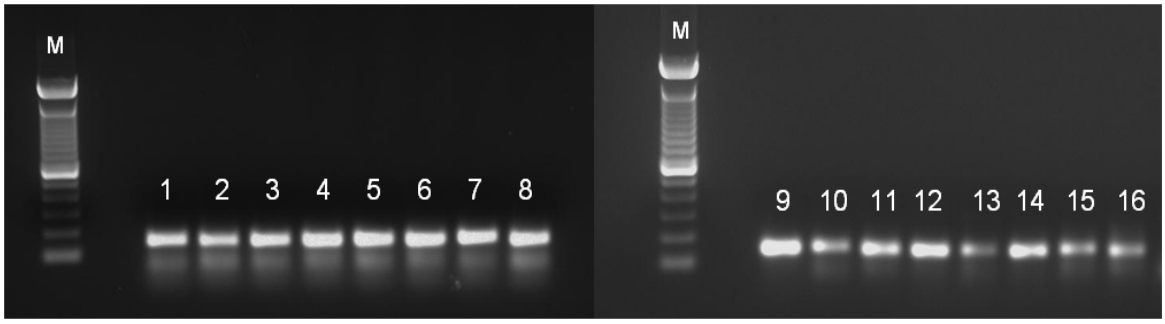

Figure 7.3.4 RT-PCR results with the designed HA primers tested with 16HA types. On gel: lane 1 to 16 represent subtype of H1 to H16. M: Marker 100bp (Inivtrogen)

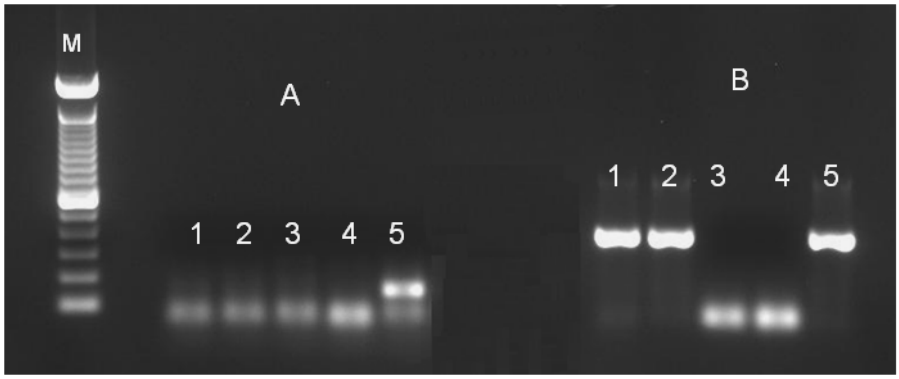

Figure 7.3.5 RT-PCR specificity test for A) HA primer set and B) control NDV primer set. Lanes 1) with RNA from NDV virus strain La Sota, 2) with RNA from NDV virus strain Ulster strain, 3) with RNA from chicken faecal sample, 4) negative control and 5) positive control. M) Marker 100bp (Inivtrogen).

Subtyping of AIV

Specific capture-probes were designed for subtyping each of the 16 HA genes. The probes were located within the region amplified by the HA primers. The first set of probes was tested for subtyping of H1, H2, H4 and H7. Figure 7.3.6 shows the RT-PCR results of such tests. In this

RT-PCR, the capture-probes were used as the forward primers while the HA_Rev was used as the reverse primer. The RT-PCR was amplified successfully (Figure 7.3.6).

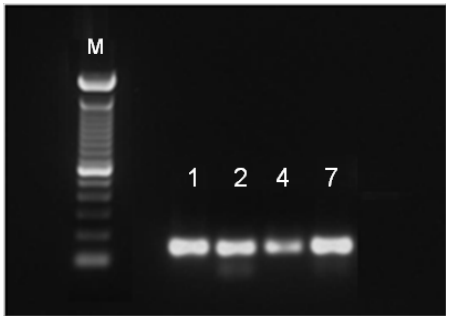

Figure 7.3.6 Subtyping of AIV by RT-PCR. Lane 1, 2, 4 and 7 represent the corresponding HA subtypes H1; H2; H4 and H7 respectively.

The designed H1, H2, H4 and H7 probes were further tested for their specificity. Each probe was used as a forward primer in a RT-PCR to amplify the RNA targets extracted from reference strains from H1 to H16. Figure 7.3.7 (a, b, c and d) shows the results of such experiment. Using the designed probe H1 (Figure 7.3.7 a) for example, a RT-PCR amplicon of 166 bp was obtained with RNA target from AIV reference strain subtype H1.

A strong signal was observed for the particular (H1) subtype. However, amplicons with the same size are observed also with the RNA targets from other subtypes of H3, H6, H9 and H12. Similar results were observed with the designed H2, H4 and H7 subtype probes (Figure 7.3.7 b, c and d). The quantification of gel bands using ImageJ software (National Institute of Health, USA) reveals that the strongest non-specific band for H1, H2, H4 and H7 had relative band intensities of 75.07%, 96.33%, 42.38%, 89.83% respectively.

The observation of non-specific bands could be due to the difference in the melting temperature (T_m) of probe (56.4°C) that was used as a forward primer and the reverse primer (50.4°C) in the RT-PCR reactions and overlapping of the target sequences. Immobilizing the capture probe on the solid substrate may reduce the probe T_m [185] and also the non-specific binding. Further optimization of the test in terms of selection of new probe sequence, RT-PCR reaction conditions and sequencing of RT-PCR product to understand the non-specificity is needed.

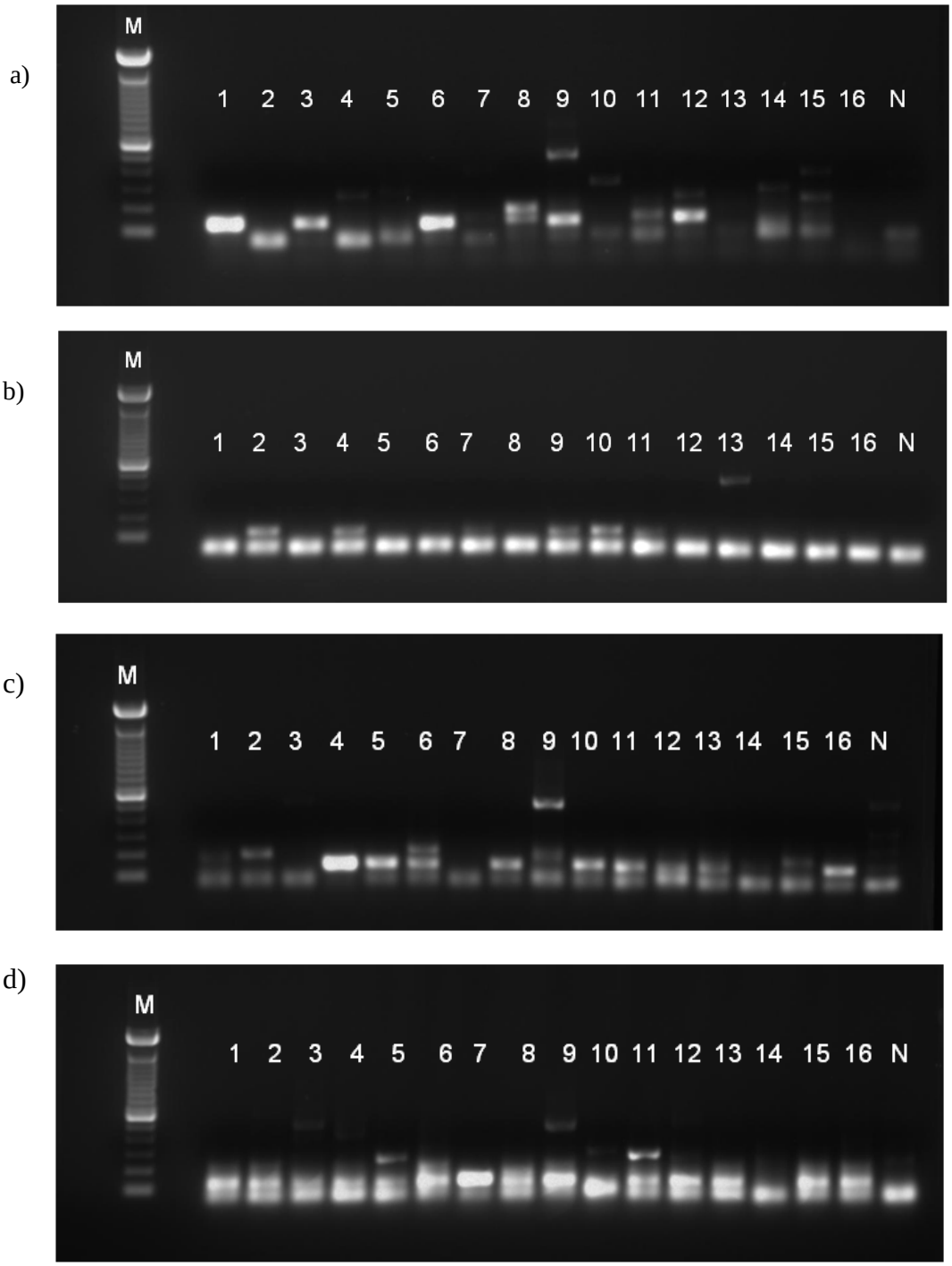

Figure 7.3.7 Specificity test of the probes for sub-typing of a) H1, b) H2, c) H4 and d) H7subtype using RT-PCR with RNA extracted from 16 different HA subtypes. On gel: lane 1 to 16 represent H1 to H16, respectively. N, negative control.

7.3.4 Conclusion

A set of primer for RT-PCR amplifying the cleavage region of the HA gene for all the 16 HA subtypes (H1-H16) of AIV has been designed and tested successfully. Using the designed primers in a RT-PCR with RNA isolated from chicken faecal or NewCastle disease virus, no amplification was observed. The amplified region could be a good target for further differentiating all the 16 HA subtypes as well as for pathotyping of the AIV isolates. With an attempt to subtyping of AIV using different probes, 16 HA capture-probes were designed and four capture-probes of H1, H2, H4 and H7 were tested using RT-PCR. However, non-specificity of RT-PCR amplifications was observed when the designed capture-probes were used as one of primer in the RT-PCR. The newly developed method needs to be further optimized in such directions for development of one-step multiplex RT-PCR for detection and subtyping of AIV using solid-phase RT-PCR.

Chapter 8

Immunoassay

This chapter focuses on the development of two immunological assays; a fluorescent DNA barcode-based assay and a fluorescent bead-based assay for rapid detection of AIV. In both assays, the target AIV is sandwiched between the AIV nucleoproteins monoclonal antibody and the AIV matrix protein monoclonal antibody. Fluorophore-tagged oligonucleotides and fluorescent beads are used as the detection signals in the fluorescent DNA barcode-based immunoassay and the fluorescent bead-based immunoassay, respectively. The advantages of each method for rapid detection of the AIV are presented and discussed.

8.1 Detection of avian influenza virus by fluorescent DNA barcode-based immunoassay with sensitivity comparable to PCR

Manuscript published in the Analyst, (2010) 135, 337-342.

Detection of avian influenza virus by fluorescent DNA barcode-based immunoassay with sensitivity comparable to PCR†

Cuong Cao,[a] Raghuram Dhumpa,[b] Dang Duong Bang,[b] Zohreh Ghavifekr,[b] Jonas Høgberg[b] and Anders Wolff*[a]

Received 13th August 2009, Accepted 30th November 2009
First published as an Advance Article on the web 15th December 2009
DOI: 10.1039/b916821b

In this paper, a coupling of fluorophore-DNA barcode and bead-based immunoassay for detecting avian influenza virus (AIV) with PCR-like sensitivity is reported. The assay is based on the use of sandwich immunoassay and fluorophore-tagged oligonucleotides as representative barcodes. The detection involves the sandwiching of the target AIV between magnetic immunoprobes and barcode-carrying immunoprobes. Because each barcode-carrying immunoprobe is functionalized with a multitude of fluorophore-DNA barcode strands, many DNA barcodes are released for each positive binding event resulting in amplification of the signal. Using an inactivated H16N3 AIV as a model, a linear response over five orders of magnitude was obtained, and the sensitivity of the detection was comparable to conventional RT-PCR. Moreover, the entire detection required less than 2 hr. The results indicate that the method has great potential as an alternative for surveillance of epidemic outbreaks caused by AIV, other viruses and microorganisms.

Introduction

Avian influenza viruses (AIV), belonging to the *Orthomyxoviridae* family, have attracted global concern due to the potential pandemic threat for human health and enormous economic losses. It has killed millions of poultry and hundreds of people not only in Asia but also throughout Europe and Africa.[1–3] To control the epidemic diseases, there has been a surge of interest in sensitive, specific and rapid detection of AIV.

Several decades ago, traditional viral detection methods such as Madin-Darby canine kidney (MDCK) cell culture,[4] complement fixation (CF),[5] or hemagglutinin-inhibition (HI)[6] were mostly used. These approaches are laborious and time-consuming (*e.g.*, up to 4–10 days for the viral culture). Furthermore, in some cases the techniques are insufficient due to lack of specificity. Recently, reverse transcriptase PCR (RT-PCR) has emerged as the most sensitive method for AIV detection and pathotyping.[3,7] RT-PCR involves an extraction of viral nucleic acids (RNA), an *in vitro* reverse transcription process to synthesize cDNA from the viral RNA, followed by an enzymatic amplification and detection of the cDNA. Although very sensitive, specific, and much faster than the aforementioned procedures, RT-PCR also has some drawbacks such as a complicated procedure, high cost, and high false positive rate arising from cross contaminations between samples. Furthermore, it still requires a day and experienced personnel to obtain results.

Immunoassays could be an alternative for detection of AIV *via* immunoreactions between surface antigens (nucleoproteins, matrix proteins) of the AIV and their developed antibodies. Many studies have been devoted to the development of enzyme-linked immunosorbent assay (ELISA),[7–10] immunochromatographic strip test,[1,11] or microsphere immunoassay (MIA) for detection of AIV.[12] Although these immunoassays have been shown to be rapid, inexpensive to perform and possible to automate, they have lower sensitivity compared to those obtained from RT-PCR.[8] Bio-barcode immunoassay, proposed by Nam *et al.*, is the only approach for detection of biological targets that can obtain PCR-like sensitivity without the enzymatic amplification.[13,14] Typically, the bio-barcode immunoassay utilizes two types of particles: (1) a magnetic microparticle (MMP) functionalized with antibody (primary antibody) which is to capture and isolate the target analyte from the sample solution, and (2) another particle (gold nanoparticle, polystyrene or silica microparticle) anchored with secondary antibodies, which is specific to the same target, and double-stranded DNA.[13–16] Only one strand of the double-stranded DNA is covalently immobilized onto the secondary particle probe, and after the sandwiching immunoreaction, the complementary DNA strand can easily be released by increasing the temperature. The DNA surrogates for the target of interest and is therefore called a DNA bio-barcode. The surrogate DNA bio-barcode can subsequently be detected by PCR, DNA microarrays, colorimetric assays, or fluorophore-based assays. Unlike other conventional sandwich immunoassays, where the signal intensity is limited by number of antigenic valences for specific binding of reporter-tagged antibody, each particle is functionalized with a multitude of DNA strands and thus many DNA barcodes are released for each positive binding event resulting in amplification of the assay. Although the bio-barcode amplification assays have

[a]*DTU-Nanotech, Department of Micro and Nanotechnology, Technical University of Denmark, DTU Building 345 East, DK-2800 Kongens Lyngby, Denmark. E-mail: Anders.Wolff@nanotech.dtu.dk*
[b]*DTU-VET, Laboratory of Applied Micro-Nanotechnology, Department of Poultry, Fish, and Fur Animals, The National Veterinary Institute, Technical University of Denmark, Hangovej 2, DK-8200 Aarhus N, Denmark*

† Electronic Supplementary Information (ESI) available: Compared images before and after dissociating Cy5-biobarcodes from the immunocomplexes; and high resolution image of the Cy5-DNA barcode arrays. See DOI: 10.1039/b916821b

been the focus of many studies for detection of oligonucleotides and proteins, there have been no publications dedicated to bio-barcodes for detection of pathogenic organisms. In this paper, we will address a detection strategy that incorporates the benefits of fluorophore-DNA barcodes as a representatively optical reporter with the use of bead-based immunoassay for the detection of AIV. The method has not only a wide dynamic range of detection but also a sensitivity equivalent to that of RT-PCR which outperforms all detection limits of immune-based tests so far. This, in combination with the shorter detection time and possibility of adapting the method for detection of other viruses or microorganisms, make it a potential tool for surveillance of infectious diseases.

Materials and methods

Virus strain

An inactivated AIV virus subtype H16N3 was used as a model for developing the method. The AIV strain was propagated in SPF chicken eggs (Lohmann Tierzucht, Cuxhaven, Germany) and harvested from the allantoic fluid. The virus sample was prepared and titrated by Haemagglutin (HA) test at a concentration of 1:128 according to the guidelines of the European Union (EU) Council Directive 92/40/EEC.[17] A Newcastle Diseases Virus (NDV) Ulter strain was used to test the specificity of the assay. Both of the virus strains were kindly prepared by Poultry Virus Laboratory, National Veterinary Institute, Technical University of Denmark (DTU-VET).

Chemicals

Magnetic microparticle (Dynabeads® M-270 Amine, diameter 2.8 μm) was purchased from Invitrogen Dynal AS (Oslo, Norway). Polystyrene microparticle (Polybead® amino microsphere, diameter 1 μm), glutaraldehyde kit, and BioMag®Plus amine protein coupling kit were supplied by Polysciences Europe GmbH, Germany. Influenza type A virus nucleo-protein monoclonal antibody (NP mAb) and influenza type A virus matrix-protein monoclonal antibody (MP mAb) were purchased from Statens Serum Institut, Denmark. Oligonucleotide sequences were obtained from TAG Copenhagen A/S, Denmark; primers used in RT-PCR were obtained from DNA Technology, Aarhus, Denmark (Table 1). Other essential chemical reagents were of analytical grade and supplied by Pierce, Sigma-Aldrich, or Fluka unless otherwise stated. Ultrapure water (18.2 mΩ/cm) produced by a Millipore Milli-Q system was used to prepare the chemical solutions when needed.

Table 1 List of primers and oligonucleotide sequences used in this study

Oligonucleotides	Sequence (5′ → 3′)
Oligo 1	Amino-C6-AAAAAAAAAA AGG AAG GTG TGG ACG ACG TCA AGT CAT CAT GGC C
Oligo 2	Cy5-C GCC ATG ATG ACT TGA CGT CGT CCA CAC CTT CCT
Forward primer	AGA TGA GTC TTC TAA CCG AGG TCG
Reverse primer	TGC AAA AAC ATC TTC AAG TCT CTG

Preparation of magnetic microparticle immunoprobe

The amino-functionalized magnetic microparticle (MMP) was coated covalently with the NP mAb by using a BioMag®Plus amine protein coupling kit according to the manufacturer's protocol and a procedure reported previously with some modifications.[18] Briefly, 100 μl of MMP solution containing 2×10^8 beads (approximately 3 mg) was equilibrated and washed intensively 2 times with a mixture of 3 ml EDTA (0.05 mM) and 6 ml pyridine wash buffer (0.01 M, pH 6). The MMPs were separated after each washing step by a MultiSep magnetic separator (Polysciences Inc.). Then, 3 ml of 5% glutaraldehyde was added to activate the MMPs for about 3 h at room temperature while shaking vigorously. After the activation, the MMPs were washed two times, and suspended in 6 ml pyridine wash buffer. 1 ml of NP mAb (80 μg/ml) was added to the glutaraldehyde-activated MMP suspension; the mixture was gently mixed and incubated for about 10 hr at room temperature to ensure covalent coupling, followed by the washing step with 6 ml pyridine wash buffer. Afterwards, 3 ml BSA (0.2 mg/ml) was added to the solution for an additional 5 hr to block the non-specific adsorption of other proteins. The unreacted aldehyde sites were subsequently deactivated by 10 ml of 1 M glycine solution (pH 8) for 1 hr at room temperature. It should be noted that the washing step with pyridine buffer was repeated after each reaction to eliminate any remaining free reactants. The resulting MMP immunoprobes were then suspended in 1 ml of 0.15 M PBS solution and stored at 4 °C for up to 1 month without loss of activity.

Preparation of polystyrene microbead immunoprobe (PMP)

The experimental steps for the preparation of PMP immunoprobes were carried out by covalently immobilizing MP mAb and barcode DNA complementary strand (Oligo 1) onto the Polybead® amino microsphere by using the glutaraldehyde kit.[19] In brief, after washing and normalizing 1 ml of PMPs (approximately 2.28×10^{10} beads/ml) by PBS buffer, the PMPs were separated from the supernatant by centrifuging at 10 000 rpm for 10 min. Then, the PMP pellet was resuspended in 1 ml PBS buffer and reacted with 1 ml of 8% glutaraldehyde for 5 hr at room temperature. The reaction was performed in a 5 ml vial and stirred gently by a magnet bar to avoid settlement of the PMPs. The activated PMPs were centrifuged, washed, and resuspended in 1 ml PBS as described above. 10 μl of MP mAb (1 mg/ml) was added to the solution to conjugate with PMPs and incubated for 2 hr at room temperature with gentle stirring. Afterwards, 200 μl of 100 μM barcode DNA complementary strand (Oligo 1) was added continuously while stirring gently, and left to react overnight. The beads were washed 2 times with PBS buffer and unreacted glutaraldehyde sites of the PMP immunoprobes were deactivated by mixing with 1 ml of 0.2 M ethanolamine. The supernatant was removed by centrifuging at 13 000 rpm for 10 min, and 1 ml of 10% BSA was added to further block the unbound regions of the particle surface (30 min incubation). After washing with PBS and centrifugation, the resulting particle pellet was resuspended in 2 ml PBS buffer. Finally, 200 μl of 100 μM DNA barcode (Oligo 2) was added and incubated with the PMP immunoprobe for 1 hr. The barcode PMP

immunoprobe was washed and collected by centrifugation and resuspended in 2 ml of storage buffer. The final PMP probe was stored at 4 °C in a dark container to reduce photobleaching of the fluorophore. By using this method, the average numbers of mAb molecules and barcode DNA strands were respectively determined at about 1457 and 1.45×10^4 per polystyrene particle which are slightly lower than those reported previously.[19]

Immunoreaction and optical detection

In a typical experiment, a sandwiched immunoassay of MMP immunoprobe/AIV/PMP immunoprobe was carried out, and then the DNA bio-barcodes were collected by a magnetic separation and thermal dehybridization. Briefly, 30 μl of MMP immunoprobes was incubated with 40 μl of various 10-fold dilutions of the inactivated H16N3 with a HA titre of 1:128 in an Eppendorf tube. The reaction was kept for 30 min at room temperature on a rotating mixer. 30 μl of PMP immunoprobes was added and incubated for 30 min. When the immunoreaction had finished, the MMP immunoprobe/AIV/PMP immunoprobe complexes were separated in the magnetic separator, and the supernatant was removed. The reacted complexes were washed 3 times with 0.15 M PBS buffer, and 30 μl of pure and DNA-free water was added to the magnetically collected pellet. Finally, to release the surrogate DNA barcodes, the complexes were heated to 75 °C for 15 min, immediately followed by magnetic separation. The upper aqueous solution containing the released surrogate DNA barcode strands was collected and spotted onto a microscope slide by using a non-contact inkjet Nano-plotter 2.1 (GeSiM, Germany). Fluorescence measurement was carried out by a scanner ScanArray Lite (Packard Bioscience, USA) with appropriate settings for the Cy5 fluorophore.

RT-PCR

Detection of AIV by RT-PCR for matrix gene (M1) was performed according to a procedure published elsewhere with some modifications.[7,20] 25 μl RT-PCR reaction contained 12 μl of RNase free water, 5 μl RT-PCR buffer, 10 pmol of each primer (Table 1),[20] 1 μl of dNTP, 1 μl of enzyme mix and 5 μl of viral sample. RT-PCR was performed in a thermal cycler (Biometra, Germany) with reverse transcription at 56 °C for 30 min and enzyme activation at 95 °C for 15 min followed by 40 cycles with denaturation at 94 °C for 30 s, annealing 58 °C for 1 min, and extension at 72 °C for 1 min. The final extension step was carried out at 72 °C for 7 min. The obtained RT-PCR products were analysed using 1.5% agarose gel electrophoresis.

Results and discussion

The experimental procedure of the fluorescence-DNA barcode-based immunoassay is depicted in Fig. 1. The detection is initiated by sandwiching the target virus between the MMP immunoprobes and the PMP immunoprobes. After separation of the sandwich immunocomplex by a magnetic field, the surrogate

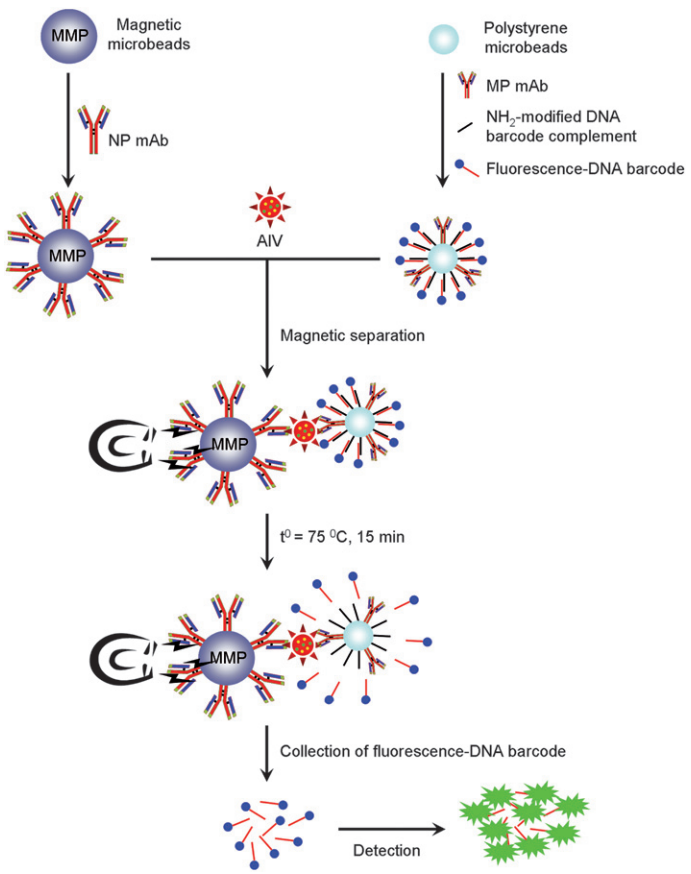

Fig. 1 Overall scheme illustrating procedure of the fluorophore-DNA barcode-based immunoassay for detection of AIV.

fluorophore-DNA barcodes are released by heating the immunocomplex at 75 °C for 15 min, and collected. Because the barcode immunoprobe particle can carry thousands of the representative barcodes, a single antibody–antigen binding event is translated to a multitudinous number of surrogate DNA barcodes leading to amplification of the assay. The fluorophore-DNA barcodes are then detected by any fluorescence readout available. In our lab, the most convenient way to detect the liberated DNA barcode strands was to spot them onto a microscope slide as microarrays following by a scanometric analysis, the entire detection required less than 2 hr to complete. It should be noticed that the Cy5- DNA barcode can be printed and measured directly without the dissociation step from the immunocomplex; however, due to the micro-sized nature of the microbeads the fluorescence was not dispersed leading to the fluctuation of the final results. Furthermore, the 3-D shape of the microbeads could hinder the Cy5-DNA barcodes located underneath leading to deterioration of the signal. To obtain more uniform fluorescent spot, the Cy5-barcode was released from the particles by heating and the results showed that the spot homogeneity was much better (See Fig. S1, ESI†). Therefore, the dissociation step is required in the protocol.

There are many factors that may limit performance of the DNA barcode-based immunoassay. These factors include the type of particles or antibodies, attachment chemistry, effectiveness of removal and washing steps, *etc.* Among them, immunological affinity of the immunoprobes towards their target analyte plays the most important role; it could be a key factor to determine the success or failure of the whole assay and their immunological activity could be deteriorated after the chemical immobilization. It is therefore necessary to ensure that the immunoprobes are able to capture the virus after enduring the chemical conjugation process. To determine this, conventional RT-PCR was exploited as a straightforward approach to validate the usefulness of the immunoprobes: The MMP and PMP immunoprobes were successively incubated with 10^{-3} dilution of the HA-titrated H16N3, and the captured viruses were collected by magnetic separation or centrifugation (in case of the PMP immunoprobes) as described in the method section. After the incubation period, the samples were washed several times with 1 ml of PBS buffer with 0.05% Tween 20 (pH 7.4). Finally, 50 μl DNA-free water was added to dissolve the collected complexes for the RT-PCR analysis. False-positive or false-negative results could be obtained if the washing step is not performed adequately in any immunoassays. For this reason, the washing supernatants were also collected in 1 ml aliquots to be analyzed with RT-PCR. Fig. 2A shows the gel electrophoresis image of the RT-PCR products. As seen, both of the MMP and PMP immunoprobes were PCR positive, and neither secondary product nor contamination was observed. Moreover, both washing solutions were virus-free after 4 times of washing as shown by PCR negative signals in lane 3 and 5, indicating that the positive bands (lane 2 and 4) resulted solely from specific interactions between the virus and the immunoprobes. A number of viruses were still observed in the washing solution until the third washing step (data not shown). This could be because of blocking effect of the microbeads or non-specific interactions of the beads and the viruses, and this might contribute to a false-positive result of the assay if the washing step is not carried out

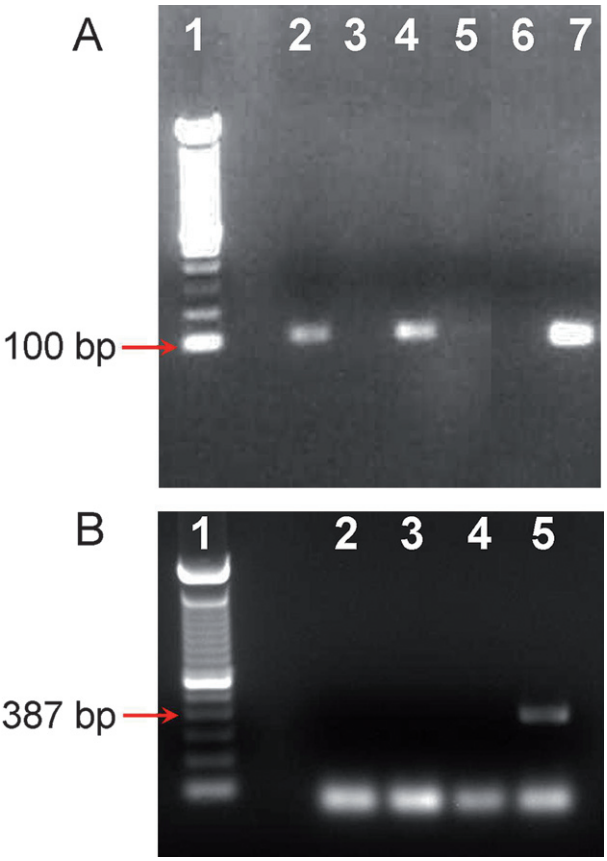

Fig. 2 (A) Agarose gel electrophoresis image illustrating validation of the immunoprobes by RT-PCR for H16N3 AIV (HA titers = 1:128). On gel, lane 1: 100 bp DNA ladder (Qiagen); lane 2: MMP immunoprobe sample (virus dilution 10^{-3}); lane 3: Washing solution of MMP immunoprobe sample (4^{th}); lane 4: PMP immunoprobe sample (virus dilution 10^{-3}); lane 5: Washing solution of PMP immunoprobe sample (4^{th}); lane 6: Negative control (virus free); lane 7: Positive control (virus dilution 10^{-3}). (B) Investigation of non-specific binding of Newcastle Disease Virus (NDV, HA titers = 1:128) on the immunoprobes. On gel, lane 1: DNA ladder; lane 2: NP mAb coated magnetic microbead sample (virus dilution 10^{-2}); lane 3: MP mAb coated magnetic microbead sample (virus dilution 10^{-2}); lane 4: Negative control (virus free); lane 5: Positive control (virus dilution 10^{-2}).

carefully. Non-specific interaction of the immunoprobes with other viruses is also important information that should be elucidated to evaluate the specificity of the immunoprobes. Newcastle Disease Virus (NDV) was used as the control virus because NDV is the viral infectious disease that is closely related to AIV in poultry. Briefly, NP mAb and MP mAb were conjugated to the magnetic beads. The immunoreactions with NDV were performed as described above. Subsequently, the immunocomplex was collected by a magnetic force; the captured NDV was then determined by RT-PCR and gel electrophoresis that were well-established at DTU-VET.[21] As shown in Fig. 2B, both of the PCR products obtained from NP mAb and MP mAb coated microbeads were negative indicating that the non-specific binding of NDV was negligible. Overall, this result shows how many times the washing step is required, and indicates that the immunoprobes were prepared successfully; they are sufficient and specific for catching the AIV in the next experiments.

To realize the principle illustrated in Fig. 1, a practical experiment was implemented to detect the AIV subtype H16N3. A series of 10-fold dilutions of the virus were prepared and incubated with the immunoprobes. Fig. 3A illustrates that the spot intensities were intuitively differentiated and proportional to a certain range of viral dilutions (see Fig. S2 (ESI) for high resolution image of the arrays†). The proportional relation was observed on all 3 replicates of the experiment. More quantitatively, Fig. 3B shows the generalized logarithmic correlation between the fluorescence values and the diluted concentrations of the virus. As seen, this method is able to reliably detect AIV with a very wide dynamic range of virus titres spanning from 1:128 up to 1:128 $\times$ 10^{-5} (five orders of magnitude) in which the fluorescence intensities were proportional to a log scale of the viral dilutions. The spot intensities at the dilutions higher than 1:128 $\times$ 10^{-5} were poorly discriminated because their signals did not exceed 2 or 3 times of standard deviation from the blank measurement (negative control sample, horizontal line); the limit of detection (L.O.D) was therefore proposed to be approximately 1:128 $\times$ 10^{-5} dilutions of the HA titre of the virus.

To further evaluate the effectiveness of the strategy, the same 10-fold dilutions of the virus samples were analyzed by conventional RT-PCR assay. The results of the fluorophore-DNA barcode-based detection of H16N3 AIV agreed remarkably well with the RT-PCR analysis. A proportional relationship was also obtained for the concentration range of 1:128 to 1:128 $\times$ 10^{-5} by RT-PCR (Fig. 4). Viral concentrations lower than 10^{-5} of dilution could also not be detected by RT-PCR owing to the extremely low number of virus particles. Therefore, the results suggest that the fluorophore-DNA barcode-based immunoassay described in this study is as sensitive as RT-PCR, it could be an alternative for detection of AIV where RT-PCR is not available.

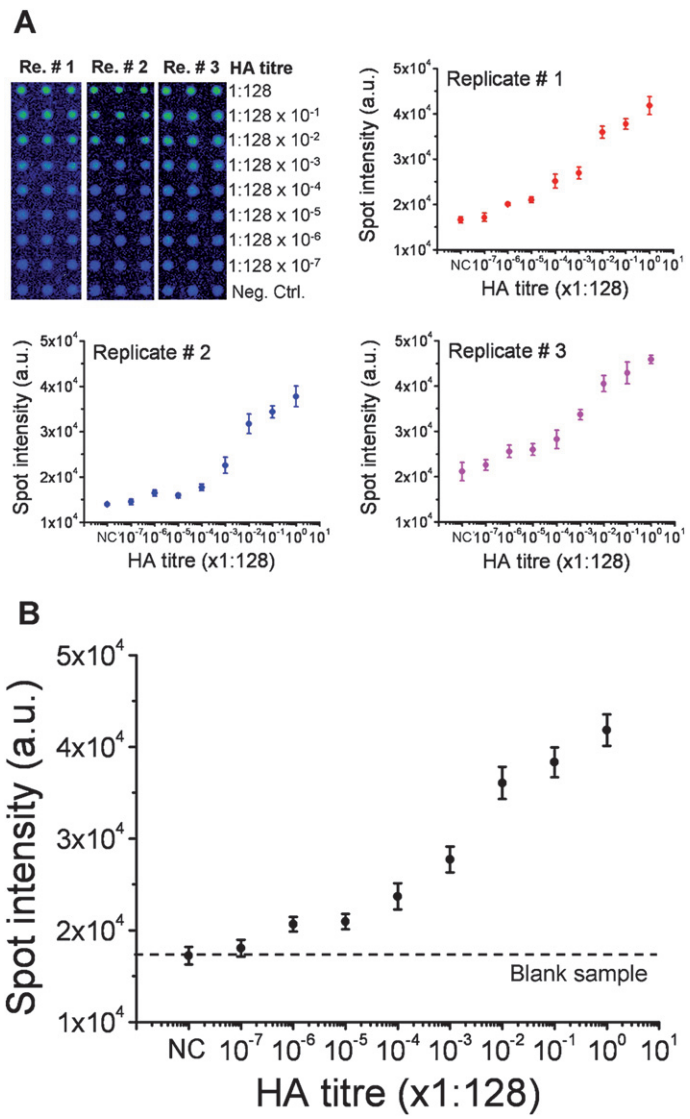

Fig. 3 Detection of fluorescent DNA barcodes. Scanometric image showing three replicated microarrays of surrogate Cy5-DNA barcode strands and their corresponding fluorescence intensity to the diluted concentrations of H16N3 AIV (A); and (B) generalized correlation of the average intensity and the diluted concentrations for the detection of H16N3 AIV (HA titre 1:128). NC negative control signal.

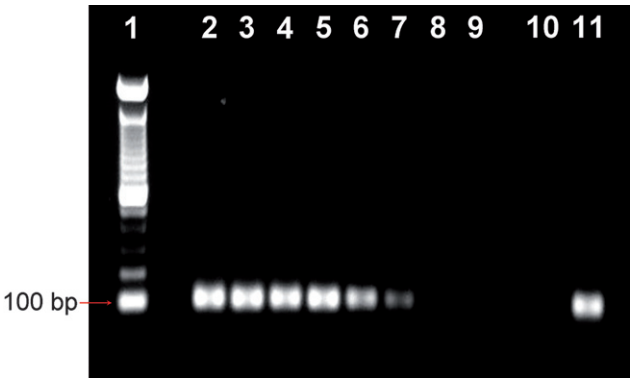

Fig. 4 Detection of H16N3 inactivated AIV (HA titers, 1:128) by RT-PCR. On gel, Lane 1: 100 bp DNA ladder (Qiagen); Lane 2–9: 10-fold dilutions of the virus pool ranging from the original HA titre 1:128 to 1:128 $\times$ 10^{-7}, respectively; Lane 10: Negative control (virus free); Lane 11: Positive control. The virus strain was not recognized at dilutions higher than 1:128 $\times$ 10^{-5}.

Conclusion

An effective method using fluorophore-DNA barcode combined with bead-based immunoassay was described for the first time to detect AIV. The single immuno-recognition events were translated into multitude numbers of the Cy5-tagged DNA barcodes which could be quantitatively measured by a fluorescence readout device. The H16N3 AIV strain could be detected with PCR-like sensitivity and a wide dynamic range of up to five orders of magnitude. Although simple in design and concept, the method introduced has PCR-comparably sensitive, is less time-consuming (less than 2 hr for the entire detection), highly applicable, and can be carried out using simple laboratory equipment. For these reasons, the assay deserves attention as an alternative for the surveillance and clinical detection of AIV outbreaks.

Acknowledgements

We would like to thank Dr. Kurt Handberg and the Poultry Virus Laboratory, National Veterinary Institute, Technical University of Denmark in Aarhus for providing AIV and NDV strains. We thank Dr. Sun Yi for her help with the nano-plotter and the laser scanner. This work was supported by the Danish Research Council for technology and production sciences (FTP) grant no. 274-05-0017 and by the Technical University of Denmark (DTU), Food Pathogen Project No. 8, Grant No. 150627.

Notes and references

1 S. Cui, C. Chen and G. Tong, *J. Virol. Methods*, 2008, **152**, 102–105.
2 D. J. Alexander, *Zoonoses Public Health*, 2008, **55**, 16–23.
3 J. Pasick, *Transboundary and Emerging Diseases*, 2008, **55**, 329–338.
4 S. R. Shih, K. C. Tsao, H. C. Ning, Y. C. Huang and T. Y. Lin, *J. Virol. Methods*, 1999, **81**, 77–81.
5 S. Sato, H. Ochiai and S. Niwayama, *J. Med. Virol.*, 1988, **24**, 395–404.
6 R. T. Schwarz and H. D. Klenk, *J. Virol.*, 1974, **14**, 1023–1034.
7 M. Munch, L. P. Nielsen, K. J. Handberg and P. H. Jorgensen, *Arch. Virol.*, 2001, **146**, 87–97.
8 S. Velumani, Q. Du, B. J. Fenner, M. Prabakaran, L. C. Wee, L. Y. Nuo and J. Kwang, *J. Virol. Methods*, 2008, **147**, 219–225.
9 Q. He, S. Velumani, Q. Du, C. W. Lim, F. K. Ng, R. Donis and J. Kwang, *Clin. Vaccine Immunol.*, 2007, **14**, 617–623.
10 G. Sala, P. Cordioli, A. Moreno-Martin, M. Tollis, E. Brocchi, A. Piccirillo and A. Lavazza, *Avian Dis.*, 2003, **47**, 1057–1059.
11 S. Cui and G. Tong, *Journal of Veterinary Diagnostic Investigation*, 2008, **20**, 567–571.
12 D. Deregt, T. L. Furukawa-Stoffer, K. L. Tokaryk, J. Pasick, K. M. B. Hughes, K. Hooper-McGrevy, S. Baxi and M. K. Baxi, *J. Virol. Methods*, 2006, **137**, 88–94.
13 J. M. Nam, S. I. Stoeva and C. A. Mirkin, *J. Am. Chem. Soc.*, 2004, **126**, 5932–5933.
14 J. M. Nam, C. S. Thaxton and C. A. Mirkin, *Science*, 2003, **301**, 1884–1886.
15 J. M. Nam, S. J. Park and C. A. Mirkin, *J. Am. Chem. Soc.*, 2002, **124**, 3820–3821.
16 Y. P. Bao, T. F. Wei, P. A. Lefebvre, H. An, L. X. He, G. T. Kunkel and U. R. Muller, *Anal. Chem.*, 2006, **78**, 2055–2059.
17 CEC, *Official Journal of the European Commission*, 1992, **L167**, 1–15, The Hemagglutination Assay (HA) is a quantification of viruses by hemagglutination, *i.e.* agglutination (binding together) of red blood cells. The highest dilution of virus causing complete agglutination of the red blood cells is defined as a HA titre unit.
18 J. M. Nam, K. J. Jang and J. T. Groves, *Nat. Protoc.*, 2007, **2**, 1438–1444.
19 B. K. Oh, J. M. Nam, S. W. Lee and C. A. Mirkin, *Small*, 2006, **2**, 103–108.
20 E. Spackman, D. A. Senne, T. J. Myers, L. L. Bulaga, L. P. Garber, M. L. Perdue, K. Lohman, L. T. Daum and D. L. Suarez, *J. Clin. Microbiol.*, 2002, **40**, 3256–3260.
21 P. H. Jørgensen, K. J. Handberg, P. Ahrens, H. C. Hansen, R. J. Manvell and D. J. Alexander, *J. Vet. Med. B*, 1999, **46**, 381–387.

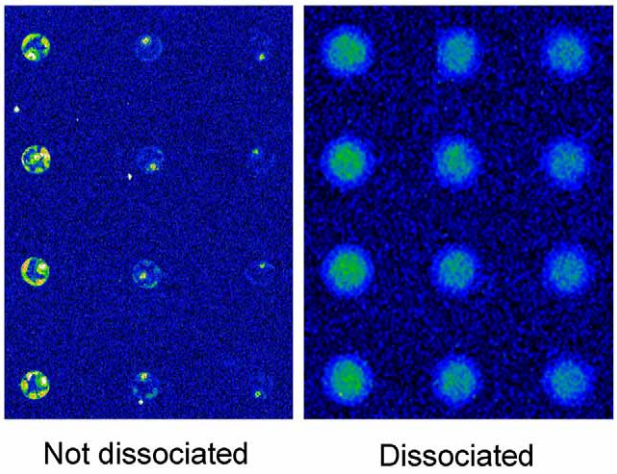

Fig. S1. Compared images before and after dissociating Cy5-biobarcodes from the immunocomplexes.

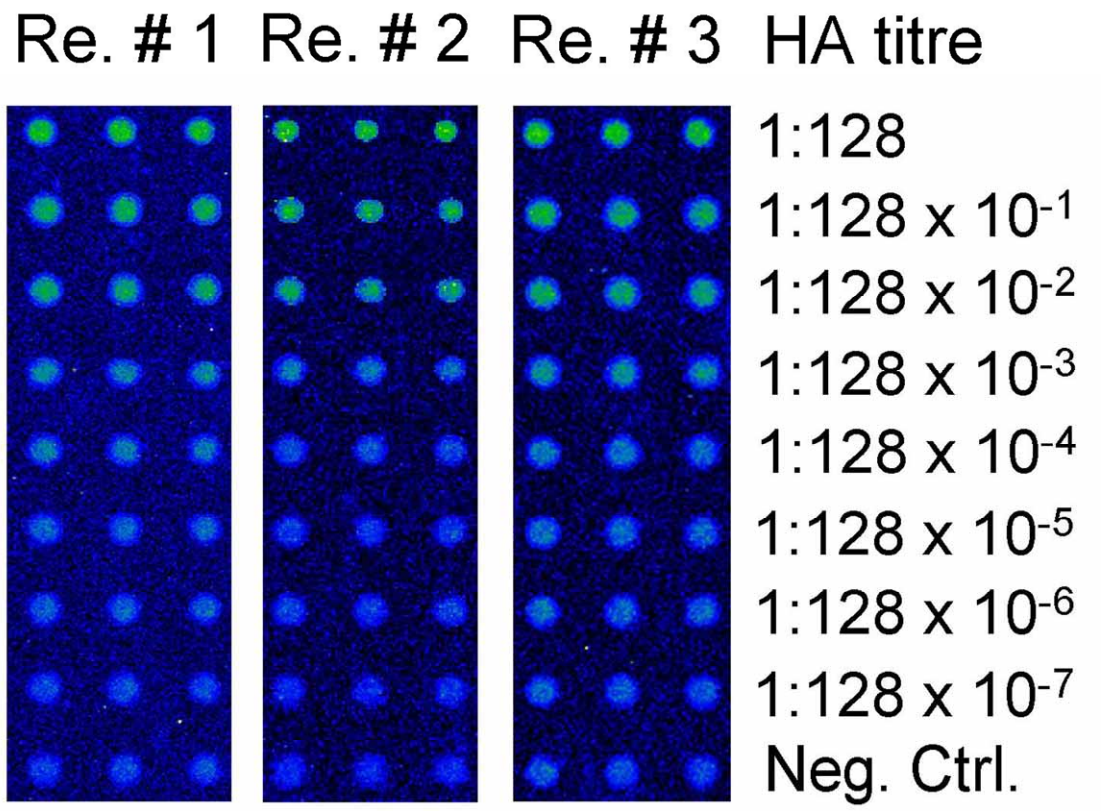

Fig. S2. High resolution image of the Cy5-DNA barcode arrays.

8.2 Development of a fluorescent bead-based immunoassay for rapid detection of Avian influenza virus

8.2.1 Introduction

Currently, the POC tests or other commercial tests for AIV detection are largely based on immunoassays. These assays are rapid (5 to 30 minutes) but have low sensitivity, 10^5 to 10^6 of 50% tissue culture infectious dose/ ml ($TCID_{50}$/ml) [186]. The low sensitivity of these tests is a major concern for mass screening of the AIV. This problem has been addressed in the previous study of the development of a fluorophore-DNA barcode and bead-based immunoassay. Using the developed method the AIV can be detected with PCR-like sensitivity. However, the developed assay needs a heat step to release the barcode oligonucleotide for quantitative detection, therefore applying such assay for a POC or an integrated LOC is complicated. An alternative simple approach would be to detect the fluorescence signal directly with a simple optical detection system that is suitable for on-field screening tests.

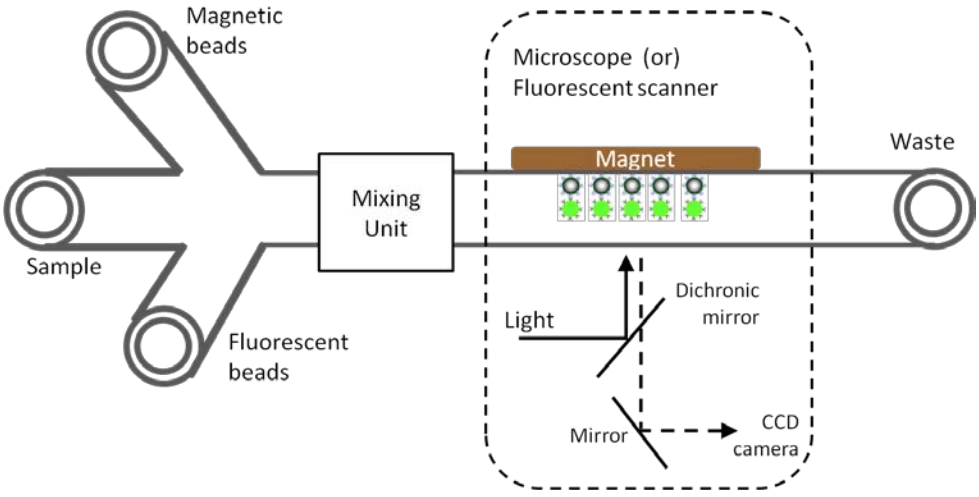

Figure 8.2.1: Schematic of a lab-on-a-chip (LOC) for fluorescent bead based detection system

In the immunoassay based on fluorescence detection, nano and micro beads conjugation with antibodies or antigen have been used to obtain high sensitive sensing for detection of infectious disease[187]. These fluorescent beads carry a high amount of fluorophores that generate a photo-stable and strong fluorescent signal. Moreover, with a high surface-to-volume ratio (SVR), the beads provide better binding sites for the targets. A fluorescent immunoassay (FIA) has been

developed for the detection of antibodies against nucleoprotein (NP), matrix and non-structural proteins of AIV[188] and also for multiplex detection of both NP and H5[189] using commercial spectrophotometer instrument (Luminex, USA). In these studies, the sensitivity of the assays were low (1:3200 dilution of the serum) i.e., can only detect higher concentration, which could be due to the use of fluorescent reporter dye. In addition, an expensive instrument is needed for the analysis. In this study, a fluorescent bead-based immunoassay was developed to detect the avian influenza virus suitable for a simple POC test using LOC (Figure 8.2.1).

8.2.2 Materials and Methods

Virus and antibodies

In order to compare the result with the previous study, the H16N3 inactivated virus of the same batch with the HA titre of 128HAU. Monoclonal antibody (mAb) against the AIV nucleoprotein (NP) (HYB 340-05) and matrix proteins (MP) (HYB 344-01) of AIV were purchased from Staten Serum Institute (Copenhagen, Denmark) with a concentration of 100 mg/ml.

Antibody conjugation to beads and fluorophore

a) *NP antibody conjugation to magnetic bead*

Super-paramagnetic polystyrene carboxylic acid beads (Myone, Invitrogen, Denmark) with 1.05 µm diameter were used. The antibody was conjugated to the beads using protein coupling kit (PolyLink protein coupling kit for COOH microparticles, Polysciences, Eppelheim, Germany) according to the manufacturer´s instruction with modifications. Briefly, 250 µl of beads were washed twice with 1 ml of coupling buffer (50 mM MES, pH 5.2, 0.05% Proclin 300) and the beads were re-suspended in 100 µl of the same buffer. A magnetic separator (Dynal MPC, Invitrogen, Copenhagen, Denmark) was used to separate the beads in all the washing steps. The functional carboxyl groups on the surface of the bead were activated by adding 100 µl of 1-ethyl-3-(3-dimethylaminopropyl) carbodiimide (EDC) (10 mg/ml) to the bead suspension and incubated for 30 min at room temperature on a rotator. To remove the excess EDC the beads was washed once with coupling buffer (500 µl). The activated beads were mixed with 100 µg of mAb NP diluted in coupling buffer in a total volume of 500 µl and incubated over night at room temperature on a rotator. The un-reacted sites on the surface of the beads were de-activated by mixing with 500 µl of 0.2 M ethanolamine and incubating for 30 min at room temperature. The

beads were further blocked with 1 ml of PBS containing 0.5% Casein (blocking buffer) and incubated for 30 min at room temperature. Finally, the beads were restored in 250 µl of PBS containing 1% Tween20 (storage buffer).

b) *Conjugation of MP antibody on fluorescent carboxyl beads*

The MP antibody was conjugated onto the surface of the (Ø1 µm) fluorescent carboxyl beads (ex:441nm, em:486nm) that were purchased from Polysciences (Eppenheim, Germany). A similar coupling procedure as mentioned above was performed. Briefly, the fluorescent beads (75 µl) were washed twice with 500 µl of coupling buffer and re-suspended in 480 µl of coupling buffer**.** Twenty µl of EDC (200 mg/ml) was added to the bead re-suspension and incubated for 30 min at room temperature. After a washing to remove all the excess EDC, 50 µg of MP antibody was added and incubated overnight on a rotator at room temperature. The remaining steps were as described earlier, and finally the beads were suspended in 75 µl of storage buffer. During the procedure, the fluorescent beads were collected by centrifugation (Z233 M-2, Hermle Labortechnik GmBH, Wehningen, Germany) at 10,000 rpm for 5 min at room temperature. Both magnetic and fluorescent beads can be stored at 4 ^{o}C for up to 2 months without loss of activity.

Antibody conjugation confirmation

The presence of NP-mAb on the surface of carboxyl magnetic bead was confirmed by secondary goat anti-mouse antibody labelled with Alexa Fluor-488 SFX (Invitrogen, Taastrup, Denmark). Five µl of Alexa Fluor-488-labelled antibody was added to 5µg of NP-mAb coated magnetic beads and uncoated magnetic beads and mixed for 30 min at room temperature. Later, the beads were washed 3 times with 1 ml of PBS and finally restored in 25 µl. Five µl of bead mixture was transferred to a microscopic glass slide and the images were captured using a fluorescent microscope (model DMRB, Leica, Germany) with FITC filter set (450 to 490-nm bandpass excitation filter and 530 nm emission filter).

Development of fluorescent immunoassay

A scheme of the fluorescent immunoassay (FIA) assay using fluorescent beads is shown in Figure 8.2.2. In brief, 5 µl of magnetic beads were added to 100 µl of H16N3 virus with HA titre value of 128 HAU (undiluted allantoic fluid) and incubated for 30 min on the rotator. After the incubation, 0.5 µ1 of MP antibody conjugated fluorescent beads were added to the mixture and incubated for further 30 min. In this, step a sandwich complex of magnetic bead-virus-fluorescent bead was formed. The complex was separated and washed 4 times with 10 mM PBS containing 0.05% of Tween20 (washing buffer) using a magnetic separator and finally the complex was restored in 20 µl of washing buffer.

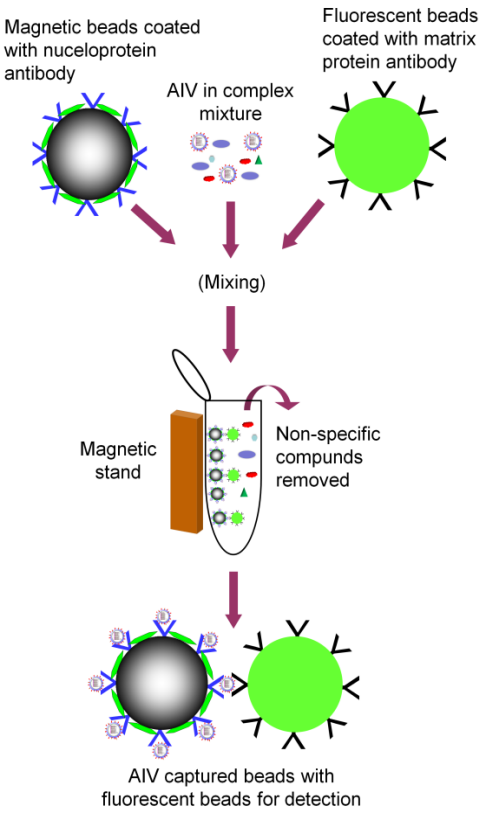

Figure 8.2.2 A scheme representing fluorescent bead based immunoassay for detection of AIV

The complex (entire volume) was transferred on a microscopic slide (without cover slip) and scanned using a fluorescence scanner (LaVision Biotech, Bielefeld, Germany) with FITC filter set. To avoid the interference of the beads during the scanning and for obtaining uniform results, a magnetic strip (IKEA, Aarhus, Denmark) was placed under the slide to pull down all the beads on the slide surface before scanning. A blank sample with 100 µl of washing buffer was used as a negative control and the assay was performed accordingly. To determine the sensitivity of the developed FIA, 10-fold serial dilutions of H16N3 virus were made and the assay was performed in triplicates.

During the pilot experiments, the beads blocked with BSA as blocking buffer in the mAb conjugation procedure showed aggregation of the beads resulted in higher non-specific signal. Therefore, the BSA was replaced with Casein in the blocking buffer and used for the assay. Although Casein reduced the aggregation of beads, the non-specific interaction was controlled with the addition of Tween20.

In the FIA the effect of agglutination i.e., magnetic bead-virus-magnetic bead was studied using the magnetic bead based assay. In that assay, magnetic beads were incubated with three dilutions of 10^{-1}, 10^{-2} and 10^{-3} of H16N3 virus (128 HAU) for 30 min at room temperature. After the incubation, magnetic beads were washed 3 times with the washing buffer and the agglutination effect was observed during the washing steps.

8.2.3 Results and discussions

Immunoassay based on ELISA is time-consuming (1-2 days) due to the immobilization of antibody on the microtiter wells (2D surface), washing and the planar assay for detection, where as the use of beads accelerate the kinetic reaction in a shorter time[190]. In this study, the FIA was developed using the two mAb specific for NP and MP of AIV for rapid detection of the AIV. In the preliminary experiments, it is noted that high non-specific signals were observed when the tosylactivated (hydrophobic) magnetic beads and the fluorescent beads (hydrophilic) were used. To reduce the non-specific signals, in the developed FIA, magnetic beads and fluorescent beads with the same surface chemistry, i.e. carboxylic acid (hydrophilic), were selected for the conjugation of mAb's. The conjugation of mAb (NP) to the magnetic beads was confirmed by the secondary antibody labelled with Alexa Fluor-488 (Figure 8.2.3 a). The antibody on the surface of fluorescent beads was not confirmed by the secondary labelled antibody due to the strong signal from fluorescent beads which override the fluorophore.

a) 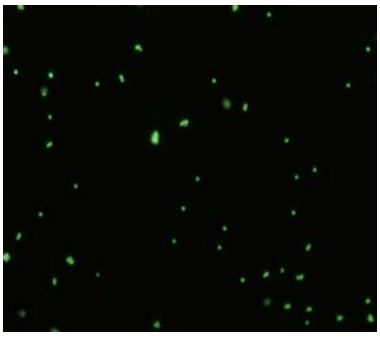 b) 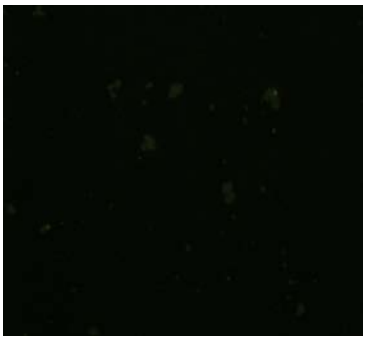

Figure 8.2.3: Microscopic images using fluorescence microscopy (Leica, Germany), with FITC filter setting. The images confirming a) the presence of mAb (NP) on the surface of magnetic beads and b) no signal on uncoated beads.

Fluorescent immunoassay

Figure 8.2.4 shows the images taken with fluorescent scanner for the FIA performed with H16N3 virus and buffer. The two images differentiated by the quantity of fluorescent beads (white spots) confirm the capture of virus by magnetic bead and the formation of sandwich immunoassay.

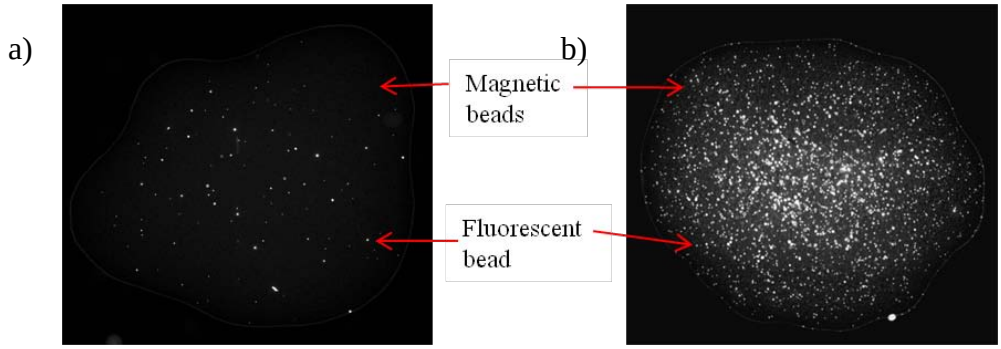

Figure 8.2.4: Images from fluorescent scanner for the FIA with a) buffer and b) H16N3 virus (undiluted allantoic fluid with 128HAU). The white spots are the fluorescent beads with the magnetic beads at the background.

A low background and a low aggregation could be achieved in the developed FIA due to the combined effect of Casein as a blocking buffer and the presence of the Tween20. The replacement of BSA (Figure 8.2.5a) by Casein proved beneficial in reducing the non-specific binding. This could be due to the Casein protein having a smaller molecular mass i.e., more molecular surface compared to BSA and acts as an effective blocking agent[191]. The use of Tween20 in the storage buffer lowered the surface tension of the beads and thus reduced the non-specific interaction (Figure 8.2.5b).

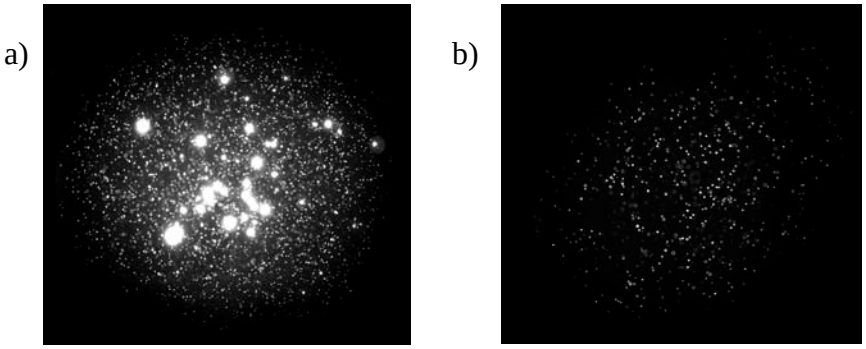

Figure 8.2.5: Images from fluorescent scanner for the FIA with a) BSA blocked beads showing aggregates and b) buffer sample without Tween20 showing higher non-specific signal.

Image analysis

The images were analyzed by using ImageJ (Image processing and analysis in Java, National Institute of Health, USA). It is freely available software and provides a cost effective solution for fluorescence quantification. The acquired image (16-bit) was converted into 8 bit gray scale, which has intensity of pixel range from 0 (black) to 255 (white) (Figure 8.2.6 a). The brighter dots with gray values above 255 were also counted as having a gray value of 255. The signal from the background and magnetic beads were removed from image processing by setting the threshold or lowest intensity (min) to 60 (Figure 8.2.6 b).

a) b)

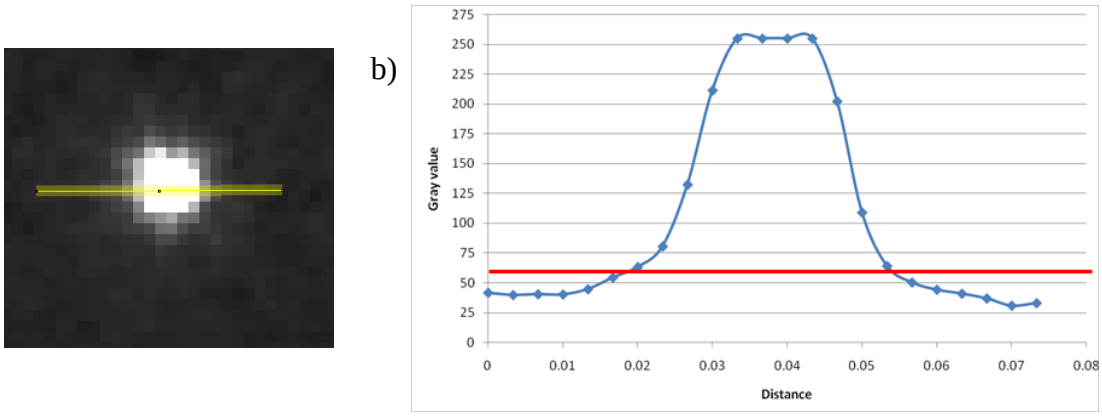

Figure 8.2.6 Analysis of 8-bit gray scale image using ImageJ. a) Fluorescent bead with the region (yellow) used for plot profile. b)Profile showing the distribution of grayscale (0 to 255) across the fluorescent bead. The gray scale value below 60 (red line) was considered as background.

Using these settings, a histogram was plotted with the distribution of pixel intensity (gray scale) for 61-254 and the number of pixels found for each gray value of the image. Figure 8.2.7 shows such histogram of the images taken for H16N3 virus (undiluted) and the blank sample performed in triplicates. By comparing the two series it is noted that the virus sample (undiluted H16N3) has higher pixel counts for all the gray scale value (61 to 254) compared to the blank sample. This effect is due to the presence of the fluorescent beads and therefore represents the fluorescent emissions.

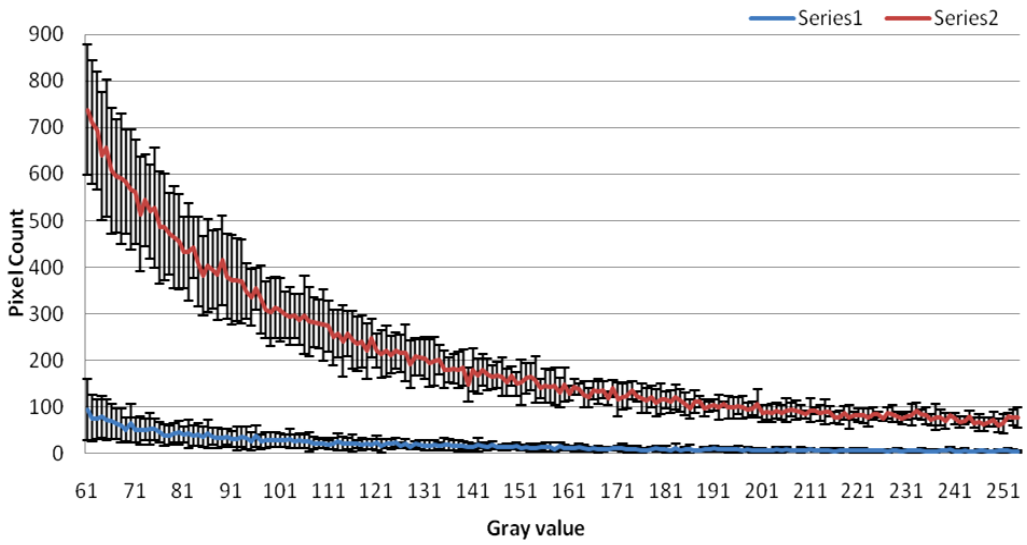

Figure 8.2.7 Histogram showing the intensity of gray value for FIA images of virus sample (series 1) and blank sample (series 2).

The sensitivity of FIA was determined by using 10-fold serial dilutions of the H16N3 virus (128 HAU). The total fluorescent intensity of the images was calculated by summing the gray intensity of all pixels in the range of 61-255 using ImageJ software. As seen in Figure 8.2.8, there were 10 fold differences in the signal intensity of the undiluted virus (55,507± 6,570) comparison to the negative control (buffer) (5,158±2,885). Up to the 10^{-2} dilution of the virus there was a significant difference between the virus and the negative control (buffer). At the dilution of 10^{-3}, there was a sudden decrease in the signal intensity (3,816±1,870) down to the range of the negative control. Similar results were observed for other dilutions of 10^{-3} and 10^{-4} with signal intensity of 6410±4135 and 7753±1324 respectively. At a lower dilution of virus (10^{-6}) there was a positive signal observed (21,830 ±10,505) and declined (10^{-7}) to the negative control.

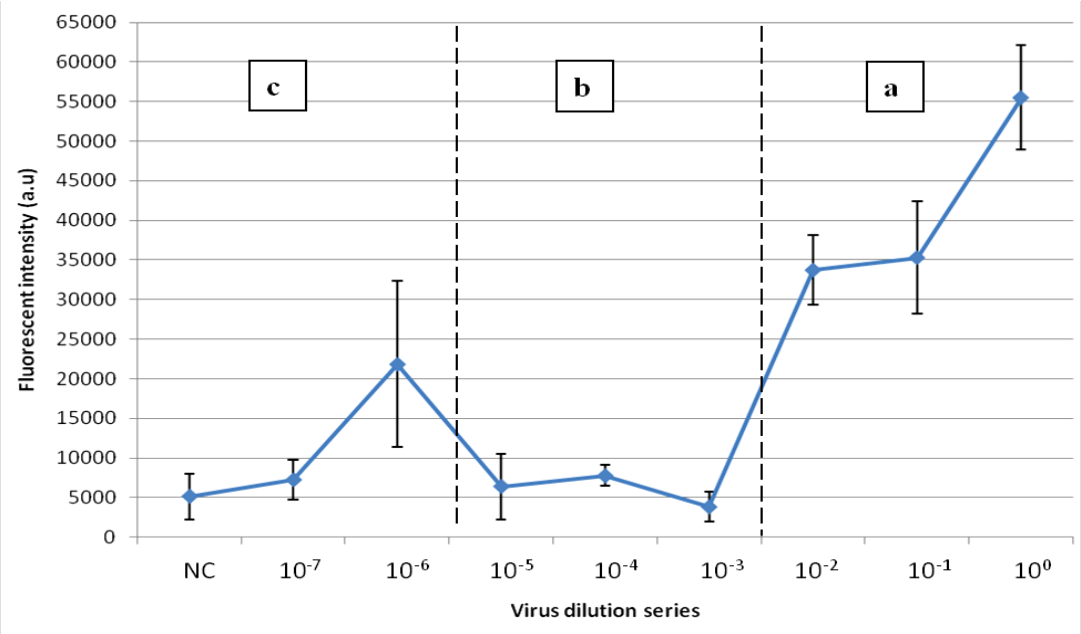

Figure 8.2.8 Sensitivity of the FIA assay using a ten fold serial dilutions of H16N3 virus (128 HAU). The ten fold serial dilutions of the virus range from 10^{0} to 10^{-7} were made and used for the FIA assay. NC is a negative control (buffer). Based on the fluorescent intensities from the dilutions, results were divided into three zones of a, b and c (see the discussion).

The observed phenomenal curve is due to the steric hindrance for the fluorescent beads to form sandwich assay. This effect can be explained similar to the formation of immunoprecipitation or agglutination curve [192]. In the FIA, with constant amount of mAb conjugated magnetic beads and the decreasing amount of virus, an agglutination curve is generated. This may be divided into three zones (Figure 8.2.8): a) excess of virus (10^{0} to 10^{-2} dilution); where there are so many virus particles in relation to magnetic beads that only a single magnetic bead will bind to each virus particle. There are therefore no steric hindrance which occurs when 2 or more magnetic beads bind to a single virus particle, leaving no room for binding of fluorescent beads; b) the equivalence zone (10^{-3} to 10^{-5} dilution); where the low concentration of virus cause magnetic beads to form agglutination and create steric hindrance for binding to fluorescent beads; c) very low amount of virus (10^{-6} to 10^{-7} dilution), where the virus concentration is too low to form agglutination and the fluorescent beads have the possibility to form sandwich. For 10^{-6} dilution the signal deviation was higher, which could be due to the difference within the binding of AIV to the magnetic beads (for e.g., 1:1 or 1:3 respectively) that the increased or decreased the

binding of fluorescent beads to form the immunocomplex. The agglutination is formed due to the specific interaction between the virus and mAb coated magnetic beads and this effect was not controlled with the use of Tween20, which meant to reduce the non-specific interaction between the magnetic and fluorescent beads.

To test the effect of agglutination, the magnetic bead based immunoassay was performed using three dilutions of 10^{-1}, 10^{-2} and 10^{-3} of H16N3 virus and the results are shown in (Figure 8.2.9). The agglutination of magnetic beads was increasing with the dilution of virus and was visible to the naked eye

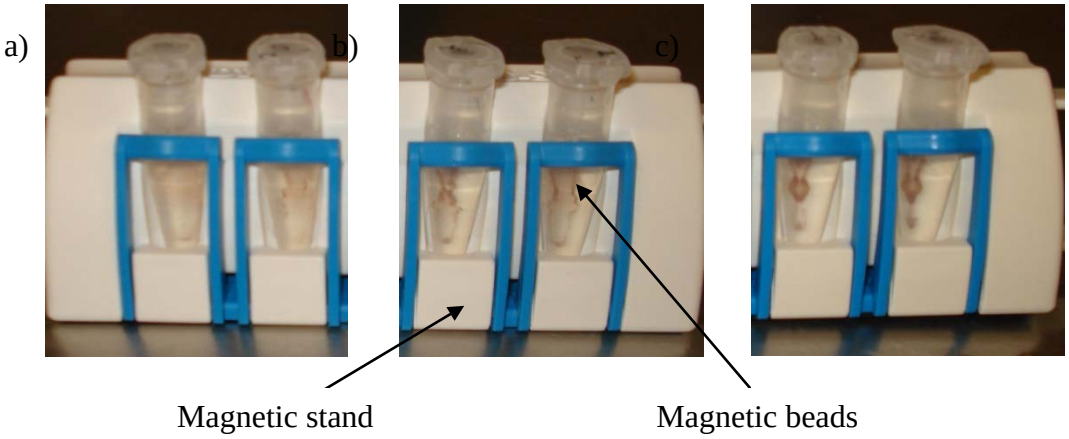

Figure 8.2.9 Images of agglutination test. The mAb conjugated magnetic beads were used to capture the H16N3 virus in a) 10^{-1}, b)10^{-2} and c)10^{-3} dilutions and an increasing effect of the agglutination was observed.

8.2.4 Conclusion

A simple fluorescent bead-based immunoassay (FIA) has been developed for rapid detection of virus in less than 2h. The FIA has detection limit of 10^{-2} dilution of the H16N3 virus (128 HAU). For further dilutions of the virus, no linear response was obtained due to the steric hindrances. If the FIA is further optimized such as reducing the size of magnetic bead, sensitivity similar of the method could be similar or higher than RT-PCR could be achieved. The developed FIA can be easily integrated with LOC and using portable fluorescent scanner, the system can be used as a sensitive tool for screening of AIV in the fields.

Chapter 9

Summary and Outlook

Avian influenza virus (AIV) is a contagious disease among birds. Infection of AIV in poultry industries has killed several millions of birds and suffered massive economic loss. Contact with AIV infected poultry has spread the infection to humans and threatening the world with a human pandemic influenza. Therefore a simple, fast and reliable diagnostic method is needed urgently for early detection and surveillance of AIV. The combination of rapid diagnostics with the microfluidic lab-on-a-chip (LOC) technology offer great potential to create portable point-of-care (POC) diagnostic system to detect and monitor infectious disease on field or at resource-limited settings. This Ph.D-study has been focused on development of rapid diagnostic methods for the identification and subtyping of the AIV towards POC diagnostics.

The key challenge in the realization of POC diagnostics is the sample preparation that has been addressed in this study with the development of an immunomagnetic bead-based assay (Section 6.1). The magnetic beads conjugated with mAb were used successfully for immuno-separation, concentration and purification of AIV from spiked chicken faecal sample. The effective removal of RT-PCR inhibitors using magnetic bead-captured virus was observed. More importantly the developed method was used directly for RT-PCR without additional RNA release steps. The developed method was also realized and performed in a magnetic microsystem with microfludics (Section 6.2). This indicates the possibility to integrate the developed of sample preparation in a total analysis microsystem for AIV diagnostic.

Further efforts were made to miniaturize the RT-PCR for AIV using microfluidic chip made of SU-8 and COC (Section 6.3). The use of SU-8 chip for RT-PCR showed inhibition effect by unknown factor. Efforts to address the inhibition were not successful due to insufficient information of chemical materials used for chip fabrication and also the batch-to-batch variation in fabrication. Although further optimization was planned to perform RT-PCR on SU-8 with different enzyme kits, no attempts were made due to the shortage of chip supply. The

performance of RT-PCR on COC chip was studied and successfully detected in less than two hours. These chips constitute a simple and cheap alternative (disposable chips) suitable for POC diagnostics.

In section 7.1, a DNA microarray based solid-phase PCR platform for sub-typing of AIV to overcome the limitation of real-time RT-PCR in discriminating and sub-typing a number of targets, e.g. H5&H7 subtypes of the AIV simultaneously were developed. A combined approach of reverse-transcription amplification of RNA extracts in the liquid-phase and sequence-specific nested PCR on the solid phase has been achieved. This approach with fewer steps generated a new method with high sensitivity and specificity comparable to in-tube multiplex PCR towards the development of a POC diagnostics. The developed solid-phase RT-PCR method was further incorporated into a microchip to reduce the sample volume and detection time 2h to 1h (Section 7.2).

As any subtype among the 16HA types (H1-H16) of the AIV could emerge as a pandemic influenza virus, it is important to develop a method that could not only detect but also subtype all the 16HA subtypes of AIV in one step. A multiplex DNA microarray based solid-phase RT-PCR for simultaneously detection and subtyping all the 16HA was initiated by designing new set of primers and probes (Section 7.3). The designed primer successfully identified all the 16 HA subtypes. Further, among the 16 probes that were designed to subtype the 16 HA, four probes were tested for RT-PCR which showed non-specificity. The developed method needs further optimization for subtyping using solid-phase PCR.

In Chapter 8, two immunological assays; a fluorescent DNA barcode-based assay and a fluorescent bead-based assay was developed that could be used for rapid detection of AIV in less than 2h. Both the fluorophore-tagged oligonucleotides and fluorescent beads can be used as the detection signals in the immunoassay for AIV. The bead based DNA barcode immunoassay offers an alternative approach for detecting AIV with PCR-like sensitivity. While, the developed fluorescent immunoassays can be integrated with LOC and using portable fluorescent scanner, it can be used as a sensitive tool for screening of AIV in the fields.

In this thesis, several approaches for rapid detection of AIV have been developed. The different steps of a molecular diagnostic LOC such as sample preparation (magnetic beads), RT-PCR amplification and detection (DNA microarray) have been demonstrated in different microfluidic system. The integration of all these steps in to one system will ensure the realization of a true LOC in the near future. This total integrated LOC will be a good tool for on-site rapid screening of AIV, especially the infectious agents and can improve the quality of life and economic.

List of references

[1] J. S. M. Peiris, M. D. de Jong, and Y. Guan, "Avian Influenza Virus (H5N1): a Threat to Human Health," *Clin. Microbiol. Rev.*, vol. 20, no. 2, pp. 243-267, Apr.2007.

[2] OIE, "Avian influenza. Chapter 2.3.4.," *OIE(world Organization for animal health) Terrestrial Manual.*, 2009.

[3] D. J. Alexander, "A review of avian influenza in different bird species," *Vet. Microbiol.*, vol. 74, no. 1-2, pp. 3-13, May2000.

[4] "http://www.who.int/csr/disease/avian_influenza/country/cases_table_2008_06_19/en/index.html,".

[5] International Monetary Fund Report, " THE GLOBAL ECONOMIC AND FINANCIAL IMPACT OF AN AVIAN FLU PANDEMIC AND THE ROLE OF THE IMF,"Feb.2006.

[6] D. J. Alexander, "An overview of the epidemiology of avian influenza," *Vaccine*, vol. 25, no. 30, pp. 5637-5644, July2007.

[7] V. J. Munster, C. Baas, P. Lexmond, J. Waldenstr+¦m, A. Wallensten, T. Fransson, G. F. Rimmelzwaan, W. E. P. Beyer, M. Schutten, B. r. Olsen, A. D. M. E. Osterhaus, and R. A. M. Fouchier, "Spatial, Temporal, and Species Variation in Prevalence of Influenza A Viruses in Wild Migratory Birds," *PLoS Pathog*, vol. 3, no. 5, p. e61, May2007.

[8] "http://www.ifpma.org/index.php?id=4169," 2010.

[9] P. Palese and Shaw.M.L, "Orthomyxoviridae: The viruses and their replication," in *Fields virology*. D. M. Knipe and Howley P.M, Eds. 2007, pp. 1647-1689.

[10] T. P. Weber and N. I. Stilianakis, "Inactivation of influenza A viruses in the environment and modes of transmission: A critical review," *J. Infect.*, vol. 57, no. 5, pp. 361-373, Nov.2008.

[11] M. C. Joseph, A. S. Kirk, and W. G. Laver, "Approaches and strategies for the treatment of influenza virus infections," *Antiviral Chemistry & Chemotherapy*, vol. 10, no. 4, pp. 155-185, 1999.

[12] K. Subbarao and J. Katz, "Avian influenza viruses infecting humans," *Cell. Mol. Life Sci.*, vol. 57, no. 12, pp. 1770-1784, Oct.2000.

[13] D. A. Steinhauer, "Role of Hemagglutinin Cleavage for the Pathogenicity of Influenza Virus," *Virology*, vol. 258, no. 1, pp. 1-20, May1999.

[14] S. Bertram, I. Glowacka, I. Steffen, A. K++hl, and S. P+¦hlmann, "Novel insights into proteolytic cleavage of influenza virus hemagglutinin," *Rev. Med. Virol.*, vol. 20, no. 5, pp. 298-310, 2010.

[15] "http://www.accessexcellence.org/RC/VL/GG/influenza.php," 2010.

[16] M. Vey, M. Orlich, S. Adler, H. D. Klenk, R. Rott, and W. Garten, "Hemagglutinin activation of pathogenic avian influenza viruses of serotype H7 requires the protease recognition motif R-X-K/R-R," *Virology*, vol. 188, no. 1, pp. 408-413, May1992.

[17] G. W. Wood, J. W. McCauley, J. B. Bashiruddin, and D. J. Alexander, "Deduced amino acid sequences at the haemagglutinin cleavage site of avian influenza A viruses of H 5 and H 7 subtypes," *Arch. Virol.*, vol. 130, no. 1, pp. 209-217, Mar.1993.

[18] D. A. Senne, B. Panigrahy, Y. Kawaoka, J. E. Pearson, J. S++ss, M. Lipkind, H. Kida, and R. G. Webster, "Survey of the Hemagglutinin (HA) Cleavage Site Sequence of H5 and H7 Avian Influenza Viruses: Amino Acid Sequence at the HA Cleavage Site as a Marker of Pathogenicity Potential," *Avian Dis.*, vol. 40, no. 2, pp. 425-437, Apr.1996.

[19] J. W. Drake, "Rates of spontaneous mutation among RNA viruses," *Proc. Natl. Acad. Sci. U. S. A.*, vol. 90, no. 9, pp. 4171-4175, May1993.

[20] F. Carrat and A. Flahault, "Influenza vaccine: The challenge of antigenic drift," *Vaccine*, vol. 25, no. 39-40, pp. 6852-6862, Sept.2007.

[21] T. Ito, H. Goto, E. Yamamoto, H. Tanaka, M. Takeuchi, M. Kuwayama, Y. Kawaoka, and K. Otsuki, "Generation of a Highly Pathogenic Avian Influenza A Virus from an Avirulent Field Isolate by Passaging in Chickens," *J. Virol.*, vol. 75, no. 9, pp. 4439-4443, May2001.

[22] N. J. Cox and K. Subbarao, "Global Epidemiology of Influenza: Past and Present," *Annu. Rev. Med.*, vol. 51, no. 1, pp. 407-421, Feb.2000.

[23] K. S. Li, Y. Guan, J. Wang, G. J. D. Smith, K. M. Xu, L. Duan, A. P. Rahardjo, P. Puthavathana, C. Buranathai, T. D. Nguyen, A. T. S. Estoepangestie, A. Chaisingh, P. Auewarakul, H. T. Long, N. T. H. Hanh, R. J. Webby, L. L. M. Poon, H. Chen, K. F. Shortridge, K. Y. Yuen, R. G. Webster, and J. S. M. Peiris, "Genesis of a highly pathogenic and potentially pandemic H5N1 influenza virus in eastern Asia," *Nature*, vol. 430, no. 6996, pp. 209-213, July2004.

[24] W. Ma, R. E. Kahn, and J. A. Richt, "The pig as a mixing vessel for influenza viruses: Human and veterinary implications," *Journal of Molecular and Genetic Medicine*, vol. 3, no. 1, pp. 158-166, 2009.

[25] G. Neumann, T. Noda, and Y. Kawaoka, "Emergence and pandemic potential of swine-origin H1N1 influenza virus," *Nature*, vol. 459, no. 7249, pp. 931-939, June2009.

[26] R. G. Webster, W. J. Bean, O. T. Gorman, T. M. Chambers, and Y. Kawaoka, "Evolution and ecology of influenza A viruses," *Microbiol. Mol. Biol. Rev.*, vol. 56, no. 1, pp. 152-179, Mar.1992.

[27] E. Spackman, "The ecology of avian influenza virus in wild birds: What does this mean for poultry?," *Poult. Sci.*, vol. 88, no. 4, pp. 847-850, Apr.2009.

[28] B. Olsen, V. J. Munster, A. Wallensten, J. Waldenstrom, A. D. M. E. Osterhaus, and R. A. M. Fouchier, "Global Patterns of Influenza A Virus in Wild Birds," *Science*, vol. 312, no. 5772, pp. 384-388, Apr.2006.

[29] W. B. Karesh, R. A. Cook, M. Gilbert, and J. Newcomb, "Implications of wildlife trade on the movement of avian influenza virus and other infectious diseases," *J. Wildl. Dis.*, vol. 43, no. 3_Supplement, p. S55-S59, July2007.

[30] R. G. Webster, M. Yakhno, V. S. Hinshaw, W. J. Bean, and K. Copal Murti, "Intestinal influenza: Replication and characterization of influenza viruses in ducks," *Virology*, vol. 84, no. 2, pp. 268-278, Feb.1978.

[31] T. C. Harder and O. Werner, "Avian influenza report," Flying Publisher, Paris,2006.

[32] A. S. Beare and R. G. Webster, "Replication of avian influenza viruses in humans," *Arch. Virol.*, vol. 119, no. 1, pp. 37-42, Mar.1991.

[33] M. N. Matrosovich, T. Y. Matrosovich, T. Gray, N. A. Roberts, and H. D. Klenk, "Human and avian influenza viruses target different cell types in cultures of human airway epithelium," *Proc. Natl. Acad. Sci. U. S. A.*, vol. 101, no. 13, pp. 4620-4624, Mar.2004.

[34] S. J. Baigent and J. W. McCauley, "Influenza type A in humans, mammals and birds: Determinants of virus virulence, host-range and interspecies transmission," *BioEssays*, vol. 25, no. 7, pp. 657-671, 2003.

[35] K. Subbarao * and J. Katz, "Avian influenza viruses infecting humans," *Cell. Mol. Life Sci.*, vol. 57, no. 12, pp. 1770-1784, Oct.2000.

[36] M. Koopmans, B. Wilbrink, M. Conyn, G. Natrop, H. van der Nat, H. Vennema, A. Meijer, J. van Steenbergen, R. Fouchier, A. Osterhaus, and A. Bosman, "Transmission of H7N7 avian influenza A virus to human beings during a large outbreak in commercial poultry farms in the Netherlands," *The Lancet*, vol. 363, no. 9409, pp. 587-593, Feb.2004.

[37] K. Ungchusak, P. Auewarakul, S. F. Dowell, R. Kitphati, W. Auwanit, P. Puthavathana, M. Uiprasertkul, K. Boonnak, C. Pittayawonganon, N. J. Cox, S. R. Zaki, P. Thawatsupha, M. Chittaganpitch, R. Khontong, J. M. Simmerman, and S. Chunsutthiwat, "Probable Person-to-Person Transmission of Avian Influenza A (H5N1)," *N. Engl. J. Med.*, vol. 352, no. 4, pp. 333-340, Jan.2005.

[38] B. B. Carolyn, J. M. Katz, W. H. Seto, P. K. S. Chan, D. Tsang, W. Ho, K. H. Mak, W. Lim, J. S. Tam, M. Clarke, S. G. Williams, A. W. Mounts, J. S. Bresee, L. A. Conn, T. Rowe, J. Hu-Primmer, R. A. Abernathy, X. Lu, N. J. Cox, and K. Fukuda, "Risk of Influenza A (H5N1) Infection among Health Care Workers Exposed to Patients with

Influenza A (H5N1), Hong Kong," *The Journal of Infectious Diseases*, vol. 181, no. 1, pp. 344-348, /1.

[39] Stefan Riedel, "Crossing the species barrier: the threat of an avian influenza pandemic," *Proceedings (Baylor University. Medical Center)*, vol. 19, no. 1, pp. 16-20, 2006.

[40] B. Lupiani and S. M. Reddy, "The history of avian influenza," *Comp. Immunol. Microbiol. Infect. Dis.*, vol. 32, no. 4, pp. 311-323, July2009.

[41] "http://www.who.int/csr/disease/avian_influenza/country/cases_table_2008_06_19/en/index.html,".

[42] International Monetary Fund Report, " THE GLOBAL ECONOMIC AND FINANCIAL IMPACT OF AN AVIAN FLU PANDEMIC AND THE ROLE OF THE IMF,"Feb.2006.

[43] Sherry Cooper, "In The Avian Flu Crisis: An Economic Update,"Mar.2006.

[44] B. Hoye, V. Munster, H. Nishiura, M. Klaassen, and R. Fouchier, "Surveillance of wild birds for avian influenza virus," *Emerg. Infect. Dis.*, vol. 16, no. 12 2010.

[45] K. Subbarao and T. Joseph, "Scientific barriers to developing vaccines against avian influenza viruses," *Nat Rev Immunol*, vol. 7, no. 4, pp. 267-278, Apr.2007.

[46] F. Carrat and A. Flahault, "Influenza vaccine: The challenge of antigenic drift," *Vaccine*, vol. 25, no. 39-40, pp. 6852-6862, Sept.2007.

[47] M. F. Boni, "Vaccination and antigenic drift in influenza," *Vaccine*, vol. 26, no. Supplement 3, p. C8-C14, July2008.

[48] F. B. Johnson, "Transport of viral specimens," *Clin. Microbiol. Rev.*, vol. 3, no. 2, pp. 120-131, Apr.1990.

[49] "http://classes.midlandstech.edu/carterp/Courses/bio225/chap13/ss2.htm," 2010.

[50] "http://www.ifpma.org/index.php?id=4221," 2010.

[51] J. T. M. Voeten, R. Brands, A. M. Palache, G. J. M. van Scharrenburg, G. F. Rimmelzwaan, A. D. M. E. Osterhaus, and E. C. J. Claas, "Characterization of high-growth reassortant influenza A viruses generated in MDCK cells cultured in serum-free medium," *Vaccine*, vol. 17, no. 15-16, pp. 1942-1950, Apr.1999.

[52] K. A. Moresco, D. E. Stallknecht, and D. E. Swayne, "Evaluation and Attempted Optimization of Avian Embryos and Cell Culture Methods for Efficient Isolation and Propagation of Low Pathogenicity Avian Influenza Viruses," *Avian Diseases Digest*, vol. 5, no. s1, p. e142-e143, Mar.2010.

[53] Cynthia Goldsmith, "http://www.cdc.gov/media/subtopic/library/diseases.htm," Centers for Disease Control and Prevention, 2010.

[54] G. Cattoli and I. Capua, "DIAGNOSING AVIAN INFLUENZA IN THE FRAMEWORK OF WILDLIFE SURVEILLANCE EFFORTS AND ENVIRONMENTAL SAMPLES," *J. Wildl. Dis.*, vol. 43, no. 3_Supplement, p. S35-S39, July2007.

[55] OIE (World Organization for Animal Health), "Avian influenza. In: Manual of diagnostic tests and vaccines for terrestrial animals. Chapter 2.7.12," 2009.

[56] C. Cao, R. Dhumpa, D. D. Bang, Z. Ghavifekr, J. Hogberg, and A. Wolff, "Detection of avian influenza virus by fluorescent DNA barcode-based immunoassay with sensitivity comparable to PCR," *Analyst*, vol. 135, no. 2, pp. 337-342, 2010.

[57] S. Velumani, Q. Du, B. Fenner, M. Prabakaran, L. C. Wee, L. Y. Nuo, and J. Kwang, "Development of an antigen-capture ELISA for detection of H7 subtype avian influenza from experimentally infected chickens," *J. Virol. Methods*, vol. 147, no. 2, pp. 219-225, Feb.2008.

[58] D. A. J. Tyrrell and R. C. Valentine, "The Assay of Influenza Virus Particles by Haemagglutination and Electron Microscopy," *J. Gen. Microbiol.*, vol. 16, no. 3, pp. 668-675, June1957.

[59] D. M. Knipe and Howley P.M, "Principles of Virology," in *Fields virology* Lippincott Williams & Wilkins, 2007, p. 42.

[60] G. Cross, "Hemagglutination inhibition assays," *Seminars in Avian and Exotic Pet Medicine*, vol. 11, no. 1, pp. 15-18, Jan.2002.

[61] J. C. Pedersen, "Hemagglutination-Inhibition Test for Avian Influenza Virus Subtype Identification and the Detection and Quantitation of Serum Antibodies to the Avian Influenza Virus," in *Avian Influenza Virus*, 436 ed 2008, pp. 53-66.

[62] "http://www.aht.org.uk/science_eqflu.html," 2010.

[63] R. G. Webster and C. H. Campbell, "An Inhibition Test for Identifying the Neuraminidase Antigen on Influenza Viruses," *Avian Dis.*, vol. 16, no. 5, pp. 1057-1066, /10.

[64] J. C. Pedersen, "Neuraminidase-Inhibition Assay for the Identification of Influenza A Virus Neuraminidase Subtype or Neuraminidase Antibody Specificity," in *Avian Influenza Virus*, 436 ed. E. Spackman, Ed. Humana Press, 2008, pp. 67-75.

[65] Thomas Walton and Erica Suchman, "The Double Agar Gel Immunodiffusion Test for Viral Infection," 2007.

[66] E. Spackman, D. L. Suarez, and D. A. Senne, *Avian Influenza Diagnostics and Surveillance Methods* Blackwell Publishing Ltd., 2008, pp. 299-308.

[67] "http://nfs.unipv.it/nfs/minf/dispense/immunology/agabint.html," 2010.

[68] P. R. Woolcock and C. J. Cardona, "Commercial Immunoassay Kits for the Detection of Influenza Virus Type A: Evaluation of Their Use with Poultry," *Avian Dis.*, vol. 49, no. 4, pp. 477-481, /12.

[69] T. H. Chua, T. M. Ellis, C. W. Wong, Y. Guan, S. X. Ge, G. Peng, C. Lamichhane, C. Maliadis, S. W. Tan, P. Selleck, and J. Parkinson, "Performance Evaluation of Five Detection Tests for Avian Influenza Antigen with Various Avian Samples," *Avian Dis.*, vol. 51, no. 1, pp. 96-105, Mar.2007.

[70] A. L. Shafer, J. B. Katz, and K. A. Eernisse, "Development and Validation of a Competitive Enzyme-Linked Immunosorbent Assay for Detection of Type A Influenza Antibodies in Avian Sera," *Avian Dis.*, vol. 42, no. 1, pp. 28-34, /1.

[71] D. S. Song, Y. J. Lee, O. M. Jeong, Y. J. Kim, C. H. Park, J. E. Yoo, W. J. Jeon, J. H. Kwon, G. W. Ha, B. K. Kang, C. S. Lee, H. K. Kim, B. Y. Jung, J. H. Kim, and J. S. Oh, "Evaluation of a competitive ELISA for antibody detection against avian influenza virus," *J Vet Sci*, vol. 10, no. 4, pp. 323-329, Dec.2009.

[72] M. Shahid, M. Abubakar, S. Hameed, and S. Hassan, "Avian influenza virus (H5N1); effects of physico-chemical factors on its survival," *Virol. J*, vol. 6, no. 1, p. 38, 2009.

[73] C. Thomas and D. E. Swayne, "Thermal Inactivation of H5N1 High Pathogenicity Avian Influenza Virus in Naturally Infected Chicken Meat," *J. Food Prot.*, vol. 70, pp. 674-680, Mar.2007.

[74] S. Isbarn, R. Buckow, A. Himmelreich, A. Lehmacher, and V. Heinz, "Inactivation of Avian Influenza Virus by Heat and High Hydrostatic Pressure," *J. Food Prot.*, vol. 70, pp. 667-673, Mar.2007.

[75] D. M. Knipe and Howley P.M, "Principles of Virology," in *Fields virology* Lippincott Williams & Wilkins, 2007, pp. 37-43.

[76] "http://www.virology.ws/2009/07/06/detecting-viruses-the-plaque-assay/," 2010.

[77] D. M. Knipe and P. M. Howley, *Field virology*, 5th ed. Philadelphia, PA: Lippincott Williams & Wilkins, 2010.

[78] L. J. REED and H. Muench, "A simple method of estimating fifty per cent endpoints," *Am. J. Epidemiol.*, vol. 27, no. 3, pp. 493-497, May1938.

[79] J. Pasick, "Advances in the Molecular Based Techniques for the Diagnosis and Characterization of Avian Influenza Virus Infections," *Transboundary and Emerging Diseases*, vol. 55, no. 8, pp. 329-338, 2008.

[80] "http://www.gene-quantification.de/poster-rt-pcr.jpg," 2010.

[81] E.Starick, A.Rømer-Oberdørfer, and O.Werner, "Type- and Subtype-Specific RT-PCR Assays for Avian Influenza A Viruses (AIV)," *Journal of Veterinary Medicine, Series B*, vol. 47, pp. 295-301, 2000.

[82] R. A. M. Fouchier, T. M. Bestebroer, S. Herfst, L. Van Der Kemp, G. F. Rimmelzwaan, and A. D. M. E. Osterhaus, "Detection of Influenza A Viruses from Different Species by PCR Amplification of Conserved Sequences in the Matrix Gene," *J. Clin. Microbiol.*, vol. 38, no. 11, pp. 4096-4101, Nov.2000.

[83] M. S. Lee, P. C. Chang, J. H. Shien, M. C. Cheng, and H. K. Shieh, "Identification and subtyping of avian influenza viruses by reverse transcription-PCR," *J. Virol. Methods*, vol. 97, no. 1-2, pp. 13-22, Sept.2001.

[84] M. Munch, L. P. Nielsen, K. J. Handberg, and P. H. J++rgensen, "Detection and subtyping (H5 and H7) of avian type A influenza virus by reverse transcription-PCR and PCR-ELISA," *Arch. Virol.*, vol. 146, no. 1, pp. 87-97, Jan.2001.

[85] M. J. Carter and B. W. J. Mahy, "Incomplete avian influenza virus contains A defective non-interfering component," *Arch. Virol.*, vol. 71, no. 1, pp. 13-25, Mar.1982.

[86] "http://home.cc.umanitoba.ca/~umbouc00/PLNT7690/presentation/TaqMan.html," 2010.

[87] I. M. Mackay, K. E. Arden, and A. Nitsche, "Real-time PCR in virology," *Nucleic Acids Res.*, vol. 30, no. 6, pp. 1292-1305, Mar.2002.

[88] D. Klein, "Quantification using real-time PCR technology: applications and limitations," *Trends in Molecular Medicine*, vol. 8, no. 6, pp. 257-260, June2002.

[89] E. Spackman, D. A. Senne, T. J. Myers, L. L. Bulaga, L. P. Garber, M. L. Perdue, K. Lohman, L. T. Daum, and D. L. Suarez, "Development of a Real-Time Reverse Transcriptase PCR Assay for Type A Influenza Virus and the Avian H5 and H7 Hemagglutinin Subtypes," *J. Clin. Microbiol.*, vol. 40, no. 9, pp. 3256-3260, Sept.2002.

[90] M. J. Slomka, V. J. Coward, J. Banks, B. Z. L¦ndt, I. H. Brown, J. Voermans, G. Koch, K. J. Handberg, P. H. Jørgensen, M. Cherbonnel-Pansart, V. Jestin, G. Cattoli, I. Capua, A. Ejdersund, P. Thoren, and G. Czifra, "Identification of Sensitive and Specific Avian Influenza Polymerase Chain Reaction Methods Through Blind Ring Trials Organized in the European Union," *Avian Dis.*, vol. 51, no. s1, pp. 227-234, Mar.2007.

[91] G. M. Air, "Sequence Relationships among the Hemagglutinin Genes of 12 Subtypes of Influenza A Virus," *Proc. Natl. Acad. Sci. U. S. A.*, vol. 78, no. 12, pp. 7639-7643, /12.

[92] E. Spackman, D. A. Senne, T. J. Myers, L. L. Bulaga, L. P. Garber, M. L. Perdue, K. Lohman, L. T. Daum, and D. L. Suarez, "Development of a Real-Time Reverse Transcriptase PCR Assay for Type A Influenza Virus and the Avian H5 and H7 Hemagglutinin Subtypes," *J. Clin. Microbiol.*, vol. 40, no. 9, pp. 3256-3260, Sept.2002.

[93] C. W. Lee and D. L. Suarez, "Application of real-time RT-PCR for the quantitation and competitive replication study of H5 and H7 subtype avian influenza virus," *J. Virol. Methods*, vol. 119, no. 2, pp. 151-158, Aug.2004.

[94] J. Banks, E. C. Speidel, J. W. McCauley, and D. J. Alexander, "Phylogenetic analysis of H7 haemagglutinin subtype influenza A viruses," *Arch. Virol.*, vol. 145, no. 5, pp. 1047-1058, May2000.

[95] C. R÷hm, T. Horimoto, Y. Kawaoka, J. Snss, and R. G. Webster, "Do Hemagglutinin Genes of Highly Pathogenic Avian influenza Viruses Constitute Unique Phylogenetic Lineages?," *Virology*, vol. 209, no. 2, pp. 664-670, June1995.

[96] M. J. Slomka, T. Pavlidis, J. Banks, W. Shell, A. McNally, S. Essen, and I. H. Brown, "Validated H5 Eurasian Real-Time Reverse Transcriptase–Polymerase Chain Reaction and Its Application in H5N1 Outbreaks in 2005–2006," *Avian Dis.*, vol. 51, no. s1, pp. 373-377, Mar.2007.

[97] A. S. Arafa, A. A. Selim, M. K. Hassan, and M. M. Aly, "Genetic Characterization of Variant Strains of Highly Pathogenic Avian Influenza H5N1 That Escaped Detection by Real-Time Reverse TranscriptaseΓÇôPCR Diagnostic Tests," *Avian Dis.*, vol. 54, no. s1, pp. 673-676, Mar.2010.

[98] E. Spackman, H. S. Ip, D. L. Suarez, R. D. Slemons, and D. E. Stallknecht, "Analytical validation of a real-time reverse transcription polymerase chain reaction test for Pan-American lineage H7 subtype Avian influenza viruses," *J Vet Diagn Invest*, vol. 20, no. 5, pp. 612-616, Sept.2008.

[99] J. Stockton, J. S. Ellis, M. Saville, J. P. Clewley, and M. C. Zambon, "Multiplex PCR for Typing and Subtyping Influenza and Respiratory Syncytial Viruses," *J. Clin. Microbiol.*, vol. 36, no. 10, pp. 2990-2995, Oct.1998.

[100] S. K. Poddar, "Influenza virus types and subtypes detection by single step single tube multiplex reverse transcription-polymerase chain reaction (RT-PCR) and agarose gel electrophoresis," *J. Virol. Methods*, vol. 99, no. 1-2, pp. 63-70, Jan.2002.

[101] B. Chaharaein, A. R. Omar, I. Aini, K. Yusoff, and S. S. Hassan, "Detection of H5, H7 and H9 subtypes of avian influenza viruses by multiplex reverse transcription-polymerase chain reaction," *Microbiol. Res.*, vol. 164, no. 2, pp. 174-179, 2009.

[102] Z. Xie, Y. s. Pang, J. Liu, X. Deng, X. Tang, J. Sun, and M. I. Khan, "A multiplex RT-PCR for detection of type A influenza virus and differentiation of avian H5, H7, and H9 hemagglutinin subtypes," *Mol. Cell. Probes*, vol. 20, no. 3-4, pp. 245-249, June2006.

[103] E. Spackman, D. A. Senne, L. L. Bulaga, S. Trock, and D. L. Suarez, "Development of Multiplex Real-Time RT-PCR as a Diagnostic Tool for Avian Influenza," *Avian Dis.*, vol. 47, pp. 1087-1090, 2003.

[104] P. q. Li, J. Zhang, C. P. Muller, J. x. Chen, Z. f. Yang, R. Zhang, J. Li, and Y. s. He, "Development of a multiplex real-time polymerase chain reaction for the detection of influenza virus type A including H5 and H9 subtypes," *Diagn. Microbiol. Infect. Dis.*, vol. 61, no. 2, pp. 192-197, June2008.

[105] S. Payungporn, P. Phakdeewirot, S. Chutinimitkul, A. Theamboonlers, J. Keawcharoen, K. Oraveerakul, A. Amonsin, and Y. Poovorawan, "Single-Step Multiplex Reverse Transcription–Polymerase Chain Reaction (RT-PCR) for Influenza A Virus Subtype H5N1 Detection," *Viral Immunol.*, vol. 17, no. 4, pp. 588-593, Dec.2004.

[106] S. Payungporn, S. Chutinimitkul, A. Chaisingh, S. Damrongwantanapokin, C. Buranathai, A. Amonsin, A. Theamboonlers, and Y. Poovorawan, "Single step multiplex real-time RT-PCR for H5N1 influenza A virus detection," *J. Virol. Methods*, vol. 131, no. 2, pp. 143-147, Feb.2006.

[107] B. Hoffmann, T. Harder, E. Starick, K. Depner, O. Werner, and M. Beer, "Rapid and highly sensitive pathotyping of avian influenza A H5N1 virus using real-time RT-PCR," *J. Clin. Microbiol.*, p. JCM, Dec.2006.

[108] I. M. Frayling, E. Monk, and R. Butler, "PCR-Based Methods for Mutation Detection," in *Molecular Diagnostics*. W. B. Coleman and G. J. Tsongalis, Eds. Humana Press, 2005, pp. 65-74.

[109] J. Li, S. Chen, and D. H. Evans, "Typing and Subtyping Influenza Virus Using DNA Microarrays and Multiplex Reverse Transcriptase PCR," *J. Clin. Microbiol.*, vol. 39, no. 2, pp. 696-704, Feb.2001.

[110] M. J. Heller, "DNA MICROARRAY TECHNOLOGY: Devices, Systems, and Applications," *Annu. Rev. Biomed. Eng.*, vol. 4, no. 1, pp. 129-153, Aug.2002.

[111] "http://upload.wikimedia.org/wikipedia/en/a/a8/NA_hybrid.svg," 2010.

[112] L. C. Wang, C. H. Pan, L. L. Severinghaus, L. Y. Liu, C. T. Chen, C. E. Pu, D. Huang, J. T. Lir, S. C. Chin, M. C. Cheng, S. H. Lee, and C. H. Wang, "Simultaneous detection and differentiation of Newcastle disease and avian influenza viruses using oligonucleotide microarrays," *Vet. Microbiol.*, vol. 127, no. 3-4, pp. 217-226, Mar.2008.

[113] X. Han, X. Lin, B. Liu, Y. Hou, J. Huang, S. Wu, J. Liu, L. Mei, G. Jia, and Q. Zhu, "Simultaneously subtyping of all influenza A viruses using DNA microarrays," *J. Virol. Methods*, vol. 152, no. 1-2, pp. 117-121, Sept.2008.

[114] Z. w. Zhang, Y. m. Zhou, Y. Zhang, Y. Guo, S. c. Tao, Z. Li, Q. Zhang, and J. Cheng, "Sensitive Detection of SARS Coronavirus RNA by a Novel Asymmetric Multiplex Nested RT-PCR Amplification Coupled With Oligonucleotide Microarray Hybridization," in *Microarrays in Clinical Diagnostics*, 114 ed. T. O. Joos and P. Fortina, Eds. Humana Press, 2005, pp. 59-78.

[115] A. Gall, B. Hoffmann, T. Harder, C. Grund, D. Hoper, and M. Beer, "Design and Validation of a Microarray for Detection, Hemagglutinin Subtyping, and Pathotyping of Avian Influenza Viruses," *J. Clin. Microbiol.*, vol. 47, no. 2, pp. 327-334, Feb.2009.

[116] P. P. Cheung, Y. H. C. Leung, C. K. Chow, C. F. Ng, C. L. Tsang, Y. O. Wu, S. K. Ma, S. F. Sia, Y. Guan, and J. S. M. Peiris, "Identifying the species-origin of faecal droppings used for avian influenza virus surveillance in wild-birds," *J. Clin. Virol.*, vol. 46, no. 1, pp. 90-93, Sept.2009.

[117] L. Monteiro, D. Bonnemaison, A. Vekris, K. G. Petry, J. Bonnet, R. Vidal, J. Cabrita, and F. Megraud, "Complex polysaccharides as PCR inhibitors in feces: Helicobacter pylori model," *J. Clin. Microbiol.*, vol. 35, no. 4, pp. 995-998, Apr.1997.

[118] P. Rådström, R. Knutsson, P. Wolffs, M. Danhlenborg, and C. Löfström, "Pre-PCR Processing of Samples," in *PCR Detection of Microbial Pathogens*, 216 ed 2002, pp. 31-50.

[119] R. Peter, K. Rickard, W. Petra, L. Maria, and L. Charlotta, "Pre-PCR Processing : Strategies to Generate PCR-Compatible Samples," *Mol. Biotechnol.*, vol. 26, pp. 133-146, Feb.2004.

[120] C. S. Ginny and C. P. Helen, "Analytical molecular biology: quality and validation," RSC,UK, 1999, pp. 91-96.

[121] C. T. Suin and C. Y. Beow, "DNA, RNA, and Protein Extraction: The Past and The Present," *Journal of Biomedicine and Biotechnology*, 2009.

[122] D. L. Suarez, A. Das, and E. Ellis, "Review of Rapid Molecular Diagnostic Tools for Avian Influenza Virus," *Avian Dis.*, vol. 51, no. s1, pp. 201-208, Mar.2007.

[123] "RNAse Kit, www.qiagen.com," 2010.

[124] T. B. Rasmussen, +. Uttenthal, M. Hakhverdyan, S. Belβk, P. R. Wakeley, S. M. Reid, K. Ebert, and D. P. King, "Evaluation of automated nucleic acid extraction methods for virus detection in a multicenter comparative trial," *J. Virol. Methods*, vol. 155, no. 1, pp. 87-90, Jan.2009.

[125] J. H. Knepp, M. A. Geahr, M. S. Forman, and A. Valsamakis, "Comparison of Automated and Manual Nucleic Acid Extraction Methods for Detection of Enterovirus RNA," *J. Clin. Microbiol.*, vol. 41, no. 8, pp. 3532-3536, Aug.2003.

[126] S. Berensmeier, "Magnetic particles for the separation and purification of nucleic acids," *Appl. Microbiol. Biotechnol.*, vol. 73, no. 3, pp. 495-504, Dec.2006.

[127] D. Tewari, C. Zellers, H. Acland, and J. C. Pedersen, "Automated extraction of avian influenza virus for rapid detection using real-time RT-PCR," *J. Clin. Virol.*, vol. 40, no. 2, pp. 142-145, Oct.2007.

[128] L. Bissonnette and M. G. Bergeron, "Diagnosing infections–current and anticipated technologies for point-of-care diagnostics and home-based testing," *Clinical Microbiology and Infection*, vol. 16, no. 8, pp. 1044-1053, 2010.

[129] World Health Organisation, "WHO recommendations on the use of rapid testing for influenza diagnosis," *World Health Organization*, July2005.

[130] P. Yager, T. Edwards, E. Fu, K. Helton, K. Nelson, M. R. Tam, and B. H. Weigl, "Microfluidic diagnostic technologies for global public health," *Nature*, vol. 442, no. 7101, pp. 412-418, July2006.

[131] J. Mairhofer, K. Roppert, and P. Ertl, "Microfluidic Systems for Pathogen Sensing: A Review," *Sensors*, vol. 9, pp. 4804-4823, 2009.

[132] N. Crews, C. Wittwer, and B. Gale, "Continuous-flow thermal gradient PCR," *Biomedical Microdevices*, vol. 10, no. 2, pp. 187-195, Apr.2008.

[133] J. El-Ali, I. R. Perch-Nielsen, C. R. Poulsen, D. D. Bang, P. Telleman, and A. Wolff, "Simulation and experimental validation of a SU-8 based PCR thermocycler chip with integrated heaters and temperature sensor," *Sens. Actuators A*, vol. 110, no. 1-3, pp. 3-10, Feb.2004.

[134] C. Zhang and D. Xing, "Miniaturized PCR chips for nucleic acid amplification and analysis: latest advances and future trends," *Nucleic Acids Res.*, vol. 35, no. 13, pp. 4223-4237, July2007.

[135] K. Y. Lien and G. B. Lee, "Miniaturization of molecular biological techniques for gene assay," *Analyst*, vol. 135, no. 7, pp. 1499-1518, 2010.

[136] Y. Zhang and P. Ozdemir, "Microfluidic DNA amplification--A review," *Anal. Chim. Acta*, vol. 638, no. 2, pp. 115-125, Apr.2009.

[137] L. Chen, A. Manz, and P. J. R. Day, "Total nucleic acid analysis integrated on microfluidic devices," *Lab Chip*, vol. 7, no. 11, pp. 1413-1423, 2007.

[138] C. Zhang, J. Xu, W. Ma, and W. Zheng, "PCR microfluidic devices for DNA amplification," *Biotechnology Advances*, vol. 24, no. 3, pp. 243-284, May2005.

[139] M. A. Shoffner, J. Cheng, G. E. Hvichia, L. J. Kricka, and P. Wilding, "Chip PCR. I. Surface Passivation of Microfabricated Silicon-Glass Chips for PCR," *Nucleic Acids Res.*, vol. 24, no. 2, pp. 375-379, Jan.1996.

[140] D. J. Beebe, G. A. Mensing, and G. M. Walker, "PHYSICS AND APPLICATIONS OF MICROFLUIDICS IN BIOLOGY," *Annu. Rev. Biomed. Eng.*, vol. 4, no. 1, pp. 261-286, Aug.2002.

[141] D. Holmes and S. Gawad, "The Application of Microfluidics in Biology," in *Microengineering in Biotechnology*, 583 ed 2008, pp. 55-80.

[142] X. Chen and D. F. Cui, "Microfluidic devices for sample pretreatment and applications," *Microsyst Technol*, vol. 15, no. 5, pp. 667-676, May2009.

[143] M. A. Dineva, L. Mahilum-Tapay, and H. Lee, "Sample preparation: a challenge in the development of point-of-care nucleic acid-based assays for resource-limited settings," *The Analyst*, vol. 132, no. 12, pp. 1193-1199, 2007.

[144] D. Li, "Microfluidic Lab-on-a-Chip Devices for Biomedical Applications," in *Microfluidics Based Microsystems*, 0 ed. S. Kaka+º, B. Kosoy, D. Li, and A. Pramuanjaroenkij, Eds. Springer Netherlands, 2010, pp. 377-397.

[145] M. A. M. Gijs, "Magnetic bead handling on-chip: new opportunities for analytical applications," *Microfluid Nanofluid*, vol. 1, no. 1, pp. 22-40, Nov.2004.

[146] O. Olsvik, T. Popovic, E. Skjerve, K. S. Cudjoe, E. Hornes, J. Ugelstad, and M. Uhlen, "Magnetic separation techniques in diagnostic microbiology," *Clin. Microbiol. Rev.*, vol. 7, no. 1, pp. 43-54, Jan.1994.

[147] I. Safarik and s. Mirka, "Use of magnetic techniques for the isolation of cells," *Journal of Chromatography B: Biomedical Sciences and Applications*, vol. 722, no. 1-2, pp. 33-53, Feb.1999.

[148] D. Horaík, M. Babic, H. Mackova, and M. J. Benes, "Preparation and properties of magnetic nano- and microsized particles for biological and environmental separations," *J. Sep. Science*, vol. 30, no. 11, pp. 1751-1772, 2007.

[149] "Dynabeads; www.invitrogen.com/," 2010.

[150] I. Safarik and M. Safarikova, "Magnetic techniques for the isolation and purification of proteins and peptides," *BioMagnetic Research and Technology*, vol. 2, no. 1, p. 7, 2004.

[151] "Hysteresis Loop http://www.ndt-ed.org/EducationResources/CommunityCollege/MagParticle/Physics/HysteresisLoop.htm," 2010.

[152] J. Andreassen, "One micron magnetic beads optimised for automated immunoassays," *Clinical laboratories International*, vol. in: April ed. 2005.

[153] D. L. Leslie-Pelecky and R. D. Rieke, "Magnetic Properties of Nanostructured Materials," *Chem. Mater.*, vol. 8, no. 8, pp. 1770-1783, Jan.1996.

[154] K. Y. Lien, J. L. Lin, C. Y. Liu, H. Y. Lei, and G. B. Lee, "Purification and enrichment of virus samples utilizing magnetic beads on a microfluidic system," *Lab Chip*, vol. 7, no. 7, pp. 868-875, May2007.

[155] Y. Li, C. Zhang, and D. Xing, "Fast identification of foodborne pathogenic viruses using continuous-flow reverse transcription-PCR with fluorescence detection," *Microfluid Nanofluid*, pp. 1-14, July2010.

[156] R. Hartung, A. Br+¦sing, G. Sczcepankiewicz, U. Liebert, N. H+ñfner, M. D++rst, J. Felbel, D. Lassner, and J. K+¦hler, "Application of an asymmetric helical tube reactor for fast identification of gene transcripts of pathogenic viruses by micro flow-through PCR," *Biomedical Microdevices*, vol. 11, no. 3, pp. 685-692, June2009.

[157] L. Kang-Yi, L. Wang-Ying, L. Yu-Fang, W. Chih-Hao, L. Huan-Yao, and L. Gwo-Bin, "Microfluidic Systems Integrated With a Sample Pretreatment Device for Fast Nucleic-Acid Amplification," *Microelectromechanical Systems, Journal of*, vol. 17, no. 2, pp. 288-301, Apr.2008.

[158] "http://www.optolabcard.com/," 2010.

[159] "http://www.labonfoil.eu/," 2010.

[160] P. Abgrall, V. Conedera, H. Camon, A. M. Gue, and N. T. Nguyen, "SU-8 as a structural material for labs-on-chips and microelectromechanical systems," *Electrophoresis*, vol. 28, no. 24, pp. 4539-4551, 2007.

[161] M. Agirregabiria, F. J. Blanco, J. Berganzo, M. T. Arroyo, A. Fullaondo, K. Mayora, and J. M. Ruano-Lopez, "Fabrication of SU-8 multilayer microstructures based on successive CMOS compatible adhesive bonding and releasing steps," *Lab Chip*, vol. 5, no. 5, pp. 545-552, 2005.

[162] J. M. Ruano-Lopez, M. Agirregabiria, G. Olabarria, D. Verdoy, D. D. Bang, M. Bu, A. Wolff, A. Voigt, J. A. Dziuban, R. Walczak, and J. Berganzo, "The SmartBioPhone[trade mark sign], a point of care vision under development through two European projects: OPTOLABCARD and LABONFOIL," *Lab Chip*, vol. 9, no. 11, pp. 1495-1499, 2009.

[163] Joel Voldman, "Dielectrophoretic traps for cell manipulation," in *BioMEMS and Biomedical Nanotechnology, Biomolecular sensing, Processing and Analysis*, IV ed. Mauro Ferrari, Rashid Bashir, and Steve Wereley, Eds. US: Springer, 2006.

[164] M. Bally, R. Dhumpa, and J. V÷r÷s, "Particle flow assays for fluorescent protein microarray applications," *Biosens. Bioelectron.*, vol. 24, no. 5, pp. 1195-1200, Jan.2009.

[165] M. Andersson, K. Elihn, K. Fromell, and K. D. Caldwell, "Surface attachment of nanoparticles using oligonucleotides," *Colloids and Surfaces B: Biointerfaces*, vol. 34, no. 3, pp. 165-171, Apr.2004.

[166] A. J. Goldman, R. G. Cox, and H. Brenner, "Slow viscous motion of a sphere parallel to a plane wall--II Couette flow," *Chem. Eng. Sci.*, vol. 22, no. 4, pp. 653-660, Apr.1967.

[167] K. C. Chang and D. A. Hammer, "Influence of Direction and Type of Applied Force on the Detachment of Macromolecularly-Bound Particles from Surfaces," *Langmuir*, vol. 12, no. 9, pp. 2271-2282, Jan.1996.

[168] C. Carisson, M. Johnson, and B. Akerman, "Double bands in DNA gel elctrophoresis caused by bis-intercalating dyes," *Nucleic Acids Res.*, vol. 23, no. 13, pp. 2413-2420, July1995.

[169] O. Tu, T. Knott, M. Marsh, K. Bechtol, D. Harris, D. Barker, and J. Bashkin, "The influence of fluorescent dye structure on the electrophoretic mobility of end-labeled DNA," *Nucleic Acids Res.*, vol. 26, no. 11, pp. 2797-2802, June1998.

[170] A. Prakash, M. Amrein, and K. Kaler, "Characteristics and impact of <i>Taq</i> enzyme adsorption on surfaces in microfluidic devices," *Microfluid Nanofluid*, vol. 4, no. 4, pp. 295-305, Apr.2008.

[171] T. B. Christensen et al, "PCR biocompatibility of lab-on-a-chip and MEMS materials,", 17 ed 2007, p. 1527.

[172] W. Rychlik, "Selection of primers for polymerase chain reaction," *Mol. Biotechnol.*, vol. 3, no. 2, pp. 129-134, Apr.1995.

[173] J. Brownie, S. Shawcross, J. Theaker, D. Whitcombe, R. Ferrie, C. Newton, and S. Little, "The elimination of primer-dimer accumulation in PCR," *Nucleic Acids Res.*, vol. 25, no. 16, pp. 3235-3241, Aug.1997.

[174] M. Y. R. N. VIRREIRA, F. A. U. S. TORRICO, C. A. R. I. TRUYENS, C. R. I. S. ONSO-VEGA, M. A. R. C. SOLANO, Y. V. E. S. CARLIER, and M. I. C. H. SVOBODA, "COMPARISON OF POLYMERASE CHAIN REACTION METHODS FOR RELIABLE AND EASY DETECTION OF CONGENITAL TRYPANOSOMA CRUZI INFECTION," *Am. J. Trop. Med. Hyg.*, vol. 68, no. 5, pp. 574-582, May2003.

[175] "An Internal Amplification Control System Based on Primer-Dimer Formation for PCR Product Detection by DNA Hybridization," *J. Food Prot.*, vol. 69, pp. 2280-2284, Sept.2006.

[176] Dang Duong Bang and et.al., "A total integrated Lab-on-a-chip systems for rapid detection of Campylobacter spp. in broiler chicken Validation trial," 2009.

[177] P. Nunes, P. Ohlsson, O. Ordeig, and J. +. Kutter, "Cyclic olefin polymers: emerging materials for lab-on-a-chip applications," *Microfluid Nanofluid*, vol. 9, no. 2, pp. 145-161, Aug.2010.

[178] "National center for biotechnology information: Influenza virus resource database (IVRD) [http://www.ncbi.nlm.nih.gov/genomes/FLU/]," 2009.

[179] A. Gall, B. Hoffmann, T. Harder, C. Grund, and M. Beer, "Universal Primer Set for Amplification and Sequencing of HA0 Cleavage Sites of All Influenza A Viruses," *J. Clin. Microbiol.*, vol. 46, no. 8, pp. 2561-2567, Aug.2008.

[180] K. Tsukamoto, H. Ashizawa, K. Nakanishi, N. Kaji, K. Suzuki, M. Okamatsu, S. Yamaguchi, and M. Mase, "Subtyping of Avian Influenza Viruses H1 to H15 on the

Basis of Hemagglutinin Genes by PCR Assay and Molecular Determination of Pathogenic Potential," *J. Clin. Microbiol.*, vol. 46, no. 9, pp. 3048-3055, Sept.2008.

[181] N. Jindal, Y. Chander, M. de Abin, S. Sreevatsan, D. Stallknecht, D. A. Halvorson, and S. M. Goyal, "Amplification of four genes of influenza A viruses using a degenerate primer set in a one step RT-PCR method," *J. Virol. Methods*, vol. 160, no. 1-2, pp. 163-166, Sept.2009.

[182] R. Wang, L. Soll, V. Dugan, J. Runstadler, G. Happ, R. D. Slemons, and J. K. Taubenberger, "Examining the hemagglutinin subtype diversity among wild duck-origin influenza A viruses using ethanol-fixed cloacal swabs and a novel RT-PCR method," *Virology*, vol. 375, no. 1, pp. 182-189, May2008.

[183] R. Wang and J. K. Taubenberger, "Methods for molecular surveillance of influenza," *Expert Rev Anti Infect Ther*, vol. 8, no. 5, pp. 517-527, May2010.

[184] M. F. Polz and C. M. Cavanaugh, "Bias in Template-to-Product Ratios in Multitemplate PCR," *Appl. Environ. Microbiol.*, vol. 64, no. 10, pp. 3724-3730, Oct.1998.

[185] M. Dufva, J. Petersen, M. Stoltenborg, H. Birgens, and C. B. V. Christensen, "Detection of mutations using microarrays of poly(C)10-poly(T)10 modified DNA probes immobilized on agarose films," *Anal. Biochem.*, vol. 352, no. 2, pp. 188-197, May2006.

[186] S. Marche and T. van den Berg, "Evaluation of Rapid Antigen Detection Kits for the Diagnosis of Highly Pathogenic Avian Influenza H5N1 Infection," *Avian Dis.*, vol. 54, no. s1, pp. 650-654, Mar.2010.

[187] P. Tallury, A. Malhotra, L. M. Byrne, and S. Santra, "Nanobioimaging and sensing of infectious diseases," *Advanced Drug Delivery Reviews*, vol. 62, no. 4-5, pp. 424-437, Mar.2010.

[188] D. S. Watson, S. M. Reddy, V. Brahmakshatriya, and B. Lupiani, "A multiplexed immunoassay for detection of antibodies against avian influenza virus," *J. Immunol. Methods*, vol. 340, no. 2, pp. 123-131, Jan.2009.

[189] B. Lupiani, B. Mozisek, P. W. Mason, C. Lamichhane, and S. M. Reddy, "Simultaneous Detection of Avian Influenza Virus NP and H5 Antibodies in Chicken Sera Using a Fluorescence Microsphere Immunoassay," *Avian Dis.*, vol. 54, no. s1, pp. 668-672, Mar.2010.

[190] J. Baudry, C. Rouzeau, C. Goubault, C. Robic, L. Cohen-Tannoudji, A. Koenig, E. Bertrand, and J. Bibette, "Acceleration of the recognition rate between grafted ligands and receptors with magnetic forces," *Proceedings of the National Academy of Sciences*, vol. 103, no. 44, pp. 16076-16078, Oct.2006.

[191] P. Rachel Pearce and R. Bruce, "Comparison of blocking agents for ELISA," *NuncBulletin*, vol. 7, pp. 1-3, 1997.

[192] H. Bak, J. Kyhse-Andersen, and O. R. T. Thomas, "High-throughput immunoturbidimetric assays for in-process determination of polyclonal antibody concentration and functionality in crude samples," *Journal of Chromatography B*, vol. 848, no. 1, pp. 142-150, Mar.2007.